RITSUMEIKAN

International Collaborative Research Project

Report

May 2025 - January 2026

Ritsumeikan High School

SSH
Super Science High school

Foreword

It is our great pleasure to present this volume of research reports, which represents the culmination of this year's International Collaborative Research Project. Over the course of the year, high school students from diverse regions of the world have engaged in sustained scientific inquiry, working collaboratively across borders to develop research questions, design and conduct investigations, analyze data, and communicate their findings. We trust that this experience has contributed not only to their intellectual growth, but also to their personal development as globally minded individuals.

Contemporary society continues to confront a range of complex and interrelated challenges, including environmental sustainability, energy security, disaster preparedness, and the ethical implications of rapidly advancing technologies. Such issues transcend national boundaries and disciplinary frameworks, requiring cooperative efforts grounded in scientific understanding. In this context, the capacity to collaborate across cultures and borders is indispensable. Through their participation in this program, students have cultivated essential competencies, including critical thinking, scientific reasoning, and effective teamwork. Equally important, they have gained firsthand experience in navigating the practical dimensions of international collaboration, such as overcoming linguistic and cultural differences, coordinating across time zones, and reaching consensus through constructive dialogue.

For many years, Ritsumeikan High School has been committed to fostering educational practices that promote international engagement and mutual understanding. Over nearly two decades, we have advanced initiatives in international collaborative research at the secondary school level. While such endeavors were once constrained by the limitations of communication, ongoing developments in information and communication technology have enabled more continuous and meaningful exchanges among students worldwide. This year, we were privileged to collaborate with partner schools from a wide range of countries and regions. Throughout the program, student teams demonstrated perseverance, intellectual curiosity, and a spirit of cooperation as they pursued shared research objectives. The presentations delivered at the International Collaborative Research Fair stand as a testament to the quality of their work and the depth of their engagement. It is our hope that this compilation will serve both as a record of these accomplishments and as an inspiration for future participants.

We would like to extend our sincere gratitude to all students and teachers involved in this program, as well as to the administrators, guardians, and supporting institutions whose contributions have made these activities possible. We also wish to express our deep appreciation to the Ministry of Education, Culture, Sports, Science and Technology (MEXT) for its continued support of the International Collaborative Research Project as part of its broader efforts to promote international exchange.

To the students who have participated in this program: as you continue along your academic and professional paths, we encourage you to draw upon the experiences and insights gained through this endeavor. The ability to engage collaboratively in the pursuit of knowledge, across differences in culture and perspective, will remain an invaluable asset in an increasingly interconnected world. We look forward with great anticipation to your future contributions to society.

April 2026
Ritsumeikan High School
SSH Department

Table of Contents

Participating Schools 3
Year Schedule 4
Research Topics 5
International Collaborative Research Fair 6
Research Reports 7
- Group 1 (QASMT - Atsukou) 8
- Group 2 (NGSPSSW - ISTHS) 15
- Group 3 (NGSPSSW - RishoRits) 21
- Group 4 (NGSPSSW - Rits) 25
- Group 5 (NGS-YK - Tokai) 32
- Group 6 (NGS-YK - FUKUKO) 38
- Group 7 (G.T. College - TGUSHS) 43
- Group 8 (BMD - Saijo) 49
- Group 9 (BMD - OKU Tennoji) 53
- Group 10 (MPHS - Seisho) 57
- Group 11 (SBC - KFNHS) 61
- Group 12 (SBC - Ichijô SHS) 65
- Group 13 (PSHS-EVC - Ichijô SHS) 69
- Group 14 (PSHS-EVC - Akashikita) 75
- Group 15 (PSHS-SRC - sensan) 82
- Group 16 (SST - Yokkaichi) 90
- Group 17 (SST - Akashikita) 96
- Group 18 (KSHS - SGHS) 101
- Group 19 (KSHS - WUHSHS) 106
- Group 20 (KSHS - Rits) 112
- Group 21 (CD - Rits) 119
- Group 22 (CD - Rit'sm) 127
- Group 23 (CUD - KagoChuo) 134
- Group 24 (KVIS - Kobe) 139
- Group 25 (PDS - RishoRits) 142
- Group 26 (PDS - Minami) 146
- Group 27 (PCSHSM - Ryuichi) 149
- Group 28 (PCSHSM - Ikunishi) 154
- Group 29 (PCSHSTRG - NGT) 158
- Group 30 (PCSHSTRG - Matsusho) 163
- Group 31 (SPSM - RishoRits) 167

Participating Schools

Total 43 Schools

Australia	Queensland Academy for Science Mathematics and Technology
Cambodia	New Generation School, Preah Sisowath High School New Generation School, Preah Yukunthor High School
Hong Kong	GT College
Indonesia	Budi Mulia Dua High School Mutiara Persada High School
Malaysia	Sekolah Menengah Kebangsaan St. Bernadette's Convent
The Philippines	Philippine Science High School - Eastern Visayas Campus Philippine Science High School - SOCCSKSARGEN Region Campus
Singapore	School of Science and Technology, Singapore
Taiwan	Kaohsiung Municipal Kaohsiung Senior High School
Thailand	Chitralada School Chulalongkorn University Demonstration Secondary School Kamnoetvidya Science Academy Patumwan Demonstration School Princess Chulabhorn Science High School Mukdahan Princess Chulabhorn Science High School Trang Srinakharinwirot University; Prasarnmit Demonstration School (Secondary)
Japan	Akashikita Senior High School Chiba Prefectural Funabashi High School Ehime Prefectural Matsuyama Minami High School Fukushima Prefectural Fukushima High School Hyogo Prefectural KOBE High School Hyogo Prefectural Nagata High School Ichijô Senior High School Ikueinishi High School Institute of Science Tokyo High School Kagoshimachuo High School Kanagawa Prefectural Atsugi High School Matsushogakuen High School Miyagi Prefecture Sendai Daisan High School Nara Prefectural Seisho High School Risho Gakuen Osaka Ritsumeikan Junior & Senior High School Ritsumeikan High School Ritsumeikan Moriyama High School Ryugasakidaiichi Senior High School Saijo High School Seishingakuen High School Tennoji High School Attached To Osaka Kyoiku University Tokai University Takanawadai Senior High School Tokyo Gakugei University Senior High School Waseda University Honjo Senior High School Yokkaichi High School

Year Schedule

On May 9, we held the first learning session for Japanese students, introducing the project's objectives, significance, and annual schedule, along with guidance for international collaborative research. A week later, on May 15, we hosted an orientation for overseas teachers, explaining the project's purpose and key considerations. Schools then registered their available research fields—math, physics, chemistry, biology, earth science, and information science—and were matched into collaborative research groups.

The first plenary meeting between Japanese and overseas schools was held online on May 23. It included an overview of the project, exchange activities, schedule confirmation, and introductions of the research groups. At the second plenary meeting on May 30, Ritsumeikan High School led cultural exchange activities, such as school and language introductions, to help build rapport within groups. Native English-speaking staff from Ritsumeikan supported the first group meetings to facilitate initial research topic discussions.

From that point on, each group held regular meetings to advance their research. After each meeting, activity reports were submitted via Google Forms and automatically published on the project homepage to visualize each group's progress.

On July 11, we held a teachers' meeting for Japanese schools to share updates and confirm that all groups had finalized their research themes and summer plans. Ritsumeikan offered additional support to groups that needed it. After the summer break, on September 5, the second learning session for Japanese students was held. Students presented their research progress and plans, organized by subject, and received feedback from partner school teachers.

On September 12, overseas teachers gathered online to share updates. Then, on October 3, we held the third plenary meeting with both domestic and international schools. The session began with a lecture on data analysis titled "Analyzing Results" by Mr. Koichiro Hiromatsu of Ritsumeikan High School in Japan. Students then gave interim presentations in breakout rooms, with feedback provided by international graduate students from Ritsumeikan University.

The fourth plenary meeting took place on December 19, covering research report writing, final presentation preparation, and a mini-lecture on effective slide design. Groups then met in breakout rooms to plan for the International Collaborative Research Fair (ICRF).

The ICRF was held on January 24, 2025. After a keynote lecture, students gave presentations in four breakout sessions organized by research field. A post-activity questionnaire was conducted, followed by random breakout sessions for participants to reflect on the year's experience through informal discussions. Each group submitted an English-language report summarizing their research.

All project activities were conducted online. Ritsumeikan organized all sessions and meetings via Zoom. Slack was used for communication, with dedicated group channels. Activity reports were submitted using Google Forms, and content was automatically published to the project homepage using Google Sites and Google Apps Script.

Research Topics

Group	Research Topic
Group 1	Investigating GI and AMP Properties of Rice to Tackle Food Security Issues
Group 2	Water Quality Testing Using a Smartphone
Group 3	Antibacterial Effect of Different Soaps
Group 4	Changes in Vitamin C Content Over Time Based on Fruit Storage Methods
Group 5	Effects of Biodiversity on Plant Growth and Environment in Terrariums
Group 6	The Effect of Mass on the Magnetic Levitation and Stability in a Model Maglev Train
Group 7	The Role of Lactobacillus in Yakult in Enhancing Potato Growth
Group 8	Extraction of Anthocyanin from Blueberry (Vaccinium corymbosum) as a Sensitizer for Dye-Sensitized Solar Cells
Group 9	Differences in Antibacterial and Insect Repellent Properties Among Bitter Gourd (Momordica Charantia)
Group 10	Creation of Natural Yeast Bread Utilizing Regional Specialties and Antioxidant Capacity Titration
Group 11	How Touch Frequency Affects Leaf Closure in Mimosa Pudica
Group 12	Eco Friendly Paper
Group 13	Design, Fabrication, and Experimental Evaluation of Toroidal Propellers
Group 14	Comparative Study on the Biodiversity of Native Trees found in Japan and the Philippines
Group 15	Determining the Efficiency of Plant-Based Biocoagulants on Improving Water Quality
Group 16	Investigation of Water Hyacinth Root Exudates in Polystyrene Microplastic Adsorption
Group 17	How Might We Find a Sustainable and Environmentally Friendly Air Conditioning Method?
Group 18	Food Preference and Decoy Effect on Slime Mold
Group 19	Effects of Blade Design on Electricity Output in Waterwheel-Type Generator
Group 20	Light your life, More lightly - Design and Evaluation of Paper-Based Zinc-Air Batteries for Emergency Light
Group 21	Comparison of the Effectiveness of Fruits in Inhibiting Oral Bacteria
Group 22	The Efficacy of Extract from Thai and Japanese Piper nigrum L. to Inhibit Stachybotrys chartarum
Group 23	Make a Disinfectant from the Different Bactericidal Effects of Medicinal Herbs
Group 24	Making more Bio-nanofiber from Fruits Unique to Each Other's Countries.
Group 25	Innovative Bioplastic Materials from Food Industries Wastes for skin regeneration
Group 26	A Study on the Allelopathic Effects of Specific Plants
Group 27	A Study on the Degradation of PLA Using Cutinase from Tomato Peel-associated Fungi and the Chemical Factors Influencing the Reaction
Group 28	A Comparative Study of Bioplastic Production from Orange Peels in Thailand and Japan
Group 29	A Comparative Study of Soil Quality, Carbon Sequestration and Growth Patterns of Sakura (Cherry Blossom) in Japan and Sritrang (Blue Jacaranda) in Thailand
Group 30	The Difference of Microorganisms and Water Quality of Water Sources between Japan and Thailand.
Group 31	Microbial Decontamination and Structural Integrity of Recycled Polycaprolactone (PCL) Masks for Sterile Medical Casts

International Collaborative Research Fair

Date/Time	January 24th, 2036, 12:00～17:00 (JST)
Format	Online（Zoom）
Language	English
Scale	34 Research Topics　/ Approximately 250 participants 45 Schools（20 overseas schools、25 Japanese schools）
Schedule	12:00-12:10　Opening Ceremony Opening Address 12:10-12:50　Special Lecture Through the science lecture, participating students gained a deeper understanding of global-scale research activities and the importance of collaboration with researchers around the world. The lecture helped make these ideas more concrete and relatable. 13:00-15:30　Science Project Presentation Presentations were held in four breakout sessions. Each group gave a joint presentation using the slides they had prepared collaboratively. Each presentation lasted 10 minutes, followed by a 5-minute Q&A session. Teachers from participating schools acted as commentators and provided advice. 15:30-16:00　Feedback Session All participants completed a post-event questionnaire. Japanese students also completed an AAR survey 16:00-16:45　Group Discussion and Reflection Students from both domestic and overseas schools were randomly assigned to groups to reflect on their collaborative research experience and share advice for future participants. 16:30-17:00　Closing Ceremony Instructions were given regarding the submission of final reports, followed by closing remarks.

Research Reports

Using GI and AMP Properties of Rice as Proxies to Tackle Food Insecurity around the Globe

Sicheng He[1], Jarren Huang[1], Manuel Joseph[1], Wakana Ichikawa[2], Kana Iwamoto[2], Jun Tokutake[2]
[1] *Queensland Academy for Science, Mathematics and Technology (Australia)*
[2] *Kanagawa Prefectural Atsugi High School (Japan)*

Abstract

This study aims to identify rice varieties that are the most suitable to serve as a solution to food insecurity by examining and comparing the glycaemic index (GI) and antimicrobial activity of antimicrobial peptides (AMPs) derived from each rice variety, as they each shed light on different yet complementary aspects of the food security pillars set out by the FAO (Food and Agriculture Organization of the United Nations). To identify cross-country trends in rice performance between Australia and Japan, this study attempts to focus on rice varieties that are both commercially available and amongst the most commonly consumed in both countries. In both locations, Sushi Rice (Polished Koshihikari), Brown Rice, and Arborio Rice were analyzed. The results reveal systematic differences between rice varieties when discussing them in terms of the selected biological indicators, with brown rice consistently aligning most closely with the defined GI and AMP criteria.

Keywords: Food Insecurity; Glycaemic Index; Antimicrobial Peptides; Rice; Cross-locational Comparison

1. Introduction

For decades, food security has proven a pressing and ubiquitous issue with long-term implications. In 2025 alone, an estimated 2.3 billion people were blighted by food insecurity[1]. In response to this crisis, the FAO (Food and Agriculture Organization of the United Nations) created the four pillars of food security that consist of *availability*, *stability*, *access*, and *utilisation*[14]. Since rice is considered a dietary staple in more than 90 countries[2], its prominence and acceptability prove useful to tackle issues threatening the four pillars[3]. This investigation attempts to find the most suitable out of a selection of common rice varieties across locations in Australia and Japan as solutions to food insecurity, determined through two measurable biological traits, glycaemic index (GI), which reflects post-meal blood-glucose response and nutritional utilisation[4], and antimicrobial peptides (AMPs), which inhibit the growth of fungus in storage and influence post-harvest losses.

For the purpose of our research, AMP levels can be proxies to address the "supply side" of rice[5], which includes *availability* and *stability*, as consistently stronger antifungal activity implies a lower post-harvest loss[6] and stronger resilience to environmental variation[5], and thus a consistent yield. Complementarily, GI reflects both *access,* as one of the most common issues people face with rice involves its high GI linked to an increased risk of type 2 diabetes[7], and *utilisation,* since, by definition, GI is a proxy for the "ability to absorb and metabolize nutrients", reflecting the criterion laid out by the FAO[5]. Through a cross-national study using several varieties of rice, this investigation aims to quantify effects derived from the rice's characteristics and location on GI and AMP antifungal activity in order to identify resilient, health-aligned rice options for food security.

2. Glycaemic Index

2.1 Methodology

This experiment involves simulating the oral and intestinal phases of the digestion of rice, and then measuring the amount of glucose extracted over time, providing an estimation of the glycaemic index.

2.1a) Glucometer Calibration: The glucometer was first calibrated using glucose standards of 0 to 200mg/dL D-glucose solution with intervals of 50mg/dL. Each standard was measured using the same glucometer and strips used for experimental samples (≥3 replicates per concentration). With such data, a linear calibration trend representing glucometer reading against glucose concentration[8] can be created, and used to convert raw glucometer readings for digestion samples to actual glucose concentrations.

2.1b) In vitro Digestion: For **sample preparation,** portions of rice were washed and cooked with a ratio of 1:1(mass) to water, before being divided into 50.0g samples and homogenised manually in a ceramic mortar. Each sample was then placed into a conical flask, situated in a 37.0 °C water bath[9, 15], and closely monitored. Next, 120.0mL of distilled water was pre-adjusted to a neutral pH[10] of 7.0 ± 0.05 using 1 M sodium hydroxide (NaOH) or 1 M hydrochloric acid (HCl) solutions, and added to each flask. In the **simulated oral phase**, 30 mL of 3.4% (w/v) α-amylase (source: Aspergillus oryzae) was added to each flask and monitored for 30 minutes with occasional stirring. Subsequently, at the 30-minute mark, a 25.0mL aliquot of the rice solution was extracted using a pipette and set aside for analysis. Immediately after, for the **simulated intestinal digestion phase**, 15 mL of 1% (w/v) pancreatin (source: porcine pancreas) was added to the flask and thoroughly mixed[11]. Finally, a further 25.0mL aliquots were taken at the 50, 70, and 90-minute mark for analysis[16].

2.1c) Aliquot analysis: The 25.0mL aliquots were first cooled to room temperature and diluted to 100.0mL using distilled water. Using a pre-calibrated glucometer (section 2.1a), a test strip was placed into each solution, and the glucose concentration (mmol/L) was measured.

2.1d) Data processing: For each rice sample, glucose concentration was plotted against time. The area under the curve (AUC_{Sample}) was calculated using a regression via Desmos Graphing Calculator by $y = M(1 - e^{-kx})$, where y is glucose concentration and x is time[12] (Figure 1). If a function is regressed and labelled $f(x)$, the AUC is calculated using:

$$AUC = \int_0^{90} f(x)\,dx$$

The data collected using a reference food under the same procedures above (White Bread was our choice) was regressed, and the Area Under the Curve was also calculated, the value denoted as $AUC_{Reference}$. The hydrolysis index (HI) for each rice sample was calculated[12] as $HI = \frac{AUC_{Sample}}{AUC_{Reference}} \times 100$. The estimated GI can be calculated using the equation[12] $GI = 39.71 + 0.549 \times HI$. The values are recorded for each sample.

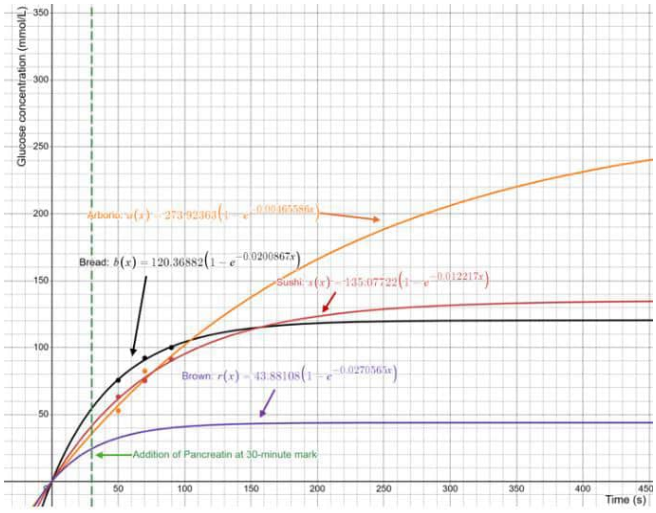

Figure 1. Sample graph for GI calculations

2.2a - Australian Processed Results

Table 1. ***Calculated Average Glycaemic Index for Each Variety (Australia)***

Rice Type	Area Under Curve (4s.f.) / $mmol \cdot L^{-1} \cdot s$				Average A.U.C.	Hydrolysis Index (relative to white bread)	glycaemic Index
	Trial 1	Trial 2	Trial 3	Trial 4			
Arborio Rice	4647	4513	4969	4399	4628	0.795	83.33
Sushi Rice	4627	4783	4493	4806	4677	0.803	83.8
Brown Rice	2470	2421	2353	2640	2471	0.424	62.47
White Bread	5824						

2.2j - Japanese Processed Results

Table 2. ***Calculated Average Glycaemic Index for Each Variety (Japan)***

Rice Type	Area Under Curve (4s.f.) / $mmol \cdot L^{-1} \cdot s$				Average A.U.C.	Hydrolysis Index (relative to white bread)	glycaemic Index
	Trial 1	Trial 2	Trial 3	Trial 4			
Carnaroli Rice	2622	2800	2544	2927	2723	0.467	64.74
Sushi Rice	2063	2490	2238	2400	2298	0.394	61.05
Brown Rice	2458	2277	2539	3178	2613	0.504	66.66
White Bread	5824						

3. Antimicrobial Peptides

3.1 AMP Methodology

This experiment involves extracting antimicrobial peptides (AMPs) from three varieties of rice, and then determining the effectiveness of each AMP against Penicillium Chrysogenum on an agar medium by measuring the radius of the zone of inhibition.

3.1a) Sample preparation: 80g of uncooked rice was ground into fine particles using a blender. Each of the powdered samples was added to 400 mL of 0.2% sodium hydroxide solution and stirred for 30 minutes. Once stirred, they were centrifuged at 3,000×g for 10 min to remove any undissolved residue from the samples. Then, 6 mol/L hydrochloric acid dropwise was added to the samples to neutralize the solution to pH 5.0 (the isoelectric point of rice proteins), after which all three neutralized solutions were centrifuged at 3,000 ×g again, and the precipitate was collected.

3.1b) Extraction of AMP: 200 mL of distilled water was added to the dried precipitate, and the environment was adjusted to the optimal pH (2.0) for enzyme activity using hydrochloric acid solution. Next, pepsin (0.1%, 2 mL) was added and incubated for 2 hours at 37℃. Pepsin was inactivated by adjusting to pH 7.0 ±0.1 with 0.2% sodium hydroxide solution.

3.1c) Evaluation of Antimicrobial Activity: Penicillium Chrysogenum was smeared on PDA (Potato Dextrose Agar) medium. Paper discs were soaked in the liquids and placed individually on every nine mediums prepared in advance, as explained below. To assess antimicrobial peptide activity, the nine heat-sterilized media are divided into four equal sections with a marker. Labelled the sections as water (control), Arborio rice, Koshihikari (Sushi) rice, and brown rice. Place each culture medium in a 25°C incubator and observe the inhibition zone area. If zones of inhibition are identified in the water (control) section, the specific batch should be discarded.

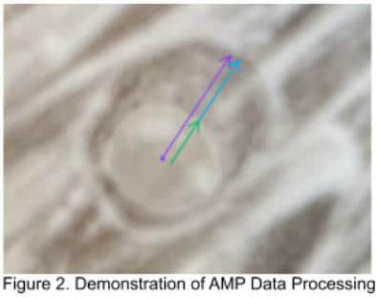

Figure 2. Demonstration of AMP Data Processing

3.1d) Data processing: A photo of each agar plate was taken with a ruler for scaling (Figure 2, right). Next, using a digital ruler scaled with the ruler in the photo, the longest line (purple) from the center of the disk to the outer edge of the zone of inhibition was drawn, and the length of such a line was measured and recorded. To exclude the impact of the disk itself on fungal growth, the radius of the disk (green) was then subtracted, leaving the distance reflecting the inhibition zone of solely the AMP mixture (blue).

3.2a - Australian Processed Results

Table 3. ***Effect of AMP extracted from different types of rice (Australia)***

Rice type	Average of processed radius of inhibition zone / *cm*				Total Average across all trials
	Trial 1 (11/17/25)	Trial 2 (12/02/25)	Trial 3 (12/03/25)	Trial 4 (12/04/25)	
Arborio Rice	0.396	0.225	N/T	0.258	0.293
Sushi Rice	0.457	0.121	N/T	0.379	0.325
Brown Rice	0.367	0.325	0.429	N/T	0.374

3.2j - Japanese Processed Results

Table 4. ***Effect of AMP extracted from different types of rice (Japan)***

Rice type	Average of processed radius of inhibition zone / *cm*				Total Average across all trials
	Trial 1 (12/19/25)	Trial 2 (12/19/25)	Trial 3 (12/19/25)	Trial 4 (12/19/25)	
Arborio Rice	0.01	0.01	0.02	N/A	0.007
Sushi Rice	0.01	0.147	0.4	N/A	0.139
Brown Rice	0.01	0.22	0.2	N/A	0.107

Note: “N/T” labelled in processed results tables means “not tested”
“N/A” indicates “batches discarded due to contamination”

4. Discussion

4.1 GI Analysis of Variance

Table 5. ***ANOVA Results for the GI Experimental Data***

Source of variation	*Sum of squares*	*Degrees of freedom*	*Mean Squares*	*F-value*	*P-value*	*Critical F-value*
Between locations	864.287439	1	864.287439	203.759405	2.94626×10^{-11}	4.41387342
Between varieties	378.421838	2	189.210919	44.6072713	1.05967×10^{-7}	3.55455715
Interaction between location and variety	827.863083	2	413.931541	97.5861047	2.18211×10^{-10}	3.55455715
Within treatments	76.3507035	18	4.24170575			

To summarise, the purpose of the investigation was to determine the best rice variety to tackle the access and utilisation pillars of food security. Three varieties were considered and tested in two locations – Australia and Japan. In the two rows indicating variation between locations and between varieties, the *F-values* are significantly higher than their corresponding critical values, indicating that the variation between each factor is much larger than the variation within. This, accompanied by the low *p-value* indicating an extremely low likelihood of the variation being attributed to randomness, indicates that there is a significant effect of location and variety on the GI of rice grown. In the row representing interaction, the *F-value* being much larger than the critical value, along with the low *p-value*, suggests that the effect of location differs depending on the rice variety. Overall, in all three cases, the null hypothesis is rejected, and the alternative hypothesis is adopted due to ANOVA indicators suggesting a statistically meaningful variation between treatments. Moreover, the test implies that the means of treatments can be used in analysis as a representation of the treatment as a whole.

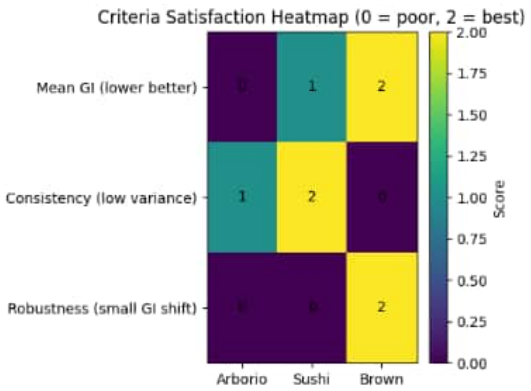

Figure 3. Heat Map for GI Criteria

To determine the best rice variety for food insecurity, three criteria were developed: magnitude, consistency, and robustness. Arborio rice had the worst average GI from a health standpoint, with 74.38, followed by sushi rice at 72.59. This suggests that, for the purpose of our research, brown rice has the best nutritional profile, with a GI of 65.21. Sushi rice was the most consistent within each location, with an average variance of 2.52, followed by arborio rice and brown rice, with average variances of 4.03 and 6.18, respectively. Finally, in terms of robustness, both arborio and sushi rice exhibit a large GI shift of approximately 20 between Australia and Japan, while brown rice only differs by 4.4 between locations. Statistically, this difference can also be considered insignificant as it is below Tukey's HSD at 4.62. Overall, in terms of glycaemic index, brown rice offers the best solution for tackling food security due to its healthy nutritional profile consistent across two locations.

4.2 AMP Analysis of Variance

Table 6. ***ANOVA results for the AMP experimental data***

Source of variation	*Sum of squares*	*Degrees of freedom*	*Mean Squares*	*F-value*	*P-value*	*Critical F-value*
Between locations	0.10733889	1	0.10733889	8.54231143	0.01277552	4.74722535
Between varieties	0.01322433	2	0.00661217	0.52621364	0.6038649	3.88529383
Interaction between location and variety	0.00711811	2	0.00355906	0.28323901	0.75823883	3.88529383
Within treatments	0.15078667	12	0.01256556			

When the three criteria used in the GI analysis are applied to AMP as well, the first criterion, adequacy, shows that the mean inhibition zone radii followed the order of "brown rice (0.274) ≈ sushi rice (0.267) > arborio (0.213)." However, because these values did not exhibit statistically significant differences in the ANOVA, it can only be stated that brown rice and sushi rice showed slightly higher numerical tendencies. For the second criterion, consistency, sushi rice displayed considerable variability in its values, whereas Arborio and brown rice showed more stable measurements, with brown rice in particular exhibiting low variance ($s^2 = 0.0027$ in Japan and $s^2 = 0.0041$ in Australia). Regarding the third criterion, robustness, the interaction effect was not significant ($F=0.28<F\text{-}crit=3.89$, $p=0.758$), indicating that no specific variety experienced an environment-dependent performance decline and that no variety can be considered vulnerable. In summary, although a significant main effect of= location was observed for antifungal activity ($p=0.0128$), neither the variety effect nor the Location×Variety interaction was significant. This suggests that while AMP activity differs overall between countries, the differences among varieties are small relative to within-experiment variability, and the varieties remain stable across environments. Therefore, in this study, variety evaluation cannot be based on mean statistical superiority but on numerical tendencies and within-group consistency. Overall, brown rice demonstrated the most favorable balance between the magnitude of inhibitory effect and reproducibility.

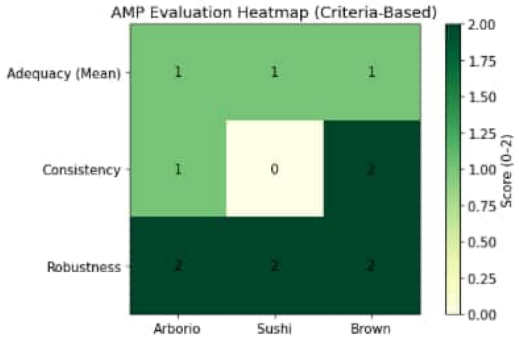

Figure 4. Heat Map for AMP Criteria

4.3 Final Evaluation

This investigation aimed to determine the best rice as a solution to issues threatening the four pillars of food security. According to data collected representing both GI and AMP properties, brown rice displays the best and most consistent overall biological profile to meet the demands of production, storage, and consumption. The substantial performance of brown rice compared to others in the 'consistency' criterion, alongside numerically and marginally favourable 'adequacy' criterion values in the AMP experiment, indicates a higher level of crop resilience and thus promising *availability* for consumers. Moreover, its robustness across locations in both experiments demonstrates consistency in both crop resilience and nutrition, therefore meeting the criteria for *stability*. Further, the notably low GI of brown rice improves accessibility for consumers with type 2 diabetes, indicating sufficient *access*, and also supports *utilisation* due to low GI supporting claims of a healthy nutritional profile. Overall, brown rice offers the most effective solution to tackle food insecurity out of the options considered.

5. Limitations

5.1 GI Limitations

Within the procedure for measuring the GI index of the chosen rice, several limitations have been presented, such as the official cooking instructions on the packaging being discarded in favour of maintaining the same ratio of rice to water mass; thus, it may not be an accurate representation of the real cooking process. Furthermore, the time that the rice was cooked for was not timed and recorded, thus leading to the possibility of a higher GI index measured if the rice was left to cook for longer[13]. Additionally, the method is not fully in alignment with the INFOGEST protocol; it is a hybrid and modified in-vitro starch hydrolysis method as a result of highschool lab restrictions and an incomparable data type of final results in order to calculate GI. For example, we did not perform a gastric phase, add bile salts in the intestinal phase, nor did we measure using an enzymatic assay like GODOP or Dinitro Salicylic Acid (DNS method), as they would not yield distinct quantitative results for us to model and regress. This implies that our methodology provides a simplified, estimating model of hydrolysis, and cannot claim to be a replica of the complex physiological conditions of the entire human digestive process. A larger-scale limitation of the method lies in its attempt to quantify an inherently in-vivo physiological response. While in-vitro analysis can measure rates of carbohydrate digestion, they fail to capture key in-vivo factors such as gastric emptying, hormonal regulation, insulin response, and inter-individual metabolic variation. As such, a reliance on in-vitro measurements introduces systematic bias and reduces the ecological validity of GI values.

5.2 AMP Limitations

There are several limitations to the AMP methodology and assessment of results. First, although some studies have shown rice AMPs work against *Cutibacterium acnes*, a bacterial species, our experiment used *Penicillium chrysogenum*, a filamentous fungus with distinct cellular structures; hence, results may not correspond directly. Secondly, the methodology was time-consuming, thus each school had to skip or shorten certain steps to save time; this possibly made our results unreliable in the end. As for the process itself, the AMP assay used a crude peptide mixture (alkaline solubilisation followed by pepsin digestion) rather than purified AMPs, limiting molecular specificity,

meaning that we could not isolate the effect of a specific rice AMP. Additionally, antifungal activity was tested against only *Penicillium chrysogenum*, reducing ecological generalisability. In terms of results, inhibition zones from disc diffusion are only semi-quantitative, so AMP results represent relative trends that complement GI as a proxy for rice suitability in food-security assessment.

5.3 Limitations of Overall Assumptions

On a broader scale, our overall framework of GI and AMP as targeted proxy indicators for food security can only represent so much that it may not encompass or fully represent other aspects within the pillars, such as economic access or cultural acceptability. Although our focus on rice moderately compensates for this limitation as it is one of the most widely cultivated and consumed staple crops globally[2] and spans a broad price range, there need be such variables to quantify said factors. The combination of GI and AMP is an explicit methodological choice about focusing on health-related attributes, as our team deems it the most practical and relevant focus regarding food insecurity. Moreover, our restricted experimental scope (three varieties, two countries, one cooking method) bounds our conclusions and interpreted patterns within a specific domain; hence, a natural extension would be to consider more measurable variables, such as yield or price per kilojoule, and quantify the weighting of each variable based on stakeholder consultation or multi-criteria decision analysis.

6. Conclusion

To conclude the research, our aim was to determine which variety of rice and the growth, storage, and consumption environment are more applicable to Food Security. Considering the discussions on both GI and AMP, while the figures between the two countries were consistent in some parts and varied in others, brown rice best aligns with our selected proxy indicators and is more effective than the other two types. Looking ahead, to address the limitations mentioned above, there is room for methodological improvement. Specifically, using equipment with similar performance in each school, using the same microorganisms in AMP evaluations as in previous studies, and considering a wider and broader experimental scope, which includes using more diverse rice selections, testing against a wider selection of bacteria and fungi, and having criteria that better represent '*access*', not just based on storage and consumption. All these changes would allow our results to be more ecologically and methodologically generalisable, better for tackling a pressing issue that happens on a global scale. Finally, while this study prioritized variety, future research should investigate the impact of growth location, exploring how different environmental and geographical conditions influence these food security parameters.

7. References

[1]The World Bank. (2025). *Food Security Update*. The World Bank Group. https://thedocs.worldbank.org/en/doc/40ebbf38f5a6b68bfc11e5273e1405d4-0090012022/related/Food-Security-Update-118-September-19-2025.pdf

[2]Food and Agriculture Organization of the United Nations (FAO). (2023). *FAOSTAT: Crops and livestock products*. Food and Agriculture Organization of the United Nations. https://www.fao.org/faostat/en/#data/QCL. Parameters: All Countries, Area Harvested, Rice, 2023

[3]Fukagawa, N. K., & Ziska, L. H. (2019). Rice: Importance for Global Nutrition. *Journal of Nutritional Science and Vitaminology*, *65*(Supplement), S2–S3. https://doi.org/10.3177/jnsv.65.S2

[4]Food and Agriculture Organisation of the United Nations. (1997). *Carbohydrates in human nutrition report of a joint FAO WHO expert consultation, Rome, 14 - 18 April 1997* (p. Chapter 4). Rome FAO.

[5]Food Security Cluster Handbook. (2023, December 15). *The Four Pillars of Food Security*. Handbook.fscluster.org. https://handbook.fscluster.org/docs/231-the-four-pillars-of-food-security

[6]Baindara, P., & Mandal, S. M. (2022). Plant-Derived Antimicrobial Peptides: Novel Preservatives for the Food Industry. *Foods*, *11*(16), 2415. https://doi.org/10.3390/foods11162415

[7]Harvard School of Public Health. (2012, March 2). *Eating white rice regularly may raise type 2 diabetes risk | Harvard T.H. Chan School of Public Health*. Harvard T.H. Chan School of Public Health; HSPH. https://hsph.harvard.edu/news/eating-white-rice-regularly-may-raise-type-2-diabetes-risk/

[8]Harvey, D. (2019, January 18). *5.4: Linear Regression and Calibration Curves*. Chemistry LibreTexts. https://chem.libretexts.org/Bookshelves/Analytical_Chemistry/Analytical_Chemistry_2.1_(Harvey)/05%3A_Standardizing_Analytical_Methods/5.04%3A_Linear_Regression_and_Calibration_Curves

[9]Fernandes, Jean-M., Madalena, D. A., Pinheiro, A. C., & Vicente, A. A. (2020). Rice in vitro digestion: application of INFOGEST harmonized protocol for glycemic index determination and starch morphological study. *Journal of Food Science and Technology*, *57*(4), 1393–1404. https://doi.org/10.1007/s13197-019-04174-x

[10]Akinfemiwa, O., Muniraj, T., & Zubair, M. (2023, November 12). *Amylase*. PubMed; StatPearls Publishing. https://www.ncbi.nlm.nih.gov/books/NBK557738/

[11]Johnson, M. P., & Hillier, K. (2007). Pancreatin. *Elsevier EBooks*, 1–3. https://doi.org/10.1016/b978-008055232-3.62359-1

[12]Goñi, I., Garcia-Alonso, A., & Saura-Calixto, F. (1997). A starch hydrolysis procedure to estimate glycemic index. *Nutrition Research*, *17*(3), 427–437. https://doi.org/10.1016/s0271-5317(97)00010-9

[13]Vîrlan, A., Coșciug, L., Dinu Țurcanu, & Rodica Siminiuc. (2024). The Influence of Rice Types and Boiling Time on Glycemic Index: An In Vivo Evaluation Using the ISO 2010 Method. *Foods*, *14*(1), 12–12. https://doi.org/10.3390/foods14010012

[14]Food and Agriculture Organization of the United Nations: (2009). World Summit on Food Security: DECLARATION OF THE WORLD SUMMIT ON FOOD SECURITY . In *fao.org* (p.1). Food and Agriculture Organisation. https://www.fao.org/fileadmin/templates/wsfs/Summit/Docs/Final_Declaration/WSFS09_Declaration.pdf. Indicates the four pillars of food security.

[15]Brodkorb, A., Egger, L., Alminger, M., Alvito, P., Assunção, R., Ballance, S., Bohn, T., Bourlieu-Lacanal, C., Boutrou, R., Carrière, F., Clemente, A., Corredig, M., Dupont, D., Dufour, C., Edwards, C., Golding, M., Karakaya, S., Kirkhus, B., Le Feunteun, S., & Lesmes, U. (2019). INFOGEST static in vitro simulation of gastrointestinal food digestion. *Nature Protocols (INFOGEST)*, *14*(4), 991–1014. https://doi.org/10.1038/s41596-018-0119-1

[16]Rojas-Bonzi, P., Vangsøe, C. T., Nielsen, K. L., Lærke, H. N., Hedemann, M. S., & Knudsen, K. E. B. (2020). The Relationship between In Vitro and In Vivo Starch Digestion Kinetics of Breads Varying in Dietary Fibre. *Foods*, *9*(9), 1337. https://doi.org/10.3390/foods9091337

Water Quality Testing Using a Smartphone

Leehong Kim[1], Oukchhuon Molika[1], Sek Satya[1], Narumi Ikusue[2], Yui Furudate[2]
[1] *New Generation School Preah Sisowath High School (Cambodia)*
[2] *Institute of Science Tokyo High School (Japan)*

Abstract:
Simple and accessible methods for water quality assessment are increasingly required in both environmental monitoring and educational contexts. In this study, we investigated a colorimetric approach for water quality evaluation using RGB values obtained from ultraviolet–visible (UV-vis) spectrophotometric measurements and photographic images, with a particular focus on chemical oxygen demand (COD) and pH indicators. First, calibration curves were constructed using potassium permanganate solutions by analyzing both absorbance values obtained from UV–vis spectrophotometry and RGB values derived from measured spectra and photographs. RGB values were calculated by converting XYZ values using a self-developed program, and the corresponding colors were visually compared with actual solutions. To ensure consistency, measurements were conducted under a controlled environment to minimize the influence of ambient light. In addition, aqueous KMnO4 solutions after COD analysis were measured both before and after filtration to evaluate their effects on concentration determination. Furthermore, a solid pH indication film was fabricated by dropwise addition of a liquid universal indicator into wood glue, and its pH response was examined by immersing the film in strongly acidic and basic solutions.

As a result, absorbance-based UV–vis measurements provided higher precision and accuracy in determining potassium permanganate concentrations than RGB-based methods. Nevertheless, among the RGB components, a clear linear correlation with concentration was observed, demonstrating the feasibility of RGB-based quantitative evaluation. Pre-filtration samples exhibited higher measured concentrations and improved linearity compared with post-filtration samples, indicating the influence of suspended components on optical measurements. The pH indication film showed distinct color changes in the presence of strong acids and bases, confirming its fundamental pH responsiveness under extreme conditions.

In conclusion, this study demonstrated the potential of RGB-based analysis as a simplified water quality assessment method and confirmed the basic functionality of a solid pH indication film. Future developments, such as simple evaluation packages and smartphone applications capable of automatically extracting RGB values from images, may enable convenient and accessible water quality assessment for both practical and educational use.

Keywords: water quality measurement; smartphone; image analysis; color reaction

1. Introduction

Water is an essential natural resource for sustaining life, and it forms the foundation of healthy ecosystems and socioeconomic systems. With the expansion of industrialization, urbanization, and agricultural pressures, aquatic environments have increased, and the deterioration of water quality in rivers, lakes, and groundwater has become a serious global issue. Therefore, accurate and reliable measurement and assessment of water quality are critically important for sustainable water resource management.

Water quality assessment aims to provide a comprehensive evaluation based on physical and chemical parameters (e.g., pH, dissolved oxygen, and turbidity) as well as biological indicators, and standardized methodologies for such measurements have been developed over many years [(1)]. In recent years, advances in information technologies, including the Internet of Things (IoT), wireless sensor networks, and machine learning, have led to the development of new approaches that enhance the real-time capability and spatial resolution of water quality monitoring. However, precise water quality analysis generally requires expensive analytical instruments, such as UV–vis spectrophotometers. Although simple test kits based on colorimetric methods are commercially available, their reliance on visual color judgment limits their universal applicability.

As of 2023, smartphones have achieved a global penetration rate of 57% and are devices owned by most adults in many countries. Their camera capabilities have continued to improve year by year. Furthermore, smartphone applications enable simple image analysis. Application development allows

a wide range of additional functionalities to be implemented.

In this study, water quality indicators such as chemical oxygen demand (COD) were measured using colorimetric methods. By utilizing the camera and image analysis capabilities of smartphones, this study aims to establish a simple yet highly accurate analysis and evaluation method as an alternative to conventional UV–vis-based chemical analysis.

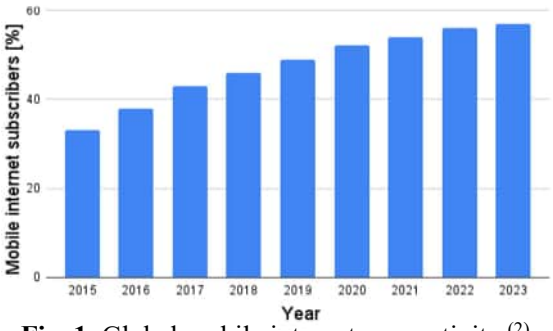

Fig. 1. Global mobile internet connectivity [2]

2.Methodology

2.1 Preparation of calibration curves for aqueous potassium permanganate ($KMnO_4$) solutions

After preparing a 10 mM aqueous $KMnO_4$ solution, its concentration was determined by redox titration using sodium oxalate ($Na_2C_2O_4$). Subsequently, a series of sample solutions were prepared by diluting the $KMnO_4$ solution of known concentration to 0, 0.125, 0.152, 0.25, 0.33, 0.40, and 0.50 mM.

The absorbance at 525 nm and the XYZ color values of each prepared solution were measured using UV-vis spectroscopy. Finally, calibration curves were constructed by plotting the absorbance against the $KMnO_4$ concentration, and by using RGB values converted from the measured XYZ values.

2.2 Preparation of calibration curves for $KMnO_4$ solutions after COD analysis [4]

Phthalic acid ($C_8H_6O_4$), lactose ($C_{12}H_{22}O_{11}$), and $Na_2C_2O_4$ were used as model water pollutants and reacted with aqueous $KMnO_4$ solutions. For $C_8H_6O_4$, the reactants were adjusted so that the residual $KMnO_4$ levels reached -27.5 and 25% of the initial dosage. For lactose, the amounts were adjusted to achieve residual levels of -20%, 0, and 20%. For $Na_2C_2O_4$, the reactions followed were conducted according to the JIS manganese method for COD determination by adding $KMnO_4$, silver nitrate ($AgNO_3$), and sulfuric acid (H_2SO_4) to yield residual levels of 80%, 60%, 20%, 0%, and -20%. For the $Na_2C_2O_4$ samples, both pre-filtered and post-filtered solutions after COD analysis were measured for absorbance at 525 nm and XYZ color values using a UV-vis spectrophotometer. Finally, calibration curves were established by plotting absorbance and converted RGB values against the concentration of the aqueous $KMnO_4$ solution.

To utilize XYZ values within the RGB color space, a matrix transformation is first applied to convert XYZ to RGB. The resulting RGB values are then uniformly scaled such that the maximum among the R, G, and B components does not exceed 255 [3].

2.3 Preparation of a universal pH indicator

A reagents mixture consisting of 120 mg of thymol blue, 150 mg of methyl red, 180 mg of bromothymol blue, and 180 mg of phenolphthalein was prepared in 150 mL of 80 vol% ethanol. The solution was diluted twofold with the ethanol of the same concentration and neutralized to pH 7.0 using 0.01 M sodium hydroxide (NaOH) (Fig. 2).

Fig. 2. Universal pH indicator

2.4 Preparation of a calibration curve between the RGB values and pH values

Sodium acetate and acetic acid were mixed to prepare buffer solutions with pH values of 5.0, 6.0, 7.0, 8.0, and 9.0 using a pH meter. 1 mL of the indicator was added to 10 mL of each pH buffer solution and the mixture was diluted to 100 mL.

As described in Section 2.1, absorption spectra and XYZ values were measured. Calibration curves were then constructed using the resulting pH values and RGB values converted from XYZ values.

2.5 Preparation of pH indication film

A liquid universal indicator, wood glue and white acrylic paint were mixed and poured into a 2cm×5cm mold, followed by nature dried (Fig. 3). The color changes of the resulting film were compared after immersion in the pH buffer solutions.

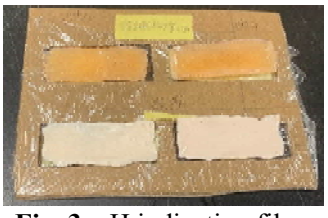

Fig. 3. pH indication films drying in a mold film

2.6 RGB measurement setup, image analysis and calibration using a smartphone

To eliminate interference from ambient light during RGB measurements, a darkroom environment was constructed using a polystyrene foam box. A smartphone (iPhone 13) camera was positioned at a small aperture on the side of the box. An LED bulb was used as the light source, and a white acrylic board was placed between the light source and the sample as a reflective diffuser to provide uniform, diffusely reflected illumination (Fig. 4).

For measurements, liquid samples were placed in front of the white acrylic board, and photographs were taken using the smartphone. The captured images were analyzed using Digital Color Meter; for each solution, RGB values were measured at five points, and the average value was used as the representative RGB value.

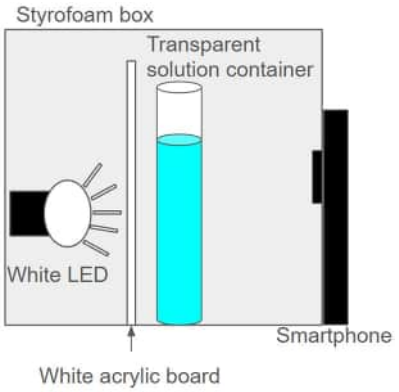

Fig. 4. Imaging setup using a smartphone

Using this imaging setup, calibration curves were constructed based on the RGB values obtained from the photographs. These calibration curves were compared with those obtained using spectrophotometric measurements, as described in Section 2.4.

3. Results and Discussion

3.1 Calibration curve for aqueous $KMnO_4$ solutions

The calibration curve relating the concentration of the $KMnO_4$ solution to absorbance exhibited excellent agreement, with a coefficient of determination (R) of 0.998 (Fig. 5).

In contrast, calibration curves based on RGB values obtained from UV-vis measurements showed correlations with concentration, with correlation coefficients (R) of 0.689 for the red value, 0.821 for the green value, and 0.747 for the blue value; however, the linearity, as indicated by the coefficients of determination (R), was low, and the plots of each RGB component appeared to follow gently curved trends resembling shallow quadratic relationships (Fig. 6). These results suggest that, within the concentration range investigated in this study, single-wavelength absorbance measurements using UV-vis spectroscopy provide a more reliable quantitative relationship with concentration than measurements based on RGB values.

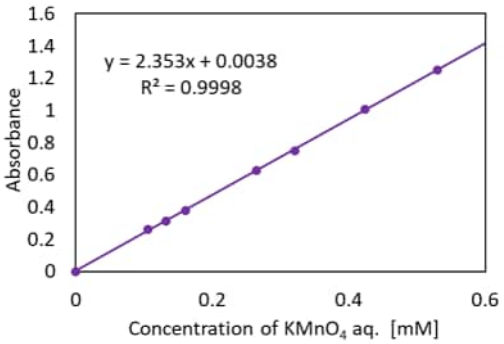

Fig. 5 Calibration curve for absorbance versus concentration of $KMnO_4$ aq.

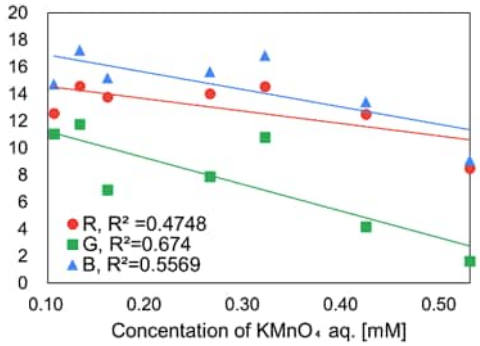

Fig. 6 Calibration curve for RGB values versus concentration of $KMnO_4$ aq.

3.2 Preparation of calibration cures for $KMnO_4$ solutions after COD analysis

For phthalic acid, the reactions were conducted under conditions in which the theoretical residual amounts of $KMnO_4$ were -27.5% and 25% relative to the initial dosage. Accordingly, the former concentration was expected to result in a colorless solution, whereas the latter was expected to yield. However, in practice, both samples exhibited a similar intensity of purple coloration (Fig.7). Similarly, for lactose, although the reactions were performed at theoretical residual levels of -20%, 0%, and 20%, all samples showed comparable purple coloration. These results indicate that phthalic acid and lactose did not react with $KMnO_4$ as predicted by corresponding stoichiometric equations.

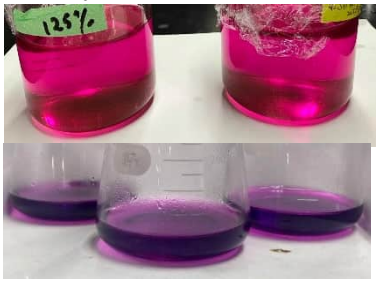

Fig. 7 $KMnO_4$ aq with added reagents (Up: phthalic acid (25% and -27.5%), Down: lactose (25%, -27.5%, 20%)

For the COD-analyzed solution before filtration, the coefficient of determination between $KMnO_4$ concentration and absorbance was 0.924 (Fig. 8). In contrast, the coefficients of determination for the RGB values were lower, being 0.674 for the red value, 0.585 for the green value, and 0.173 for the blue value (Fig. 9 Left). For the filtered solution, the coefficient of determination for absorbance decreased to 0.802 (Fig.7), while those for the RGB values were 0.788 for the green value, 0.347 for the blue value, and 0.017 for the red value (Fig. 9 Right). Under all experimental conditions, the correlations based on RGB values were weak, and higher linearity was obtained for the solution before filtration.

From these results, it is concluded that the most accurate approach is to use the COD-analyzed solution prior to filtration and to quantify $KMnO_4$ concentration based on absorbance measurements.

The reduced linearity observed after COD analysis is likely attributable to manganese ions generated during the COD analytical process, which subsequently formed suspended species that interfered with the absorbance measurements. In contrast, no significant influence on absorbance at 525 nm was observed from the other reagents used in the analysis, namely aqueous $AgNO_3$ and H_2SO_4 solutions.

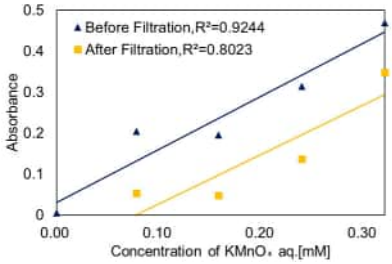

Fig. 8 Calibration curve for absorbance versus concentration of $KMnO_4$ aq. before and after filtration

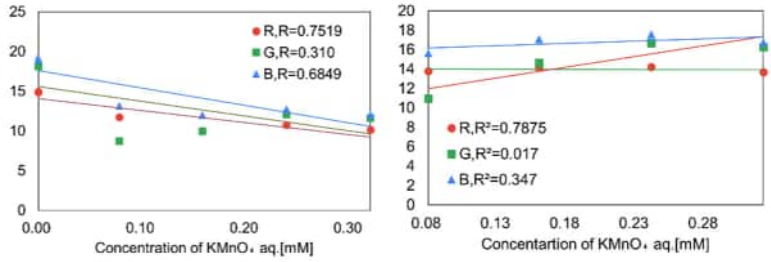

Fig. 9 Calibration curves of RGB values versus concentration of $KMnO_4$ (Left: before filtration, Right: after filtration)

3.3 Calibration curves of pH and RGB values

For the calibration curves constructed using RGB values obtained from UV-vis measurements (Fig. 10 Up), the correlation coefficients (R) were -0.830 for the red value, 0.917 for the green value, and 0.883 for the blue value. Although the green value exhibited the strongest correlation with changes in pH, it is unlikely that the linearity is as high as suggested by the correlation coefficient value.

When RGB values extracted from photographs (Fig. 10 Down) were used, the correlation coefficient was -0.872 for the red value, 0.330 for the green value, and 0.992 for the blue value. Comparison of these calibration curves shows that the correlation coefficients for the red value were similar between the two methods, whereas a substantial difference was observed for the green value. In addition, the blue value exhibited a much higher correlation coefficient when photograph-derived RGB values were used.

Furthermore, the absolute RGB values differed between the two measurement methods. For example, at pH 7.0, the blue values were 137 for the UV-vis-based measurement and 91 for the photograph-based measurement. Therefore, RGB values obtained from photographs cannot be directly applied to calibration curves constructed using RGB values derived from UV-vis measurements.

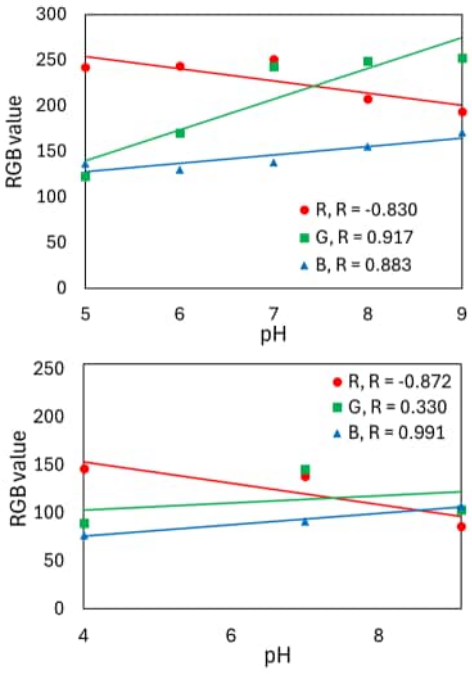

Fig. 10. Calibration curves relating RGB values versus pH
(Up: UV-vis, Down: Photographs)

3.4 pH indication film

The films prepared with one or two drops of liquid universal indicator, with or without white paint, did not exhibit a clear response when immersed in buffer solutions with pH values ranging from 4.0 to 9.0. Therefore, to confirm the pH responsiveness, the prepared film was immersed in higher concentration solutions of hydrochloric acid (HCl), H_2SO_4 and potassium hydroxide (KOH).

Fig. 11. The color changes in strong solutions

As a result, visible changes in the films were observed under these conditions (Fig. 10).

4. Conclusion

4.1 Considerations for COD measurement accuracy

In UV-Vis spectrophotometric analysis, the concentration of potassium permanganate was determined with higher precision and accuracy using absorbance measurements than using GB values.

With respect to the relationship between concentration and RGB values obtained from photographs, the red value showed a relatively strong correlation with concentration among the RGB components.

Furthermore, for aqueous $KMnO_4$ solutions after COD analysis, calibration curves constructed using solutions before filtration exhibited higher linearity and reliability than those obtained using filtered solutions.

4.2 RGB values obtained from solutions or photographs

In this study, a UV-vis spectrophotometer was used to obtain XYZ values via its dedicated software. A program was developed to convert the XYZ values of reference samples into RGB values. The colors corresponding to the converted RGB values were displayed on the screen and visually compared with the actual solution, resulting in a reasonable level of agreement (Fig. 12).

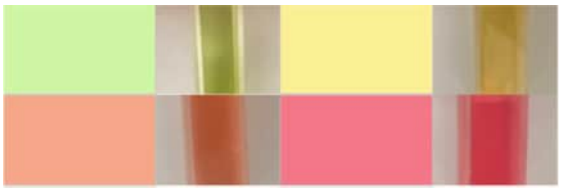

Fig. 12. Comparison of colors derived from RGB values converted from XYZ measurements

When RGB values obtained from photographs were used, R^2 values were 0.954 for the red value 0.147 for the green value, and 0.828 for the blue value (Fig.14). High linearity was observed for the red value whereas the green value and the blue value showed lower R^2.

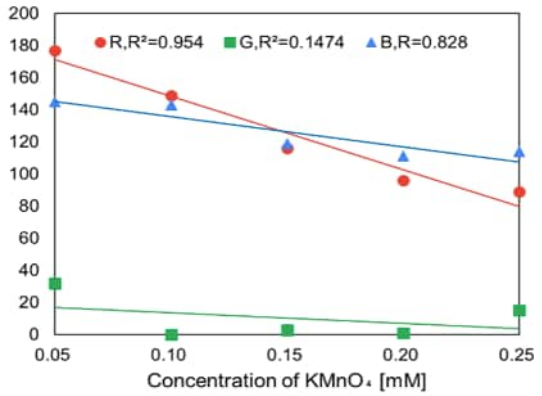

Fig. 13. RGB values obtained from photographs

The coefficients of determination for the individual RGB components differed substantially between photograph-derived RGB values and those obtained from UV–Vis measurements, indicating that the relationship between concentration and RGB values depends strongly on the measurement method. Therefore, RGB values derived from photographs cannot be directly applied to calibration curves established using UV–vis measurements. Furthermore, by conducting measurements in a controlled environment, consistent RGB values were obtained without being affected by variations in ambient light conditions.

4.3 Potential of the pH indication film

A solid pH indication film was fabricated, by dropwise addition of a liquid universal indicator to wood glue, resulting in a film that exhibits color changes in the presence of strong acids or bases. However, no noticeable color change was observed within the conventional pH range of 4 to 10, indicating that the current film has limited practical applicability for precise pH indication.

Further improvements may be achieved by optimizing the amount of indicator incorporated into the film or by employing alternative solidifying agents instead of wood glue.

5. Future prospects

In this method, the relationship between RGB values and water quality indices is not sufficiently precise, and further improvements in accuracy are required.

In addition, experiments using actual environmental samples, such as river water, have not yet been conducted; therefore, the practical applicability of this method has not been fully verified.

From this perspective, the development of simple evaluation tools, such as the pH indicator film fabricated in this study, as well as smartphone applications capable of automatically extracting RGB values of target samples from images, would be highly desirable. Although many challenges remain, the successful realization of such systems would enable anyone to assess water safety anytime and anywhere using only a smartphone and simple test kits. Moreover, these tools could serve as effective educational resources for enhancing interest in and awareness of water resources in educational settings.

6. References

1. Chapman, D. (Ed.). (1996). Water quality assessments: A guide to the use of biota, sediments and water in environmental monitoring (2nd ed.). Taylor & Francis Group (p. 5).
2. Shanahan, M. & Bahia, K. (2024). The State of Mobile Internet Connectivity 2024. GSMA.
3. Shinpaku, Y. (2017). A study on color temperature estimation using images captured by mobile device cameras（携帯端末のカメラで撮影した画像による色温度推定方法の検討）[In Japanese]. Doshisha University Miki Laboratory Monthly Report, 2. http://mikilab.doshisha.ac.jp/dia/monthly/monthly2017/2017_August/04_yshinpaku.pdf
4. Japanese Standards Association. (2024). JIS K 0102-4:2024: Testing methods for industrial water and industrial wastewater—Part 4: Organic substances. Japanese Standards Association.

Antibacterial effect of different soaps

Try Liwin[1], Rich Sopheavita[1], Bona Zarina[1], Hinata Kakei[2], Kazuki Kawaguchi[2], Haruki Tanaka[2]
[1]*New Generation Preah Sisowath High School (Cambodia)*
[2]*Risho Gakuen Osaka Ritsumeikan Junior & Senior High School (Japan)*

Abstract:
This study aims to compare the antibacterial effects antibacterial action of cheap and expensive solid soap, cheap and expensive liquid soap. The bacteria were tested on the hand before washing and after washing with each soap. The results showed that all of the soaps removed some bacteria as all are bactericidal but expensive and liquid soaps were slightly better. However, cheap soaps were still very much capable of removing bacteria if used properly. The four soaps (cheap liquid, expensive liquid, cheap solid, expensive solid) tested by the disk diffusion method on the E. coli (Escherichia coli) Bacteria and zones of inhibition measured. The results were analyzed to determine which soap showed the greatest reduction in bacteria. Overall, this study suggests that while soap type and price can influence antibacterial effectiveness, proper handwashing is essential for controlling bacterial growth. The findings also highlight that effective hygiene can be achieved using both affordable and expensive soap products.

Keywords: Soap, Bacteria, Antibacterial, Zone of Inhibition

1.Introduction

Hand hygiene is one of the most critical method uses to preventing disease from spreading all over your body, yet not all soaps are equally effective to kill all the bacteria on our hands. The average of bacterial growth on unwashed hand is estimated to be between 10,000 to 10 million bacteria at any given time and worst, it houses up to 150 different species. Soaps can be in solid or liquid shapes and vary in price and ingredients. This experiment compares the antibacterial power of cheap vs. expensive soaps in both forms. The purpose of this research is to see whether the price or soap types affects performance in killing bacteria since it is said that the bacterial growth is reduced to about 90% after using soap. There are many types of soaps available on the market, including solid and liquid soaps, with prices ranging from cheap to expensive. Many people believe that expensive soaps are more effective due to added antibacterial ingredients. However, it is important to determine whether the price and type of soap truly affect its antibacterial performance.

2. Methodology

To archive this, two different forms of soaps in two different prices are bought to be research about to compares their quality in preventing bacteria. Four different soaps were selected for this experiment: cheap solid soap, expensive solid soap, cheap liquid soap, and expensive liquid soap. The experiment was conducted by collecting bacterial samples from hands before and after washing with each type of soap. We use the glove method to record bacterial presence before washing. Each participant then washed their hands with one type of soap for 20 seconds following proper handwashing procedures. After washing, hands were pressed onto a new agar plate. The plates were then left at room temperature for 24–48 hours to allow bacterial colonies to grow. The number of bacterial colonies was observed and compared before and after washing. This process was repeated for all four soap types to ensure fair comparison. The collected data were recorded and analyzed to evaluate the antibacterial effectiveness of each soap.

(A)

(B)

(C)

(D)

Figure 1. (A) Cheap solid soap, (B) Expensive solid soap, (C) Cheap liquid soap (D) Expensive liquid soap

3.Results

The study revealed that the quality of soap may be contain in prices as it is shown that the number of bacterial growths from using expensive soaps are less than cheap soaps. Moreover, deep into this research, we have learned that both soap bars and liquid soaps has almost identical defecting bacteria rates which make no different between the two shapes of soap. The results showed that all four types of soap were able to reduce the number of bacteria on hands, but their effectiveness varied. However, although handwashing significantly reduced bacterial presence, some bacteria remained on the hands. The bacteria that were left behind continued to grow over time, as observed during the incubation period.

Haruki	Expensive liquid soap	Cheap liquid soap	Expensive Solid soap	Cheap Solid soap	Nothing (wash with water)
Day 1	30	58	15	15	145
Day 2	+17	+24	+6	+1	+43
Day 3	+3	+5	+0	+0	+4
Total	50	87	21	21	192

***Table1** Results of Haruki washing hands with different types of soaps for 3days.

Yugo (teacher)	Expensive liquid soap	Cheap liquid soap	Expensive Solid soap	Cheap Solid soap	Nothing (wash with water)
Day 1	45	123	24	25	340
Day 2	+5	+19	+53	+8	+19
Day3	+1	+1	+52	+5	+29
Total	51	143	126	38	388

***Table2** of teacher Yugo washing hands with different type of soaps for 3 days.

Kazuki	Expensive liquid soap	Cheap liquid soap	Expensive Solid soap	Cheap Solid soap	Nothing (wash with water)
Day 1	92	35	38	30	153
Day 2	+3	+14	+23	+10	26
Day 3	+1	+8	+6	+5	23
Total	96	57	67	45	202

***Table3** of Kazuki washing hands with different type of soaps for 3 days.

Hinata	Expensive liquid soap	Cheap liquid soap	Expensive Solid soap	Cheap Solid soap	Nothing (wash with water)
Day 1	20	14	32	46	74
Day 2	+7	+10	+8	+27	+16
Day 3	+8	+7	+5	+13	+9
Total	35	31	45	86	99

***Table4** of Hinata washing hands with different type of soaps for 3 days.

4.Discussion

The findings indicate that all soaps, regardless of price or form, are effective in reducing bacteria when used correctly. The higher effectiveness of expensive soaps may be due to additional antibacterial agents or moisturizing ingredients that allow longer contact with the skin.

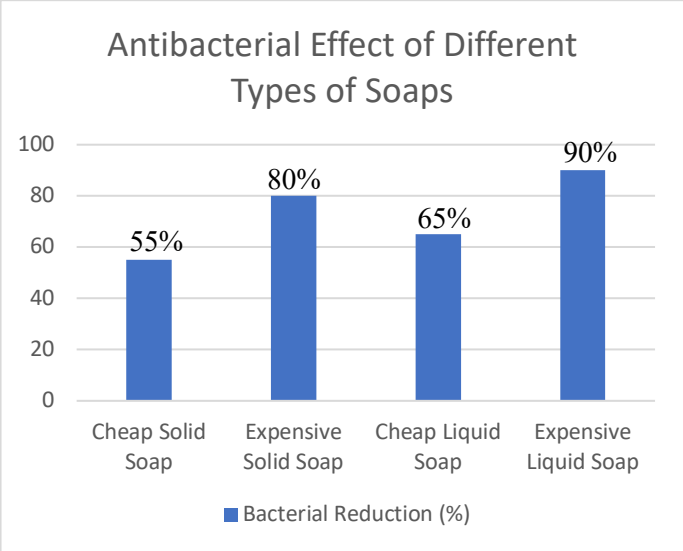

Figure 2. The results on how the different kind of soaps can kill bacteria.

The Figure 2 shows the antibacterial effectiveness of four different types of soaps. The expensive liquid soap had the lowest number of bacteria remaining, indicating the highest antibacterial effect. The cheap solid soap showed the second-highest effectiveness, followed by the expensive solid soap. The cheap liquid soap had the highest number of bacteria remaining, showing the lowest antibacterial effect. Although all soaps reduced bacteria after handwashing, some bacteria remained and continued to grow over time.

Washing hands with soap and water is one of the most effective ways to remove germs, dirt, and potentially harmful bacteria from our hands. According to the Centers for Disease Control and Prevention (CDC), handwashing with soap can significantly reduce diarrheal diseases and respiratory infections worldwide, protecting both individuals and communities from illness. (According to CDC)

This suggests that for the average person, choosing an affordable, readily accessible soap and using it correctly is more important than seeking out expensive or antibacterial products. This is especially relevant for households and community settings where resources may be limited.

5.Conclusion

In conclusion, this study shows that both cheap and expensive soaps, as well as liquid and bar forms, are effective at reducing bacteria on hands when used properly. The results align with public health evidence, which emphasizes that the act of washing thoroughly, for at least 20 seconds, is more important than the price, brand, or antibacterial label of the soap. While expensive soaps may contain additional fragrances or moisturizers, and liquid soaps may reduce cross-contamination in public settings, affordable soaps are sufficient for daily hand hygiene, making handwashing accessible to everyone. Proper technique, accessibility, and habit formation remain the key factors for preventing the spread of germs and maintaining personal and community health.

Overall, this study supports the idea that good handwashing practices with any soap are more valuable than focusing on cost or marketing claims, and that education and awareness about proper hand hygiene should be prioritized over the choice of soap type.

6. Acknowledgements

We would like to express our deepest gratitude towards Mr. Kawaguchi, who is a teacher from OsakaRits High school, for guiding and giving us advices throughout this project and Ms. Kaing Sainglin, who is a teacher majoring in biology at the Preah Sisowath High school NGS from Cambodia, for guiding, lecturing, and giving constructive feedback to us throughout this research process; In addition, this would not have been possible without their collaboration and dedication with us.

7. References

- BioTecNika. (2016). *Antibacterial soaps are not better*. https://www.biotecnika.org/2016/09/antibacterial-soaps-are-not-better-cleaner-or-safer/

- Forbes. (2015). *Antibacterial soap is no more effective than regular soap*. https://www.forbes.com/sites/daviddisalvo/2015/09/28/antibacterial-soap-is-no-more-effective-than-regular-soap-so-why-are-we-still-buying-it/

- Consultant360. (n.d.). *Antibacterial soap no more effective than regular soap*. https://www.consultant360.com/exclusives/study-antibacterial-soap-no-more-effective-regular-soap

Changes in Vitamin C Content Over Time Based on Fruit Storage Methods

Huyly Chhour[1], Linaoudom Nguon[1], Munilita Mun[1], Miu Fujii[2], Nami Higashiyama[2]
[1]*New Generation School, Preah Sisowath High School (Cambodia)*
[2]*Ritsumeikan High School (Japan)*

Abstract:

This research study was conducted to better understand the actual amount of vitamin C or ascorbic acid in orange juice, which is widely known as an essential nutrient for the body to help strengthen the immune system, but it is also a substance that is highly vulnerable and susceptible to loss of quality under various environmental conditions such as heat and light. To answer the research question of how much vitamin C is in the orange juice samples we selected for study, our research team decided to apply a quantitative analysis method, namely Redox Titration, using iodine solution as an oxidant to react with vitamin C until the mixture changes color indicating the equivalence point, with the help of starch as an indicator. Through the experimental process and careful calculation of the data obtained, we found that this method is highly effective, provides quick results, and is acceptable for accurately determining vitamin C concentration in the laboratory. Overall, we can conclude that orange juice is indeed an important source of vitamin C, but its amount can vary greatly depending on many factors such as freshness, production method, and storage. Therefore, the study concluded by recommending further comparative experiments on temperature and time factors, and advising consumers to choose to consume fresh orange juice immediately after squeezing to obtain the highest health benefits and avoid loss of nutritional value.

Keywords: Vitamin C; Storage Methods; Titration; Orange

Introduction

Vitamin C is an essential nutrient that helps provide the foundation of our immune system as well as reducing risk of other illnesses. It can be found in many fruits and vegetables, especially oranges. While consuming oranges is the primary way of boosting vitamin C level in our body, the method of storage for the oranges can be the main factor to the changes of Vitamin C content in them.

While Cambodia remains relatively warm and humid throughout the year, Japan on the other hand changes weather depending on the season. This proves to be a challenge to simulate similar weather conditions as well as temperature so we decided that these 3 storage methods would allow for the orange to be preserved in condition alike regardless of weather differences. In addition, color changes in fruits and vegetables caused by oxidation are a familiar phenomenon in our daily lives. We therefore considered the possibility that oxidation may be influenced by the components of sugar water and lemon.

Experiment 1

1. Methodology

Oranges were stored in three different conditions: in a refrigerator, at room temperature, and outdoors (Do not expose to direct light). Each orange was stored for two weeks. A starch indicator solution was prepared by dissolving 0.25 g of starch in 50 mL of water to make a 0.5% solution, and 20 mL of this solution was used for each titration. From each storage condition, 50 g of peeled mandarin orange was taken and crushed. The mixture was first filtered through two layers of gauze to separate solids and liquid. It was then filtered again using gauze and tissue paper to obtain a clearer juice sample. The iodine solution (oxidizing agent) was prepared by adding 1.3 g of iodine to 2 g of potassium iodide, dissolving the mixture with 2.5 mL of water, and then diluting it with 200 mL of water. 50μL of the iodine solution was added to the starch indicator until it turned blue-purple (50μL in Cambodia, 85 μL in Japan). Next, the orange juice was added drop by drop to the iodine-starch solution using a micropipette (5 μL per drop) until the blue-purple color became colorless. The point at which the solution became transparent was defined as the equivalence point, and the results from the three storage conditions were compared.

2. Result

- Royal D* concentration = 60mg of vitamin C /250ml of water = 0.24mg/mL = 0.00024mg/μL

  ***** powdered commercial juice from Cambodia

Let x be the amount of vitamin C it takes to neutralize iodine solution

X = V(Royal-D) x C(Royal-D) = 250μL x 0.00024mg/μL = 0.06mg

Table 1: The result in Cambodia side

Sample	Drops	Volume (μL)	Calculation (0.06/Vol)	Vitamin C Concentration	Humidity
Royal-D (Standard)	50	250	0.06 / 250	0.24 mg/mL	
Refrigerator	8	40	0.06 / 40	1.50 mg/mL	30%
Outside	11	55	0.06 / 55	1.09 mg/mL	48%
Paper Wrapped	18	90	0.06 / 90	0.67 mg/mL	45%

Table 2: The result in Japan side

Sample	Drops	Volume (μL)	Calculation (0.06/Vol)	Vitamin C Concentration	Humidity
Royal-D (Standard)	277	1385	0.06 / 1385	0.04 mg/mL	
Refrigerator	28	140	0.06 / 140	0.43 mg/mL	30%
Outside	30	150	0.06 / 150	0.41 mg/mL	62%
Paper Wrapped	20	100	0.06 / 100	0.60 mg/mL	16%

Experiment 2

1. Methodology

Oxidation was evaluated by observing changes in color. Oranges and apples were crushed using a funnel, and the juice was extracted and filtered through gauze. Filtration was performed in two steps. First, the juice was filtered through four layers of gauze. Next, it was filtered again using a setup in which two folded tissue papers were placed between two layers of gauze (two layers on each side). In addition, in Japan, samples prepared using the same method were also centrifuged at 8,000 rpm for 5 minutes in order to minimize the effects of precipitation. After that, 1.35 mL of the orange juice or apple juice was placed into each of three separate cuvettes. To each cuvette, 1.35 mL of water was added, followed by 0.3 mL of either sugar water, lime juice (lemon juice was used in the experiment conducted in Japan), or water. Sugar water was prepared by continuously adding sugar to water until no more sugar dissolved and undissolved sugar began to precipitate. This state was regarded as saturation, and the supernatant solution was collected. The cuvettes were then placed in a spectrophotometer, and absorbance was measured at 10-minute intervals.

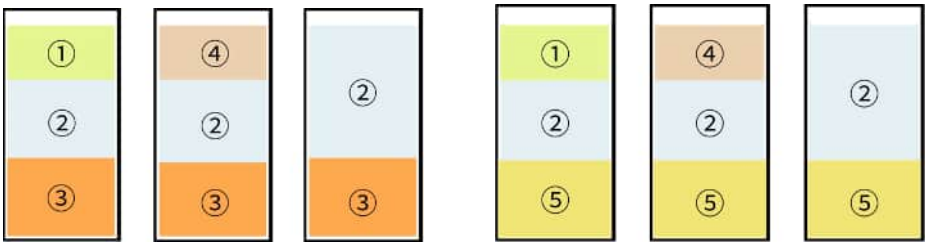

①Lime or Lemon ②Water ③Orange juice ④Sugar water ⑤Apple juice

Figure1: contents of the cuvette

2. Result

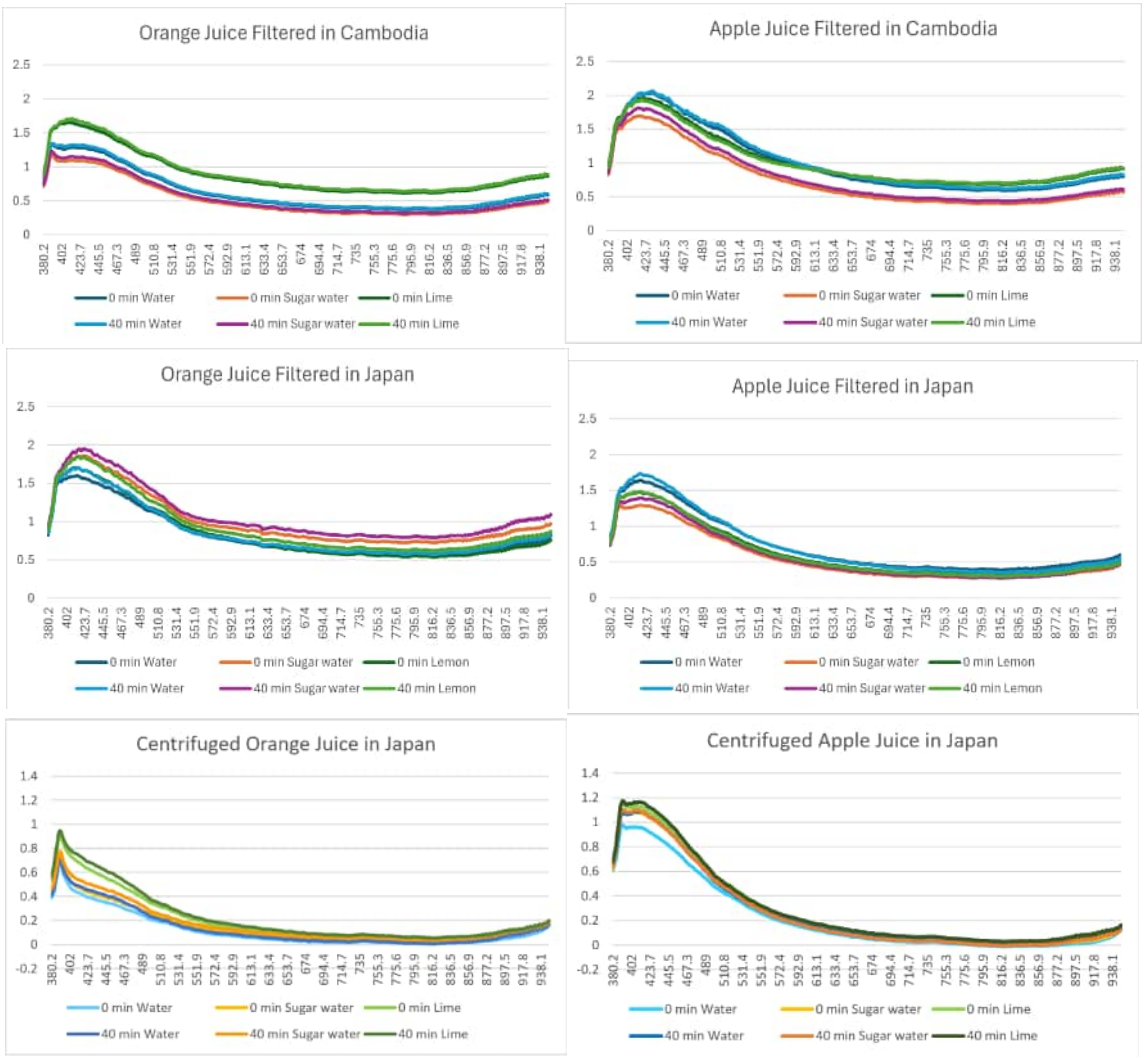

figure2: result of spectrophotometer

Table 3: Change in absorbance of orange juice (OD 423.7)

	Cambodia (Filtering)	Japan (Filtering)	Japan (Centrifuge)
Water	0.038371	0.00563	0.060159
Sugar Water	0.051872	0.078773	0.066556
Lime / Lemon	0.056168	0.173681	0.060313

Table 4: Change in absorbance of apple juice (OD 423.7)

	Cambodia (Filtering)	Japan (Filtering)	Japan (Centrifuge)
Water	0.2549	0.09538	0.12543
Sugar Water	0.1046	0.090151	0.009955
Lime / Lemon	-0.01831	0.006197	0.038029

Tables 3 and 4 present the time-dependent changes in absorbance over 40 minutes at a wavelength of 423.7 nm. These results indicate that larger values correspond to a darker change in the color of the fruit juice, meaning that oxidation progressed to a greater extent. For filtered apple juice, in both Cambodia and Japan, the samples with added lime or lemon showed the smallest change. This is likely due to the antioxidant effect of vitamin C, which is abundant in lime and lemon. In contrast, for filtered orange juice, the samples with added lime or lemon showed the largest change. Oranges contain approximately 60 mg of vitamin C per 100 g, whereas apples contain about 6 mg. In all orange samples, the color change was greater with lime or lemon than with water. Although oranges originally contain a large amount of vitamin C and therefore have strong antioxidant properties, the additional antioxidant effect from increasing vitamin C by adding lime or lemon was observed but was not as significant as in apples. For apples, similar results were obtained in both Cambodia and Japan. A notable difference was that the sample with added lime in Cambodia showed a negative change value. This is considered to be due to the influence of precipitation over time. Sugar is thought to promote oxidation because it reduces the absorption of vitamin C in the body. The dark color of the lemon juice added during centrifugation likely influenced the results. This effect was observed in apples but not in oranges. When comparing oranges and apples, no consistent trend was observed regarding the effects of the added reagents.

Discussion

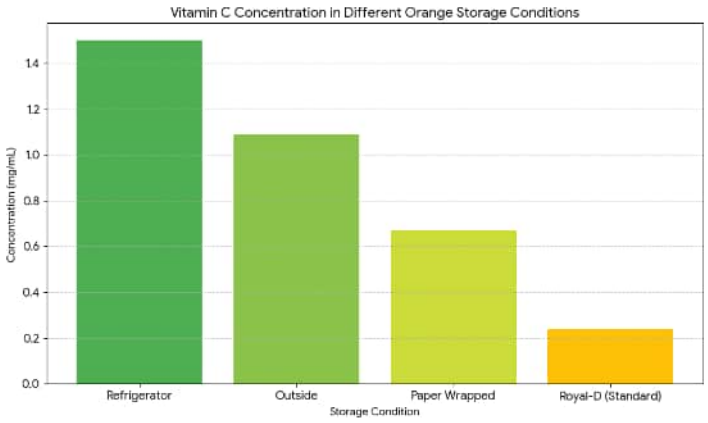

Figure 3: Vitamin C Concentration

Figure 3 shows how different storage conditions affected the vitamin C concentration in oranges. Oranges kept in the refrigerator had the highest vitamin C content, suggesting that little degradation occurred. Samples stored outside showed a lower concentration, while paper-wrapped oranges experienced a greater loss of vitamin C. The Royal-D (standard) sample had the lowest concentration, indicating the highest level of vitamin C degradation. Overall, the results suggest that cooler storage conditions help slow the loss of vitamin C.

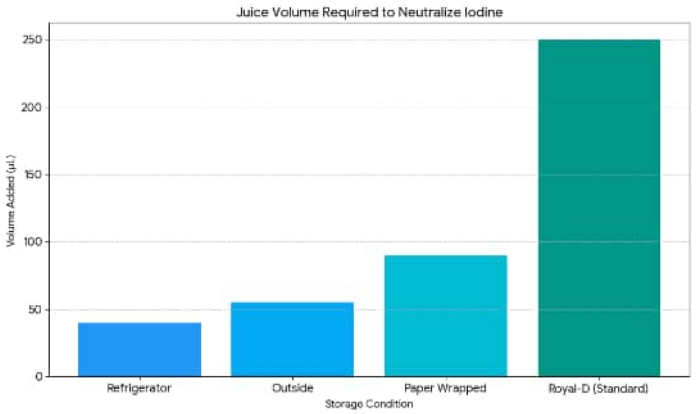

Figure 4: Juice Volume required to neutralize Iodine

Figure 4 presents the volume of orange juice required to neutralize the iodine solution for each storage condition. Refrigerated samples required the least amount of juice, which indicates a higher vitamin C concentration. In contrast, samples with lower vitamin C levels required more juice to reach the endpoint, particularly the paper-wrapped and Royal-D (standard) sample. This supports the results shown in Figure 3 and confirms the relationship between vitamin C concentration and iodine neutralization.

In this experiment conducted in Japan, the orange wrapped in paper showed the highest vitamin C content. In addition, the oranges kept outdoors contained less vitamin C than those stored in a refrigerator.

This suggests that lower temperatures may help preserve vitamin C. However, since the orange wrapped in paper and kept indoors had the highest vitamin C content, a consistent relationship between temperature and vitamin C preservation could not be confirmed from the results of this experiment. When the results were examined from the perspective of humidity, the orange stored in the place with the lowest humidity showed the highest vitamin C content. Furthermore, in most cases, the vitamin C content tends to change in accordance with the level of humidity. From these results, it can be concluded that oranges stored in low-humidity environments retain the highest amount of vitamin C. Although temperature is also thought to influence vitamin C preservation, this experiment did not clearly demonstrate its effect.

Conclusion

This study demonstrates that storage conditions have a significant effect on the vitamin C content of oranges. Among the methods tested, refrigeration was the most effective in preserving vitamin C, while storage at room temperature and paper wrapping resulted in greater losses. The iodine titration results further supported these findings, as samples with lower vitamin C concentrations required larger volumes of juice to reach the endpoint. Overall, the results suggest that oranges should be stored at low temperatures to maintain their nutritional value, and freshly prepared orange juice should be consumed as soon as possible to minimize vitamin C reduction.

In addition, experiments conducted in Japan revealed that humidity is also one of the factors influencing the vitamin C content of oranges. The results showed that oranges stored in environments with lower humidity retained higher levels of vitamin C. Therefore, based on the experimental results from both Cambodia and Japan, it can be concluded that two factors—temperature and humidity—are involved in changes in the vitamin C content of oranges depending on the storage method.

References

Lee, S. K., & Kader, A. A. (2000). Preharvest and postharvest factors influencing vitamin C content of horticultural crops. Postharvest Biology and Technology, 20(3), 207–220. https://doi.org/10.1016/S0925-5214(00)00133-2

Soceanu, A., Matei, N., Dobrinas, S., & Popescu, V. (2021). Degradation kinetic modelling of ascorbic acid from orange juice. Proceedings, 70(1), 55. https://doi.org/10.3390/foods_2020-07693

University of Canterbury. (n.d.). Determination of vitamin C concentration by titration. https://www.canterbury.ac.nz/content/dam/uoc-main-site/documents/pdfs/d-other/Determination-of-Vitamin-C-Concentration-by-Titration.pdf

https://fooddb.mext.go.jp/details/details.pl?ITEM_NO=7_07040_7

https://medipalette.lotte.co.jp/post/94

Effects of biodiversity on plant growth and environment in terrariums

Lao Panharoth[1], Tim Angelie[1], Thong Puthika[1], Shihoko Kurofuchi[2], Leo Kawasaki[2]
[1]*Preah Yukunthor New Generation School (Cambodia)*
[2]*Tokai University Takanawadai Senior High School (Japan)*

Abstract

Biodiversity plays a fundamental role in maintaining ecosystem function, productivity, and stability. Through ecological research, it has shown that ecosystems with higher species diversity are consistently more resilient and efficient than those with limited diversity. This study investigates the effects of biodiversity on ecosystem ability using controlled environments, such as terrariums. Two types of terrariums. Hence why, two types of terrariums were prepared. biodiverse systems containing plants and soil invertebrates, and control systems containing plants only. The terrariums were observed over a two-month period, during which plant growth, environmental conditions, and signs of nutrient cycling were monitored. Biodiversity was quantified using the Shannon Diversity Index. Results showed that biodiverse terrariums maintained stable, rainforest-like conditions, exhibited active decomposition, and demonstrated greater plant recovery following environmental stress. In contrast, non-biodiverse terrariums experienced progressive plant decline, including yellowing, wilting, and decomposition. These findings demonstrate that biodiversity enhances ecosystem resilience and supports essential ecological processes, even at small scales. The experiment highlights the importance of biodiversity conservation and illustrates how ecosystem degradation may impact environmental sustainability in the future.

Keywords: Biodiversity, environment, terrarium

1. Introduction

While most studies of biodiversity occur in large field systems, controlled environments such as a terrarium can provide a simplified view to observe them. A terrarium, with its semi-closed off design is a perfect fit to mimic nature making sure our biodiversity can thrive in conditions we want while making sure their function still works. Since external inputs are limited, the balance of the system heavily relies on interactions among its organisms. This makes the terrarium an ideal environment for studying how biodiversity directly influences ecological processes. By creating terrariums with different levels of species diversity, it becomes possible to observe on a small scale the same ecological patterns that shape entire landscapes, but under conditions that are easier to control and monitor.

This study aims to investigate how biodiversity influences ecosystem stability and function in a terrarium setting. By comparing the terrariums with different levels of species richness and functional diversity, the experiment seeks to highlight the role of biodiversity in processes such as nutrient cycling, productivity, and resilience.

2. Methodology

The experiment was conducted in the project work room of NGS-Preah Yukunthor highschool, for the Cambodian side, as for the japanese side, the experiment was conducted within the science room of the Tokai University Takanawadai Senior High School.

The experiment was done for a little over 2 months (Sep-Nov), with the usage of the Shannon Index method, as well as doing observations once in the afternoon and taking 1 top photo and 4 photos on each of our terrariums, every 2 days. Furthermore, the terrarium was made by the following steps below:

1. LECA and soil were laid at the bottom of two terrariums.
2. LECA is for drainage.
3. We put hydro cotyle itoprides, pilea glauca, moss, Pteris multifida, and Davilla termini in both.
4. We put springtails, isopods, pot worms, earth worms, and black ants in only one side.
5. In Japan, there were 57 isopods, 15 pot worms, and 15 earth worms.
6. In Cambodia, there were 17 isopods, 30 pot worms, and 30 earth worms.
7. In both countries, there were 30 Springtails and 15 Black ants.

8. We kept watering the two terrariums about for two months, taking photos of them three times a week, measuring the plants' growth, their temperature, and pH in the terrariums once a week.

Terrariums received bright indirect light; biodiverse ones were mostly sealed with occasional misting (every 2-3 days), while non-biodiverse needed more frequent spraying due to humidity loss. Invertebrate counts were springtails (30 both), isopods (17 Cambodia/57 Japan), potworms/earthworms (30/15), ants (15 both). Observations occurred every 2 days with top and side photos, diversity assessed via Shannon index is species proportion. Plant health tracked growth, color, wilting, and smells indicating decomposition/recycling.

Table 1. Information about the terrariums.

Parameter	**Japan with Biodiversity**	**Cambodia with Biodiversity**	**Cambodia No Biodiversity**	**Japan No Biodiversity**
Dimensions (cm)	37×21×24	20×10×30	6×6×16	31×21×24
Total invertebrates	117	92	0	0
Shannon index (H')	1.226	1.339	0	0
Soil/Drainage	Garden soil/LECA	Garden soil/LECA	Garden soil/LECA	Garden soil/LECA
Plants	5 species	5 species	5 species	5 species

As shown in **Table 1**, biodiverse terrariums contained springtails (30), isopods (Cambodia: 17, Japan: 57), potworms (Cambodia: 30, Japan: 15), and ants (15). Observations occurred every 2 days with 1 top and 4 side photos. Shannon index $H' = -\Sigma(Pi \times \ln(Pi))$ with Pi calculated as = species proportion. Biodiverse terrariums maintained sealed conditions with minimal misting; controls required frequent spraying.

3. Results

Biodiverse terrariums maintained rainforest-like conditions with active decomposition. As seen in **Table 1**, higher Shannon indices correlated with plant recovery after stress (Cambodia biodiversity: pennywort propagated rapidly by Oct 1). Controls showed progressive decline: yellowing by Oct 4, wilting by Oct 22, rotting odors by Oct 27. For Cambodia's terrarium with biodiversity, it seems to be more diverse than Japan's terrarium with biodiversity, calculated through the Shannon Index method, with a 1.339 and a 1.226, respectively.

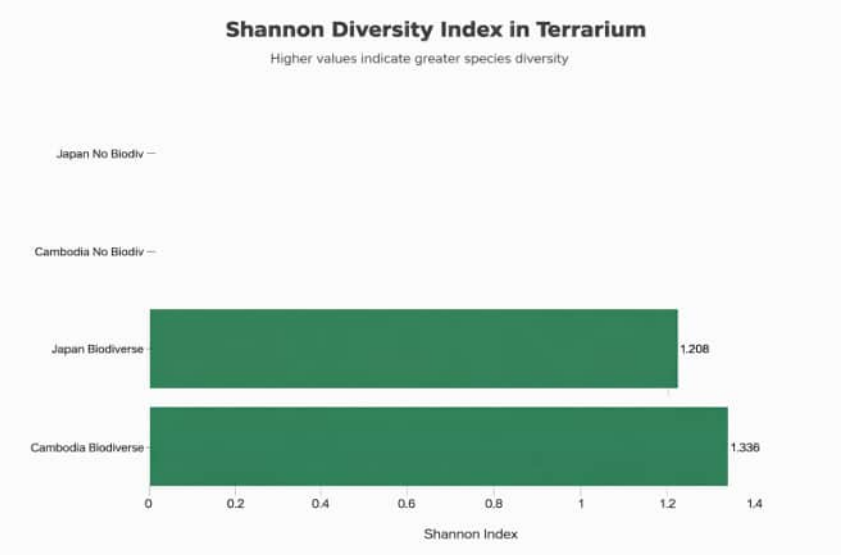

Figure1. Shannon Diversity Index comparison across terrariums. Higher values indicate greater species evenness supporting ecosystem function.

4. Discussion

Invertebrates enhanced nutrient recycling per **Table 1** compositions, buffering plants against moisture/light stress that devastated controls. School events disrupted Japanese watering, yet diversity mitigated impacts better than sterile setups.

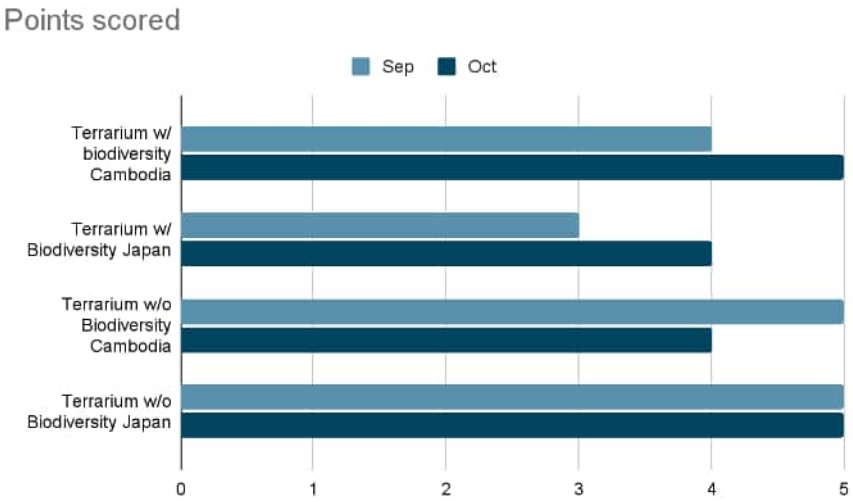

Figure 2. The health of terrariums using the Shannon Index method calculations throughout the periods.

5. Conclusion

This study demonstrates biodiversity's critical role in terrarium ecosystem stability. Biodiverse setups (Table 1) with Shannon indices 1.226-1.339 outperformed controls (H' = 0), showing rapid plant recovery post-stress, sustained rainforest-like conditions, and active nutrient cycling via invertebrate decomposition. Controls exhibited progressive decline culminating in plant death, lacking essential functional diversity.

These findings scale field ecology principles (Tilman, 1997) to classroom experiments, validating biodiversity's universal importance for ecosystem resilience. Terrariums emerge as powerful educational tools demonstrating nutrient cycling, water conservation, and species interactions in miniature. Future studies could quantify biomass accumulation, CO_2 regulation, and long-term carbon sequestration to further bridge microcosm and macroecosystem research.

6. References

Patanaponpaiboon, P., Ninomiya, I., & Ogino, K. (n.d.). Ecosystem conservation by means of man-made ecosystems in Thailand.*ThaiScience*.

https://www.thaiscience.info/Article/ThaiScience/Article/63/10039947.pdf

Christine I. B. Wallis and Yvonne C. Tiede. (2021, December 31). Biodiversity and ecosystem functions depend on environmental conditions and resources rather than the geodiversity of a tropical biodiversity hotspot.

https://doi.org/10.1038/s41598-021-03488-1

Graham R. Martin, Rory Crawford. (2014, November 7).Reducing bycatch in gillnets: A sensory ecology perspective, Global Ecology and Conservation.

https://doi.org/10.1016/j.gecco.2014.11.004

World Health Organization. (2023, December 6). Biodiversity.

https://www.who.int/news-room/fact-sheets/detail/biodiversity

Tilman, D. (1997). Community diversity and ecosystem productivity. *Nature*, 387(6632), 25-26.

https://doi.org/10.1038/387025a0

Loreau, M., Naeem, S., Inchausti, P., Bengtsson, J., Grime, J. P., Hector, A., Hooper, D. U., Huston, M. A., Raffaelli, D., Schmid, B., Tilman, D., & Wardle, D. A. (2001). Biodiversity and ecosystem functioning: Current knowledge and future challenges. *Science*, 294(5543), 804-808.

https://doi.org/10.1126/science.1064088

Tilman, D., Naeem, S., Knops, J., Reich, P. B., Siemann, E., & Wedin, D. (1997). *Biodiversity and ecosystem properties*. Science,278(5345), 1865–1869. https://doi.org/10.1126/science.278.5345.1865c

(PDF) Biodiversity and Ecosystem Properties

Loreau, M., Naeem, S., Inchausti, P., Bengtsson, J., Grime, J. P., Hector, A., Hooper, D. U., Huston, M. A., Raffaelli, D., Schmid, B., Tilman, D., & Wardle, D. A. (2001). *Biodiversity and ecosystem functioning: Current knowledge and future challenges*. *Science, 294*(5543), 804–808.

https://www.science.org/doi/10.1126/science.1064088

Appendix1: the observation checklists

Week	Plant Growth (Height, Leaf Number, Color)	Soil Condition (Moisture, pH, Organic Matter)	Microclimate (Temperature, Humidity)	Plant Health (Color, Mold, Pests)	Notes/Comments
1	Height: ● Leaves Color	Moist Dry PH:	Temp:	Healthy Yellow leaves Mold Pests	
2	Height: ● Leaves Color	Moist Dry PH:	Temp:	Healthy Yellow leaves Mold Pests	
3	Height: ● Leaves Color	Moist Dry PH:	Temp:	Healthy Yellow leaves Mold Pests	
4	Height: ● Leaves Color	Moist Dry PH:	Temp:	Healthy Yellow leaves Mold Pests	
5	Height: ● Leaves Color	Moist Dry PH:	Temp:	Healthy Yellow leaves Mold Pests	
6	Height: ● Leaves Color	Moist Dry PH:	Temp:	Healthy Yellow leaves Mold Pests	
7	Height: ● Leaves Color	Moist Dry PH:	Temp:	Healthy Yellow leaves Mold Pests	
8	Height: ● Leaves Color	Moist Dry PH:	Temp:	Healthy Yellow leaves Mold Pests	

The Effect of Mass on the Magnetic Levitation and Stability of Maglev Trains

Bunleap Pove[1], Chantheary Saing[1], Vysal Van[1], Takuma Sato[2], Niina Kato[2]
[1]*New Generation School, Preah Yukunthor High School (Cambodia)*
[2]*Fukushima Prefectural Fukushima High School (Japan)*

Abstract:

The technology of maglev trains rely on a core concept based on magnetic forces stating that the same magnetic poles repel each other, and opposite magnetic poles attract each other. Maglev trains adopt two systems: EMS, and EDS. Following this, a general model of maglev trains applying the same concept of magnetic forces mentioned will be assembled to show the levitation system of maglev trains-alongside test its disadvantage of being inefficient when carrying a heavier load. The report tests this by applying coins or mass atop the model train and measuring the relation between levitation distance between the train and the base, and the extra mass added. During these tests, it was to be concluded that with increasing load, the efficiency of the overall train's levitation is decreased.

Keywords: EMS (Electromagnetic suspension), EDS (Electrodynamic suspension); Levitation

1. Introduction

Public transportation, notably by train, is essential for those living in urban cities, and the technological advances in this field have led to the development of magnetic levitation technology, eventually up to the creation of Maglev trains (Matan, 2023a). In April of 2015, the Series L0 in Japan achieved a record speed of 603km/h --showing just how superior maglev trains are when compared to conventional trains in terms of speed (Genness World Records, 2015). Despite this, many still don't understand the principles and science behind these trains (Adhamy, 2024).

Maglev trains rely on a universally known fact about magnetic forces stating that the same magnetic poles repel each other, and opposite magnetic poles attract each other (Matan, 2023b). Alongside this, two different systems (EMS, EDS) are used according to different train lines (Topics, 2022). This study aims to explore the basics of these two systems and create a model that simulates a real-world application of these trains (Finio, 2023), alongside testing its disadvantage of being inefficient when carrying higher loads with a goal of educating the public on how these futuristic trains work (Finio, 2023; Matan, 2023a).

2. Description

In maglev train transportation, there are two parts which are crucial for levitation: the track and the train (Matan, 2023a). Maglev technology generally utilizes the attractive and repulsive forces between magnets -hence the division of two different systems: EMS, and EDS (Topics, 2022). In *electromagnetic suspension* (EMS), the magnets supporting the train are set up under the track so these magnets can attract those on the track (Figure 1) (Matan, 2023a). The electromagnets fitted on the train then attract them to the track, which lifts the train (Matan, 2023b). When the train rises slightly, the magnet moves closer to the track and the attractive force increases, making the train move upward until it contacts the rail (Serway & Jewett, 2006). Proximity sensors and feedback-control systems help correct this instability by adjusting the current to the electromagnets in real time to prevent physical contact (Serway & Jewett, 2006; Matan, 2023a; Topics, 2022). By interaction between the alternating polarities of the train's electromagnets with the track's permanent magnets, the train moves. Whereas in *electrodynamic suspension* (EDS), this system uses superconducting magnets on the train and track which create a magnetic field inducing repulsive forces resulting in levitation and propulsion of the train (Adhamy, 2024). The sides of the track have magnetic coils which create an overlapping and alternating pattern of north, south magnetic fields. Since opposite poles induce a repulsive force, this allows for the train to levitate (Matan, 2023b). This system is unique because it uses supercooled, superconducting magnets which are known to have a stronger magnetic field compared to electromagnets in normal room temperatures thus increasing efficiency and speed

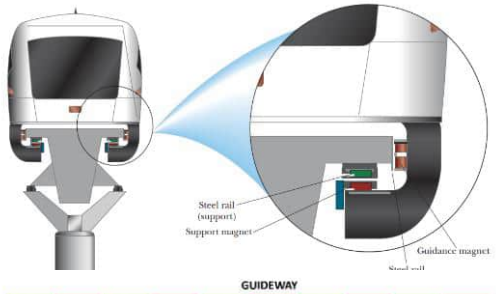

Figure 1: EMS System

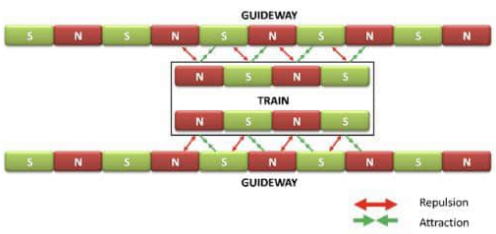

Figure 2: EDS

of the whole system (Adhamy, 2024). As for the propulsion of EDS trains, normal electromagnets set in the guideway with opposite polarity are changed consecutively, creating a constant attraction and repulsion forced between the superconducting magnets on the train and the electromagnets on the guideway (Figure 2) (Adhamy, 2024; Topics, 2022).

3. Methodology

To showcase the levitation and repulsion system of maglev systems—a simple model is assembled (Figure 3). A cardboard strip acts as the base of the module, and plastic angles on the sides of this base act as the guiderail for the hollow wooden block acting as the maglev train itself. The wooden block has a mass of 116.0g. A pair of monopolar magnetic tape, with a width of 0.9cm and a height of 0.3cm each, is then set up onto the bottom of the wooden block, facing opposite to another pair that is set up onto the cardboard base- with the top and bottom magnetic strips having opposite polarities, to showcase the levitation of the train based on magnetic principles. Following the assembly of this model, an experiment is done by placing the maglev train on the track to track the relation of distance between the wooden block and bottom magnetic strip with an increasing variable of mass on the train to showcase a real-world application of maglev systems on how efficiency of the system is affected as the mass of the train increases. In observing and recording the data of this distance between the train and the magnetic strip, three data sets were made to find the average of these data sets. In each of these data sets, exactly 25g weights were added continuously atop the wooden block until a total of 200g was achieved on top of the wooden block. In the process of collecting data from this observation, only a single person had observed and measured the distance to avoid user error. A camera was used alongside a ruler to further increase the reliability of the results. To clarify further, the same exact model was used for testing in both regions. Data tables were made to collect the data, before graphing.

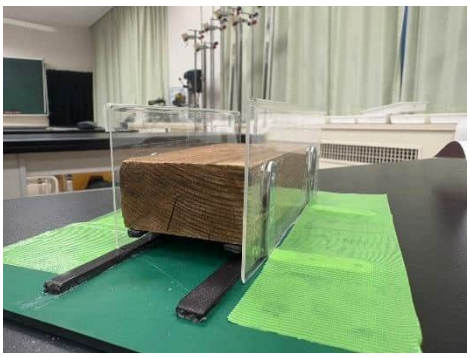

Figure 3: Maglev Model

4. Results

The study revealed that as more mass was added atop the wooden block, a clear pattern of decreasing levitation distance between the bottom magnetic strips and the wooden block was observed. This trend indicates that the magnetic force generated by the system was gradually overcome by the increasing gravitational force caused by the added mass. As a result, the block was pulled closer to the magnetic base, reducing the levitation height. This observation suggests that in real-world applications of maglev systems, efficiency and stability may decrease as the load increases, especially if the magnetic strength is not adjusted to compensate for the added weight.

After collecting the data and organizing it into tables that included the sum and average values of the levitation distances using the model in Cambodia (Figure 4), a consistent downward trend in levitation distance became evident. Repeated trials helped reduce random error and increased the reliability of the results, allowing for more accurate comparisons between different mass increments. The most notable change occurred when the mass increased from 75 g to 100 g, where a significant decrease in levitation distance of 1.1 cm was recorded. This sudden drop suggests the system may be approaching its maximum load capacity, beyond which the magnetic force is no longer sufficient to counteract the gravitational force acting on the wooden block. Additionally, minor variations in earlier data points may be attributed to experimental limitations such as slight misalignment of the magnetic strips or measurement uncertainty. Overall, the processed data strongly supports the conclusion that increasing mass has a measurable and increasingly pronounced effect on levitation distance.

To further illustrate this relationship, a bar graph was created to visually represent the change in levitation distance as mass increased. The graph clearly demonstrates an inverse relationship between mass and levitation height, reinforcing the conclusion that increased mass negatively impacts the performance and reliability of magnetic levitation systems.

CAMBODIAN STATISTICS			
Test Variables		*Levitation Distance (cm)*	
Count	*Mass (g)*	*Sum*	*Average*
3	0	14.5	4.8
3	25	14	4.6
3	50	12	4
3	75	11.5	3.8
3	100	8.3	2.7
3	125	7.2	2.4
3	150	7	2.3
3	175	6.1	2
3	200	5.1	1.7

Figure 4. Cambodian Statistics Table

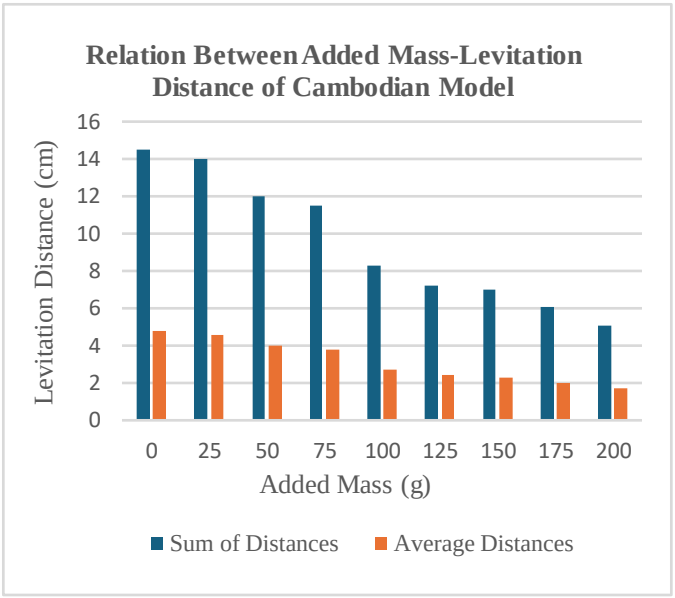

Figure 5. Bar Graph of Cambodian Statistics

When the model was tested in Japan with the same methodology, a difference was observed in the statistics table (Figure 6). At 0g of mass added, the Japanese model had a levitation distance of 3.6cm, compared to the Cambodian model that had a levitation distance of 4.8cm which indicates a 1.2cm difference or a 25% decrease.

JAPAN STATISTICS			
Test Variables		*Levitation Distance (cm)*	
Count	*Mass (g)*	*Sum*	*Average*
3	0	10.8	3.6
3	25	9	3
3	50	6.5	2.2
3	75	5.5	1.8
3	100	3.9	1.3
3	125	3.4	1.1
3	150	3	1
3	175	1.6	0.5
3	200	0.8	0.3

Figure 6. Japanese Statistics Table

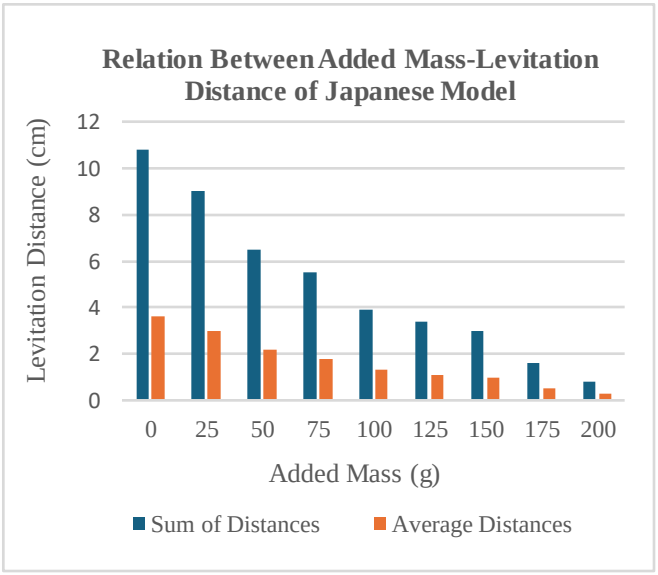

Figure 7. Bar Graph of Japanese Statistics

5. Discussion

The results indicate that mass is an important variable in magnetic levitation systems. One can determine how the magnetic levitation of these systems is affected negatively based on the mass added atop the model maglev train. Through testing, we can determine that the effect of mass has a downwards-linear effect on the overall levitation distance between the bottom magnetic strip and the wooden block (Figure 9).

SUMMARY STATISTICS							
Test Variables		*Levitation Distance (cm)*					
Count	*Mass (g)*	*Sum (CAM)*	*Sum (JP)*	*Average (CAM)*	*Average (JP)*	*Total Sum*	*Total Average*
3	0	14.5	10.8	4.8	3.6	25.3	4.2
3	25	14	9	4.6	3	23	3.8
3	50	12	6.5	4	2.2	18.5	3.1
3	75	11.5	5.5	3.8	1.8	17	2.8
3	100	8.3	3.9	2.7	1.3	12.2	2
3	125	7.2	3.4	2.4	1.1	10.6	1.75
3	150	7	3	2.3	1	10	1.65
3	175	6.1	1.6	2	0.5	7.7	1.25
3	200	5.1	0.8	1.7	0.3	5.9	1

Figure 8. Summary Statistics (JAP- Japanese, CAM- Cambodia)

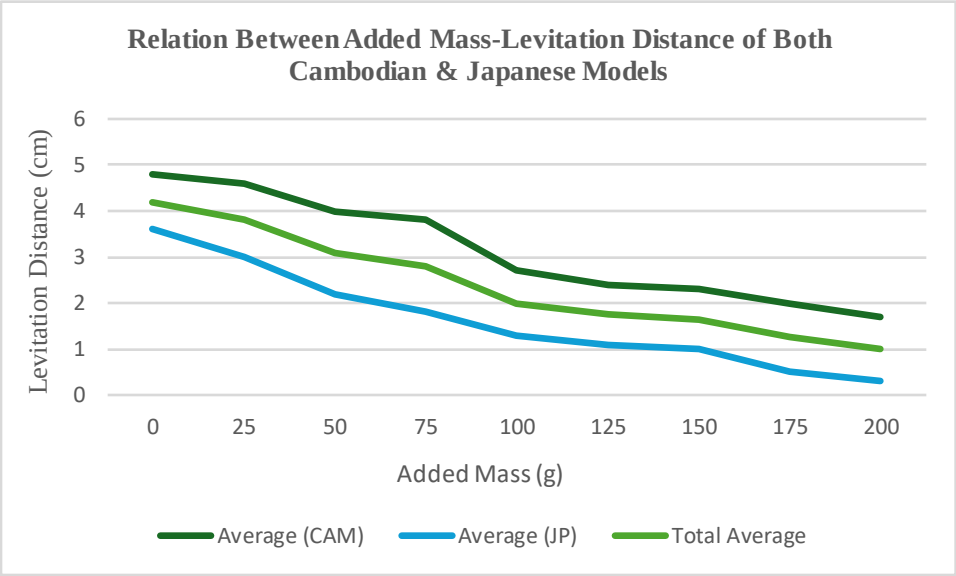

Figure 9. Line Graph of Summary Statistics (Average Values of Levitation Distance)

6. Conclusion

In conclusion, this research aimed to show the levitation systems of maglev trains based on the concept of contrasting and the same magnetic poles (repel, attract). According to the data shown above, provided with a line graph performed by testing on the maglev train model, the study revealed that the efficiency of maglev trains declines according to a higher mass or load. It can be concluded that mass plays a major role in the efficiency of these trains.

7. Acknowledgements

We would like to express our deepest gratitude towards Mr. Phoeurn Lafy, who currently is a physics teacher at Preah Yukunthor High School, for guiding, lecturing, and giving constructive feedback to us throughout this research process. In addition, this would not have been possible without his collaboration and dedication to us.

8. References

Adhamy, A. (2024, July 1). *How it works: EDS Maglev Trains*. BBC Science Focus Magazine. https://www.sciencefocus.com/science/how-it-works-eds-maglev-trains

Fastest maglev train. (2015, June 26). *Guinness World Records*.

https://www.guinnessworldrecords.com/world-records/fastest-maglev-train

Finio, B. (2023, February 4). *Build a Floating Maglev Train. Retrieved from* https://www.sciencebuddies.org/science-fair-projects/project-ideas/Phys_p093/physics/maglev-train-weight?ytid=KQH2UhHss6c&ytsrc=description

Matan. (2023a, May 17). *How maglev trains work in detail | Description, Example & Application. Your Physicist*. https://your-physicist.com/how-maglev-trains-work-in-detail/#:~:text=EMS%20uses%20electromagnets%20on%20the%20train%20and%20the,field%20from%20the%20track%E2%80%99s%20electromagnets%2C%20resulting%20in%20levitation.

Matan. (2023b, June 11). *What is magnetic levitation and how does it work? – Electricity – Magnetism*. https://www.electricity-magnetism.org/what-is-magnetic-levitation-and-how-does-it-work/

Serway, R. A., & Jewett, J. W. (2006). *Principles of physics: A calculus-based text* (4th ed.). Thomson Brooks/Cole.

Topics, S. (2022, September 1). *How a Maglev Train Works (EMS and EDS)? Interesting Science.* https://sciencetopic03.blogspot.com/2021/11/how-maglev-train-works-ems-and-eds.html

The Role of *Lactobacillus* in Yakult in Enhancing Potato Growth

Cai Kai Hin Kelvin[1], Chu Cheuk Kiu[1], Tsang Jin Yi Jacob[1], TANAKA Himeha[2], NISHIO Tomoka[2]
[1]*G.T. (Ellen Yeung) College (Hong Kong, China)*
[2]*Tokyo Gakugei University Senior High School (Japan)*

Abstract:

Potatoes are a popular food in both Japan and Hong Kong. They are a major source of starch and rich in mineral ions, making them a popular food source in developing countries. While several bacteria are known to have plant-activating properties, this study evaluated the plant-activating properties of *Lacticaseibacillus paracasei strain Shirota*. Experiments showed that the average mass of potatoes in the experimental group was heavier than that of potatoes in the control group. Furthermore, the leaves of the experimental group were found to be healthier. This led to the conclusion that strain Shirota (a lactic acid bacterium) was involved in promoting potato growth.

Keywords: Potato; Lacticaseibacillus paracasei strain Shirota; Potato growth

1. Introduction

Potatoes are a nutritious crop that is a major source of carbohydrates (starch) and is rich in vitamins B6 and C, potassium, iron, and other minerals. Compared to fruits, potatoes are easier to cultivate, require less space, and have a shorter growing period than many vegetables. For these reasons, potatoes are widely used as a major source of energy and nutrients in developing countries and other regions.

Given this background, it is important to achieve low-cost, high-yield potato cultivation. This study investigated bacteria that contribute to potato growth promotion. Several bacteria have been reported to be involved in plant-activating functions such as promoting plant growth and improving disease resistance; these are generally collectively referred to as 'Plant Growth-Promoting Rhizobacteria (PGPR).'

In this study, we focused on *lactobacillus* with potential as a PGPR and evaluated their effects on plants. Specifically, we investigated the growth of seed potato sprouts using a lactic acid beverage containing *Lacticaseibacillus paracasei strain Shirota*. The growth rate of sprouts was evaluated using the number of leaves as an indicator, and we examined whether *Lacticaseibacillus paracasei strain Shirota* has a growth-promoting effect. It is hypothesised that *lactobacillus* added into the soil results in statistically significant difference between the control and experimental group on the growth rate.

2. Methodology

Rogosa Agar plates, which selectively cultivate bacteria, were made by dissolving Rogosa Agar powder in water. To reduce the concentration of *Lacticaseibacillus paracasei strain Shirota* from Yakult for easier cultivation, we diluted the Yakult to 10^{-1} and 10^{-2} concentrations, then slurred the solutions evenly onto the Rogosa Agar plates and put the slurred plates in the incubator at 36°C for around 3 days. After cultivating the bacteria, purification was done to ensure that only *Lactobacillus* was cultivated. The plates with *Lactobacillus* are streaked with an inoculation loop, then the 2 plates are placed upside down in a warm incubator at 36°C for around 2 days.

To prepare the *Lactobacillus* at a suitable concentration for injecting it into the soil, a colony of the *Lactobacillus* is suspended in 2 separate shaking tubes with 45 mL of MEB solution, incubated in a shaking incubator at 34°C and 180 rpm for 48 hours. Transfer 1 mL of the solution into a cuvette after pipetting up and down. Using the spectrophotometer, measure the OD value of the bacteria. Use the formula v1c1=v2c2 (where v1 is the original volume, c1 is the data from the spectrophotometer, v2 is the unknown volume needed, and c2 is 1.0) to determine the volume of liquid medium required to be added to adjust the OD value from 600 to 1.0. Adjust the OD value by centrifuging the MEB with *Lactobacillus* at a maximum of 5000rpm for 15 minutes. Then, add or extract MEB in the shaking tube until the OD value becomes 1.0 (determined by the above equation).

Sprout the potatoes in a warm and moist environment and cut out 10 eyes from the potatoes. Heat a screwdriver with a Bunsen Burner and poke holes in the bottom of the two boxes to let water pass out. Put soil into the boxes and bury the 5 potato eyes in each of the boxes. Gently spray 30mL of the MEB with *Lactobacillus* using a pipette. Water the potatoes once or twice a week, depending on the state of the weather. After a few months, gently remove the potatoes from the soil to compare their size by weighing the potatoes grown, measuring the diameter of the leaves, and measuring the length of the roots.

Figure 1: Centrifuge

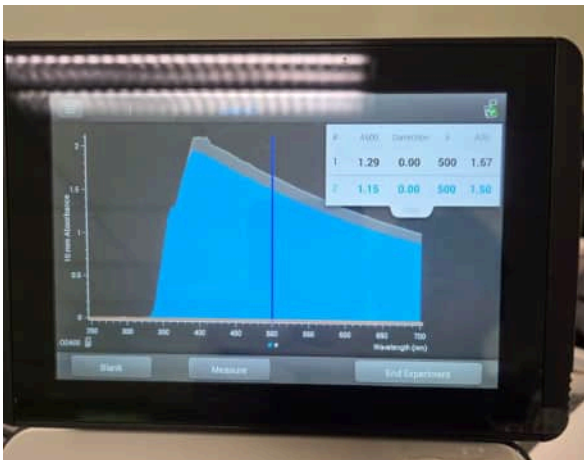

Figure 2: Measured OD value

3. Results

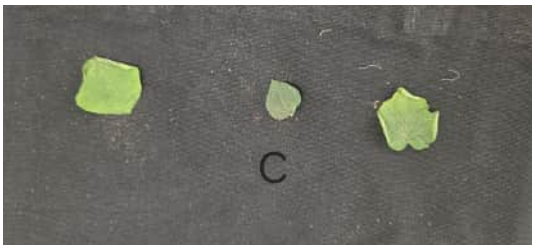

Figure 3: Leaves of the control group

Figure 4: Leaves in the experimental group

Leaves of the experimental group	Mass of leaves for experimental group (g)	Mass of leaves for control group (cm)
Experimental 1	0.146	0.221
Experimental 2	0.151	0.089
Experimental 3	0.172	0.157

Figure 5: Table of data for mass of leaves

Leaves of the control group	Diameter of leaves for experimental group(g)	Diameter of the leaves for control group (cm)
Control 1	3.1	2.1
Control 2	3.7	3.2
Control 3	4.5	3.3

Figure 6: Table of data for diameter of leaves

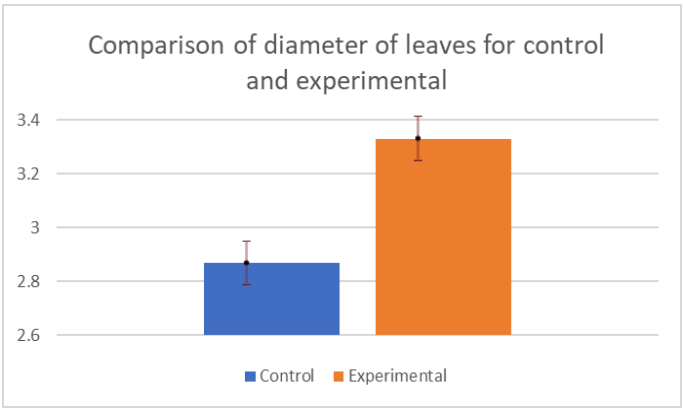

Figure 7: Bar chart of the comparison of the diameter of leaves for the control and experimental groups

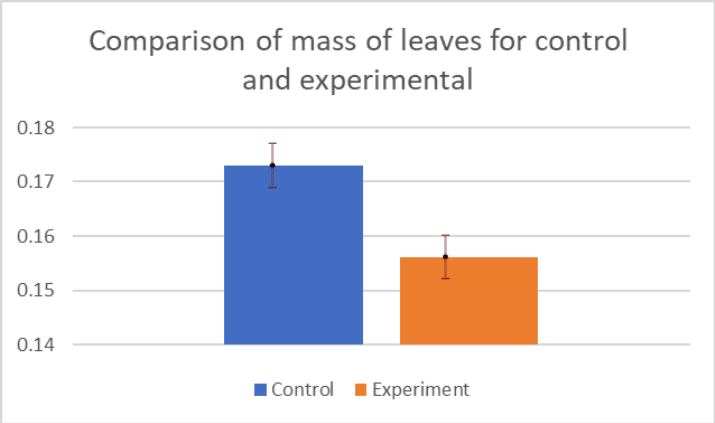

Figure 8: Bar chart of the comparison of the mass of leaves for the control and experimental groups

Potatoes of the control group (g)	Potatoes of the experimental group (g)
0.755	3.265
0.276	2.299

Figure 9: Comparison of the mass of potatoes for the control and experimental groups

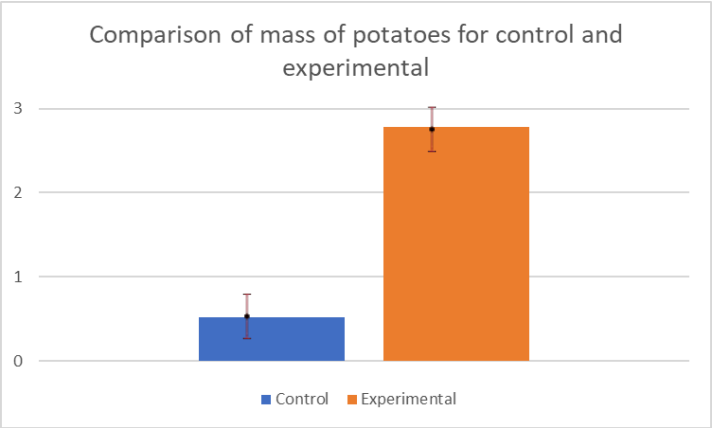

Figure 10: Comparison of data for the mass of potatoes of the control and experimental group

Figure 11: Potato tubers of the experimental group

Figure 12: Potato tubers of the control group

]Description of the Table on Leaf Growth

The first table compares the growth data of potato leaves between the experimental and control groups.

Experimental Group (with *Lactobacillus*):

Sample 1: The average leaf mass was 0.146g, with a diameter of 3.1cm.

Sample 2: The average leaf mass was 0.151g, with a diameter of 3.7cm.

Sample 3: The average leaf mass was 0.172g, with a diameter of 4.5cm.

Control Group (without *Lactobacillus*):

Sample 1: The average leaf mass was 0.221g, with a diameter of 2.1cm.

Sample 2: The average leaf mass was 0.089g, with a diameter of 3.2cm.

Sample 3: The average leaf mass was 0.157g, with a diameter of 3.3cm.

Key Observation: The average leaf diameter in the experimental group (3.1-4.5 cm) was generally larger than that in the control group (2.1-3.3 cm). Regarding leaf mass, the data from the experimental group (0.146-0.172g) were more clustered, while the control group showed greater variation with both a higher (0.221g) and a lower value (0.089g).

Description of the Table on Potato Tuber Yield

The second table directly compares the fresh weight of the harvested potato tubers.

The two tubers from the Control Group (without *Lactobacillus*) weighed 0.755g and 0.276g, respectively.

The two tubers from the Experimental Group (with *Lactobacillus*) weighed 3.265g and 2.299g, respectively.

Key Observation: The mass of potato tubers in the experimental group (2.299g and 3.265g) was significantly higher than that in the control group (0.276g and 0.755g). Notably, the smallest tuber in the experimental group (2.299g) was heavier than the largest tuber in the control group (0.755g).

4. Discussion

The experimental group, which consisted of potato plants with injected Lacticaseibacillus paracasei strain Shirota, exhibited better growth compared to the control group. Some potato plants in the control setup have wrinkled and dull leaves, indicating the plant as unhealthy and nutrient-deprived. On the other hand, the plants in the experimental group all expressed fresh and lush leaves, indicating healthy plant growth. However, the overall difference in the diameter of leaves is small, with the diameter of leaves of the experimental group slightly longer than that of the control. The potato tubers of the experimental group are also significantly larger and heavier than those of the control group by approximately 2g. This shows that *Lactobacillus*, when infiltrated into the soil and absorbed by potato roots, can help in promoting leaf and potato tuber growth.

The experiments prove that *Lactobacillus* can certainly promote plant growth, proving our hypothesis as correct and aligning with other research as a Plant Growth-Promoting Rhizobacteria. The reason the *Lacticaseibacillus paracasei strain Shirota* promotes plant growth should be because it secretes bacteriocins, which inhibit the growth of bacteria. This may help in the growth of potato plants and account for the larger potato tubers in the experimental group.

Possible follow-ups on the project can include investigating how *Lacticaseibacillus paracasei strain Shirota* could help in enhancing plant growth, as the proposed ideas are just theories. We could also test whether *Lactobacillus* affects the nutritional value of the potato itself.

Nevertheless, our project also has some limitations. Yakult is also a sweet drink, which may attract pests such as ants. Diluting the drink is needed, but this may reduce the concentration of *lactobacillus* and therefore the benefits. Even though Yakult is a relatively organic and affordable fertiliser, using it for large-scale farms may be expensive and not economically feasible in the long term.

In conclusion, Yakult is an affordable drink present in numerous countries around the world. The ease to obtain *Lacticaseibacillus paracasei* strain, which is present as the only bacteria in the drink, could make Yakult a low-cost biofertiliser for small-scale farmers. This could greatly improve potato crop yield and quality in developing countries and places where no chemical fertilisers are available. This could help promote sustainable farming in the long run.

5. Conclusion

The experimental results suggest that *Lacticaseibacillus paracasei strain Shirota* can act as a potential Plant Growth-Promoting Rhizobacteria (PGPR), supporting healthier potato growth when compared to the control group. Potato plants treated with the *lactobacillus* showed fresher leaves and larger tubers, indicating improved vitality and yield, but the mechanism is still unknown. Further study on the effect of bacteriocin on the plant growth and soil microbiome might unravel the potential strategies to use Yakult as a low-cost and convenient fertiliser and serve as a feasible option.

6. References

Bhattacharyya, P. N., and D. K. Jha. “Plant Growth-Promoting Rhizobacteria (PGPR): Emergence in Agriculture.” World Journal of Microbiology and Biotechnology, vol. 28, no. 4, 24 Dec. 2011, pp. 1327–1350, https://doi.org/10.1007/s11274-011-0979-9.

Singh, Dhiraj K, et al. “Potatoes: The Food for Nutritional Security.” Potatoes: The Food for National Security, 27 Feb. 2020, www.researchgate.net/publication/339527705_Potatoes_The_Food_for_Nutritional_Security.

King, Janet C., and Joanne L. Slavin. “White Potatoes, Human Health, and Dietary Guidance.” Advances in Nutrition, vol. 4, no. 3, 1 May 2013, pp. 393S401S, https://doi.org/10.3945/an.112.003525.

Silva, et al. “Biotechnological Potential of Lacticaseibacillus Paracasei Shirota for Bioemulsifier, Bacteriocin and Lipase Production.” Brazilian Journal of Microbiology, 10 Oct. 2024, https://doi.org/10.1007/s42770-024-01534-4.

de Medeiros, N.S., da Nóbrega, F.F., Lopes, P.S. et al. Biotechnological potential of Lacticaseibacillus paracasei Shirota for bioemulsifier, bacteriocin and lipase production. Braz J Microbiol 55, 3229–3238 (2024). https://doi.org/10.1007/s42770-024-01534-4

Extraction of Anthocyanin from Blueberry (Vaccinium corymbosum) as a Sensitizer for Dye-Sensitized Solar Cells

Neisya Raharema[1], Luqman Taufiqurrahman[1], Comachi Kuwahara[2], Reika Shimizu[2]

[1]*Budi Mulia Dua International High School (Indonesia)*

[2]*Saijo High School (Japan)*

Abstract:
DSSC are capable of generating electricity from natural and synthetic light sources and generating electrical and thermal power, compared to crystalline silicon solar panels: DSSC offers low cost, the capability to be installed on non-uniform surfaces, and superior electrical performance. Natural dyes with abundant and sustainable sources that could replace the synthetic counterparts in DSSC. In this study, anthocyanin pigments were extracted from blueberries (Vaccinium corymbosum) and evaluated for their feasibility as a natural sensitizer in a DSSC system. The methods were to extract pigment from blueberries, make the TiO_2 paste, apply TiO_2 paste on TCO glass, fire TiO_2 paste on TCO glass, apply the dye, make a counter electrode, assemble DSSC, and measure electricity. The assembled DSSC successfully generated electrical voltage under sunlight exposure. The measured voltage increased with increasing light illuminance, indicating a photoresponsive behavior of anthocyanin-sensitized cells. Therefore, the way of using natural and sustainable resources for DSSC has been achieved. Further studies involving control experiments and efficiency measurements are required to evaluate its performance relative to other sensitizers and to assess its potential for practical applications.

Keywords: Blueberry; Anthocyanin; Dye-Sensitized Solar Cell; TCO glass; TiO_2 paste

1. Introduction

The dye-sensitized solar cells (DSSC) are capable of generating electricity from natural and synthetic light sources and generating electrical and thermal power, compared to crystalline silicon solar panels: DSSC offers low cost, the capability to be installed on non-uniform surfaces, and superior electrical performance (Ghahremani et al., 2024). Alternative options are increasing from time to time; one of the examples is natural dyes with abundant and sustainable sources that could replace the synthetic counterparts in DSSC (Shukor et al., 2023). Anthocyanin is a natural dye with inherent red, blue, and purple pigments that can be found in fruits, vegetables, and flowers. From previous analysis, anthocyanin has been validated as an applicable option of photosensitisers in DSSC. The photosensitiser is responsible for light absorption and initiating electrical flow in DSSC (Shukor et al., 2023). This research has an objective to test anthocyanin from blueberry extract as a sensitizer of dye-sensitized solar cells (DSSC).

2. Methodology

A. Tools and Materials

This study used titanium dioxide (TiO_2) powder, polyvinyl alcohol (PVA) as a binder for the TiO_2 paste, distilled water, 96% ethanol, blueberries, white vinegar as a source of acetic acid, Lugol's solution as an electrolyte (I^-/I_3^-), carbon from the candle wick combustion used as counter electrode, and isopropyl alcohol. The tools used included TCO glass as a conductive substrate, a measuring cylinder, pH indicator paper, a magnetic stirrer, a lab spatula, masking tape, a heating oven, aluminum foil, a pipette, and a multimeter.

B. Procedure

1) Blueberry Pigment Extraction

A total of 25 mL ethanol and 25 mL distilled water were mixed. 6 ml white vinegar with pH 2 was added to the mixture while stirring. About 10 grams of blueberries were crushed and added to the solvent solution. The mixture was stored 24 hours in the refrigerator in a sealed container. Afterward, the solution was filtered to obtain a purple extract.

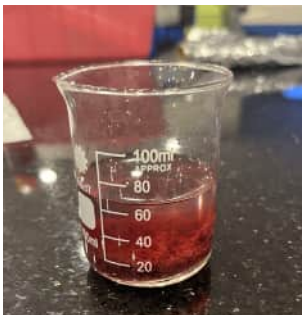

Figure 1. Blueberry Pigment Extraction

2) TiO_2 Paste Preparation

Prepare 2×2 cm² TCO glass with an active area of 1.5×1.5 cm² for electrical testing. The TiO_2 paste was prepared by mixing 1 gram TiO_2 powder, 1.5 grams PVA, and 13.5 mL distilled water. The mixture was stirred using a magnetic stirrer at 45°C for approximately 45 minutes until a homogeneous paste was obtained.

3) TiO_2 Paste Coating on TCO Glass and Heating the TiO_2 Coating

The TCO glass is cleaned using isopropyl alcohol. Masking tape is applied to form a 1.5 × 1.5 cm² square area. TiO_2 paste is applied to the area using a lab spatula until evenly distributed. Then heated in an oven at 250°C for 60 minutes with the TiO_2 layer facing upwards. This process aims to burn the binder and strengthen the TiO_2 adhesion to the substrate. Then, the glass is allowed to cool to room temperature.

4) Dye Sensitization Process

The heated TiO_2 layer was covered again with masking tape to a 1.5 × 1.5 cm² area. Blueberry extract was spread onto the TiO_2 surface, then left for 30 minutes to allow the dye to fully absorb.

5) Counter Electrode Preparation

Masking tape was applied to create a 1.5 × 1.5 cm² area on 2 × 2 cm² TCO glass. The combustion product from the candle wick was then used to create a dense carbon layer.

6) DSSC Assembly

The anode electrode (dye-sensitized TiO_2) and the cathode electrode (carbon) were arranged facing each other, leaving a small gap. 0.25 ml of Lugol's solution were dripped into the gap using a pipette between the two electrodes (Figure 2a). The cell assembly was clamped using binder clips, with the TiO_2 layer facing directly toward the carbon electrode as shown in Figure 2b.

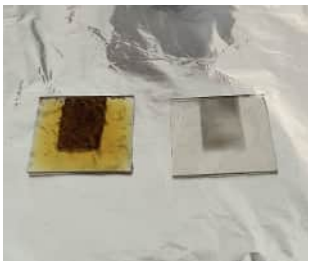

Figure 2a. DSSC assembly process

Figure 2b. DSSC final assembly

7) Electrical Measurements

Electrical properties were measured by connecting a multimeter to the DSSC, with the positive lead connected to the dye-sensitized TiO_2 electrode and the negative lead to the carbon electrode. The cell was then exposed to sunlight. The open-circuit voltage (Voc) was recorded.

Figure 3. DSSC Electrical Measurement

3. Results

Table 1. Light Illuminance & Voltage

Light Illuminance (lux)	**Voltage (mV)**
3600	**280**
7000	**300**
25000	**357**
30000	**522**

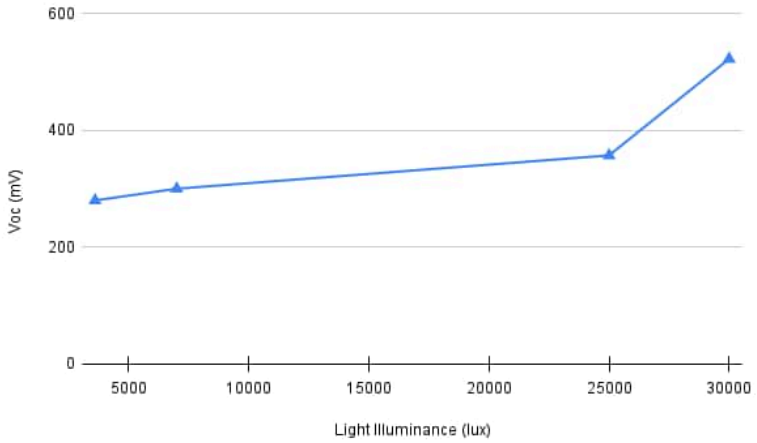

Graph 1. The relation between the given voltage and light illuminance

Based on the graphic, it proves that blueberries can be a sensitizer for dye-sensitized solar cell. From the data it shows the light illuminance increases correspondingly to the voltage, when the number of light intensity increases the number of voltage also increases.

4. Discussion

In a previous journal, the data of voltage are quite comparable with the average voltage 450 mV (Abidin et al., 2020). The rise of the illumination level affects the increase of conductivity of the TiO_2 electrode that makes the voltage increase. The effectiveness of using blueberries as a sensitizer in this DSSC medium requires further research, as it has not been compared to DSSC medium with other sensitizers. Further research is also needed to determine which is more effective compared to other natural sensitizers.

5. Conclusion

Though there is preliminary research on this topic of using blueberry anthocyanin as a sensitizer for DSSC solar cells, we conducted an experiment ourselves. Because the light illuminance increased correspondingly to the voltage in our experiment results, the results indicate that anthocyanin extracted from blueberries can function as a sensitizer under the tested conditions. compared to crystalline silicon solar panels. Alternative options have been coming up such as using natural dye or sustainable resources. This study suggests that blueberry-derived anthocyanin is a potential natural sensitizer for DSSC applications, although further comparative studies are required. Further research is necessary to determine the effectiveness of using blueberries and whether they are a viable alternative to other options. With some further research, we may be able to come up with a solution that solves the problems of generating electricity efficiently and more sustainable.

6. References

Ghahremani, A., Adams, S. D., Norton, M., Khoo, S. Y., & Kouzani, A. Z. (2024). Delamination techniques of waste solar panels: a review. *Clean Technologies*, *6*(1), 280-298. https://doi.org/10.3390/cleantechnol6010014

Shukor, N. I. A., Chan, K. Y., Thien, G. S. H., Yeoh, M. E., Low, P. L., Devaraj, N. K., ... & Yap, B. K. (2023). A green approach to natural dyes in dye-sensitized solar cells. *Sensors*, *23*(20), 8412. https://doi.org/10.3390/s23208412

Abidin, Z., Maulana, E., Mudjirahardjo, P., Fadillah, M.V. (2020). Dye pH variation on blueberry anthocyanin based dye sensitized solar cell. *Bulletin of Electrical Engineering and Informatics, 9*(3), 950-955. https://doi.org/10.11591/eei.v9i3.1969

Differences in Antibacterial and Insect Repellent Properties Among Bitter Gourd (*Momordica Charantia*)

Mutiara Putri Setiawan[1], Muhammad Rayhan Arkana Majid[1], Alif Anggabaya Jalanidi[1], Nanami Oishi[2], Nao Matsumoto[2], Ichika Morihira[2]
[1]*Budi Mulia Dua International High School (Indonesia)*
[2]*Tennoji High School Attached to Osaka Kyoiku University (Japan)*

Abstract:
The increasing prevalence of antibiotic-resistant bacteria has highlighted the need for alternative antibacterial agents derived from natural sources. Bitter gourd (Momordica charantia) contains bioactive compounds such as cucurbitacin, which are known to exhibit antibacterial properties. However, differences in antibacterial activity among various parts of the bitter gourd have not been fully clarified. In this study, the fruit was divided into edible flesh and inner pulp with seeds, and each part was further separated into upper, middle, and lower sections. Extracts from each section were prepared and tested for antibacterial activity against Escherichia coli using agar plate assays. The results showed no significant differences in antibacterial activity among the upper, middle, and lower sections of the bitter gourd. However, the pulp and seed extracts exhibited stronger antibacterial effects than the edible flesh, as bacterial growth was inhibited in areas close to the filter paper. These findings suggest that the inner pulp and seeds of bitter gourd, which are commonly discarded during food preparation, may contain higher levels of antibacterial compounds and have potential for use as natural antibacterial resources.

Keywords: Bitter gourd; antibacterial activity; cucurbitacin; Escherichia coli; natural antibacterial agents; plant extracts

1. Introduction
In recent years, antibiotics have been widely used to treat bacterial infections. However, bacteria that are resistant to antibiotics are increasing and have become a serious problem around the world. Because of this, it is important to find new antibacterial substances that do not depend too much on synthetic antibiotics. Natural substances are especially useful. If antibacterial substances are found in familiar foods, they are safe and easy to obtain. Bitter gourd, also called bitter melon, is a vegetable with a strong bitter taste. One of its bitter components is cucurbitacin. Previous studies have shown that cucurbitacin has antibacterial effects. However, it is not clear which parts of bitter gourd have stronger antibacterial activity. Also, the white inner part of bitter gourd is usually removed and thrown away when cooking, but it may contain useful substances. In this study, bitter gourd was divided into two parts: the edible part and the white inner part. Each part was then divided into upper, middle, and lower sections, making six parts in total. The antibacterial activity of each part was tested using agar plates to see if there were differences between the parts. The purpose of this study was to find out whether the antibacterial activity of bitter gourd is stronger in certain parts and whether the white inner part, which is often discarded, is useful. If these points can be clarified, this research may help with better use of food and the use of natural antibacterial substances.

2. Methodology
【In Indonesia】

1. Preparation of Bitter Gourd (Momordica Charantia)
Fresh bitter gourd was washed thoroughly with water to remove dirt and impurities. The bitter gourd was then sliced into thin pieces, and the seeds along with the inner white pulp were removed, as the bioactive compounds are mainly present in the green outer flesh. The sliced bitter gourd was dried in an oven at approximately 50 °C until completely dry. After drying, the material was crushed using a mortar and pestle (or blender) to obtain a fine powder.

2. Extraction with Solvent

One gram of the bitter gourd powder was placed into a clean glass container. Ethanol was added to the powder in a ratio of 1:3 (w/v), resulting in 3 mL of ethanol per gram of powder. The mixture was stirred to ensure complete contact between the solvent and the plant material. The container was loosely covered with aluminum foil and gently heated at 40–50 °C to enhance the extraction process. After heating, the mixture was allowed to stand at room temperature for 1–2 days to allow diffusion of bioactive compounds into the ethanol.

3. Filtration

After the extraction period, the mixture was filtered using filter paper or gauze to separate the solid plant residue from the liquid extract. The filtrate obtained was the ethanol extract containing dissolved bitter compounds.

4. Concentration

The ethanol solvent was removed by allowing the filtrate to evaporate over warm water. After evaporation, a crude extract remained in the container. This extract contained concentrated bitter compounds, including cucurbitacin, and was used for further observation and analysis.

The process to filtratiom result with experimental equipment: 100 gr bitter gourd, filter paper, blender, 500 mL beaker glass, 3 mL ethanol.

Measure out bitter gourd in pieces

Drying process

Bleding ingredients to powder

Ethanol process in 3 days

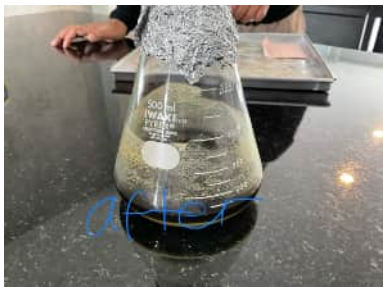

After filtration

【In Japan】

All equipment used in the experiment was sterilized using an autoclave. Agar plates were prepared in advance.

Agar Plate Preparation Method

1. While stirring, 15g of agar, 10g of high-protein peptone, 2g of yeast extract, 1g of $MgSO_4 \cdot 7H_2O$, and 1L of distilled water were thoroughly mixed.
2. The mixture was poured into petri dishes and sterilized in an autoclave along with the other experimental equipment.

The other experimental equipment: 200ml beaker, filter paper, medicine spoon, bacteria spreader, micro tube, micro tip, 200ml of distilled water.

Fig.1 The way it is divided parts **Fig.2** fruit flesh of Bitter gourd **Fig.3** The way of filtering

① The Bitter gourd was divided into top, middle, and bottom sections starting from the stem end. In each section, the pulp and seeds were separated from the fruit flesh. (Fig. 1) (Fig. 2)
② The fruit flesh was ground using a mortar, while the pulp and seeds were finely chopped with a knife.
③ Next, a homogenizer was used to further process the samples into a paste-like consistency. At this stage, distilled water was added to the pulp and seed mixture due to its low moisture content.
④ Each paste was then centrifuged.
⑤ After centrifugation, the supernatant was collected and filtered under vacuum using a bottle-top filter. (Fig.3)
⑥ Powdered E. coli culture medium was mixed with distilled water and filtered through a sterile filter. The filtered solution was incubated overnight in a shaking water bath at 37 °C.
⑦ The cultured E. coli was diluted to 10^{-5}. Using a micropipette, 100 μL of the diluted bacterial suspension was spread onto agar plates with a Conradi rod sterilized over an alcohol lamp.

Each Bitter gourd filtrate was diluted to 10^{-1}, 10^{-2}, 10^{-3}, and 10^{-4}, and 60 μL of each dilution was dispensed onto filter paper placed on the agar plates. To prevent droplets from falling directly onto the agar surface, the petri dish lids were inverted.

The prepared Agar plates were incubated in an electric incubator for 2–3 days.

3.Results

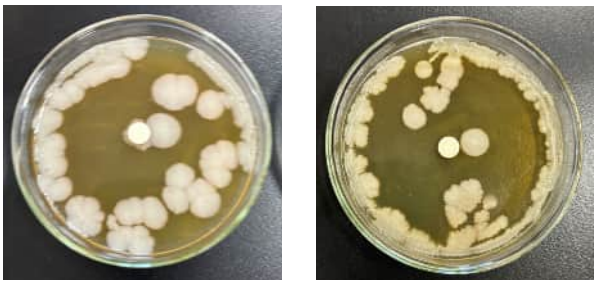

Fig.4 Agar plates of pulp and seeds after culturing

On the agar plates containing the fruit flesh, bacterial colonies grew evenly over the whole surface. In contrast, on the agar plates containing the pulp and seeds, colonies grew only in areas far from the filter

paper. There were no noticeable differences in colony growth among the top, middle, and bottom parts of the bitter gourd.

4. Discussion

Although no significant differences in antimicrobial activity were observed among the upper, middle, and lower sections of the Bitter gourd, the results indicate that the pulp and seeds exhibit greater antimicrobial activity than the edible flesh. This finding may be attributed to previous studies reporting that the pulp and seeds contain higher concentrations of cucurbitacin compared to the edible portion. Future studies should explore the correlation between antimicrobial activity and cucurbitacin content, should further opportunities for experimentation arise.

The antibacterial results discussed in this study were obtained from collaborative data provided by the Japanese research team, as direct antibacterial testing could not be conducted due to experimental limitations.

5. Reflections

- Insufficient experimental planning led to an inadequate number of trials and necessitated last-minute changes to the research theme.
- Failure to thoroughly verify and follow experimental procedures.
- Inadequate review of prior research.
- Insufficient communication with the partner school.
- Realization that sustaining collaborative research was challenging, ultimately resulting in each team pursuing separate research themes.

6.References

Tetsuya Ozeki,(2012),Research on Bitter Component Masking Technology for Health Foods Using Specialized Spray Nozzles
https://www.urakamizaidan.or.jp/research/jisseki/2012/vol21urakamif-01ozeki.pdf

Cucurbitacin B and Its Derivatives: A Review of Progress in Biological Activities by Wenzhe Nie, Yalan Wang, Xinlu Tian, Jinying Liu, Zhanhui Jin, Junjie Xu, Miaohai He, Qingkun Shen, Hongyan Guo, and Tian Luan

Creation of Natural Yeast Bread Utilizing Regional Specialties and Antioxidant Capacity Assay

Shodai Nagano[1], Reiko Inomoto[1], Ayumu Yamamoto[1], Nafeisa Khairunnisa Y.[2], Nathania Setiawan[2], Kannaya Alexandra Sutrisno[2]

[1]*Nara Prefectural Seisho High School (Japan)*

[2]*MUTIARA PERSADA Multi Community School (Indonesia)*

Abstract:

In this international collaborative research, we comparatively evaluated the antioxidant capacity and fermentation applicability of two types of plant-based fermented breads produced using region-derived yeasts: Indonesian sapodilla-based sourdough bread and Japanese rice-flour bread fermented with kudzu-derived yeast. Antioxidant capacity was assessed using the DPPH radical-scavenging assay with 80% ethanol extracts of yeast samples. Among the five kudzu-derived yeast strains, one strain (strain C, provisionally designated as Rhodotorula sp.) exhibited markedly high DPPH radical-scavenging activity. Although kudzu is regarded as an invasive alien species in Japan, utilizing its biomass as a yeast isolation source and fermentation resource may contribute to regional industrial revitalization in Gose City, Nara and to sustainable food systems. This report demonstrates the potential value of underutilized regional plants in enhancing the functionality and diversifying the raw materials of fermented bread.

Keywords: yeast; antioxidant capacity; underutilized plant resources; kudzu; sapodilla

1. Introduction

Growing consumer interest in health and sustainability has increased attention toward alternative fermented bread products such as sourdough and rice-flour bread. Sourdough fermentation has been suggested to improve glycemic response and enhance nutrient bioavailability, while rice-flour bread is valued for being gluten-free and easily digestible. This study investigated the potential application of yeasts isolated from sapodilla fruit, which is abundant in Indonesia, and from kudzu (Yoshino kudzu), an invasive alien species in Japan, as fermentation starters for bread production. In particular, kudzu biomass—typically targeted for removal—was examined as a food resource, to contribute to regional industrial revitalization in Gose City, Nara and to sustainable food systems. This societal relevance was positioned as a key motivation for the study. This study includes the following objectives;

- To compare the antioxidant activities of yeast strains isolated from kudzu leaves and sapodilla using the DPPH radical-scavenging assay with 80% ethanol extracts.
- To conduct provisional species identification of promising yeast strains and select candidates for fermentation applications.

2. Methodology

Samples and Yeast Strains

Kudzu-derived yeasts (Japan):

Five wild yeast strains (A–E) isolated from kudzu leaves were maintained on koji extract medium. A1 and A2 represent independent replicates (sample 1 and sample 2) of the same strain.

Sapodilla-derived system (Indonesia):

Sapodilla fruit was crushed and mixed with a medium containing malt extract, sucrose, and distilled water. After sterilization, the mixture was cultured to promote yeast growth, followed by stepwise cultivation and selective isolation of yeasts on YPD agar plates.

Extraction Solvent and Target Strains

All extractions were performed using 80% ethanol. Water extraction was initially attempted under the same conditions as ethanol extraction; however, no DPPH data were obtained from water extracts. Therefore, all antioxidant evaluations reported here are based on 80% ethanol extracts.

Extraction Procedure

Yeast cells were suspended in 80% ethanol and subjected to ultrasonic treatment (5 min, output according to instrument specifications). After treatment, samples were centrifuged at 5,000 × g for 10

min, and the supernatant was collected. Extracts were concentrated or diluted as needed for measurement and stored at −70°C. The procedure facilitated partial cell disruption.

DPPH Radical-Scavenging Assay

DPPH solution was prepared in 99.5% ethanol, and Trolox was used as the standard. Samples were mixed with the reaction solution, blank-corrected, incubated for 30 min at 25°C in the dark, and absorbance was measured at 517 nm. Each sample was measured in triplicate, and radical-scavenging activity (%) was calculated.

Bread-Making Test (Overview)

Small-scale trial baking was conducted using sapodilla-derived starters and selected kudzu-derived yeasts to confirm basic compatibility with fermentation and baking conditions. Detailed sensory evaluation is not included in this report.

Statistical Analysis

One-way ANOVA and Tukey's multiple comparison test were performed. Sample sizes (n) for each group are shown in the Results section. Normality and homoscedasticity were tested, and data transformation was applied when necessary. SPSS software was used.

3. Results

Premise of Antioxidant Activity Measurements

All antioxidant evaluations were based on DPPH assays using 80% ethanol extracts. No measurable DPPH data were obtained from water extracts.

Strain	Absorbance (517 nm)	Radical-scavenging activity (%)
A1	1.018 ± 0.001	1.84 ± 0.06
A2	0.921 ± 0.000	11.33 ± 0.00
B1	0.894 ± 0.000	13.94 ± 0.04
B2	0.964 ± 0.001	7.11 ± 0.06
C1	0.792 ± 0.000	23.88 ± 0.02
C2	0.766 ± 0.000	26.36 ± 0.01
D1	0.868 ± 0.000	16.50 ± 0.01
D2	0.925 ± 0.000	10.86 ± 0.00
E1	1.019 ± 0.000	1.77 ± 0.01

Figure 1. Absorbance at 517 nm and Radical-Scavenging Activity of Kudzu-Derived Yeast

One-way ANOVA revealed significant differences among strains except between strains A and E ($\alpha = 0.05$). Tukey's test confirmed that strain C exhibited significantly higher DPPH radical-scavenging activity than all other strains. Each group had $n = 3$ (independent extraction and measurement replicates). Morphological observations and contextual characteristics suggested provisional identification as Rhodotorula sp., although definitive species identification requires additional molecular analyses.

4. Discussion

Interpretation of Antioxidant Activity

Strain C showed the highest DPPH radical-scavenging activity based on 80% ethanol extracts, suggesting the involvement of lipophilic antioxidant components such as carotenoids. However, the DPPH assay is an in vitro chemical evaluation and does not directly indicate in vivo effects; therefore, claims regarding health benefits or functional labeling must be made cautiously. Although strain C was provisionally identified as Rhodotorula sp., definitive identification requires sequence analysis of ITS regions, 26S rDNA D1/D2 domains, and phylogenetic analysis. Functional interpretations based on provisional identification should remain limited.

Challenges Toward Practical Application

To apply wild yeasts to fermented foods, evaluations beyond antioxidant capacity are required,

including:

- **Fermentation activity (CO_2 production):** Assessment of leavening ability via CO_2 generation or dough expansion.
- **Tolerance to sugar and salt:** Evaluation of growth and fermentation under high-sugar and high-salt conditions.
- **Baking stability:** Quantification of antioxidant retention during baking.
- **Safety assessment:** Screening for pathogenicity, toxicity, resistance genes, and compliance with food hygiene standards.
- **Identification of active compounds:** Chemical identification and quantification of carotenoids, phenolics, etc. (HPLC, LC–MS).
- **Improved taxonomic identification:** Molecular identification (ITS, 26S) and phylogenetic analysis.

Stepwise evaluation of these factors will enable the selection of starter yeasts that balance functionality and practical usability.

Social Significance

Kudzu is often targeted for removal as an invasive alien species; however, utilizing its biomass as a yeast isolation source and fermentation resource represents a promising approach linking invasive species management with circular use of regional resources. While the potential contributions to regional industrial revitalization in Gose City, Nara and to sustainable food systems are noteworthy, practical implementation requires safety verification, regulatory review, supply-chain development, and collaboration with local stakeholders. Demonstration studies and implementation planning incorporating these elements are future challenges.

5. Conclusion

This study demonstrated that yeasts isolated from sapodilla and kudzu plant resources exhibit antioxidant capacity based on 80% ethanol extracts and may serve as candidates for fermentation applications. In particular, kudzu-derived strain C showed the highest DPPH radical-scavenging activity. Future work should include comprehensive evaluations of fermentation power, stress tolerance, active compound identification, safety assessment, and regulatory compliance, thereby advancing demonstration studies toward circular utilization of regional plant resources.

6. Acknowledgements

We express our sincere gratitude to Inoue Tengyokudo Co., Ltd. and Sanwa Starch Industry Co., Ltd. for their invaluable advice and support throughout this study.

7. References

1) Inoue Tengyokudo Co., Ltd., Fujino, F., Nishio, M., Kitada, Z., Nara Prefectural Institute of Industrial Development, Tsuzuki, M., Ohashi, M., & Shimizu, H. Isolation of useful sake-brewing yeasts from kudzu flowers and development of sake [Kuzu no hana kara no yuyo seishu kobo no bunri to seishu no kaihatsu] (In Japanese).
2) Kazuka, T., Takeda, K., & Nakata, H. (2012). Characteristics of yeasts isolated from enrichment cultures using koji extract medium (In Japanese). Journal of the Brewing Society of Japan, 107(4), 271–278.
3) Yamamoto, A. (2010). Isolation of wild sake-brewing yeasts from cherry blossoms (In Japanese). Bulletin of Hachinohe National College of Technology, 45, 45–48.
4) Tayama, K., Izumi, C., Fujikawa, M., Kanehiro, Y., Mabuchi, R., Okamoto, Y., Takano, Y., & Tanimoto, S. (2016). Isolation of yeasts suitable for rice flour bread making and characteristics of trial breads (In Japanese). Journal of the Japan Society of Food Life Sciences, 27(1), 22–30.
5) Imamura, M. (2012). Descriptive sensory evaluation: Application of the QDA method in product development (In Japanese). Chemistry and Biology, 50(11), 818–822.
6) Dojindo Laboratories. (2025). DPPH radical scavenging activity assay kit (Product No. D678): Technical manual. Dojindo Laboratories.
7) Buzzini, P., Innocenti, M., Turchetti, B., Libkind, D., Mulinacci, N., & Pagnoni, U. M. (2007).

Potential of Rhodotorula species for the production of carotenoids and lipids. FEMS Yeast Research, 7(2), 241–250.
8) Brand-Williams, W., Cuvelier, M. E., & Berset, C. (1995). Use of a free radical method to evaluate antioxidant activity. Lebensmittel-Wissenschaft & Technologie, 28(1), 25–30.
9) Liu, Y., Zhang, Y., & Wang, J. (2020). Isolation and characterization of wild yeast from fruits using Yeast Extract Peptone Dextrose (YPD) medium. Fermentation, 6(1), Article 25. https://doi.org/10.3390/fermentation6010025
10) Mark, R. (2016). How to make wild yeast water. Rosemary Mark. https://www.rosemarymark.com
11) Rahman, A., Putri, D. R., & Hidayat, S. (2021). Utilization of natural yeast from fruits in food fermentation processes. Journal of Science and Technology Innovation, 3(2), 45–52.
12) Suryani, D., Lestari, R., & Pratama, A. (2022). Utilization of natural yeast from mango fruit in bread making. BEST Journal (Biology Education, Science and Technology), 5(2), 45–52.
13) Collar, C. (2008). Enriching nutrition and health through bread: A review. Journal of Food Science and Technology, 45(4), 312–320.
14) Forseth, I. N., & Innis, A. F. (2004). Kudzu (Pueraria montana): History, physiology, and ecology of an invasive plant. Critical Reviews in Plant Sciences, 23(5), 401–413.
15) Kusumawati, N., [Other Authors]. (2020). Utilization of sapodilla (Manilkara zapota) as a source of local yeast for sourdough production. Journal of Indonesian Food and Nutrition, 12(2), 85–94.
16) Maioli, M., [Other Authors]. (2008). Sourdough-leavened bread improves postprandial glucose and insulin plasma levels in subjects with impaired glucose tolerance. Diabetes Care, 31(9), 1784–1786. https://doi.org/10.2337/dc08-0275
17) Minervini, F., [Other Authors]. (2014). Ecological parameters influencing microbial diversity and stability of traditional sourdough. International Journal of Food Microbiology, 171, 136–146. https://doi.org/10.1016/j.ijfoodmicro.2013.11.021
18) Pellegrini, N., & Agostoni, C. (2015). Nutritional aspects of gluten-free products. Journal of the Science of Food and Agriculture, 95(12), 2380–2385. https://doi.org/10.1002/jsfa.7101
19) Poutanen, K., Flander, L., & Katina, K. (2009). Sourdough and cereal fermentation in a nutritional perspective. Food Microbiology, 26(7), 693–699. https://doi.org/10.1016/j.fm.2009.07.011

How Touch Frequency Affects Leaf Closure In Mimosa Pudica

Eita Nagafuchi[1], Karen Sugawara[1], Subaru Takahashi[1], Kasturi D/O Saseekumar[2], Keerthana Sree D/O Gurunathan[2], Liynnette D/O Jeiprakasam[2]

[1]Chiba Prefectural Funabashi High School (Japan)
[2]SMK St. Bernadette's Convent (Malaysia)

Abstract:
This experiment examined the response of Mimosa pudica to repeated mechanical stimulation, focusing on the relationship between touch frequency and leaf closure speed. Specimens from Japan and Malaysia were used to compare responses across locations. Plants were touched at regular intervals, and the speed and completeness of leaf closure were recorded over multiple trials. Initial stimulation caused rapid and complete closure. With repeated stimulation, responsiveness gradually declined, showing slower movement, delayed reactions, or incomplete folding. This indicates habituation to repeated, non-harmful stimuli. The hypothesis was partially supported, as responses varied among specimens. Overall, the study highlights adaptive plant behavior patterns.

Keywords: Mimosa pudica; Mechanical stimulation; Leaf closure; Touch frequency; Responsiveness adaptation

1. Introduction

Mimosa pudica, commonly known as the "sensitive plant," is well known for its rapid leaf-folding response to mechanical and temperature stimuli. When touched, the plant exhibits a sudden movement in which its leaves fold inward, a phenomenon believed to serve as a defensive mechanism against potential threats. This unique behavior makes Mimosa pudica an ideal subject for studying plant sensitivity and adaptive responses.

This experiment focuses on specimens from Japan and Malaysia, providing an opportunity to compare the responsiveness of plants from different regions. Studying these plants allows us to explore how repeated mechanical stimulation affects leaf closure speed and whether habituation occurs over time. Additionally, this study is driven by curiosity about the physiological process behind leaf folding and reopening, a fascinating mechanism that remains not widely understood. By investigating these responses, we aim to gain insight into plant behavior and environmental adaptations.

Figure 1. Mimosa Pudica

Figure 2. Touching Mimosa Pudica

2. Methodology

Preparation

A healthy Mimosa pudica plant was selected for the experiment to ensure accurate and reliable observations. The plant was placed in a well-lit environment with stable temperature and minimal external disturbance. Prior to the experiment, the plant was allowed to rest for 30 minutes so that all leaves were fully open and had recovered from any previous stimulation. This ensured that the plant's responses were solely due to the experimental procedure.

Hypothesis

The hypothesis for this study is that Mimosa pudica will show a measurable and consistent response when exposed to specific external stimuli, and that the movement may vary depending on the type, strength, and frequency of the stimulus.

Setting of Variables

The independent variable in this experiment was the number of touches applied to the Mimosa pudica leaf. The dependent variable was the time taken for the leaf to close after being touched. Controlled variables included light intensity, temperature, watering conditions, type and age of the plant, amount of force applied during each touch, and the time of day. Keeping these factors constant ensured that changes in leaf-closing time were due only to the number of touches.

Experimental Procedure

One leaf was selected for each trial to maintain consistency. The leaf was gently touched using a fingertip to avoid damage to the plant. Touches were applied at fixed frequencies, such as once, depending on the trial. Care was taken to apply the same amount of force during each touch.

Observation and Recording

Immediately after touching the leaf, a stopwatch was started. The response of the leaf was carefully observed, and the time taken for the leaf to close was recorded. All observations were noted accurately to ensure precise data collection.

Repetition of Experiment

After each trial, the leaf was allowed to reopen completely before the next test was conducted. The experiment was repeated three times for each touch frequency to improve the reliability and accuracy of the results. All readings obtained from each trial were recorded.

6. Data Collection and Analysis

The recorded times from repeated trials were used to calculate the average time taken for leaf closure at each touch frequency. The results were organized into a data table for further analysis and interpretation.

3. Results

Table 1. Time required for leaves to close (JAPAN)

	1st plant	2nd plant	3rd plant
1st attempt	2.39	3.39	3.62
2nd attempt	3.37	4.16	1.8
3rd attempt	3.62	5.26	1.34
4th attempt	no data	4.48	3.69
5th attempt	no data	4.91	3.62

The table shows that the leaf closure time of Mimosa pudica from Japan generally increased or became inconsistent with repeated stimulation, indicating reduced responsiveness over time.

Table 2. Time required for leaves to close (MALAYSIA)

	1st plant	2nd plant	3rd plant
1st attempt	2.01	1.28	1.4
2nd attempt	1.54	1.23	1.7
3rd attempt	1.51	0.96	1.11

The table shows that Mimosa pudica from Malaysia closed its leaves faster overall, with only slight changes across repeated attempts, suggesting weaker habituation compared to Japan.

4. Discussion

The results of this study support the hypothesis that Mimosa pudica exhibits a measurable and consistent response when exposed to external stimuli, with the nature of the response varying depending on the frequency of stimulation over time. In the experiment, each leaf was touched only once per trial, following a consistent method and under controlled conditions, including constant light, temperature, and humidity. During the initial attempts, all plants responded quickly, with leaf closure times ranging from 2.39 to 3.62 seconds, indicating that the plants were fully sensitive and capable of responding efficiently to the touch stimulus.

However, as the trials were repeated, the time taken for leaf closure generally increased, and in some cases the leaves did not close fully. This pattern suggests that repeated exposure over time reduces the plant's responsiveness, even when the stimulus is applied only once per attempt. Differences between the three plants, such as the faster responses of Plant 3 in the second and third attempts compared to slower responses of Plant 2, may be due to natural variation in leaf sensitivity, recovery time, or slight differences in leaf condition. The slowing or incomplete closure observed in later trials is likely caused by temporary fatigue or reduced turgor pressure in the motor cells of the leaves, which limits the plant's ability to respond immediately. Overall, the experiment demonstrates that Mimosa pudica not only responds consistently to a single touch stimulus but also exhibits adaptive behavior, adjusting its response when the same stimulus is repeated over time. These findings align with the hypothesis, confirming that the movement of Mimosa pudica is measurable, consistent, and influenced by the frequency of exposure to stimuli.

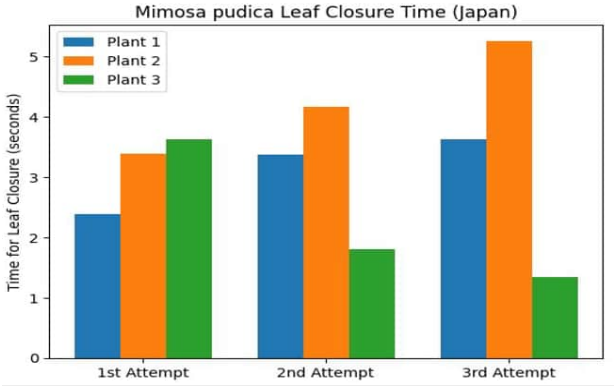

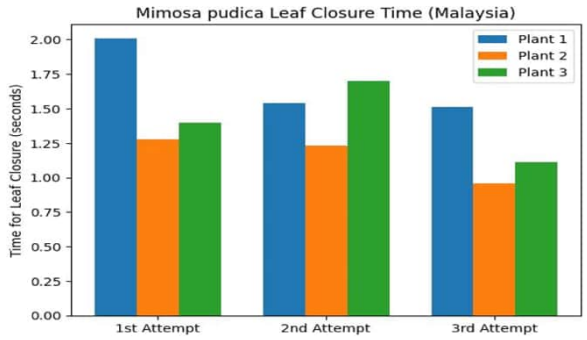

5. Conclusion

The hypothesis of this study stated that Mimosa pudica will show a measurable and consistent response when exposed to specific external stimuli, and that the movement may vary depending on the type, strength, and frequency of the stimulus. Based on the results, the experiment confirmed that Mimosa pudica responds reliably to a single touch, with measurable leaf closure times recorded across all plants. The speed and completeness of leaf closure varied slightly between repeated trials and among different plants, likely due to temporary fatigue or natural differences in sensitivity. Therefore, the hypothesis is accepted, as the plants exhibited a clear, consistent response to the stimulus, and the variations observed align with the expectation that the type and frequency of stimulation can influence the response. Overall, this study demonstrates that Mimosa pudica can detect external stimuli and adjust its behavior accordingly, highlighting the plant's adaptive response mechanisms.

6. Acknowledgements

I would like to express my sincere gratitude to my family for their constant encouragement and support throughout this project. I am thankful to my friends who assisted during the experiment, whether by helping with data collection, observing the plant, or providing moral support during long hours of work. I would also like to sincerely thank the school gardener for helping us locate and provide a healthy Mimosa pudica plant, without which this study would not have been possible. Lastly, I appreciate the availability of resources and materials that allowed this research to be conducted successfully, and everyone who motivated and inspired me to complete this project.

7. References

Britannica. (n.d.). Mimosa pudica: Sensitive plant. Retrieved January 16, 2026, from https://www.britannica.com/plant/sensitive-plant

Nature Communications. (2022). Rapid leaf movement in Mimosa pudica triggered by electrical and calcium signaling. Nature Communications. Retrieved January 16, 2026, from https://www.nature.com/articles/s41467-022-34106-x

MDPI Plants. (2020). Mechanism of thigmonastic movement in Mimosa pudica. Plants, 9(5), 587. https://www.mdpi.com/2223-7747/9/5/587

Pearson Education. (n.d.). Leaflets of Mimosa pudica (sensitive plant, touch-me-not). Retrieved January 16, 2026, from https://www.pearson.com/channels/biology/asset/abe00017/leaflets-of-mimosa-pudica-common-names-sensitive-plant-touch-me-not-have-a-remar-3

Eco-friendly paper

Himeno Nakayama[1], Ryoka Ono[1], Saeka Nishibori[1], Dharmini a/p Jayandaran[2], Nur Alia Natasha Binti Abdul Hafiz[2], Sharon a/p Michel[2]
[1]*Ichijô Senior High School (Japan)*
[2]*SMK St Bernadette's Convent (Malaysia)*

Abstract:
This research explores producing recycled paper from food and agricultural waste in Japan and Malaysia, using orange peels, banana stem fibers, and eggshells to reduce waste and create eco-friendly alternatives. Banana stem fibers were processed into pulp and formed into paper sheets, then coated with an eggshell–starch layer, while orange peel fibers were mixed with calcium carbonate to produce paper sheets. Results showed that banana stem paper with eggshell coating was smoother, whiter, stronger, and moderately flexible, with no cracking under light bending. In contrast, orange peel and pineapple peel sheets were brittle, though orange peel paper remained light and retained its shape. Fiber type and the form and application method of calcium carbonate were found to greatly influence paper quality. Despite some limitations, both projects demonstrate the potential for creating decorative, craft, or temporary packaging materials from waste, highlighting the environmental significance and potential for further optimization of sustainable paper production.

Keywords: natural fibers; eco-friendly materials; food waste recycling; Sustainable development; Recycled paper

1. Introduction

Our research focuses on making recycled paper from food waste. Food loss is a serious problem in Japan, Malaysia, and around the world, and we wanted to find a way to reduce food waste by reusing parts of food that are usually thrown away. In Japan, about 2.33 million tons of food waste come from households every year, and one common example is fruit peels, with orange peels being the most frequently discarded fruit peels in Japanese homes. Similarly, in Malaysia, large amounts of agricultural and food waste are generated daily, including fruit waste and plant residues from farming activities. A previous study by Uwajima Higashi High School in Ehime Prefecture attempted to make paper using kaya leaves and orange peels, showing that paper can be produced from plant fibers but was not strong enough, which inspired further exploration of alternative waste materials. Another common food waste is eggshells; in Japan, more than 200,000 tons of eggshells are discarded every year, accounting for about 80% of all eggs used, and previous studies have shown that eggshells can be used in paper production to improve paper properties. Eggshell waste is also commonly produced in Malaysia from households and food industries. Based on these facts, we decided to use orange peels and eggshells in Japan, and banana stems and eggshells in Malaysia, which are familiar foods and agricultural wastes, to produce eco-friendly paper. This research contributes to Sustainable Development Goals (SDGs) Goal 12 (Responsible Consumption and Production) and Goal 15 (Life on Land).

2. Methodology

Japanese Team Method: The Japanese team produced paper using orange peel fibers with calcium carbonate and cornstarch as a binder. After multiple trial-and-error attempts, the final method involved heating the mixture, followed by blending to form a fiber pulp. The pulp was then formed into sheets and dried. This final trial produced the material closest to paper, forming thin, sheet-like structures, although the material remained relatively fragile.

Malaysian Team Method: The Malaysian team initially attempted paper production using pineapple peels mixed with eggshell-derived calcium carbonate and cornstarch; however, the material became brittle after drying due to the separation of the calcium carbonate. The method was then improved by switching to banana stem fibers. The fibers were cleaned, soaked, boiled, and blended to form pulp, which was shaped into paper sheets using a mould and deckle. After drying, eggshell-derived calcium carbonate was applied as a surface coating using a starch binder to improve surface quality.

Table 1. Measurement of the ingredients

Parameter	Japanese Team (Orange Peel Paper)	Malaysian Team (Banana Stem Paper
Fiber source	Orange peels	Banana stem
Water volume (ml)	600	480
Fiber mass (g)	33	297
Calcium carbonate amount (g)	6	8

3. Results

Paper sheets were successfully produced using both banana stem fibers and orange peel fibers with the addition of calcium carbonate. The banana stem fibers formed paper sheets with a relatively flat structure. After applying an eggshell-derived calcium carbonate coating, the banana stem paper appeared visibly whiter, smoother, and more uniform, with improved surface firmness and moderate flexibility. No cracking was observed during light bending of the coated banana stem paper. In contrast, orange peel fibers mixed with pure calcium carbonate produced a thin sheet with a wavy surface. After drying, the orange peel paper became hard and dry with very limited flexibility and cracked easily when bent. Although it could not be used in the same manner as conventional paper, the orange peel material was light, thin, and maintained its shape, giving it a paper-like appearance and indicating potential for non-functional applications.

Table 2. Comparison of Banana Stem Paper and Orange Peel Paper

Property	Banana Stem Paper (Eggshell $CaCO_3$ Coating)	Orange Peel Paper ($CaCO_3$ in Pulp
Fibre source	Banana stem	Orange peel
Calcium carbonate source	Eggshell-derived	Commercial (pure)
Method of $CaCO_3$ application	Surface coating	Mixed into pulp
Surface appearance	Smooth, uniform	Wavy, uneven
Colour	Whiter	Light brown/orange

Firs**t** attempt

Second attempt

Figure 1. Banana Stem Paper

first attempt

second attempt

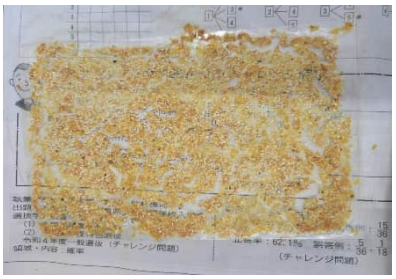

Figure 2. Orange Peel Paper

4. Discussion

Both the Malaysian and Japanese teams observed that the method of adding calcium carbonate and the type of fiber used significantly affected the quality of the paper. The Malaysian team found that mixing eggshell-derived calcium carbonate directly into pineapple peel pulp caused the sheets to become brittle due to separation after drying. However, when they switched to banana stem fibers and applied the calcium carbonate as a surface coating instead, the paper became smoother, whiter, firmer, and retained its flexibility. Similarly, the Japanese team also experienced brittleness when eggshell powder was mixed into orange peel pulp. Replacing it with pure commercial calcium carbonate improved sheet formation and reduced brittleness, resulting in a more stable paper-like material.

In nutshell, both studies show that fiber type and the form and method of calcium carbonate application play crucial roles in determining the quality of paper. Improper mixing methods can cause brittleness, while suitable fibers and surface coating techniques can improve smoothness, strength, and flexibility. These findings highlight the importance of optimizing materials and processing methods to enhance the performance of eco-friendly paper made from waste materials.

5. Conclusion

Both the Malaysian and Japanese teams explored the use of food and agricultural waste to create eco-friendly paper-like materials. The Malaysian team successfully produced paper from banana stem fibers and enhanced its quality by coating it with eggshell-based calcium carbonate, which improved its whiteness, surface smoothness, and strength. Meanwhile, the Japanese team developed paper from orange peels, which, although not very strong or flexible, was lightweight, thin, and able to retain its shape. This made it suitable for decorative purposes, crafts, and temporary packaging. Together, these projects demonstrate that waste materials can be repurposed into useful, sustainable alternatives to conventional paper.

In conclusion, both projects highlight the strong potential of using food and agricultural waste to produce environmentally friendly paper-like materials. Paper made from orange peels proved to be lightweight and shape-retaining, making it suitable for decorative and temporary uses, while paper made from banana stem fibers and coated with eggshell-based calcium carbonate showed improved strength, smoothness, and whiteness. Despite certain limitations, these studies emphasize the importance of waste reuse and show that with better materials, testing, and methods, the quality and performance of such eco-friendly paper can be further improved in the future.

6. Acknowledgements

We would like to acknowledge the collaborative efforts between the participating schools in Japan and Malaysia, which made this joint research project possible. We also thank our families and local communities for providing food and agricultural waste materials used in this study. In addition, we appreciate the support of external organizations and previous studies that inspired our research on sustainable paper production.

7. References

Leong, S. K., & Abd Rahman, R. (2007). Potentiality of banana (Musa) stem as raw material in chemical non-wood pulping. Science Research Journal, 4(1), 1–8. https://journal.uitm.edu.my/ojs/index.php/SRJ/article/view/3442

Nik Idris, N. F., & Nik Yusuf, N. A. A. (2021). Investigation and properties of waste banana peel composite for paper making consist of egg shell. Malaysian Journal of Bioengineering Technology, 3(1), 15–22. https://journal.umk.edu.my/index.php/mjbet/article/view/1542

Adli, M. H. Z., Sharil, M. A. M., & Nawi, A. A. (2023). Paper bag production using banana stem via kraft pulping process. Malaysian Research in Industrial Engineering, 6(2), 45–52. https://penerbit.uthm.edu.my/periodicals/index.php/mari/article/view/9345

Uwajima Higashi High School
https://uwajimahigashi-h.esnet.ed.jp/uploads/r31nen11.pdf

Consumer Affairs Agency, Government of Japan
https://www.no-foodloss.caa.go.jp/whats.html

Design, Fabrication, and Experimental Evaluation of Toroidal Propellers

Miyu Masutani[1], Ten Nakagawa[1], Jim Albrecht S. Cadion[2], Chad Dejon V. Cervantes[2], Angelo Paulo L. Tabang[2]

[1]*Ichijo high school (Japan)*

[2]*Philippine Science High School - Eastern Visayas Campus in Leyte (Philippines)*

Abstract:

Propellers play a crucial role in the performance of aerial and marine vehicles by converting rotational motion into thrust for the mobility of the vehicle. Conventional propellers have been extensively studied and optimized; however, recent interest has emerged in an alternative design like the toroidal propellers due to their potential advantages in noise reduction and flow efficiency. Despite the claims made for this propeller design, experimental data on toroidal propellers remain limited, particularly at small scales suitable for unmanned aerial systems.To address both quantitative performance and practical feasibility, we employed two complementary experimental approaches. A controlled thrust measurement setup was used to obtain thrust, power, and efficiency data, while a lightweight motor–propeller configuration was tested to evaluate the ability of the toroidal propeller to generate sufficient lift, based on its geometry. Together, these approaches can provide a comprehensive evaluation of toroidal propeller behavior. The project's findings indicate that conventional propellers consistently produced higher thrust coefficients than the toroidal propeller across all tested rotational speeds, with the toroidal propeller demonstrating lower power coefficients and relatively higher efficiencies. However the toroidal propeller design was unable to generate sufficient thrust for lift in the qualitative motor experiment. This limitation is attributed to constraints in blade thickness, width, and pitch angle. Overall, the results suggest that while toroidal propellers may offer efficiency advantages under specific operating conditions, their performance is highly dependent on geometric optimization, and without appropriate design refinement, they may be unsuitable for small-scale applications requiring significant thrust.

Keywords: toroidal propeller; thrust coefficient; power coefficient; efficiency; additive manufacturing

1. Introduction

Propellers are essential components in propulsion systems, where their design affects thrust, efficiency, and overall performance. Conventional propellers, with distinct blade tips, are widely used due to their simple design and established performance. Toroidal propellers, featuring a continuous looped blade, are proposed to reduce tip vortices, potentially improving efficiency and reducing noise. This project experimentally compared toroidal and conventional propellers using two approaches. First, conducted by the Philippine students, a thrust-measuring stand quantified performance parameters such as thrust, revolutions per minute, and power consumption. Second, conducted by the Japanese students, a toroidal propeller was tested for the flight of a lightweight mass. These experiments can provide practical insight into the advantages and constraints of toroidal propeller designs at small scales.

2. Methodology

2.1 Overall Experiment Workflow

Figure 1 Overall Experimental Workflow

The overall methodology followed a sequential process from propeller design to data analysis. A flowchart summarizing the complete experimental procedure is shown in Figure 1, illustrating the relationship between design, fabrication, calibration, testing, and post-processing stage. The project started with the 3D modelling of the propellers with equal diameters of 200cm through an open-source Computer-Aided Design (CAD) platform Tinkercad. Software programming was then done to account for the python and arduino codes for sensor calibration, propeller disk area

computation, experiment proper, and data reading through serial communication. After confirmation of equal propeller disk areas, the propellers were then created through additive manufacturing. Before beginning the experimental data collection, the 1kg Load Cell and HX711 amplifier, ACS712 current sensor, and 30A Electronic Speed Controller (ESC) were calibrated to ensure accurate data readings. The ESC was operated within the 0–1 A range during testing to capture low-current propeller performance accurately. Parameters such as time, throttle, current, voltage, power, thrust, and RPM were measured through nine tests to increase the reliability of measured data, with each test having 47 incremental throttle configurations of 10 from ranges 1000 µs-1470 µs. This extensive range allowed the capture of propeller performance across low to moderate speeds, providing a robust dataset for calculation of thrust coefficient, power coefficient, and efficiency. The Python data-acquisition software was programmed to let logged data be post-processed to Excel and enabled analysis of trends, statistical evaluation of consistency, and comparison between the toroidal and conventional propellers under controlled experimental conditions.

2.2 Experimental Setup 1

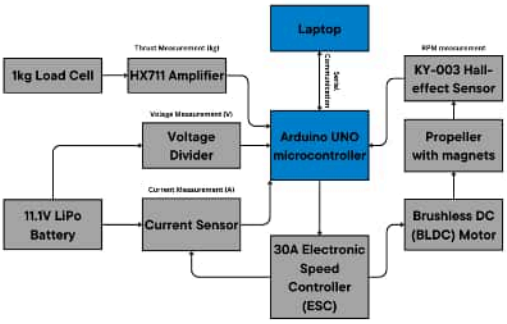

Figure 2 General System Architecture Diagram

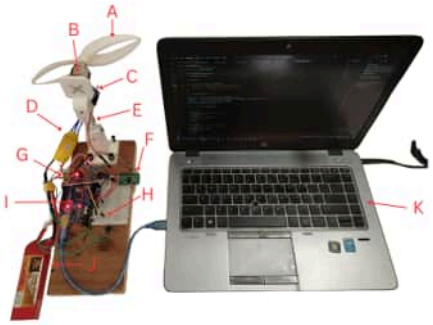

Figure 3 A: Propeller, B: BLDC Motor C: KY-003 Hall-effect Sensor, D: 30A ESC, E: 1kg Load Cell, F: HX711 amplifier, G: ACS712 current sensor, H: Voltage Divider, I: Arduino UNO microcontroller, J: 11.1V LiPo Battery, K: Laptop

Figures 2 & 3 show the system architecture and the actual experimental setup, respectively. The system architecture diagram illustrates all hardware connections, including the microcontroller, ESC, motor, sensors, voltage divider, battery, and the computer running the Python data acquisition software. The experimental setup picture highlights the physical arrangement of these components, with labels for the motor, load cell, Hall-effect sensors, voltage divider, microcontroller, battery, and computer.

The setup was designed to measure thrust, rotational speed, and electrical power of the propellers under controlled conditions. A brushless DC motor mounted on a thrust stand was controlled via PWM signals from the Arduino UNO microcontroller. Thrust was measured using a 1kg load cell with HX711 amplifier, rotational speed via a KY-003 Hall sensor and propeller magnet, and electrical power from the voltage divider and ACS712 current sensor. Both propellers were fabricated to have equal blade area and diameter for a fair comparison. Sensor readings and motor control were synchronized and logged in real time, with nine trials conducted per propeller. Post-processed data were automatically tabulated in Excel using the Python program and was used to calculate propeller efficiency as well as thrust and power coefficients with the following equations for static propeller testing:

$$\eta = \frac{Thrust}{Power}$$

Eq. 1 Propeller Efficiency

$$C_t = \frac{Thrust}{\rho n^2 D^4}$$

Eq. 2 Thrust Coefficient

$$C_p = \frac{Power}{\rho n^3 D^5}$$

Eq. 3 Power Coefficient

The propeller efficiency (η) was calculated as the ratio of output thrust force in Newtons (N) to electrical input power in Watts (W), as shown in Eq. 1. Thrust coefficient (C_t) and power coefficient (C_p) were calculated using Eq.2 and Eq.3 respectively, which accounts for air density (ρ) of 1.225 $\frac{kg}{m^3}$ at sea level, rotations per second (n), and a constant propeller diameter (D) of 0.2m, allowing a dimensionless comparison between the toroidal and conventional propellers.

2.3 Experimental Setup 2

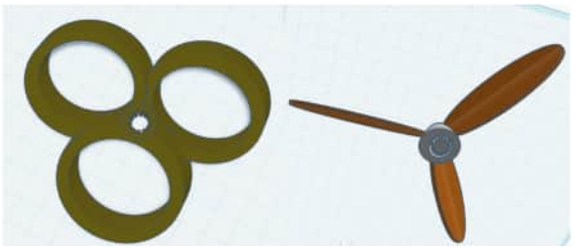

Figure 4 3D model of Propellers

Figure 5 Experimental Setup 2

The experimental process began with the design of a propeller using the CAD software Tinkercad as shown in Figure 4.. Several propeller models were created digitally, after which the finalized design was fabricated using a 3D printer. The printed propeller was then mounted onto a 3 V DC motor manufactured in Japan and powered by an AA battery.

Figure 5 shows the experimental setup used. To evaluate the basic thrust capability of the propeller, the motor–propeller assembly was tested under stationary conditions. To minimize the total system mass and isolate the performance of the propeller, the battery was kept on the ground, while only the motor and propeller assembly were allowed to operate freely. The setup was intended to determine whether the propeller alone could generate sufficient thrust for lift.

3. Results

3.1 Results for Experiment 1

After nine experimental trials, where time, throttle input, current, voltage, power, thrust, and RPM were recorded. These measured parameters were subsequently used to calculate the C_t, C_p, and propeller efficiency. As summarized in Table 1, the normal propeller consistently exhibited higher thrust coefficients across the tested rotational speed range, indicating greater thrust production. In contrast, the toroidal propeller demonstrated lower power coefficients and significantly higher efficiencies, particularly at higher rotational speeds. This trend suggests that while the toroidal propeller generated less thrust overall, it operated more efficiently by requiring less power relative to thrust produced. These results highlight a trade-off between thrust generation and efficiency when comparing conventional and toroidal propeller geometries.

NORMAL PROPELLER				TOROIDAL PROPELLER			
RPS	C_t	C_p	Efficiency	RPS	C_t	C_p	Efficiency
13.565	0.411	5.723	0.002	15.206	0.064	4.625	0.045
13.565	0.665	5.899	0.004	15.206	0.072	4.729	0.049
21.765	0.394	1.375	0.005	17.317	0.064	3.289	0.055
21.765	0.484	1.396	0.006	17.317	0.071	3.435	0.058
26.380	0.387	0.696	0.007	19.365	0.062	2.419	0.065
26.380	0.434	0.812	0.007	19.365	0.071	2.528	0.072
29.300	0.389	0.591	0.009	21.302	0.066	2.021	0.075
29.300	0.440	0.608	0.010	21.302	0.072	1.997	0.084
34.696	0.376	0.397	0.011	23.615	0.065	1.553	0.086
34.696	0.416	0.407	0.012	23.615	0.072	1.565	0.095
38.435	0.366	0.306	0.013	25.983	0.065	1.207	0.102
38.435	0.389	0.336	0.013	25.983	0.070	1.233	0.108
40.981	0.368	0.243	0.014	27.841	0.066	1.049	0.111
40.981	0.391	0.287	0.014	27.841	0.071	1.065	0.117
43.487	0.363	0.217	0.015	30.598	0.062	0.798	0.125
43.487	0.390	0.208	0.016	30.598	0.063	0.838	0.121
45.839	0.369	0.204	0.016	33.180	0.059	0.694	0.125
45.839	0.387	0.192	0.016	33.180	0.064	0.721	0.131
47.909	0.371	0.171	0.016	35.317	0.060	0.620	0.135
47.909	0.388	0.201	0.017	35.317	0.063	0.626	0.141
50.028	0.369	0.150	0.018	36.446	0.062	0.604	0.139
50.028	0.386	0.158	0.018	36.657	0.063	0.596	0.142
51.904	0.372	0.148	0.018	39.391	0.058	0.493	0.146
51.904	0.384	0.152	0.018	39.496	0.062	0.524	0.146
53.852	0.369	0.139	0.018	40.983	0.060	0.476	0.152
53.852	0.384	0.142	0.019	40.996	0.061	0.483	0.152
55.991	0.376	0.130	0.019	42.798	0.061	0.451	0.154
55.991	0.396	0.133	0.020	43.191	0.063	0.441	0.162
58.493	0.377	0.119	0.020	44.817	0.061	0.403	0.165
58.493	0.387	0.119	0.020	45.080	0.063	0.422	0.162
59.909	0.379	0.116	0.020	46.859	0.061	0.395	0.162

Table 1 RPS, C_t, C_p, and Efficiency Data Table for Both Propellers

3.2 Results for Experiment 2

During testing, the fabricated toroidal propeller was unable to generate sufficient thrust to achieve lift. Several design-related factors were identified as possible causes of this outcome. First, the propeller was excessively thin, which limited its ability to effectively interact with the surrounding air and generate thrust. Second, the propeller lacked sufficient thickness and blade width, reducing the volume of air displaced during rotation and resulting in weak forward force. Third, the blade angle was nearly flat, preventing effective backward air acceleration, which is essential for thrust generation.

4. Discussion

4.1 Discussion for Experiment 1

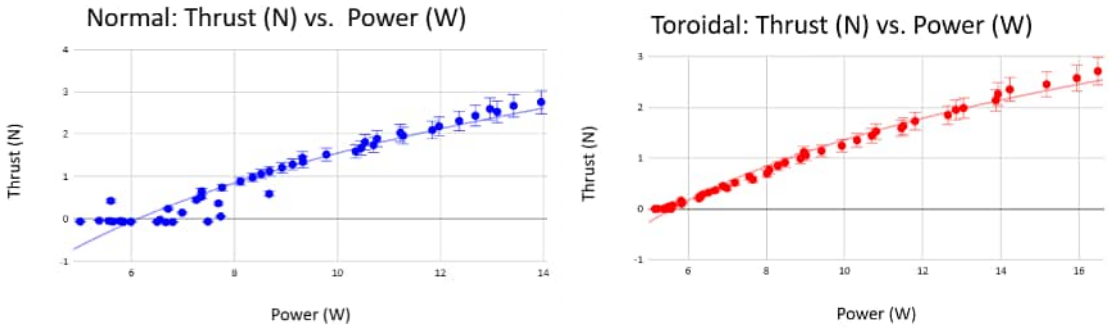

Figure 6 Thrust (N) vs Power (W)

For the Thrust (N) vs. Power (W) graphs, both the normal and toroidal propellers follow a nonlinear, logarithmic trend. However, the normal propeller gains small amounts of thrust at low power levels and increases rapidly as power rises before leveling off at higher power levels. This suggests that the normal propeller performs less consistently at lower power levels. On the other hand, the toroidal propeller follows a tighter and more consistent spread as the power level increases, although it still gains small amounts of thrust at lower power levels that levels off at higher power levels.

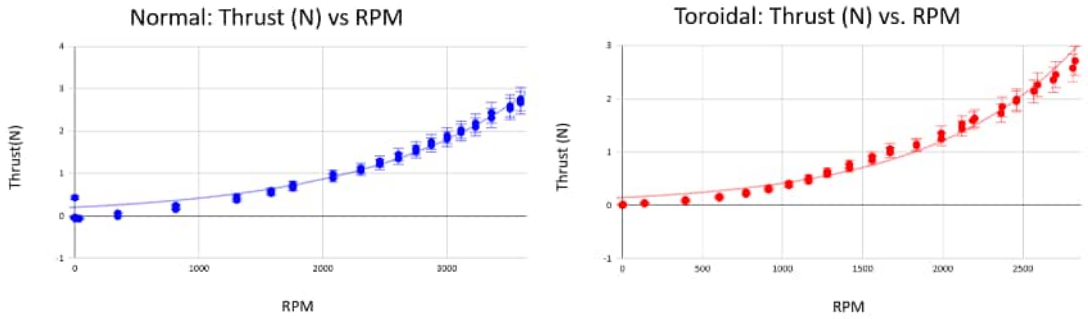

Figure 7 Thrust(N) vs Revolutions per Minute (RPM)

For the Thrust (N) vs. RPM graphs, the normal and toroidal propeller follow an exponential trend. For the normal propeller, thrust increases with RPM exponentially, At low RPM, thrust remains around zero and even slightly negative at times, indicating minimal thrust generation. As RPM increases, thrust rises rapidly and the scatter becomes more consistent, while at low RPM, the scatter shows less consistency. For the toroidal propeller, it exhibits a smoother and more consistent performance across different RPM ranges. Thrust remains around zero at lower RPM, and increases steadily as the RPM increases.

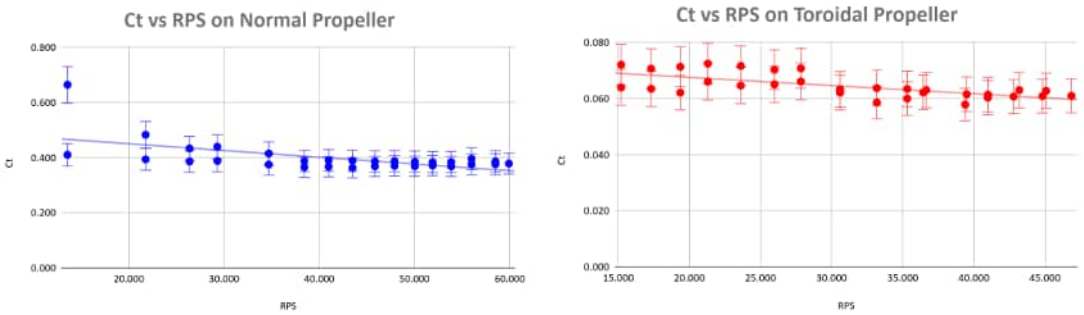

Figure 8 Thrust Coefficient (C_t) vs Rotations per Second (RPS)

For the normal propeller, the thrust coefficient (C_t), remains relatively high across the entire RPS range, generally fluctuating between about 0.36 and 0.40. While there were some variations observed at different rotational speeds, no significant increasing trend with RPS is evident. This means that the normal propeller consistently produced thrust proportional to its rotational speed.

On the other hand, the toroidal propeller showed significantly lower C_t values, ranging only from about 0.058 to 0.072. Similar to the normal propeller, C_t does not vary significantly with increasing RPS, suggesting stable thrust behavior. However, when compared, the toroidal propeller generates significantly lower thrust coefficients at all operating speeds, implying reduced thrust production for the same rotational input.

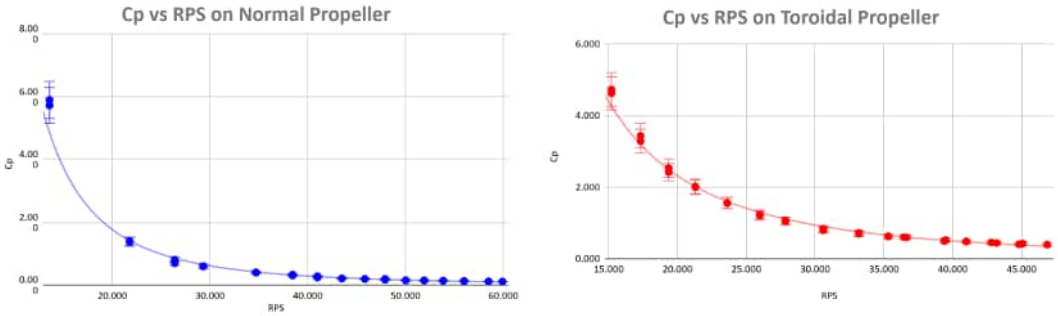

Figure 9 Power Coefficient (C_p) vs Rotations per Second (RPS)

In both graphs, the C_p and the RPS exhibit a power-law decay relationship. For the normal propeller, at low rotational speeds, the power coefficient is significantly high, exceeding 5.7, but decreases rapidly as RPS increases. As rotational speed continues to increase, the rate of decrease diminishes, and C_p approaches a lower bound of approximately 0.12 to 0.15 at high RPS.

On the other hand, for the toroidal propeller, although its C_p decreases with increasing RPS just like the normal propeller, the decline is more gradual, with values decreasing from around 4.6 at low RPS to about 0.40 to 0.60 at higher RPS. This means that the toroidal propeller maintains a relatively lower power coefficient across its operating range.

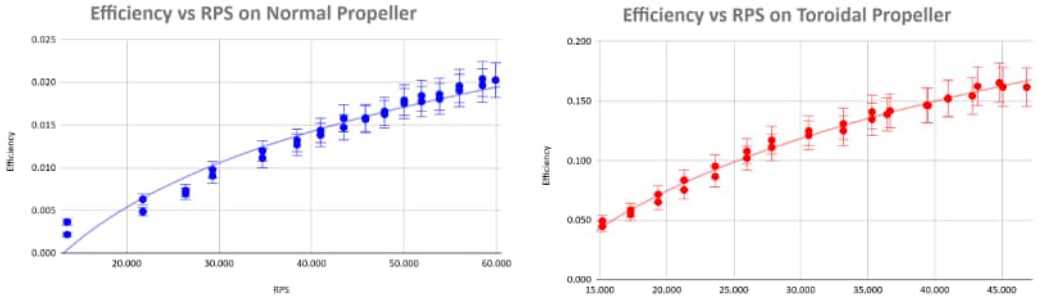

Figure 10 Efficiency vs Rotations per Second (RPS)

In both graphs, the efficiency and RPS show a logarithmic relationship. For the normal propeller's efficiency, it increases steadily as RPS increases. At low rotational speeds, efficiency values are extremely low (near 0.002 to 0.004), but they gradually rise as RPS increases, reaching a maximum of approximately 0.020 at the highest tested speeds. Despite this increase, the overall efficiency remains relatively low throughout the operating range.

On the other hand, the toroidal propeller demonstrates significantly higher efficiencies at all measured rotational speeds. Even at low RPS, efficiency values are already above 0.04, and they continue to increase with RPS, reaching values as high as 0.16. This indicates that the toroidal propeller converts input power into useful thrust much more efficiently than the normal propeller. Particularly at higher rotational speeds.

4.2 Discussion for Experiment 2

The primary factors contributing to the failure of the propeller to achieve lift were the insufficient blade thickness, inadequate blade width, and the absence of an appropriate blade pitch angle. These results highlight the importance of proper geometric parameters in propeller design. The experiment demonstrated that adequate thickness, width, and blade angle are critical for generating lift. With improvements to these design aspects, the propeller is expected to perform more effectively in future iterations.

5. Conclusion

This study experimentally compared toroidal and conventional propellers using both controlled thrust measurements and a qualitative lift evaluation. Results from the thrust stand experiment showed that the conventional propeller consistently produced higher thrust coefficients across all tested rotational speeds, while the toroidal propeller exhibited lower power coefficients and higher efficiencies, particularly at higher rotational speeds. However, the toroidal propeller was unable to generate sufficient thrust to achieve lift in the lightweight motor experiment, primarily due to limitations in blade thickness, width, and pitch angle. These findings indicate that although toroidal propellers may offer improved efficiency under certain operating conditions, their overall performance is highly dependent on geometric optimization. Consequently, without appropriate design refinement, toroidal propellers may be unsuitable for applications requiring significant thrust at small scales.

6. Acknowledgements

We acknowledge Nikus in Circuits for providing an open-source thrust stand design, which was utilized to streamline the design process of the project.

7. References

Pugna, A., Hrab, C., Hînsa, L. N., Hopârtean, A., Giurgea, C. M., & Marcu, L. (2025). Development of an experimental setup for propeller performance measurements. In *E3S Web of Conferences* (Vol. 608, p. 02013). EDP Sciences.

Žagar, L., & Jamšek, M. (2023). Comparison and analysis of toroidal and classic propellers.

Nikus in Circuits. (2021, July 12). *Brushless motor thrust stand*. Instructables. https://www.instructables.com/Brushless-Motor-Thrust-Stand/

Comparative Study On The Biodiversity Of Native Trees Found In Japan And The Philippines

Naoki Hayashi[1] , Soma Iwamoto[1] , Kotoha Kimura[1] , Keita Kodama[1]
Xyra Mae Bardelosa[2], Kimberly Zaine Eloy[2], Iris Glare Gullemas[2]
[1]*Akashi Kita High School (Japan)*
[2]*Philippine Science High School - Eastern Visayas Campus in Leyte (Philippines)*

Abstract

Forests play a crucial role in sustaining biodiversity. Lucidophyllous forests widely distributed in western Japan generally support lower biodiversity than tropical forests but maintain relatively high diversity among temperate forest ecosystems. In contrast, tropical rainforests in Southeast Asia, including the Philippines, are recognized for their exceptionally high species diversity and serve as home to many of the world's most species-rich ecosystems. This study employed a descriptive-comparative research design to assess and compare forest biodiversity between selected sites in Japan and the Philippines, with a focus on native tree species composition. Results showed that Japan recorded a slightly higher species richness (13 species) than the Philippines (11 species). Both study sites exhibited very high evenness of native tree species, with Japan (E = 0.7911) and the Philippines (E = 0.9462), indicating a balanced distribution of individuals among established taxa. However, species diversity was higher in the Philippine study site (H′ = 2.2689) than in Japan (H′ = 1.7185), although overall diversity indices in both countries remained relatively low. These findings suggest that while native tree species are evenly distributed, the total number of species constituting the forest ecosystems is limited, underscoring potential constraints on forest biodiversity in both countries. Therefore, it is recommended that future studies expand sampling areas and incorporate long-term monitoring to better capture species variability and support the development of effective, site-specific forest conservation and management strategies.

Keywords: forest biodiversity; native tree; Diversity index; Evenness index

---

1. Introduction

Biodiversity is fundamental to the health and stability of ecosystems, underpinning the complex interactions among organisms that sustain essential ecological processes (World Health Organization: WHO, 2025). Forests are among the most species-rich ecosystems, supporting diverse plant and animal life while providing essential services such as climate regulation, water cycling, and soil stabilization (Wang et al., 2025). Native tree species within these systems have co-evolved with local fauna and microbes, contributing to a balanced and resilient environment (*OCW Article Series*, n.d.). Forest conservation is therefore considered a key strategy in addressing biodiversity loss and climate change challenges.

Japan and the Philippines, though both located in East and Southeast Asia respectively, represent contrasting ecological and climatic contexts that shape their biodiversity. In Japan, forests are typically classified into four main types: coniferous forests, summer-green deciduous forests, lucidophyllous forests, and subtropical rainforests. In western Japan, where Akashi Kita High School is located, lucidophyllous forests are naturally the dominant vegetation, characterized by broad-leaved evergreen species adapted to temperate conditions (Yoshikazu, 2014). In contrast, the Philippines features predominantly tropical forests, including lowland dipterocarp forests, montane forests, and mangroves, which are rich in endemic species and shaped by a warm, humid climate with distinct wet and dry seasons (Lleno et al., 2023). Human activities such as deforestation and plantation forestry have reduced the area of evergreen broad-leaved forests in Japan, leading to the gradual emergence of mixed forests with deciduous trees. In the Philippines, tropical forests are rich in native and endemic species but face different pressures, including habitat loss. Patterns of species composition and the ecological pressures differ significantly between the two countries. Understanding these differences is important for tailoring conservation and sustainable management strategies in each context.

The main objective of this study is to compare the biodiversity of native tree species in Japan and the Philippines by examining species richness, composition, relative abundance, diversity and evenness. Also identifying environmental and climatic factors that influence their distribution, and discussing the implications of these patterns for forest conservation efforts in both countries. This study is significant because it provides insights into how climatic and ecological differences shape tree biodiversity in temperate and tropical forests, informs conservation strategies, guides sustainable forest management, and supports the protection of endemic and threatened species while addressing broader biodiversity loss challenges.

2. Methodology

In the research conducted in Japan, a forest located near Akashi Kita High School (See Figure 1) was selected as the study site. Within this forest, a 100 × 100 meter plot was established using an application. Within this plot, five 20 × 20 meter subplots were set up, and the species and number of native trees within each subplot were recorded. To distinguish trees that had already been recorded from those that had not, vinyl tape was wrapped around each tree as it was documented.

For the Philippines, a hill accessible to the public and located near Philippine Science High School - Eastern Visayas Campus in Palo, Leyte (See Figure 2) was chosen as the study area. A 100 m belt transect line was established using measuring tape and laid along the slope of the hill. The transect was divided into five consecutive segments of 20 m each. Each segment was further subdivided into 4 subsections, with data recording alternated at 5-m intervals to ensure systematic sampling coverage. At each sampling point, a 5-m perpendicular extension from the main transect line was established to form subplots. All trees within each subplot were recorded and temporarily marked with masking tape to avoid duplication in recording (Chang et. al., 2017).

Figure 1. Location of the sampling site in Japan

Figure 2. Location of the sampling site in Philippines

Collected data were analyzed to describe the diversity of native trees in terms of species richness, species composition, relative abundance, diversity and evenness of native tree species found in locations in Japan and the Philippines.

The species richness is the total number of species present in the study area. The species composition is the list of the different species present in a particular environment and their relative abundance. The relative abundance formula is expressed as:

$$P_i = \frac{n_i}{N} x\ 100$$

Where n_i is the number of individuals of the same species and N is the total number of individuals for all species.

The diversity index that was used in estimating the native tree diversity is the Shannon-Wiener Diversity Index, the formula is as follows:

$$H' = -\sum p_i \ln p_i$$

Where:
H' = Diversity index of Shannon-Weiner;
ln = natural log;
p_i = proportion (n/N) of individuals of one particular species found (n) divided by the total number of individuals (N)

The Simpson's Evenness Index was used to calculate evenness of the native tree species in the area, the formula is as follows:

$$E = \frac{H'}{ln(S)}$$

Where:
E = Evenness index
H' = Diversity of Shannon-Weinner
S = Number of species found

The criteria for evaluating the indices was based on the Fernando Biodiversity Scale which effectively facilitated the interpretation of computed values (Llait, 2024).

Table 1. Fernando Biodiversity Scale

Interpretation	Shannon-Weiner	Simpson's Evenness
Very High	3.5 and above	0.75-1.00
High	3.0-3.49	0.5-0.74
Moderate	2.5-2.99	0.25-0.49
Low	2.0-2.49	0.15-0.24
Very Low	1.9 and below	0.05-0.14

.

3. Results

The species richness differed between the two sites, with Japan recording 13 species and the Philippines recording 11 species. A total of 211 individuals were documented in Japan, while 25 individuals were recorded in the Philippines. In Japan, *Quercus phillyraeoides* was the most represented species, followed by *Quercus variabilis* and *Toxicodendron trichocarpum*. In contrast, the Philippine site exhibited a more even distribution of individuals among species, with *Peltophorum pterocarpum* and *Macaranga tanarius* having the highest number of individuals. The species composition of the study sites in Japan and the Philippines is summarized in Table 2.

Table 2. Species Composition

Japan			Philippines		
No. of Species	**Common Name**	**Scientific Name**	**No. of Species**	**Common Name**	**Scientific Name**
71	Japanese ubame oak	*Quercus phillyraeoides*	4	Yellow flame tree	*Peltophorum pterocarpum*
33	Oriental cork oak	*Quercus variabilis*	4	Parasol leaf tree	*Macaranga tanarius*
25	Japanese poison sumac	*Toxicodendron trichocarpum*	3	Midday marvel	*Oroxylum indicum*
18	Japanese blueberry	*Vaccinium bracteatum*	3	Lipa tree	*Dendrocnide meyaniana*
17	Japanese cleyera	*Cleyera japonica*	3	Vito	*Vitex parviflora*
12	Three-leaf dendropanax	*Dendropanax trifidus*	2	Narra	*Pterocarpus indicus*
11	Mochi tree / Japanese holly	*Ilex integra*	2	Burflower tree	Neolamarckia cadamba
10	Japanese evergreen oak	*Quercus glauca*	1	Common yellow-stem fig/Tibig	*Ficus Fistulosa*
9	Japanese red pine	*Pinus densiflora*	1	Griffith's ash	*Fraxinus griffithii*
2	Camphor tree	*Cinnamomum camphora*	1	Chinaberry tree	*Melia azedarach*
1	Longstalk holly	*Ilex pedunculosa*	1	Mango tree	*Mangifera indica*
1	Japanese mallotus	*Mallotus japonicus*	—	—	—
1	Japanese camellia	*Camellia japonica*	—	—	—

Relative abundance values for each species are presented in Table 3. In Japan, *Quercus phillyraeoides* accounted for the highest relative abundance at 33.6%, followed by *Quercus variabilis* at 15.6%. The remaining species each contributed less than 12% to the total composition. In the Philippines, *Peltophorum pterocarpum* and *Macaranga tanarius* both exhibited the highest relative abundance at 16%, while several species such as *Oroxylum indicum*, *Dendrocnide meyaniana*, and *Vitex parviflora* each accounted for 12%.

Table 3. Relative Abundance

Japan		Philippines	
Species	**Percentage**	**Species**	**Percentage**
Quercus phillyraeoides	33.6%	*Peltophorum pterocarpum*	16%

Quercus variabilis	15.6%	*Macaranga tanarius*	16%
Toxicodendron trichocarpum	11.8%	*Oroxylum indicum*	12%
Vaccinium bracteatum	8.53%	*Dendrocnide meyaniana*	12%
Cleyera japonica	8.06%	*Vitex parviflora*	12%
Dendropanax trifidus	5.69%	*Pterocarpus indicus*	8%
llex integra	5.21%	*Neolamarckia cadamba*	8%
Quercus glauca	4.74%	*Ficus Fistulosa*	4%
Pinus densiflora	4.27%	*Fraxinus griffithii*	4%
Cinnamomum camphora	0.948%	*Melia azedarach*	4%
llex pedunculosa	0.474%	*Mangifera indica*	4%
Mallotus japonicus	0.474%	—	—
Camellia japonica	0.474%	—	—

The Shannon–Wiener Diversity Index values are presented in Table 4. The Philippines recorded a diversity index of H′ = 2.2689, which was classified as low, while Japan recorded a lower average diversity index of H′ = 1.7185, classified as very low.

Table 4. Shannon-Weiner Diversity Index

Country	Diversity Index	Interpretation
Japan	1.7185	Very Low
Philippines	2.2689	Low

Simpson's Evenness Index values are shown in Table 5. Both study sites exhibited high evenness, with the Philippines having an evenness index of 0.9462 and Japan having an evenness index of 0.7911. Both values were interpreted as very high species evenness.

Table 5. Simpson's Evenness Index

Country	Evenness Index	Interpretation
Japan	0.7911	Very High
Philippines	0.9462	Very High

4. Discussion

Species richness refers to and quantifies the number of different species present in an area. It is a fundamental ecological measure that acts as an indicator of the variety of life within an ecosystem. Data collected from the study sites in both regions found 13 different species of native trees in Japan and 11 species in the Philippines as listed in Table 2. This indicates relatively low species richness in the Philippine locality compared to the higher value observed in the Japanese forest. This shows that between the two selected areas of study, Japan has greater species richness.

While richness does not account for the number of individuals present for each species, relative abundance on the other hand refers to the proportion of each species with respect to the total number of individuals in the community. This indicates the dominance or rarity of certain species within an area. For the study area in Japan, the Japanese ubame oak (*Quercus phillyraeoides*) is the most abundant, constituting 33.6% and dominating the population of native Japanese trees in the locale. In the Philippines, the Yellow flame tree (*Peltophorum pterocarpum*) and Parasol leaf tree (*Macaranga tanarius*) are the most dominant and make up 16% of the total population of Philippine native trees in the community.

Shannon-Wiener Diversity Index

The Shannon-Wiener Diversity Index describes the overall diversity of a biological community and accounts for both the number of species present and how evenly individuals are distributed among them. This tells the balance among taxa and stability of a community. Results show that both areas in Japan and the Philippines are on the low end of the diversity spectrum. However, the Philippines show to have higher H' value compared to Japan which demonstrates greater diversity in the Philippine chosen locale. While the Philippines had lower species richness, its greater diversity can be attributed to its more even distribution of individuals.

Simpson's Evenness Index

The Simpson's Evenness Index measures how evenly individuals are distributed among the species in a community. This shows whether certain species dominate the population of the community or if the present individuals are distributed more equally. The results reflect that the study area in the Philippines has higher evenness than the area in Japan, suggesting a more balanced ecosystem where there is no notable or significant dominance of certain species that overwhelm the others.

5. Conclusion

This comparative study revealed notable differences and similarities in the biodiversity of native tree species between selected forest sites in Japan and the Philippines. Although Japan exhibited slightly higher species richness, the Philippine site showed greater overall species diversity due to a more even distribution of individuals among species. Both study areas demonstrated very high evenness, indicating stable communities with limited dominance by any single species. However, the low diversity indices recorded in both countries suggest that the total number of species present in each ecosystem remains limited. These results indicate that high evenness does not necessarily correspond to high species diversity and emphasize the importance of considering both richness and distribution when assessing forest biodiversity. The findings underscore the need for targeted conservation efforts and sustainable forest management practices to enhance species diversity and strengthen ecosystem resilience in both temperate and tropical forest environments.

6. Acknowledgements

The researchers sincerely thank the individuals who, in one way or another, contributed their time, effort, and assistance during the conduct of this study. Special appreciation is extended to those who helped in field surveys, tree identification, and data recording in both Japan and the Philippines. Their guidance, cooperation, and support greatly contributed to the successful completion of this research.

7. References

Chang, J.-H., Shank, B. V., & Hart, D. R. (2017). A comparison of methods to estimate abundance and biomass from belt transect surveys. *Limnology and Oceanography: Methods, 15(5), 480–494.* https://doi.org/10.1002/lom3.10174

Llait, C. O. (2024). Tree Species Composition and Diversity in a Secondary Forest along the Sierra Madre Mountain Range in Central Luzon, Philippines: Implications for the Conservation of Endemic, Native, and Threatened Plants. *Journal of Zoological and Botanical Gardens*, *5*(1), 51–65. https://doi.org/10.3390/jzbg5010004

Lleno, J. V., Ligalig, R. J., Sarmiento, R. T., & Along, A. A. (2023). Tree diversity, composition, and stand structure of lowland tropical forest in Prosperidad, Agusan del Sur, Philippines. *Open Journal of Fisheries Research, 10(1S), 4810–4830.*

OCW article series. (n.d.). https://www.onecarbonworld.com/articles/why-growing-native-tree-species-can-help-save-the-planet#:~:text=Native%20tree%20species%20are%20deeply%20rooted%20in,contributing%20to%20a%20balanced%20and%20resilient%20environment.

Wang, L., Wei, F., Tagesson, T., Fang, Z., & Svenning, J. (2025). Transforming forest management through rewilding: Enhancing biodiversity, resilience, and biosphere sustainability under global change. *One Earth, 8(3), 101195.* https://doi.org/10.1016/j.oneear.2025.101195

World Health Organization: WHO. (2025, February 18). *Biodiversity*. https://www.who.int/news-room/fact-sheets/detail/biodiversity

Yoshikazu , S . (2014). Process of the formation of Japanese forest and typification of vegetation zone —From an East Asian viewpoint. Regional Studies / Komazawa University Institute of Applied Geography (ed.) (27). https://ndlsearch.ndl.go.jp/books/R000000004-I025399287

Determining the Efficiency of Plant-Based Biocoagulants on Improving Water Quality

Wendy Maxine U. Baguio[1], Miley U. Balascopo[1], Bon Matthew E. Singayao[1]
Daichi Rikiishi[2], Joe Nishiyama[2]
[1]*Philippine Science High School - SOCCSKSARGEN Region Campus (Philippines)*
[2]*Miyagi Prefecture Sendai Daisan High School (Japan)*

Abstract:

Surface water is primarily used as a drinking water source; however, many rivers and lakes continue to exhibit poor water quality due to high turbidity and organic contamination. This study evaluated the effectiveness of plant-based coagulants, specifically from aloe vera, okra, and dawn redwood nuts, to improve water quality metrics such as turbidity, TDS, pH, and conductivity. Coagulants were prepared from Aloe Vera and Okra mucilage and Dawn redwood tannin-rich extracts. Jar tests showed that aloe vera removed up to 80% of turbidity, while okra provided moderate reductions. Both coagulants had minimal impact on pH, with moderate effects on TDS and conductivity. Tannin coagulants from dawn redwood significantly reduced absorbance and increased transmission, improving water quality. These findings suggest that plant-based biocoagulants are viable, eco-friendly alternatives to traditional chemical coagulants in sustainable water treatment.

Keywords: Aloe Vera; Biocoagulant; Coagulation; Dawn Redwood; Okra

1. Introduction

Globally, the scarcity of safe, sanitized water remains a growing issue, with 2.2 billion people lacking secure access to it (United Nations, 2022). While conventional water treatment uses chemical coagulants such as aluminum sulfate (Alum) and Ferric chloride to destabilize and settle suspended particles (Ahmad et al., 2022; Singh et al., 2023), their long-term use poses significant risks. Multiple studies have linked aluminum-treated waters to neurological disorders such as dementia and Alzheimer's disease (Kurniawan et al., 2020; Krupińska, 2020), and the generation of excessive toxic sludge harms aquatic and terrestrial organisms (Ahmad et al., 2016). In response, researchers have shifted towards natural plant-based coagulants (Sen et al., 2015; Camacho et al., 2017), identifying Aloe vera and Okra (*Abelmoschus esculentus*) as promising alternatives. These natural polysaccharides provide a biodegradable, non-toxic, and safe solution for water treatment. Further research determined that Okra mucilage is a water-soluble natural polysaccharide that can destabilize colloidal suspensions and form small flocs by reducing particle surface charge, thereby encouraging particle aggregation. In contrast, Aloe vera mucilage contains polysaccharides that reduce the surface charge of colloidal particles, thereby promoting weaker attractive forces that lead to the formation of larger, more settleable flocs that can be easily discarded (Benalia et al., 2021; Abu-Jazar et al., 2022).

Beyond the well-recorded mucilaginous coagulants, this study will also investigate the unexplored potential of *Metasequoia glyptostroboides* (Dawn Redwood), which is commonly cultivated in educational landscapes, such as Miyagi Prefecture and Sendai Daisan High School. They shed cones and foliage seasonally, which contain polyphenolic compounds, particularly tannins and proanthocyanidins (Yeo et. al., 2023; Silva et. al., 2025). Tannins possess anionic properties and can be chemically modified to enhance their solubility and cationic charge (Tomasi, 2024), yielding a polymer that effectively acts as a coagulant. Tannin-based coagulants offer a promising, sustainable solution for reducing organic waste sludge by utilizing interparticle bridging to aggregate suspended solids into flocs.

2. Experimental Methods 1 (Aloe Vera and Okra Coagulant)

2.1 Extraction of bio-coagulant from *Aloe vera*

Aloe vera leaves were thoroughly washed with distilled water to remove dirt and other impurities before the rind was removed. The gel was separated from the outer leaf pulp, which contained latex, a yellow-colored substance that negatively affects coagulation. The solid gel was blended until a homogenous mixture was obtained. 200 mL of gel was incorporated with 1 L of distilled water and

stirred using a hot plate with a magnetic stirrer for 10 minutes at 100 rpm. The mixture was strained through a 50 mm mesh, and the filtrate collected was stored at 4°C until later use.

2.2 Extraction of bio-coagulant from *Abelmoschus esculentus*

Okras were thoroughly washed with distilled water before being cut into short, small pieces, simultaneously removing their seeds and any excess fiber. 100 g of the processed okra was then added to 1 L of distilled water and stirred using a hot plate with a magnetic stirrer for 2 hours at 200 rpm to extract the gel. The solution was then filtered through a 50 mm mesh to further remove fibers. The filtrate collected was stored at 4°C until later use.

2.3 Collection of Surface Water

Surface water samples were collected from a section of the Allah River flowing through Barangay Kolambog, Isulan, Sultan Kudarat, Philippines and stored in 1 L amber glass containers. These were tested on-site for water quality, providing a basis for the initial laboratory testing conducted before experimentation. After on-site testing, the samples were preserved at 4°C and analyzed within 24 hours. A field blank was also prepared to check for contamination during handling. Composite sampling was performed to ensure consistent initial water-quality measurements across all samples within each treatment group.

2.4 Water Quality Analysis

The turbidity, pH, total dissolved solids (TDS), salinity, and electroconductivity of the surface water samples were measured before and after the addition of the coagulants to determine the initial and final values per parameter.

2.4.1 Determination of Turbidity

Turbidity was measured using a turbidimeter. The device was calibrated using standards of 10 NTU and 200 NTU, as the turbidity of the surface water samples is within that range. Once calibrated, an empty glass vial was filled with the sample and placed in the device. The vial was washed with distilled water after each measurement.

2.4.2 Determination of pH, Total Dissolved Solids (TDS), Salinity, and Electroconductivity

The aforementioned water quality parameters were measured using a multiparameter meter. The device was calibrated by preparing calibration buffers and immersing the probes in their designated buffers until the readings stabilized. Once calibrated, the probes were immersed in the sample until a stable reading was achieved. The probes were washed with distilled water after each test.

2.5 Experimental Setup

The coagulants underwent a pilot test, a “jar test,” to determine their efficiency in reducing turbidity, total dissolved solids, salinity, and electrical conductivity, as well as their effect on water sample pH. While usually conducted with a coagulation-flocculation apparatus, hot plates with magnetic stirrers were used as an alternative. 500 mL of surface water was naturally cooled to room temperature (25+3°C). The coagulant was added and underwent rapid mixing for 2 minutes at 150 rpm, followed by slow mixing for 10 minutes at 60 rpm, and was allowed to settle for 20 minutes. The tested coagulant dosages of both Aloe vera and Okra were 25 mL, 50 mL, and 75 mL per 500 mL of surface water. Three trials were conducted per dosage.

3. Results and Discussion

Table 1-A. Effect of 25 mL Aloe vera Coagulant on Turbidity, TDS, and pH

Initial Turbidity (NTU)	Final Turbidity (NTU)	Efficiency Removal	Initial TDS (mg/L)	Final TDS (mg/L)	Efficiency Removal	Initial pH	Final pH	Difference in pH
136.8	36.06	**73.64%**	222	188	**15.31%**	8.179	7.962	**0.217**
130.2	34.21	**73.73%**	219	186	**15.07%**	8.181	7.961	**0.221**
132.6	35.20	**73.45%**	220	186	**15.45%**	8.176	7.957	**0.219**

Table 1-B. Effect of 25 mL Aloe vera Coagulant on Conductivity and Salinity

Initial Conductivity (µS/cm)	Final Conductivity (µS/cm)	Efficiency Removal	Initial Salinity (ppt)	Final Salinity (ppt)	Efficiency Removal
333	272	**18.31%**	0.18	0.15	**16.67%**
329	269	**18.24%**	0.17	0.14	**17.65%**
331	270	**18.43%**	0.18	0.15	**16.67%**

As you can see from Table 1-A, the 25 mL of Aloe vera achieved a high turbidity removal of approximately 73%, effectively reducing turbidity from an average of 133.2 NTU to 35.1 NTU. Total Dissolved Solids (TDS), conductivity, and salinity in Table 1-B were less distinct and showed moderate removal efficiencies (15%-18%). The pH slightly decreased by 0.22, showing successful clarification with minimal acidification of the biocoagulant.

Table 2-A. Effect of 50 mL Aloe vera Coagulant on Turbidity, TDS, and pH

Initial Turbidity (NTU)	Final Turbidity (NTU)	Efficiency Removal	Initial TDS (mg/L)	Final TDS (mg/L)	Efficiency Removal	Initial pH	Final pH	Difference in pH
135.7	31.60	**76.71%**	223	182	**18.38%**	8.209	7.980	**0.229**
133.1	31.22	**76.54%**	221	181	**18.10%**	8.201	7.975	**0.226**
134.9	31.27	**76.82%**	220	180	**18.18%**	8.207	7.976	**0.231**

Table 2-B. Effect of 50 mL Aloe vera Coagulant on Conductivity and Salinity

Initial Conductivity (µS/cm)	Final Conductivity (µS/cm)	Efficiency Removal	Initial Salinity (ppt)	Final Salinity (ppt)	Efficiency Removal
334	267	**20.06%**	0.18	0.14	**22.22%**
331	264	**20.24%**	0.18	0.14	**22.22%**
332	265	**20.18%**	0.18	0.14	**22.22%**

As you can see from Table 2-A, the 50 mL of Aloe vera achieved a high turbidity removal of approximately 76%, effectively reducing turbidity from an average of 134 NTU to 31.3 NTU, indicating that a higher dosage enhances coagulation. Total Dissolved Solids (TDS) rose to approximately 18%, while conductivity and salinity in Table 1-B improved slightly with the increase, achieving 20.1% and 22.2% respectively. The pH consistently decreased by only 0.23, showing successful clarification with minimal acidification of the biocoagulant.

Table 3-A. Effect of 75 mL Aloe vera Coagulant on Turbidity, TDS, and pH

Initial Turbidity (NTU)	Final Turbidity (NTU)	Efficiency Removal	Initial TDS (mg/L)	Final TDS (mg/L)	Efficiency Removal	Initial pH	Final pH	Difference in pH
141.7	28.18	**80.11%**	223	178	**20.18%**	8.228	7.974	**0.254**
140.9	28.15	**80.02%**	221	176	**20.36%**	8.223	7.970	**0.253**
141.3	28.16	**80.07%**	220	175	**20.45%**	8.226	7.975	**0.251**

Table 3-B. Effect of 75 mL Aloe vera Coagulant on Conductivity and Salinity

Initial Conductivity (µS/cm)	Final Conductivity (µS/cm)	Efficiency Removal	Initial Salinity (ppt)	Final Salinity (ppt)	Efficiency Removal
337	272	**19.29%**	0.19	0.15	**21.05%**
335	270	**19.40%**	0.19	0.15	**21.05%**
336	271	**19.34%**	0.19	0.15	**21.05%**

As shown in Table 3-A, the application of 75 mL of Aloe Vera coagulant resulted in very high turbidity removal, reducing the average turbidity from 141 NTU to 28 NTU. Its efficient removal (up to 80%) and consistently neutral final pH levels. The Total Dissolved Solids (TDS) removal rose to approximately 20%. According to Table 3-B, the coagulant significantly impacted the ionic properties

of the water, reducing the average conductivity from 336 µS/cm to 271 µS/cm (19.34% efficiency) and salinity from 0.19 ppt to 0.15 ppt (21.05% efficiency).

Table 4-A. Effect of 25 mL Okra Coagulant on Turbidity, TDS, and pH

Initial Turbidity (NTU)	Final Turbidity (NTU)	Efficiency Removal	Initial TDS (mg/L)	Final TDS (mg/L)	Efficiency Removal	Initial pH	Final pH	Difference in pH
149.1	60.81	**59.22%**	230	201	**12.61%**	8.213	8.001	**0.172**
153.7	62.51	**59.32%**	231	202	**12.55%**	8.231	8.056	**0.175**
126.3	51.47	**59.25%**	225	196	**12.88%**	8.247	8.059	**0.178**

Table 4-B. Effect of 25 mL Okra Coagulant on Conductivity and Salinity

Initial Conductivity (µS/cm)	Final Conductivity (µS/cm)	Efficiency Removal	Initial Salinity (ppt)	Final Salinity (ppt)	Efficiency Removal
341	288	**15.54%**	0.20	0.17	**15.00%**
340	286	**15.88%**	0.20	0.17	**15.00%**
321	272	**15.26%**	0.18	0.15	**16.67%**

As you can see from Table 4-A, the 50 mL of Okra As you can see from Table 4-A, the 50 mL of Okra achieved a moderate turbidity removal of approximately 59%, effectively reducing turbidity from a range of 126.3 NTU to 153.7 NTU to a range of 51.47 NTU to 62.51 NTU, which is noticeably lower than Aloe vera at the exact dosage. Total Dissolved Solids (TDS), conductivity, and salinity in Table 4-B were lower than their impact on turbidity, decreasing by 12.6%, 15.5%, and 15-16%, respectively. The pH slightly decreased by 0.17, showing successful clarification with minimal acidification of the biocoagulant.

Table 5-A. Effect of 50 mL Okra Coagulant on Turbidity, TDS, and pH

Initial Turbidity (NTU)	Final Turbidity (NTU)	Efficiency Removal	Initial TDS (mg/L)	Final TDS (mg/L)	Efficiency Removal	Initial pH	Final pH	Difference in pH
166.4	56.09	**66.29%**	236	200	**15.25%**	8.256	8.065	**0.191**
160.7	52.67	**67.22%**	234	198	**15.38%**	8.242	8.053	**0.189**
161.5	53.44	**66.91%**	235	199	**15.32%**	8.230	8.034	**0.196**

Table 5-B. Effect of 50 mL Okra Coagulant on Conductivity and Salinity

Initial Conductivity (µS/cm)	Final Conductivity (µS/cm)	Efficiency Removal	Initial Salinity (ppt)	Final Salinity (ppt)	Efficiency Removal
331	270	**18.13%**	0.20	0.16	**20.00%**
330	271	**17.88%**	0.20	0.16	**20.00%**
331	272	**17.82%**	0.20	0.16	**20.00%**

As shown in Table 5-A, the application of 50 mL of Okra coagulant significantly reduced turbidity from an average of 162.9 NTU to 54.07 NTU, resulting in a mean removal efficiency of 66%. The Total Dissolved Solids (TDS) also decreased by an average of 15%. Its pH difference slightly decreased by 0.193. In Table 5-B, the coagulant reduced the average conductivity from 330.7 µS/cm to 271 µS/cm (17.94% efficiency) and consistently lowered salinity from 0.20 ppt to 0.16 ppt (20.00% efficiency).

Table 6-A. Effect of 75 mL Okra Coagulant on Turbidity, TDS, and pH

Initial Turbidity (NTU)	Final Turbidity (NTU)	Efficiency Removal	Initial TDS (mg/L)	Final TDS (mg/L)	Efficiency Removal	Initial pH	Final pH	Difference in pH
166.7	51.21	**69.28%**	245	205	**16.33%**	8.210	7.929	**0.281**
167.1	51.78	**69.01%**	245	206	**15.91%**	8.232	7.953	**0.279**
166.4	51.34	**69.15%**	245	205	**16.33%**	8.225	7.941	**0.284**

Table 6-B. Effect of 75 mL Okra Coagulant on Conductivity and Salinity

Initial Conductivity (µS/cm)	Final Conductivity (µS/cm)	Efficiency Removal	Initial Salinity (ppt)	Final Salinity (ppt)	Efficiency Removal
345	296	**14.20%**	0.20	0.17	**15.00%**
344	295	**14.24%**	0.20	0.17	**15.00%**
344	294	**14.53%**	0.20	0.17	**15.00%**

As you can see from Table 6-A, increasing the amount of Okra to 75 mL of Okra significantly improved turbidity removal to approximately 69%, effectively reducing the initial high level of 166.7 NTU to 51.4 NTU. While Total Dissolved Solids (TDS), conductivity, and salinity in Table 6-B remained steady and showed removal rates from 14% to 16%. The pH decreased by 0.28, showing its neutralizing capability.

The removal efficiency of the Aloe vera coagulant for salinity and electroconductivity began to decrease at the 75 mL dosage. In contrast, improvements in turbidity reduction, total dissolved solids removal, and pH neutralization were observed. Based on overall treatment performance across all evaluated water quality parameters, the optimal Aloe vera dosage was 50 mL per 500 mL of surface water. Similarly, the removal efficiency of the okra coagulant for salinity and electroconductivity also decreased at the 75 mL dosage. In contrast, turbidity reduction, total dissolved solids removal, and pH neutralization continued to increase. Based on the overall performance across all parameters, the best dosage of okra was likewise identified as 50 mL per 500 mL of surface water. However, despite sharing the same optimal dosage, Aloe vera consistently exhibited higher removal efficiencies across all water quality parameters than Okra, indicating its superior coagulation performance over a range of 100 to 200 NTU.

4. Experimental Methods 2 (Dawn Redwood Coagulant)

4.1 Extraction of bio-coagulant from *Metasequoia glyptostroboides*

Dawn redwood nuts were washed thoroughly with distilled water to remove impurities. Two variations were tested as a coagulant, one using the pure nut and the other ground into a fine powder. 20 nuts of dawn redwood produced 17 g of powder.

4.2 Collection of Surface Water

Raw water samples were collected from the Nanakita River flowing through Sendai. Samples were collected from the mid-depth of the water to avoid bottom sediments and surface debris, and stored in 1-liter polyethylene bottles. Upon collection, the initial pH was recorded. The samples were then transported to the laboratory within 2 hours and kept at 4°C to prevent biological degradation.

4.3 Water Quality Analysis

The pH, transmission, and absorbance of the surface water samples were measured before and after the addition of the coagulants to determine the change in each parameter.

4.3.1 Determination of pH

The pH of the water samples was determined using a water-quality kit to assess the chemical environment for optimal coagulation. Water samples were placed in test vials, and their pH values were recorded.

4.3.2 Determination of Transmission and Absorbance

The transmission and absorbance of the water samples was determined using a UV-Vis spectrophotometer to assess the optical clarity of the samples. Absorbance was used as an indicator of turbidity. The device was calibrated by using distilled water as a blank at the selected wavelength.

4.4 Experimental Setup

Two primary experiments were performed. The first was to determine the differences in absorbance,

transmission, and pH between the initial and final values for both pure dawn redwood nuts and powder. The second was to determine the rate of change in absorbance using dawn redwood nut powder by measuring absorbance after 1 hour and 1 day after the coagulant was added. Transmission and pH values were also measured.

5. Results and Discussion

Table 7. Effect of Dawn Redwood Nut on Muddy Water

Initial Absorbance	Final Absorbance	Difference	Initial Transmission	Final Transmission	Difference	Initial pH	Final pH	Difference
0.784	0.400	**-0.384**	0.166	0.419	**+0.253**	5	6	**+1.0**
0.953	0.430	**-0.523**	0.113	0.420	**+0.307**	5	6	**+1.0**
0.790	0.390	**-0.400**	0.159	0.400	**+0.241**	5	6	**+1.0**

Table 8. Effect of Dawn Redwood Nut Powder on Muddy Water

Initial Absorbance	Final Absorbance	Difference	Initial Transmission	Final Transmission	Difference	Initial pH	Final pH	Difference
0.784	0.177	**-0.607**	0.166	0.664	**+0.498**	5	6	**+1.0**
0.953	0.175	**-0.778**	0.113	0.661	**+0.548**	5	6	**+1.0**
0.790	0.179	**-0.611**	0.159	0.667	**+0.508**	5	6	**+1.0**

Shown in Tables 7 and 8, the effectiveness of dawn redwood as a biocoagulant was evaluated via absorbance, transmission, chemical oxygen demand (COD), and pH. Untreated water exhibited high absorbance (up to 0.953) and low transmission (0.113), indicating significant turbidity. While treatment with pure dawn redwood nuts yielded partial clarification of the water, the use of dawn redwood nut powder significantly outperformed it, achieving larger reductions in absorbance (up to -0.778) and greater increases in transmission (up to +0.548). This suggests the powder's increased surface area enhances particle destabilization resulting in more effective coagulation. Additionally, the pH consistently rose slightly from 5 to 6 across all samples, indicating that the use of dawn redwood-based coagulants did not cause extreme pH alterations.

Table 9. Effect of Dawn Redwood Nut Powder on pH, Transmission, and Rate of Change

Percent (%)	Dosage (g)	Rate of Change	Absorbance (1 hour)	Absorbance (1 day)	Transmission	Initial pH	Final pH	Difference
10	0	**75.73%**	3.00	0.73	**18.20%**	5	5	**0.0**
10	2.50	**49.33%**	3.00	1.52	**0.10%**	5	8	**+3.0**
10	5.00	**30.00%**	3.00	2.10	**0.70%**	5	8	**+3.0**
20	0	**86.00%**	1.50	0.21	**95.80%**	5	5	**0.0**
20	2.50	**63.33%**	3.00	1.1	**0%**	5	8	**+3.0**
20	5.00	**51.20%**	3.00	1.464	**3.50%**	5	8	**+3.0**

As presented in Table 9, the effect of dawn redwood nut powder concentration and dosage on absorbance reduction, transmission efficiency, and pH variation over time was further evaluated. Results indicate that higher concentrations and dosages generally led to greater reductions in absorbance at a contact time of 1 day, indicating improved turbidity removal. However, samples treated with higher dosages exhibited a pH increase from 5 to 8, indicating a significant pH shift. Overall, the results indicate that dawn redwood nut powder exhibits dosage and concentration-dependent coagulation performance, with enhanced clarity and high pH adjustment.

6. Conclusion

This study confirms that Aloe vera, Okra, and Dawn Redwood are viable, eco-friendly coagulants, with Aloe vera demonstrating exceptional effectiveness, removing up to 80% of turbidity at a dosage of 50 mL. While the mucilaginous extracts maintained a stable pH, the tannin-rich Dawn Redwood powder was highly effective at improving transmission, specifically by enhancing particle destabilization through its increased surface area. Collectively, these results demonstrate that locally available organic materials can serve as safe alternatives to toxic chemical coagulants.

7. References

Abu-Jazar, M. S. S., Karaağaç, S. U., Abu Amr, S. S., Alazaiza, M. Y. D., Fatihah, S., & Bashir, M. J. K. (2022). Recent advancements in plant-based natural coagulant application in the water and wastewater coagulation-flocculation process: Challenges and future perspectives. Global NEST Journal, 24(4), 687–705. https://doi.org/10.30955/gnj.004380

Ahmad, T., Ahmad, K., & Alam, M. (2016). Sustainable management of water treatment sludge through 3 'R'concept. Journal of Cleaner Production, 124, 1-13.

Aziz, S. Q., & Mustafa, J. S. (2021). Step-By-Step Design and Calculations for Water Treatment Plant Units: A Recent Study. Modern Advances in Geography, Environment and Earth Sciences, 4, 45-67.

Benalia, A., Derbal, K., Khalfaoui, A., Pizzi, A., & Medjahdi, G. (2022). The use of as natural coagulant in algerian drinking water treatment plant. Journal of Renewable Materials, 10(3), 625.

Camacho, F. P., Sousa, V. S., Bergamasco, R., & Teixeira, M. R. (2017). The use of Moringa oleifera as a natural coagulant in surface water treatment. Chemical Engineering Journal, 313, 226-237.

Jiang, J. Q. (2015). The role of coagulation in water treatment. Current Opinion in Chemical Engineering, 8, 36-44.

Kurniawan, S., Abdullah, S., Imron, M., Said, N., Ismail, N., Hasan, H., Othman, A., & Purwanti, I. (2020). Challenges and opportunities of Biocoagulant/Bioflocculant application for drinking water and wastewater treatment and its potential for sludge recovery. International Journal of Environmental Research and Public Health, 17(24), 9312. https://doi.org/10.3390/ijerph17249312

Krupińska, I. (2020). Aluminium drinking water treatment residuals and their toxic impact on human health. Molecules, 25(3), 641.

Sarminingsih, A., Juliani, H., Budihardjo, M. A., Puspita, A. S., & Mirhan, S. A. A. (2024). Water quality monitoring system for temperature, pH, Turbidity, DO, BOD, and COD parameters based on internet of things in the garang watershed. Ecological Engineering & Environmental Technology, 25.

Sen, B., Sarma, H. P., & Bhattacharyya, K. G. (2015). Kinetic study of Cu (II) adsorption on Adenanthera pavonina seeds. IOSR Journal of Environmental Science, Toxicology and Food Technology, 9(8), 01–05.

Silva, L. C. D., Azevêdo, T. K. B. D., Souza, D. S. D., Nascimento, P. E. P. D., Paiva, K. L. B. D., Meza Filho, J. G. U., & Pimenta, A. S. (2025). Natural coagulant for water treatment based on cationized tannins from Terminalia Catappa bark. Revista Ambiente & Água, 20, e3060.

Singh, M. V., Kumar, A., Bhatt, N., Ren, J., Hou, H., Wang, Z., ... & Colorado, H. A. (2023). Impact of contaminated water on plants and animals: utilizing natural and chemical coagulants for treating contaminated water. ES Energy & Environment, 23, 1032.

Tomasi, I. T., Santos, S. C., Ribeiro, A., Homem, V., Boaventura, R. A., & Botelho, C. M. (2024). Coagulants from chestnut shell tannins - Synthesis, characterization and performance on water treatment. Journal of Water Process Engineering, 69, 106818. https://doi.org/10.1016/j.jwpe.2024.106818

United Nations (2023, October 19). Goal 6: Ensure access to water and sanitation for all.

https://www.un.org/sustainabledevelopment/water-and-sanitation/

Yeo, J.-Y., Lee, S., Ko, M. S., Lee, C. H., Choi, J. Y., Hwang, K. W., & Park, S.-Y. (2023). Anti-Amyloidogenic Effects of Metasequoia glyptostroboides Fruits and Its Active Constituents. Molecules, 28(3), 1017. https://doi.org/10.3390/molecules28031017

Investigation of Water Hyacinth in Polystyrene Microplastic adsorption

Gracelyn Gosal[1], Kmy Er Sze Lei[1], Ichika Hirose[2], Yui Azumaya[2], Yuzuki Hashida[2]
[1]*School of Science and Technology, Singapore (Singapore)*
[2]*Yokkaichi High School (Japan)*

Abstract:
Water hyacinth, *Pontederia crassipes*, has been used to carry out phytoremediation as the roots have been found to be able to adsorb impurities in water such as heavy metals. In previous research, water hyacinths have been found to have the ability to remove microplastics from water as an exploration of the phytoremediative capability of water hyacinths. This research aims to explore water hyacinths further to determine whether chemical interactions caused by water hyacinth root exudates or physical interactions with root structure surface play a greater role in the adsorption of polystyrene microplastics from water. Using a setup consisting of 8 identical beakers, each filled with 500ml of distilled water and a total of 0.1ml (100μL) of fluorescent polystyrene microplastic stock solution (2.5% solid) per beaker, we quantified the root exudates through Dissolved Organic Carbon (DOC) and measured other factors such as pH, temperature and root length. The results show evidence that root exudates play a greater role than physical root surface, but the extent of the impact is unclear. Overall, this proves our hypothesis that root exudates have a greater role in polystyrene microplastic adsorption compared to physical root surfaces, but may not have a significantly greater effect than it. These results allow us to further investigate the possibility of harnessing water hyacinths phytoremediative ability for microplastics and applying it in other scenarios.

Keywords: ; Water Hyacinth ; Polystyrene ; Microplastic ; Dissolved Organic Carbon

1. Introduction

In today's world, microplastics are essentially ubiquitous due to persistent pollution. Microplastics are defined as small pieces of plastic ranging in size from 1 μm to 5 mm. These microplastics do not biodegrade, remaining in the environment for hundreds of years and creating detrimental effects to flora and fauna, particularly impacting the well-being of marine life as most plastics end up in the ocean. The health of many ecosystems is affected, resulting in irreversible damage to the food chain (Cverenkárová et al., 2021). This leads to health issues as biomagnification amplifies the effect of such pollutants that cannot be broken down. Due to their small size, they are difficult to filter out of water for purification purposes. Existing solutions, such as reverse osmosis, are usually expensive and undeveloped countries cannot afford them (Mustafa et al., 2025).

Water hyacinth, *Pontederia crassipes*, is a well-known invasive species that grows rapidly and is highly destructive to ecosystems. It has been used to carry out phytoremediation as the roots have been found to be able to adsorb impurities in water such as heavy metals. Compared to other aquatic plants like duckweed, water hyacinths have a more extensive root system and higher root exudation, creating more interactions between roots and other substances or particles in the water. This positions water hyacinths as an alternative solution to removing microplastics through both physical and chemical mechanisms.

In a research by Yin et al. (2025), it has been shown that water hyacinths have the ability to remove microplastics from water as an exploration of the phytoremediative capability of water hyacinths. Specifically, their results show that water hyacinths had a removal efficiency of 55.3%, 69.1% and 68.8% for 0.5, 1 and 2 μm polystyrene particles. This efficient microplastic adsorption capability was credited to the large surface area of the extensive root network that water hyacinths have, emphasising that root caps are the primary sites for efficient microplastic entrapment. Hence, root structures play an important role in the removal of microplastics.

In a separate study by Chen et al. (2024), microplastics increased the root exudation of dissolved organic matter, which suggests that there could be a relation between root exudates and microplastic adsorption. Water hyacinths release different types of root exudates, including dissolved organic carbon, sugars, and other organic compounds, which can interact with microplastics and hence

influence their adhesion to surfaces (adsorption). Although their study did not directly study microplastic adsorption, these exudates are known to interact with surfaces and hence influence particle aggregation and adhesion. This suggests that root exudates may have a chemical role in influencing the ability of water hyacinths in microplastic adsorption.

This research aims to explore water hyacinths further to determine whether chemical interactions caused by water hyacinth root exudates or physical interactions with root structure surface play a greater role in the adsorption of polystyrene microplastics from water.

2. Methodology

This experiment is investigating whether root exudates or root structure have a greater effect on water hyacinth's ability to adsorb 1 μm polystyrene microplastics (PS).

Independent variable:

1. Condition of water hyacinth treatment (root/exudate condition)
    - Living roots
    - Boiled/killed roots
    - Root-free exudate water with plant removed
    - No water hyacinth/no exudates (PS only control)
2. Root (changed between having roots/boiled roots/no water hyacinth but root exudates present)

Dependent variables:

1. Microplastic Concentration (particles mL^-1)
2. DOC/dissolved organic matter proxy (OD254)
3. pH

Controlled variables:

1. Volume of water (500ml)
2. Microplastic type and size (1μm fluorescent polystyrene)
3. Amount of microplastics per beaker
4. Beaker type and sizes
5. Number of plants (1 plant per beaker)
6. Type of plants
7. Light placement for the plants
8. Condition and temperature of the room

Hypothesis: Root exudates have a greater role in polystyrene microplastic adsorption compared to physical root surfaces.

The setup consisted of 8 identical beakers, each filled with 500ml of distilled water. A total of 0.1ml (100μL) of fluorescent polystyrene microplastic stock solution (2.5% solid) was added to each beaker, resulting in an estimated concentration of ~4.75×10^{9} microplastic spheres per beaker.

Below are the four experimental setups that have been conducted:

1. Polystyrene microplastics with living water hyacinth roots
2. Polystyrene microplastics with boiled/killed water hyacinth roots
3. Polystyrene microplastics with root-free exudates
4. Polystyrene microplastics only (control setup)

The purpose of each setup is as follows:

1. To represent the usual environment where root structure and root exudates are present, showing the maximum adsorption as a benchmark to gauge the contribution of different factors.
2. To compare with the root-free exudates setup, and hence determine if the root structure has a

greater impact on the microplastic adsorption abilities of the water hyacinth.

3. To compare with the boiled/killed roots setup, and hence determine if the root exudates have a greater impact on the microplastic adsorption abilities of the water hyacinth.
4. To compare with other setups to negate natural background processes like microplastic sedimentation at the bottom of the beaker, confirming that any reduction in microplastic concentration in other setups is due to the presence of roots or root exudates rather than said background processes.

Water hyacinth plants with similar root lengths were selected to ensure the experiment was conducted fairly and to minimise variation in root surface area. Before the experiment, the root length was measured and recorded, as shown in Table 1 below.

Table 1. Root length (cm)

Setup	Singapore	Japan
PS + boiled roots 1	18.5	18.5
PS + boiled roots 2	21.0	12.3
PS + living roots 1	12.1	14.6
PS + living roots 2	12.0	15.2

To prepare the root-free exudate setup, the water hyacinths were placed in distilled water for 2 days to allow their roots to release root exudates into the water. Afterwards, the water hyacinth is removed, and the water containing the exudates is used for the root-free exudates setup. The water hyacinth is then boiled to kill the roots, which are used for the boiled/killed roots setup.

At regular intervals, 100μL of water samples were taken and placed onto a haemocytometer for counting fluorescent polystyrene microplastics. The concentration is average across the two duplicates for each setup.

To quantify dissolved organic carbon (DOC) from root exudates, 200 μL samples were centrifuged to pellet microplastics. The supernatant is then taken and measured at 254nm (OD254) using a UV spectrophotometer. The absorbance at 254nm (OD254) was used as a measure of DOC, representing changes in organic compounds released in root exudates.

Water temperature was measured with a thermometer throughout the experiment to ensure that adsorption was not affected by thermal variations in the climate. Water pH was measured with a calibrated pH strip to quantify the organic compounds released in root exudates.

3. Results

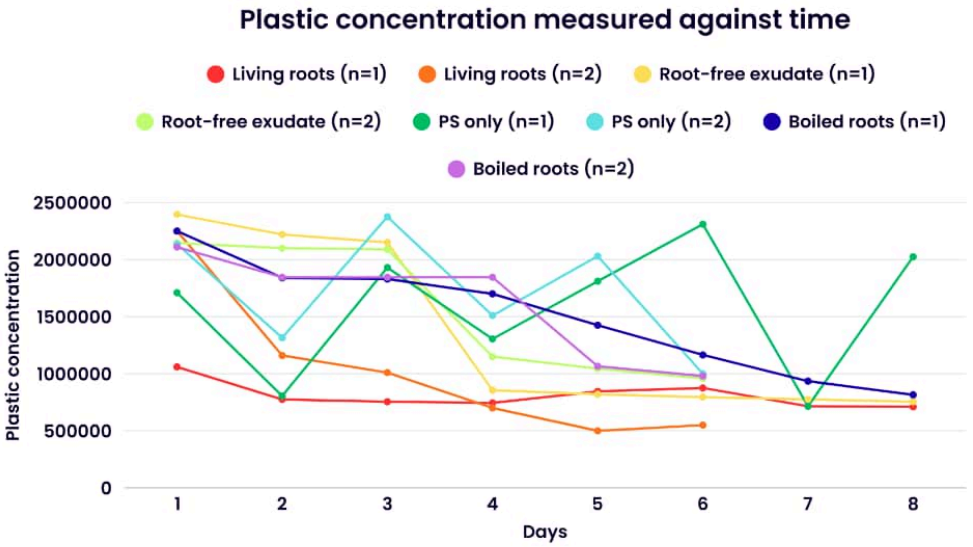

Figure 1. Plastic concentration measured against time (Japan)

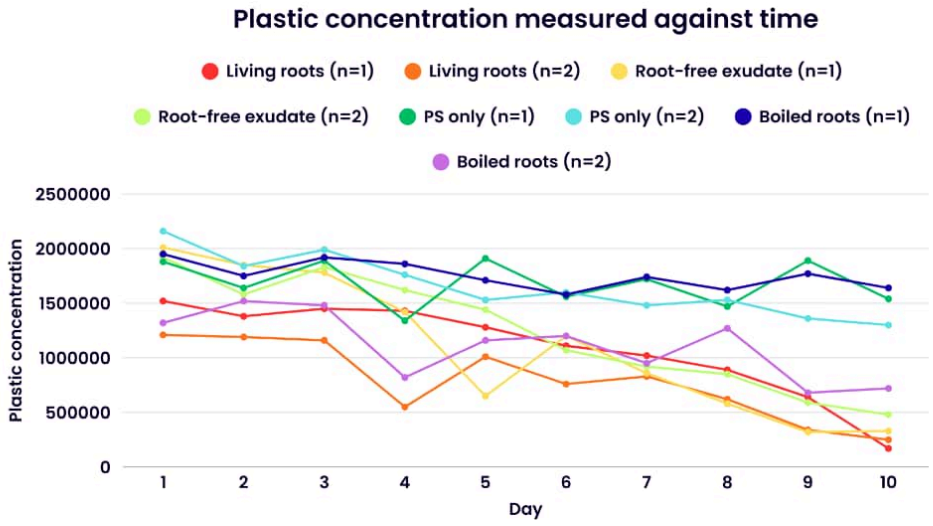

Figure 2. Plastic concentration measured against time (Singapore)

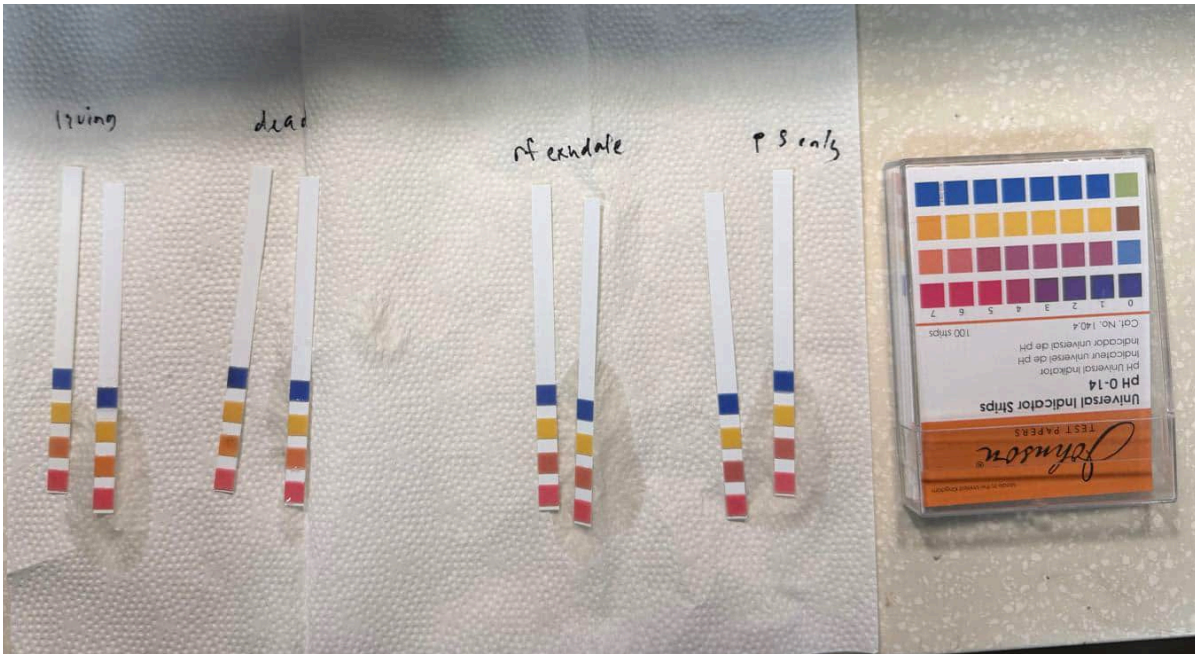

Figure 3. Day 10 pH measurement

Table 1. Overall DOC change for each setup (OD254)

Setup	Measurement on Day 1 (averaged)	Measurement on Day 10 (averaged)
PS + boiled roots 1 PS + boiled roots 2	0.130	0.560
PS + living roots 1 PS + living roots 2	0.095	0.488
PS + root-free exudates 1 PS + root-free exudates 2	0.134	0.600

4. Discussion

From the data collected, it is evident that all setups showed a decrease in PS concentration. It is worth noting that in the PS only setup for Japan, there was an increase in PS concentration. In both Japan (Fig. 1) and Singapore (Fig. 2), setups containing water hyacinth components (living roots, root-free exudates, boiled roots) generally show a greater decrease in PS concentration over time than the PS-only controls, proving that the reduction in PS concentration is not due to sedimentation or natural aggregation, but is affected by biological factors associated with water hyacinths.

In all PS + living roots setups, they had the lowest PS concentration at the end of the 10 days of data collection. This supports the initial idea that water hyacinths have the ability to adsorb microplastics, which correlates with the previous past research papers referenced. Despite the use of duplicates as a means of increasing the accuracy of our results, results are highly differing between duplicates. In

Singapore's boiled roots setup, n=1 showed barely any reduction in PS concentration, similar to that of PS only n=1. However, in n=2, it has shown a reduction that is close to that of root-free exudates setup n=2. In Japan's boiled roots setup, they have been shown to have a significant decrease in PS concentration similar to that of living roots setup n=2. This led us to conclude that Singapore's boiled roots setup n=1 is an outlier.

Based on Table 1., the measurement of DOC through (OD254) showed that all setups (excluding PS only as it was used to blank background interference) had an increase in DOC. Most notably, root-free exudates setup had a higher DOC measurement than the living roots setup. This could be due to living water hyacinths reabsorbing DOC, which root-free exudates setup lacks and hence had accumulating DOC. Through direct comparison of PS concentration and DOC changes, it can be concluded that root exudates have a larger impact on the microplastic adsorption capability of water hyacinths. Measurement of pH has also shown a slight decrease from pH7 to pH6, further proving the release of acidic root exudates and organic acids into the water, which is consistent with active chemical interactions between water hyacinth roots and microplastics.

This proves our hypothesis that root exudates have a greater role in polystyrene microplastic adsorption compared to physical root surfaces, but may not have a significantly greater effect than it. Our research has limitations regarding the sample size of 2, and especially since the two duplicates had such differing results that could lead to an unprecise conclusion on how much more important root exudates are compared to root surfaces in PS adsorption. Furthermore, 10 days of data collection limit our ability to observe the long term relationship between the two factors. The method of quantifying DOC also could be improved, as we had limited resources and hence used the UV spectrophotometer despite the existence of better methods such as Fluorescence EEM (Excitation-Emission Matrix).

5. Conclusion

Overall, the results prove our hypothesis that root exudates have a greater role in polystyrene microplastic adsorption compared to physical root surfaces through the measurement of DOC, pH and PS concentration. These results allow us to further investigate the possibility of harnessing water hyacinths phytoremediative ability for microplastics and applying it in other scenarios.

6. References

Cverenkárová, K., Valachovičová, M., Mackuľak, T., Žemlička, L., & Bírošová, L. (2021). Microplastics in the food chain. Life, 11(12), Article 1349. https://doi.org/10.3390/life11121349

Mustafa, G., Alraqibah, O., Alwaznani, E., Mustakeem, M., & Asrar, N. (2025). Challenges in capital and operation cost reduction of reverse osmosis desalination process. Desalination and Water Treatment, 322, Article 101236. https://doi.org/10.1016/j.dwt.2025.101236

Yin, J., Zhu, T., Li, X., Wang, F., & Xu, G. (2025). Phytoremediation of microplastics by water hyacinth. Environmental Science & Ecotechnology,* Article 100540. https://doi.org/10.1016/j.ese.2025.100540

Chen, Z.-w., & Hua, Z.-l. (2024). Characteristics of organic matter driven by Eichhornia crassipes during co-contamination with per(poly)fluoroalkyl substances (PFASs) and microplastics (MPs). Science of the Total Environment, 894, 170900. https://doi.org/10.1016/j.scitotenv.2024.170900

Investigation of the effect of window placement on the airflow between a room and its atmosphere

Heyi Lee[1], Avyan Mehra[1] Chisaki Kashino[2] Aoi Onuki[2]
[1]*School of Science and Technology Singapore (Singapore)*
[2]*Akashikita Senior High School (Japan)*

Abstract:

The rapid increase in the use of air conditioners worldwide has led to a significant growth in electricity consumption, as well as greenhouse gas emissions, raising concerns about the long-term sustainability of conventional cooling systems. This study explores the sustainable cooling method of passive cooling through natural ventilation as an environmentally friendly alternative to energy-intensive air conditioning. The study investigates the relationship between the number and height of window placement and the time it takes to equalise the hotter temperature inside the prototype with the cooler atmosphere outside. The results show a clear trend, with lower windows being more efficient in ventilation, consistently outperforming the higher-placed windows, suggesting that wind-based ventilation has a greater cooling effect than convection-based ventilation. The prototype 3low demonstrated the best cooling performance of the other prototypes, featuring 3 windows placed near the ground. Overall, these findings highlight the importance of strategic window placement in passive cooling techniques in architectural design. Although heavily simplified, this study demonstrates that passive cooling can play a significant role in lowering reliance on air conditioning and supporting sustainable building design.

Keywords: Passive Cooling; Natural Ventilation; Sustainability

1. Introduction

Air-conditioning units are a significant contributor to global electricity usage and are also responsible for a substantial amount of carbon emissions. According to the International Energy Agency, the use of electrical power by air conditioners and electric fans accounts for approximately 20% of the overall electrical usage by buildings globally (International Energy Agency [IEA], 2018). In addition, unless energy efficiency measures are implemented, energy usage for space cooling is expected to double by 2050. Furthermore, the usage of air conditioners is anticipated to increase from billions currently to 5.6 billion by 2050 (IEA, 2018). This growing usage is taking a significant toll on the electrical infrastructure, according to the International Energy Agency (2018).

The use of air conditioners also affects electricity consumption in measurable ways. An econometric study reveals that installing an air conditioner increases the average household electricity consumption by an estimated 36% compared to households without one. These differences are even more pronounced in hotter and more affluent regions, highlighting the direct relationship between air conditioner adoption and energy consumption (De Cian et al., 2025). In addition, residential electrical demand for cooling is predicted to increase from approximately 1,220 TWh per year in 2020 to nearly 1,940 TWh annually by 2050, reflecting both climate change and socio-economic changes that drive up the demand for cooling (Isaac & van Vuuren, 2024).

These trends are troubling in terms of environmental sustainability, as most electricity production worldwide still relies on fossil fuels, resulting in increased greenhouse gas emissions and air pollution. It is estimated that cooling alone accounts for approximately 4% of global energy-related CO_2 emissions, which is comparable to, or higher than, the contribution of the aviation sector (UNICEF, 2021). In light of these facts, conventional air conditioning systems carry considerable environmental burdens, and there is an urgent need to explore alternative approaches to mitigate this impact.

Natural ventilation is one of the most explored ways of passive cooling. Natural ventilation utilises the principles of wind pressure and convection currents to enhance airflow within buildings, thereby lowering temperatures without the need for electrical power (Ali et al., 2023). Research has proven, through detailed analysis, that incorporating natural ventilation can reduce a building's energy consumption by up to 30% or result in a similar variation when compared to a building that uses only

air conditioning methods (Integrating Natural Ventilation in Building Design, 2023). Additionally, natural ventilation enhances building ventilation and building comfort by increasing ventilation rates.

Windows are critical in these designs, as they serve as the primary means of airflow. Passive designs that incorporate strategically located windows for cross-ventilation can significantly improve airflow and indoor temperatures (Integrating Natural Ventilation in Building Design, 2023). Helpful case studies and analyses suggest that careful window positioning, combined with design features such as courtyards or sky courts, can enhance airflow and reduce mechanical cooling needs (Ali et al., 2023).

Extensive analyses of passive cooling techniques provide further evidence of the efficiency of window-related design. For instance, passive techniques concerning window design, shading, and window-to-wall ratio optimisation can lower indoor temperatures by over 2 °C, decrease cooling loads by more than 30%, and provide energy savings of nearly 30% in populated dwellings in hot environments (Santamouris et al., 2023).

Evidence strongly supports the integration of natural cooling methods at the design stage of residential settings to reduce energy consumption and environmental impacts. Window design, ventilation pathways, and other passive features can be leveraged to achieve measurable reductions in cooling demand and electricity use in buildings. This solution also contributes to several other sustainability imperatives, including reducing peak electrical load, reducing carbon emissions, and increasing resilience to a changing climate. Ultimately, passive cooling integrated into architectural design offers a viable and effective alternative to energy-intensive air conditioning systems; therefore, it should be considered for sustainable housing design.

2. Methodology

Using cardboard cutouts, 6 models were created.

Table 1. Prototypes

Label	Number of Windows	Window height from ground (cm)
1low	1	4
2low	2	4
3low	3	4
1high	1	6
2high	2	6
3high	3	6

From Table 1, you can see the 6 different prototypes made and their specifications.

Figure 1.1: 1high, 2high, 3high

Figure 1.2: 1low, 2low, 3low

An environment 10˚C warmer than the outside was created in the box using hot water. Temperature was measured continuously using a surface laser temperature sensor and a digital stick probe thermometer. A fan was placed in front of the windows, set to a constant wind speed of 1.5 m/s. A timer was started from when the temperature reached +10˚C from the outside, and stopped when the temperature equalised with the atmosphere. The experiment was repeated 2 times.

3. Results

Table 2. Results

Label	1st Time taken to Equalise Temperature (s)	2nd Time taken to Equalise Temperature (s)	Average Time taken to Equalise Temperature (s)	Standard Error (s)
1low	302	306	304	2
2low	200	244	222	22
3low	123	127	125	2
1high	252	260	256	4
2high	460	362	411	49
3high	221	238	229.5	8.5

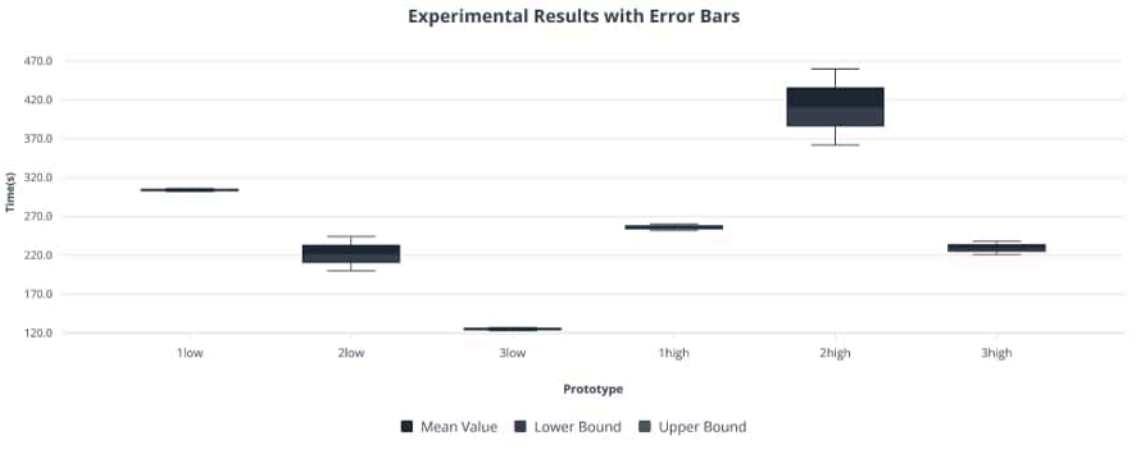

Figure 2. Average time taken for the temperature to equalise. Error bars represent standard errors.

These results indicate an apparent decrease in time taken to equalise temperature as the number of windows increases, as well as a decrease when the windows are placed lower.

4. Discussion

The results show the clear and distinct impact of window configurations on ventilation, increasing airflow while reducing indoor temperatures. This aligns with existing research showing that larger and more numerous windows improve ventilation (Ali et al., 2023).

Low windows consistently performed better than High windows, suggesting that the effect of convection currents in the surroundings was more pronounced, as they allowed cooler air to enter the prototypes more effectively than high windows, thereby displacing warmer air.

The fastest cooling time was observed in the 3low prototype. This indicates that maximising low-level openings can significantly improve natural ventilation in wind-exposed buildings. While the prototypes are simplified and may not accurately represent the cooling capacity of life-sized buildings, the observed trends are generally consistent with architectural studies. However, some limitations of

this model include air loss through cardboard, simplified geometry, and constant wind. Despite these limitations, the experiment successfully presents the fundamental principles of passive cooling and offers insight into the effectiveness of window design.

5. Conclusion

This study investigated how the number and placement in windows affect the passive cooling capability of buildings as opposed to modern air conditioning methods. The findings show that increasing the number of windows significantly improves airflow and reduces cooling time. Among the tested configurations, prototype 3low, with 3 windows placed close to the floor, provided the most effective cooling, outperforming all other prototypes.

Overall, the results highlight the importance of strategic window placement in architectural design, promoting passive cooling and reducing reliance on air conditioning systems in buildings, thereby lowering electricity consumption and greenhouse gas emissions. Although further testing with full-scale models and varying environmental conditions is needed, this experiment demonstrates that passive cooling strategies, particularly optimised window configurations, offer a promising and environmentally friendly approach to indoor thermal comfort.

6. Acknowledgements
Grammarly AI was used to format and check the grammatical accuracy of this report.

7. References

De Cian, E., Campagnolo, L., Colelli, F. P. P., Mistry, M., Xepapadeas, A., & Zappalà, G. (2025). The impact of air conditioning on residential electricity consumption *(Journal of Environmental Economics and Management, 131)*. https://doi.org/10.1016/j.jeem.2025.103122

Integrating Natural Ventilation in Building Design for Energy Efficiency. (2023). *ICSECM.org*. https://icsecm.org/integrating-natural-ventilation-in-building-design-for-energy-efficiency/

International Energy Agency. (2018). The future of cooling: Opportunities for energy-efficient air conditioning. https://www.iea.org/reports/the-future-of-cooling

Isaac, M., & van Vuuren, D. P. (2024). Inequalities in global residential cooling energy use to 2050. Nature Communications, 15. https://doi.org/10.1038/s41467-024-52028-8

Santamouris, M., et al. (2023). The effects of passive design on indoor thermal comfort and energy savings for residential buildings in hot climates: A systematic review. *Urban Climate, 49, 101466.* https://doi.org/10.1016/j.uclim.2023.101466

UNICEF. (2021). The cooling dilemma amid climate change. https://www.unicef.org/innocenti/cooling-dilemma-amid-climate-change

Food Preference and Decoy Effect on Slime Mold

Shih-You Huang[1], Yu-Hsuan Lin[1], Han-You Wu[1], Kaito Suzuki[2], Riku Saito[2]
[1]*Kaohsiung Municipal Kaohsiung Senior High School (Taiwan)*
[2]*Seishin Gakuen (Japan)*

Abstract:

Slime molds are known for their ability to make decisions despite lacking a neural system. This study investigates how different food types influence slime mold growth and explores whether the *decoy effect* occurs in slime molds. Five types of food were used to measure the growth area of slime molds after three days in a growth experiment. In a separate choice experiment, we first observed the slime mold's preference between two food options, then introduced a third (decoy) option to test whether its choice would change. Results showed that food type significantly affected slime mold growth, and that slime molds demonstrated the ability to choose between foods. The decoy effect was observed in several combinations, particularly when the two main food options had similar growth performance. This indicates that slime mold decisions are influenced by the relative attractiveness of food sources. Overall, the findings suggest that the decoy effect may be related to food type and nutritional composition, as slime mold choices were more easily influenced by foods with similar characteristics.

Keywords: slime mold; decoy effect; biological decision-making; nutritional composition; non-neural cognition

1. Introduction

The true slime mold *Physarum polycephalum* is a unicellular organism that lacks a neural system, yet it exhibits remarkably complex behaviors. It prefers moist, dark, and warm environments and forms a large multinucleate structure, known as a plasmodium, during its growth. Despite its simple biological structure, *P. polycephalum* is capable of acquiring information from its surroundings and adjusting its behavior accordingly.

Through maze experiments, it was demonstrated that slime molds form efficient pathways connecting food sources, revealing that problem-solving behavior is possible even in organisms lacking a neural system (Toshiyuki Nakagaki, 2000). This finding challenged the conventional view that complex problem-solving requires neural mechanisms.

Slime molds have also attracted attention as model organisms for studying decision-making. Research has shown that *P. polycephalum* displays preferences among different nutrient sources, such as carbohydrates and proteins (Audrey Dussutour, 2006), and can exhibit seemingly irrational decision-making behavior (T.Latty & M.Beekman, 2010). More recently, the presence of a decoy effect in slime molds has been reported, suggesting that their choices can be influenced by contextual alternatives (Jui-Yu Chou, 2025).

The "decoy effect" describes a cognitive bias where a less attractive third choice makes one of the original options more appealing. Interestingly, this "irrational" preference is not limited to higher animals; the single-celled slime mold *Physarum polycephalum* also displays it. Despite extensive study into the mold's intelligence, we still do not fully understand its nutritional requirements or how it handles these choices when encountering its natural, wild food sources.

Together, these studies demonstrate that even in the absence of a neural system, slime molds are capable of environmental sensing and decision-making. Understanding these behaviors provides valuable insight into the fundamental principles of cognition and decision-making beyond neural systems.

Figure 1, 2, slime mold we reared

Figure 3, sclerotia we made

Therefore, this study aims to further investigate the environmental detection and decision-making behavior of slime molds based on these previous findings.

2. Methodology

The aim of this study was to investigate the decoy effect in food choice behavior of *Physarum polycephalum*. To achieve this, five types of food were selected, and three types of experiments were designed.

About foods

Table1, nutritional values of five foods

Material (100g)	Water (%)	Energy (kcal)	Protein (g)	Fat (g)	Carbs (g)	Fiber (g)
O	0	389	13.2	6.9	66.3	10.6
CK	0	370	7.2	1.5	79.4	7.3
WE	90	25	0.9	0.1	6.8	5.3
M	92	22	3.1	0.3	3.3	1.0
WB	88	35	2.7	0.3	7.6	2.8

Five food types -oatmeal, corn kernel, wood ear, mushroom, and white beech mushroom- were selected. Oatmeal and corn kernel are commonly used foods for *Physarum polycephalum* and have been used in several previous studies. Wood ear, mushroom, and white beech mushroom were selected as foods expected to function as "decoys" in the decoy effect.

As shown in Table 1, these three types of mushrooms have lower nutritional values in all the listed categories compared with the two grain-based foods (oatmeal and corn kernel). Therefore, they can be regarded as sufficiently suitable decoys, irrational options with inferior nutritional value.

Growth experiment

To confirm whether oatmeal and corn kernel are indeed superior foods for *Physarum polycephalum* compared with wood ear, mushroom, and white beech mushroom, each food was provided to the organism, and its growth was observed after three days.

The amount of food provided was 0.06g per sample. For each food combination, 30 samples were prepared. Each sample contained two sclerotia measuring 0.5 cm × 0.5 cm.

We used a culture medium with filter paper for rearing *Physarum polycephalum*. Three to four sheets of tissue paper cut into approximately 5 cm × 5 cm squares were placed in a Petri dish, covered with filter paper, and moistened with purified water. This medium was used instead of a standard agar medium because *Physarum polycephalum* moves more rapidly on paper than on agar, allowing the experimental duration for each sample to be shortened.

Growth was quantified using ImageJ, an image analysis software. The day on which the culture medium was prepared was defined as day 0, and photographs were taken on day 3. The area occupied by *Physarum polycephalum* was selected using ImageJ, and growth was evaluated quantitatively by measuring this area.

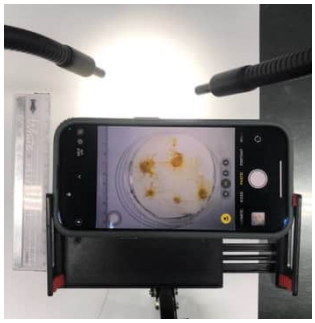

Figure 4, how we take pictures of slime mold

Preference experiment

This experiment examined food preferences of *Physarum polycephalum*. The same five food types as in the growth experiment were used. *Physarum polycephalum* was placed at the center of the medium, and two different foods were placed 0.5 cm away on the left and right sides. On the next day, it was recorded which food was eaten by *Physarum polycephalum*. Because five types of food were used, there were ten possible food pair combinations, with 30 samples for each combination. Samples were

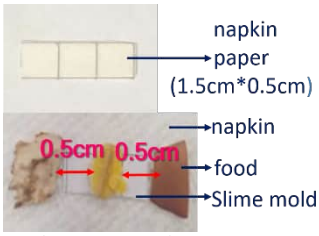

Figure 5, preference experiment setup

excluded from analysis if *Physarum polycephalum* did not eat either food, ate both foods, and died due to factors such as mold contamination. All other experimental conditions were the same as those in the growth experiment.

Decoy experiment

In this experiment, a third option was added to three food combinations that showed similar levels of preference in the preference experiment, in order to investigate whether the added food functioned as a decoy. The selected combinations were

1.corn kernel and oatmeal 2. oatmeal and mushroom 3. wood ear and mushroom

For each combination, a food that was not included in the original pair was used as the third option. Consequently, a total of nine food combinations were tested in this experiment. As in the preference experiment, the distance between the slime mold and each food was 0.5 cm. The food was placed on the left, right, and upper sides of the slime mold. All other conditions were same as those of the preference experiment.

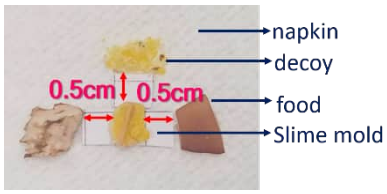

Figure 6, decoy effect experiment setup

3. Results

Growth experiment

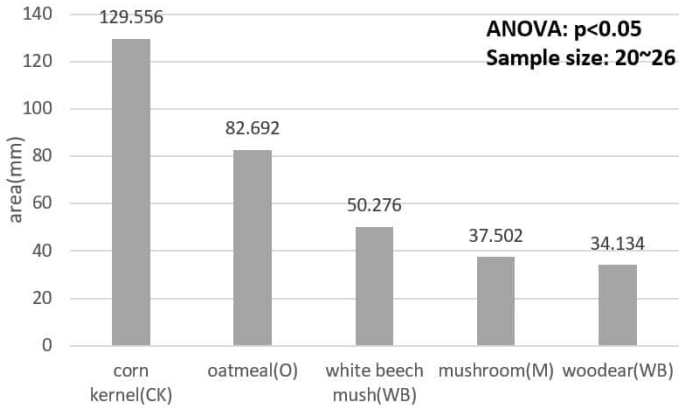

Figure 7, growth area of slime with each foods

Table 2, Tukey HSD table

Pair	Tukey HSD p-value
M vs WE	0.89
M vs WB	0.79
M vs CK	**0.001**
M vs O	**0.001**
WE vs WB	0.79
WE vs CK	**0.001**
WE vs O	**0.001**
WB vs CK	**0.001**
WB vs O	**0.045**
CK vs O	**0.001**

Figure 7 shows the results of the growth experiment. And Table 2 shows that there is a significant difference among the five types of food. However, the mushroom, white beech mushroom and wood ear shows no significant difference between each other.

In conclusion, the type of food can significantly affect slime molds growth. Among the five foods tested, corn kernels showed the greatest growth, while wood ear showed the least growth.

Food preference experiment

Table 3, results of slime mold's preference among the foods

combination	Corn Kernel	Wood Ear	Mushroom	White Beech Mushroom
Oatmeal	11:13 (30, 6, p >0.05)	9:14 (30, 7, p>0.05)	12:10 (30, 8, p >0.05)	10:12 (30, 8, p >0.05)
Corn Kernel	—	3:15 (30,12, p <0.05)	10:10 (30, 10, p >0.05)	8:15 (30, 7, p >0.05)
Wood Ear	—	—	14:14 (30, 2, p >0.05)	20:8 (40, 12, p <0.05)
Mushroom	—	—	—	25:6 (40, 9, p <0.05)

Table 3 shows the results of the preference experiment. There are three food pairs in which the slime mold shows a significant difference in preference. Therefore, we selected the three food pairs with no significant difference for the decoy effect experiment.

Decoy effect experiment

Table 4, results of decoy effect experiment

A	B	Decoy	Result (A:B, Total, Invalid, p-value)
corn kernel	oatmeal	mushroom	9:1 (31,21,$p<0.05$)
corn kernel	oatmeal	wood ear	8:8 (34,18,$p>0.05$)
corn kernel	oatmeal	white beech mushroom	13:2 (32,17,$p<0.05$)
oatmeal	mushroom	corn kernel	8:6 (32,18,$p>0.05$)
oatmeal	mushroom	wood ear	6:2 (31,23,$p>0.05$)
oatmeal	mushroom	white beech mushroom	13:3(32,16,$p<0.05$)
wood ear	mushroom	white beech mushroom	14:1 (32,17,$p<0.05$)
wood ear	mushroom	corn kernel	38:7 (50,5,$p<0.05$)
wood ear	mushroom	oatmeal	16:1 (45,28,$p<0.05$)

Table 4 shows the results of the decoy effect experiment. In Table 4, different decoys were added to the three food groups. As shown, in more than half of the groups, the results changed from no significant difference to significant difference. This indicates that adding a decoy influences the slime mold's choices, demonstrating the decoy effect.

4. Discussion

From the growth experiment, it was found that *Physarum polycephalum* grew to approximately twice the size when fed corn kernels or oatmeal compared with mushroom-based foods. This result can be regarded as reasonable, given that corn and oatmeal contain higher nutritional value. It is also consistent with our empirical expectation that organisms grow better when provided with more nutritionally rich food.

From the preference experiment, several food combinations yielded p-values below 0.05, indicating that *Physarum polycephalum* can select food non-randomly based on certain factors. Although wood ear seemed to be favored among the five food types, this preference cannot be conclusively determined. In addition, the results indicate that *Physarum polycephalum* does not prioritize foods with higher nutritional value that directly promote its growth. We think that it is similar to human behavior since we wouldn't choose what to eat only based on if the food is good for us.

From the decoy experiment, it was shown that the decoy effect occurs in *Physarum polycephalum*; however, its occurrence depends on the combination of foods, and not all foods function as effective decoys. Furthermore, the preference between the two original foods after the introduction of a decoy did not vary depending on the type of decoy. For example, in the combination of wood ear and mushroom with white beech mushroom added as a decoy, a decoy effect was observed and a preference for wood ear emerged. When the decoy was changed to oatmeal or corn kernel, the decoy effect was still observed, and the preference for wood ear was maintained. These results suggest that while the introduction of a decoy induces a preference for wood ear, the direction of this preference is independent of the decoy type and instead depends on the original food combination.

5. Conclusion

Foods with higher nutritional value promote the growth of *Physarum polycephalum*. Although *Physarum polycephalum* can select food non-randomly, the selected food is not always the one with the highest nutritional value. The decoy effect occurs in *Physarum polycephalum*, however, its occurrence depends on the combination of foods, and not all foods function as effective decoys. Furthermore, while the introduction of a decoy induces a preference for a particular food, this preference is independent of the decoy type and instead depends on the original food combination

6. References

1. Chris R. Reid, Tanya Latty, Audrey Dussutour, and Madeleine Beekman (2012). Slime mold uses an externalized spatial "memory" to navigate in complex environments. *Proceedings of the National Academy of Sciences*, 109 (43), 17490-17494. https://doi.org/10.1073/pnas.1215037109
2. Latty, T., & Beekman, M. (2011). Irrational decision-making in an amoeboid organism: Transitivity and context-dependent preferences. *Proceedings of the Royal Society B: Biological Sciences,*

278(1703), 307–312. https://doi.org/10.1098/rspb.2010.1045
3. Hao-Yun Yin, Pin-Jhu Wang, Dong-Sheng Yang, Jui-Yu Chou(2025). Context-dependent food preferences and comparative decision-making in slime mold *Physarella oblonga* . *Journal of Basic Microbiology.* https://doi.org/10.1002/jobm.70023
4. T. Nakagaki, H. Yamada, and Á. Tóth (2000). Maze-Solving by an Amoeboid Organism. *Nature, 407(6803), 470.* https://doi.org/10.1038/35035159
5. Ray, S. K., Valentini, G., Shah, P., Haque, A., Reid, C. R., Weber, G. F., & Garnier, S. (2019). Information transfer during food choice in the slime mold *Physarum polycephalum*. *Frontiers in Ecology and Evolution*, *7*, Article 67. https://doi.org/10.3389/fevo.2019.00067
6. Patino-Ramirez, F., Boussard, A., Arson, C., & Dussutour, A. (2021). Substrate and cell fusion influence on slime mold network dynamics. *Scientific Reports*, *11*(1), Article 1498. https://doi.org/10.1038/s41598-020-80320-2

Effects of Blade Design on Electricity Output in the Waterwheel-Type Generator

Tai Chunhsueh[1], Cheng Kaichi[1], Ho Wei[1], Kohaku Matsui[2], Miu Yasuda[2]
[1]*Kaohsiung Municipal Kaohsiung Senior High School (Taiwan)*
[2]*Waseda University Honjo Senior High School (Japan)*

Abstract:
On rainy days, a large amount of rainwater is discharged from roof drainage systems without being utilized. This study explores the possibility of using such rainwater for hydroelectric power generation and aims to improve the performance of a waterwheel-type generator by optimizing blade design. The research focused on identifying the conditions under which rotational efficiency and electricity output can be maximized. Three experiments were conducted to investigate the effects of blade curvature, blade setting angle, and the application of water repellent coating. In Experiment I related to blade curvature, blades with six varying curvatures were tested using a custom waterwheel-type generator developed by Kaohsiung Municipal Kaohsiung Senior High School. The results showed that Blade 4 exhibited the best performance at low flow rates, while blade curvature had little effect on performance at high flow rates. Experiment II examined the effect of blade setting angle using flat blades. The highest efficiency was achieved when the blades were aligned at 0 degrees along the radius, allowing effective momentum transfer from the water flow. Experiment III investigated the effect of applying a water repellent coating to the flat blades. Although blades without any coating showed slightly higher rotational speed, blades with water repellent coating generated higher average voltages due to improved energy conversion efficiency. These results indicate that generator performance is influenced not only by rotational speed but also by blade geometry, orientation, and surface conditions. The findings provide useful insights for optimizing rainwater-based hydroelectric power generator system, particularly for use during emergencies and disasters.

Keywords: Waterwheel-type generator; Efficiency; Blade Curvature; Blade Setting Angle; Water Repellent Coating

1. Introduction

On rainy days, a large amount of rainwater flows out from the pipes on the roof and just falls to the ground without being utilized. This observation led us to wonder if we could put this rainwater to practical use and came up with the idea of applying it to hydroelectric power generation. Such a hydroelectric power generation based on rainwater could be particularly valuable during disasters, when conventional power supplies may be disrupted. Based on this idea, we decided to focus on improving the efficiency of a waterwheel-type generator. Specifically, we modified the design of the waterwheel blades and investigated the conditions under which its rotational efficiency, and consequently its electricity output, would be maximized. In conducting this study, we referred to previous research carried out by students from Waseda University Honjo Senior High School. In their research, flat blades with and without water repellent coating were used in a waterwheel generator and a positive relationship between the use of water repellent and flow rate, as well as the use of water repellent and voltage was observed. Building on these findings, our research further examines how different blade design affect the performance of a waterwheel-type generator with three main experiments related to blade curvature, blade setting angle, and water repellent coating.

2. Methodology

Experiment I: Blade Curvature (Done by KSHS)

Experiment I related to blade curvature utilized a custom waterwheel-type generator system developed by Kaohsiung Municipal Kaohsiung Senior High School (KSHS), featuring a modified bicycle-powered AC generator. The experimental apparatus was configured as follows: (also shown in Figure 1)

- Potential Energy: Water was released from a constant head height of 2 meters to maintain consistent gravitational potential energy.
- Flow Regulation: The flow rate was manually regulated via a precision tap opening to simulate various environmental and hydraulic conditions.

About the blade design and fabrication, six distinct blades were designed with varying curvatures, defined as the perpendicular distance from the diameter line to the curved edge. To ensure structural

consistency and precision, all blades were fabricated using PLA (Polylactic Acid) via 3D printing. The blades were secured to the generator using a screw-mount system to facilitate efficient and repeatable replacement during trials. The gradient of curvature, ranging from Blade 1 (flattest) to Blade 6 (most curved), is illustrated in Figure 2.

About the data acquisition and processing, in order to ensure high data fidelity and account for the characteristics of Alternating Current (AC), following protocols were implemented:

- Voltage Measurement: Output was measured using the AC setting of a digital multimeter. For each trial, the video footage was paused at 2-second intervals to sample the instantaneous AC voltage.
- Data Smoothing: These periodic readings were averaged to obtain a reliable mean AC voltage, effectively smoothing out transient fluctuations caused by water turbulence or mechanical vibrations.
- Rotational Speed: The Revolutions Per Minute (RPM) were determined via synchronized video analysis, serving as the primary indicator of mechanical efficiency.

Under these conditions, experiments were conducted with waterwheel-type generator using each distinct blades, Blade 1 to Blade 6, and voltage and rotational speed were measured.

Figure 1: The overall experimental setup of the micro-hydroelectric generator, including digital multimeters for data recording in an outdoor environment (In KSHS)

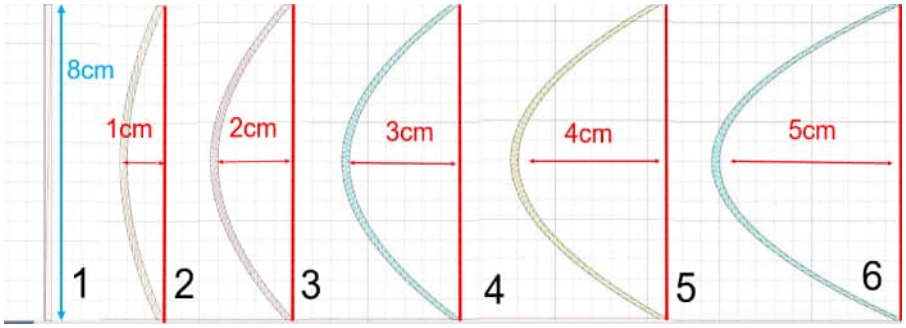

Figure 2: Comparison of blade curvatures (1–6) defined by the perpendicular distance from the diameter line to the curved edge

Experiment II: Blade Setting Angle (Done by WUHSHS)

Experiment II related to blade setting angle utilized a custom waterwheel-type generator used in the preceding research done by students from Waseda University Honjo Senior High School (WUHSHS) with a generator and voltmeter connected to it, as shown in Figure 3. Throughout this experiment, only flat blades were used in order to ensure consistency. The blades were fixed at predetermined angles using duct tape. The flow rate was manually controlled by adjusting the faucet, and for each blade angle configuration, the flow rate was varied approximately ten times. Water was supplied from a hose positioned a meter above the blades and directly toward the center of the blade. For each flow rate condition, the time required for a certain volume of water to accumulate was measured in order to

calculate the flow rate per minute. The rotational speed of the waterwheel was visually measured as revolutions per minutes. In addition, the average generated voltage per minute was calculated through video analysis. Three blade setting angles were compared: 0 degrees aligned with the radius, 30 degrees inward, and 30 degrees outward, as shown in Figure 4. The performance under each condition was evaluated to determine which blade angle produced the highest efficiency of rotational behavior and electricity output of the generator.

Experiment III: Water Repellent Coating (Done by WUHSHS)

Experiment III related to water repellent coating was conducted to examine whether applying a water repellent coating to the waterwheel blades improves the performance of the generator. The experimental environment and setup were identical to those used in Experiment II. Only flat blades were used in Experiment III as well to ensure consistency. Specifically, two experimental conditions were compared: flat blades without any coating and flat blades with a water repellent coating applied uniformly to one side of the blade surfaces that will be hit by water from the faucet.

Figure 3: The overall experimental setup of the waterwheel-type generator, including a generator and voltmeter connected to it in an outdoor environment (In WUHSHS)

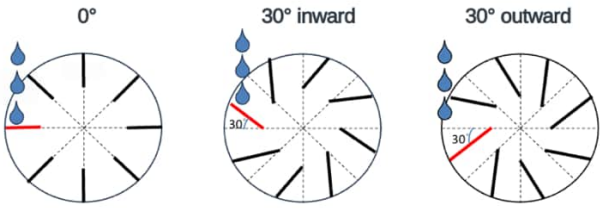

Figure 4: Comparison of blade setting angle

3. Results

Experiment I: Blade Curvature (Done by KSHS)

As an operational observations, the initial trials revealed that Blades 1 and 2 failed to generate sufficient torque to initiate the rotation of the turbine. This lack of performance is attributed to the low curvature (flatness) of the blades, which was insufficient to effectively capture the kinetic energy of the water stream. Also, as performance trends, for all functional designs (Blades 3 to 6), a consistent positive correlation was observed between the water flow rate and the generator's performance (both in RPM and Voltage). As the flow rate increased, the mechanical energy input allowed the generator to overcome internal resistance more effectively. The overall comparative performance is as follows:

- Low Flow Rates: Blade 4 demonstrated superior performance, achieving the highest voltage output. This suggests that its geometry is most efficient at capturing energy when the water momentum is limited.
- High Flow Rates: As the flow rate increased, the performance gap between Blades 3, 4, and 5 narrowed. The data indicates a convergence toward a similar performance ceiling, where the volume of water becomes the primary limiting factor rather than the specific blade geometry.

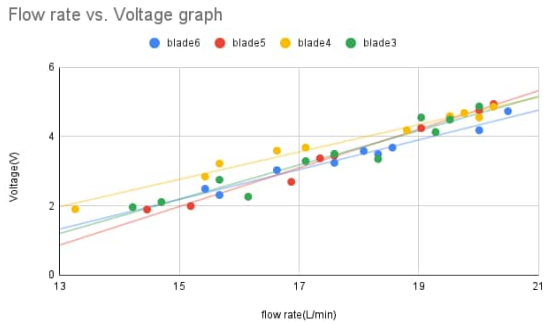

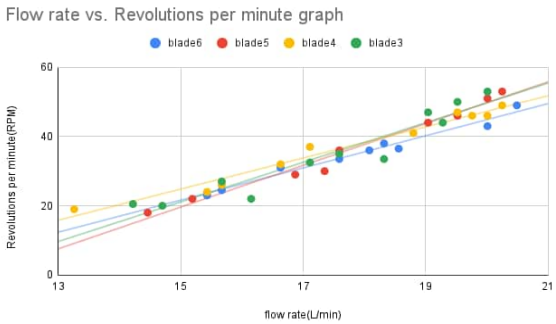

Figure 5 (Left): Graph showing the generated voltage (V) across different water flow rates (L/min) for blades 3, 4, 5, and 6

Figure 6 (Right): Graph showing the revolutions per minute (RPM) across different water flow rates (L/min) for blades 3, 4, 5, and 6

Experiment II: Blade Setting Angle (Done by WUHSHS)

As it is shown in Figure 7 and 8, the waterwheel-type generator achieved the highest efficiency when each blade was positioned 0 degrees along the radius. The next highest values were obtained when the blades were angled 30 degrees inward, followed by when they were angled 30 degrees outward.

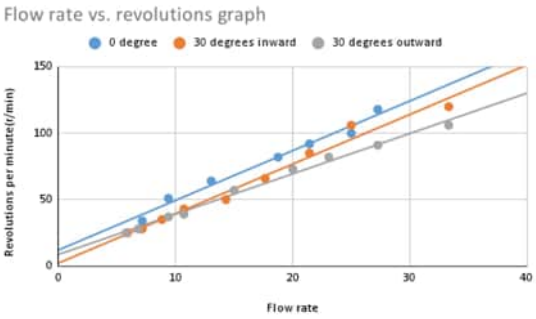

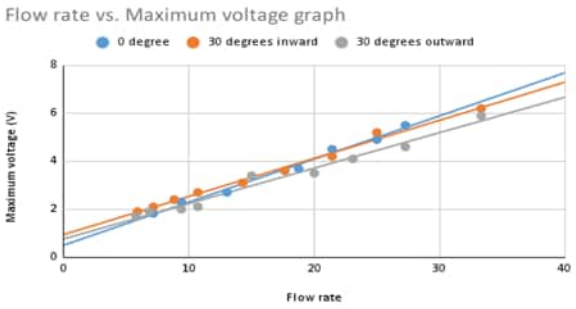

Figure 7 (Left): Graph showing the revolutions per minute (RPM) across different water flow rates (L/min) for different blade setting angles

Figure 8 (Right): Graph showing the generated maximum voltage (V) across different water flow rates (L/min) for different blade setting angles

Experiment III: Water Repellent Coating (Done by WUHSHS)

As it is shown in Figure 9 and 10, higher average voltage was obtained with water repellent coating on a surface of the blades while higher rotational speed was obtained without water repellent coating with a slight difference.

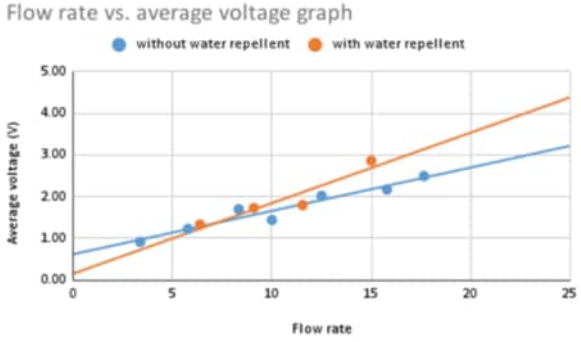

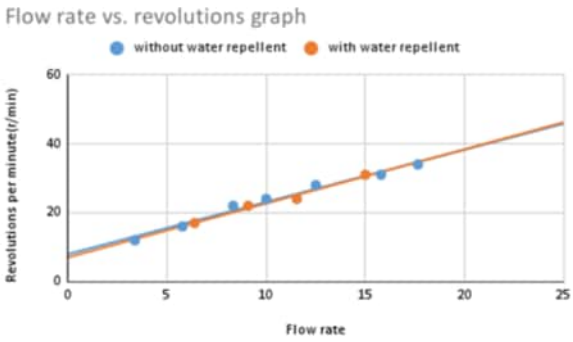

Figure 9 (Left): Graph showing the generated average voltage (V) across different water flow rates (L/min) with and without water repellent coating on blades

Figure 10 (Right): Graph showing the revolutions per minute (RPM) across different water flow rates (L/min) with and without water repellent coating on blades

4. Discussion

Experiment I: Blade Curvature (Done by KSHS)

The performance of the waterwheel is heavily dependent on the fluid-structure interaction between the water stream and the blade geometry:

- Water Contact and Splashing: For flat or low-curvature blades (Blades 1–2), water tends to splash outward upon impact. This results in a momentary impulse rather than a sustained force, failing to provide the continuous momentum required to overcome the generator's inertia.
- Momentum Transfer: Moderate curvature allows water to remain in contact with the blade surface for a longer duration. This extended contact improves momentum transfer ($P = mv$), enhancing the conversion of kinetic energy into rotational mechanical energy.
- Counter-productive Forces: A "splash-back" effect may occur in the turbine, where water is deflected in a way that creates resistance or pushes the turbine in the opposite direction. This phenomenon is more likely to occur as the curvature of the blade increases (e.g., Blade 6), as the deep pocket can trap or redirect water back toward the incoming stream, thereby reducing net power.
- Optimal Geometry: The peak performance of Blade 4 suggests it represents the "Sweet Spot"—the optimal balance between maximizing surface contact for force capture and minimizing fluid resistance or splash-back effects.

Experiment II: Blade Setting Angle (Done by WUHSHS)

The results indicate that the blade setting angle of 0 degrees exhibited the highest performance of the waterwheel. The reason for the result is likely because, at this angle, the water flow directly impacts the blades and transfers its force more effectively within minimal energy loss which therefore makes the blades receive a stronger driving force. In contrast, when the blades are tilted inward or outward, a portion of the water flows along the blade surface and slips away instead of exerting force on the blades. This results in reducing the effective momentum transfer, leading to lower rotational efficiency and electricity output.

Experiment III: Water Repellent Coating (Done by WUHSHS)

The results show that the water repellent coating affects generated average voltage and revolutions in different ways. The blades without water repellent coating exhibited slightly higher rotational speed, which may be caused by stronger water adhesion on the surface of the blades. This adhesion allows water to remain in contact with the blades for a longer time, which makes it easier to cause continued pushing of the blades and a higher rotational rate. On the other hand, blades with water repellent coating produced higher average voltages. This may have been caused by reduction of energy loss because of water retention and turbulence when coating is applied which makes water slide off the blade surface more smoothly. As a result, the torque applied to the generator results in becoming more stable and efficient which leads to improved electrical output even when rotational speed is not maximized. These findings suggest that rotational speed alone does not always determine generator performance. Instead, the efficiency of conversion from mechanical energy to electrical energy plays a significant role. Water repellent coating enhances voltage generation by improving energy transfer efficiency, while blades without water repellent coating shows slightly higher rotational speed due to increased contact between water and blades.

5. Conclusion

The study examined the effects of blade curvature, blade setting angle, and water repellent coating on the performance of a waterwheel-type generator. The results demonstrated that blade design plays an important role in determining generator efficiency on both voltage and revolution. Regarding blade curvature, Blade 4, which was a blade curved at the intermediate level, showed the best performance at low flow rates, whereas at high flow rates, blade curvature had little effect on overall performance. In addition, the highest efficiency in blade setting angle was achieved when the blades were aligned at 0 degrees along the radius, allowing effective momentum transfer from the water flow. Furthermore, although blades without water repellent coating exhibited slightly higher rotational speed, blades with water repellent coating generated higher voltages due to improved energy conversion efficiency. The results provide useful insights for optimizing rainwater-based hydroelectric power generator system.

6. References

Obayashi, M., & Yamakawa, S. (2014). *Creating a micro hydroelectric generator and studying its practicability*. Waseda University Honjo Senior High School.

Singh, D. K., & Singh, S. P. (2018). Control and Operation of a Micro-hydro Power Plant. *IFAC-PapersOnLine*, 51(1), 436-441. https://doi.org/10.1016/j.ifacol.2018.06.134

Light Your Life, More Lightly: Design and Evaluation of Paper-Based Zinc-Air Batteries for Emergency Lighting

Brian Huang[1], Natsumi Kitamura[2], Howard Lin[1], Sam Li[1], Dean Qiu[1], Tomoko Yamaguchi[2]

[1]*Kaohsiung Senior High School (Taiwan)*

[2]*Ritsumeikan High School (Japan)*

Abstract:

This study focuses on developing a paper battery that only needs salt water to generate electricity. During the research, we focused on increasing the V_{load} by changing the battery structure and changing the composition of the electrode ink. Specifically, the powder concentrations of zinc (65–80%) and graphite (40–60%) in the electrode ink varied at 5% intervals. The battery was structured with zinc as the anode and graphite as the cathode. Results show that increase in the Vload does not have much relation to the battery structure and series segmentation. However, the best combination produced a high Vload and good stability was found to be when the zinc powder was 75% and the graphite powder was 50%. These findings indicate that this paper battery can be sustained and kept stable throughout the process. Moreover, it supports that they are both environmentally friendly and can be used as emergency power sources in developing countries or areas where resources are scarce.

Keywords: Paper battery; Anode; Cathode; V_{load}; Zinc; Graphite

1. Introduction

1.1 background

With the rising crisis of e-waste and the limitations of bulky emergency power sources,our project proposes a fully biodegradable, ultra-thin paper battery. Our goal is to transform traditional bulky saltwater lamps into a flexible "printed energy" form factor, providing a sustainable and portable power solution for emergency use.

1.2 Working Principle

The battery utilizes a three-layer sandwich structure: a carbon cathode, a zinc anode, and a porous paper separator. We employ a "Saltwater Activation" mechanism, where the battery remains dry for long-term storage and is instantly activated by a few drops of saltwater through capillary action. This design prevents self-discharge and ensures power availability whenever needed.

1.3 Research Objectives and Benchmarks

Building on the work of Poulin et al. [1] and Yang et al. [2], our primary performance target is the 1.8V stable output demonstrated by Ishibashi et al. [3]. To optimize power output and minimize polarization losses, we investigate three key variables:

1. Material Concentration: Finding the optimal graphite/zinc ratio for maximum reaction efficiency.

2. Series Segmentation: Balancing voltage gain against internal resistance within a fixed area.

3. Electrode Geometry: Analyzing the impact of electrode width on concentration polarization.

The loaded voltage (V_{load}) measured under a 1 kΩ external load was used as the output performance indicator.

2. Methodology

List of Materials:

Collective term	Materials		Purpose of use
-	kraft paper		Waterproof battery casing
-	Conductive Tape		Connecting different segmentations
-	Filter paper		Electrode base
-	3% NaCl solution		Electrolyte
Electrode Paste	Active Powder		Anode
			Cathode
	colloid binder	White glue	Adhesive
		Glycerin	Moisture keeper
		Alcohol	Surface activator
		Conductive tape	Connect subunits

Paste Materials	Active powder	Colloid binder	alcohol
Cathode	Graphite powder	White glue : Glycerin = 4 : 1	Add additional alcohol 20% of total mass, not counted due to evaporation
Anode	Zinc powder		

Battery structure:

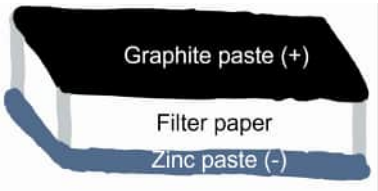

Image 1: Structure of electrode

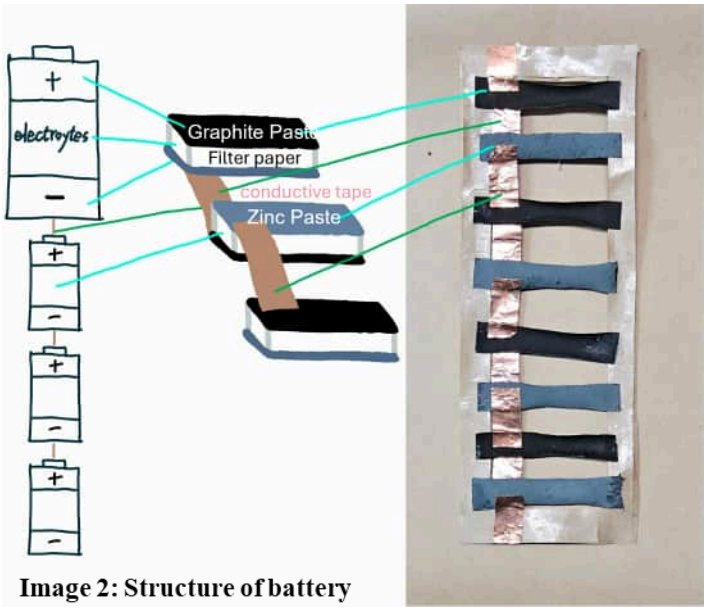

Image 2: Structure of battery

Measurement method:
Each battery was activated using **3 wt% NaCl solution (2 mL cm^{-2})**.
Voltage was measured by recording **Voc for 3 min.**
followed by **Vload under a 1 kΩ load for 2 min**.
All conditions were tested with **n = 5 independent samples.**
and results were analyzed using **box plots**.

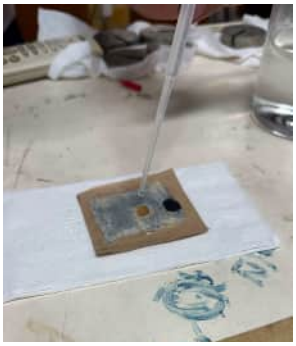

Image 3: Dropping NaCl solution

Experiment 1 (pilot study)
In Experiment 1, we actually constructed batteries and investigated whether there was a correlation between the proportion of active powder in the electrodes and the Voc. Here, we used Battery (1) shown in the photograph above.

Experiment 2 (pilot study—polarization):
In the second pilot study, we tried to decrease the area of batteries and see what happens.

Timing	Voc **(V)**
Before the polarization	0.54
After the polarization	0.20
After putting H_2O_2	0.41 - 0.42

Battery (Zn-/C+): 85%/65% dripped 3% NaCl diluted with water
Voltage decreases due to **polarization,** and it can be solved by adding H_2O_2 into it.

Experiment 3:
(1) **Purpose** : Examine the effect of powder **concentration** of paste on the voltage.
(2) **Method** : Design 5 groups of different concentrations, and paint the same number of groups (e.g., C1/A1) onto five of the batteries. The number 3 stands for the standard concentration according to literature.

3.1 Cathode	C1	C2	C3	C4	C5
Powder	40%	45%	50%	55%	60%
colloid binder	60%	55%	50%	45%	40%

3.2 Anode	A1	A2	A3	A4	A5
Powder	65%	70%	75%	80%	85%
colloid binder	35%	30%	25%	20%	15%

Experiment 4 :

(1) **Purpose** : Examine the effect of **series connection** of batteries on the electric power. (the total area remain unchanged.)

(2) **Method** : Design 5 groups of different pieces of series-connecting batteries (segmentation), and measure the output of voltages.

Segmentation	1	2	4	8	16

Image 4: Batteries with different segmentation

Experiment 5 :

(1) **Purpose** : Examine the effect of **wideness** of batteries on the electric power

(2) **Method** : Design 5 groups of different widths of electrodes, and measure the output of voltages.

widths (cm)	3	4	5	6	7

3. Results

Experiment 1

Battery	**Powder ratio (-/+)**	**Voltage (V)**	
		Maximum	**Minimum**
Battery 1	75% / 55%	0.76	0.72
Battery 2	80% / 60%	0.88	0.78
Battery 3	85% / 65%	0.54	0.52

The results are shown in the table above. We expected that a higher proportion of active powder would lead to a higher V_{load}, but the V_{load} decreased in Battery 3, which had the highest proportion.

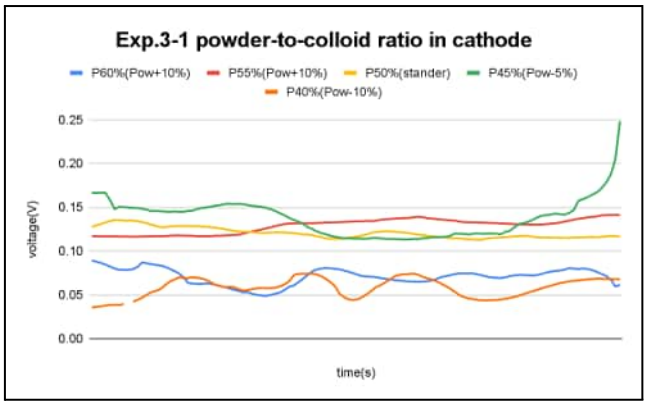

Graph 1 (Powder-to-colloid ratio in cathode)

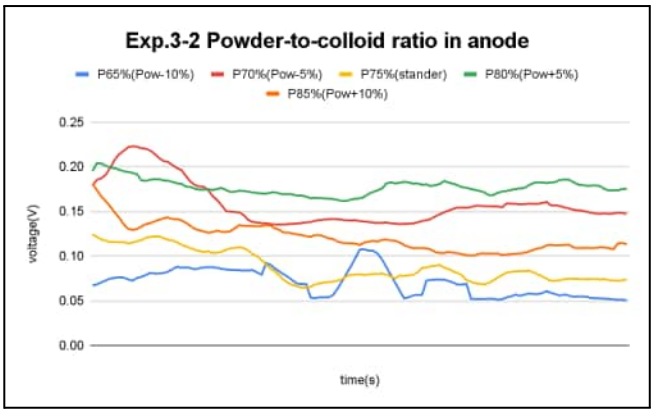

Graph 2(Powder-to-colloid ratio in anode)

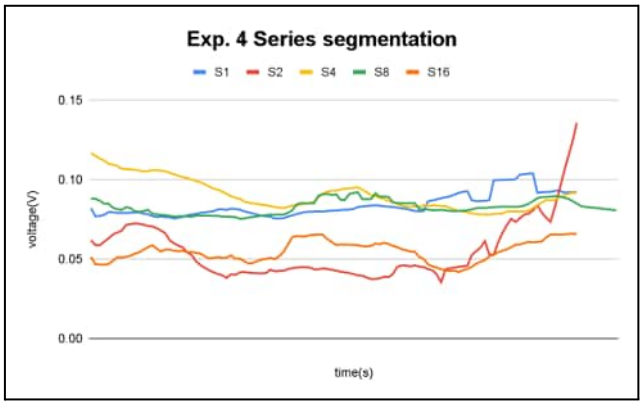

Graph 3 (Series segmentation)

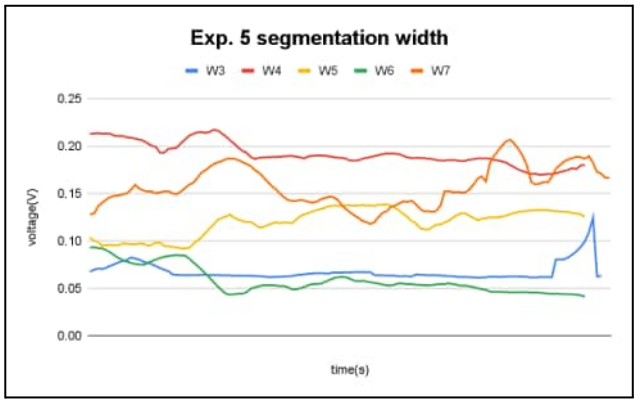

Graph 4 (Segmentation width)

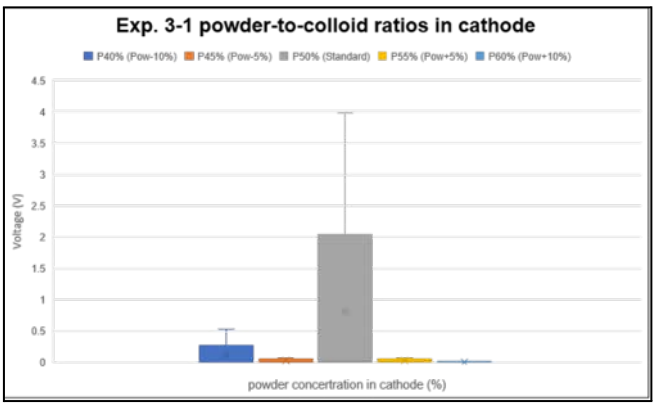

Graph 5 (Powder-to-colloid ratio in cathode)

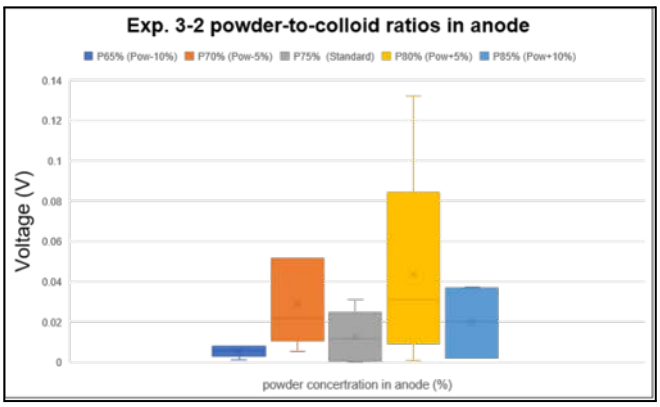

Graph 6 (Powder-to-colloid ratio in anode)

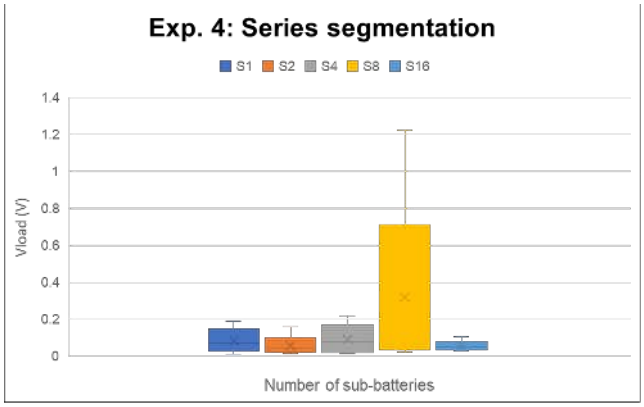

Graph 7 (Series segmentation)

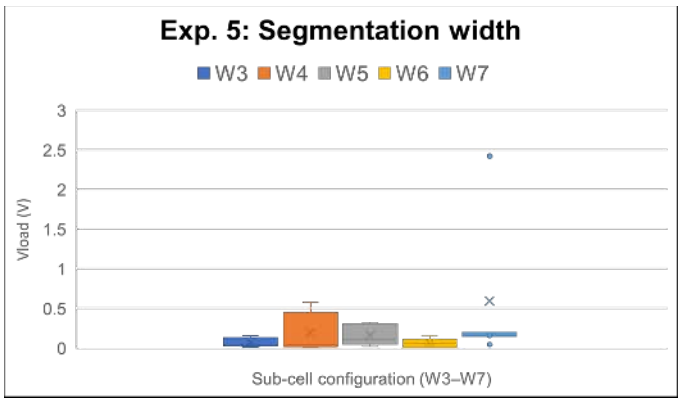

Graph 8 (Segmentation width)

4. Discussion

This study examines how electrode composition and internal geometry affect the output voltage behavior of a paper-based Zn–air battery. Although the theoretical open-circuit voltage of a Zn–air battery is approximately 1.6 V, the measured operating voltage under load is substantially lower (Graphs 5 and 6). This indicates that voltage performance is governed by polarization mechanisms and internal resistive losses rather than thermodynamic limits alone.

In Exp. 3-1 and Exp. 3-2, both the cathode and anode exhibit non-monotonic relationships between powder-to-colloid ratio and V_{load} (Graphs 1, 2, 5, and 6). At low powder ratios, insufficient active material and limited reaction sites lead to activation polarization and reduced voltage. At intermediate ratios, electronic conductivity, ionic transport, and reactant diffusion are balanced, minimizing polarization losses and maximizing V_{load}, as evidenced by higher median voltages and reduced fluctuation ranges in the box plots (Graphs 5 and 6). Excessive powder content increases internal resistance or restricts mass transport, resulting in concentration or ohmic polarization and subsequent voltage decline. These effects explain the observed optimal composition ranges for both electrodes.

In Exp. 4, series segmentation theoretically increases voltage through cell summation; however, experimental results show that voltage enhancement is non-linear (Graph 3, 7). Moderate segmentation (e.g., S8) produces a net increase in V_{load}, where the series voltage gain exceeds additional resistive losses, as reflected by the elevated median voltage in Graph 7. Excessive segmentation (e.g., S16) introduces accumulated interfacial resistance and non-uniform current distribution, offsetting voltage gain and leading to a non-monotonic voltage trend (Graph 3, 7). This demonstrates that segmentation design must balance voltage amplification against resistive penalties.

In Exp. 5, variations in segmentation width under constant total electrode area produce only minor changes in V_{load} (Graph 4, 8). This indicates that segmentation width does not directly determine total output voltage but instead influences the spatial distribution of polarization. Wider segmentation units are more prone to concentration polarization due to longer diffusion paths, while narrower units experience stronger edge effects and localized ohmic losses, resulting in redistribution rather than enhancement of voltage output (Graph 4).

From the V_{load}–time analysis across Exp. 3-1 to Exp. 5 (Graph 1–4), dynamic voltage behavior further confirms that polarization governs battery operation. Stable voltage profiles are dominated by ohmic loss, while fluctuating profiles reflect intermittent concentration polarization. High-voltage profiles maintain elevated average V_{load} but exhibit transient drops due to temporary polarization buildup (Graph 1). Voltage recovery observed after hydrogen peroxide addition at the cathode supports that oxygen depletion and gas accumulation are dominant and reversible loss mechanisms, rather than irreversible material degradation.

Across all experiments, noticeable voltage variation was observed among nominally identical battery samples (Graph 5–8). This variability primarily arises from manual fabrication processes, including non-uniform electrode coating thickness, reduced adhesion and contact instability of conductive tape under wet conditions, and non-uniform electrolyte wetting within the paper substrate. These factors introduce process-induced uncertainty but do not obscure the consistent voltage trends observed across experiments.

5. Conclusion

This study demonstrates that the output voltage of paper-based Zn–air batteries is governed by polarization trade-offs rather than material quantity alone. Both the cathode and anode exhibit non-monotonic relationships between powder-to-colloid ratio and Vload, indicating the existence of optimal composition ranges where activation, concentration, and ohmic losses are balanced. Structural design influences voltage in a constrained manner: series segmentation enhances Vload only within a limited range, beyond which accumulated interfacial resistance and current non-uniformity offset the theoretical voltage gain, while segmentation width primarily redistributes polarization behavior without significantly increasing the overall output voltage. Dynamic voltage behavior further confirms that reversible polarization processes dominate battery operation under load. Overall, effective voltage

optimization requires the co-design of electrode formulation and internal architecture, providing practical design guidelines for lightweight, water-activated, paper-based batteries intended for emergency power applications.

6. References

[1] A. Poulin, X. Aeby, and G. Nyström, "Water-activated disposable paper battery," *Scientific Reports*, vol. 12, no. 1, p. 11919, 2022.
[2] P. Yang, J. Li, S. W. Lee, and H. J. Fan, "Progress and Perspectives on Paper‐Based Batteries," *Advanced Science*, vol. 9, no. 2, p. e2103894, 2022.
[3] K. Ishibashi, S. Sasaki, S. Tokito, and Y. Takeda, "A water-activated paper battery without rare metals for wearable sensor applications," *RSC Applied Interfaces*, vol. 1, 2024.

Comparison of the Effectiveness of Fruits in Inhibiting Oral Bacteria

Nantapak Leelaporn[1], Chayaprapha Poonvutthikun[1], Saki Kaizuka[2], Wakana Suzuki[2]
[1]*Chitralada school (Thailand)*
[2]*Ritsumeikan High School (Japan)*

Abstract:
The objective of this project was to evaluate the antibacterial effectiveness of the selected Thai and Japanese fruits against oral bacteria. The pH values, citric acid content, inhibition zone diameters, minimum inhibitory concentration (MIC), and sugar content of the fruit extracts were studied. In the Thai experiment, lime had the strongest antibacterial activity, followed by starfruit and pineapple. However, in the Japanese experiment, pineapple had the highest antibacterial effectiveness while apple and orange had lower inhibitory activity. The results suggest that the abilities to inhibit oral bacteria are varied by the kinds of fruit, which may be influenced by their acidity and chemical compositions. Overall, this study highlights the potential use of certain fruits as natural antibacterial agents for oral health care.

Keywords: fruits against oral bacteria; citric acid content; sugar content; pH values; minimum inhibitory concentration; bactericidal effect; bacteriostatic effect

1. Introduction

Recently, oral health problems are becoming more common and having a greater impact on the lives of many people around the world. There has been previous research about the effect of fruits against bacteria. The purpose of this research was to find the fruits that were most effective in killing bacteria, which led to the possible solution to oral health problems. Some fruits, such as oranges, contain citric acid, which is said to have an ability to kill bacteria. Therefore, it was thought that it could be possible to create an effective mouthwash from natural fruit juice which has a low pH, a low sugar content and contains citric acid.

2. Methodology in Japan

Culturing Bacteria

1. Nutrient agar medium plates were prepared by adding 10 g of meat extract, 10 g of peptone, 3 g of NaCl, and 15 g of agar to 1000 ml of ion-changed water.
2. The inner cheek was rubbed with a cotton swab. (Both the right and left inner cheek and teeth were rubbed twice).
3. The cotton swab was put into 1 ml of ion-changed water.
4. The solution from step 3 was placed on agar plate using a micropipette.
5. The agar plates were incubated for 2 days at 37℃.

Preparing Fruits Juice

1. The fruit was peeled and cut into small pieces.
2. They were put into a blender.
3. They were put into a vacuum filter.

Experiment 1

1. Oral bacteria (bacteria samples taken from our mouth and cultivated as detailed above) were scraped off by the loop and added to ion exchange water.
2. The bacterial suspension was adjusted to an optical density (OD_{600}) of 0.005.
3. The suspension was aliquoted in 100 µl volumes into 1.5 ml tube.
4. 50 µl of regents (water (N.C), fruit juice, Clinica (P.C, Japanese mouthwash)) were added to each 1.5 ml tube.
5. A 5-fold serial dilution was performed for 10 steps.
6. 10 µl of the solution form Step 5 was placed into the nutrient agar medium plate using a micropipette.

7. The plates were incubated at 37℃ for 1 day.
8. Visible colonies were counted and the diameters of isolated were measured.

Gram staining
1. A platinum inoculating loop was put on a clean slide glass.
2. Small amounts of cultured bacteria were taken with a platinum wire, and they were added to the water on the slide glass.
3. After the solution was dried, the slide grass was passed through the fire about 3 times.
4. Crystal violet solution was dropped to the slide grass.
5. 1 minute later, the slide grass was washed by water.
6. Lugol's solution was added to the slide grass.
7. 1 minute later, the slide grass was washed by water.
8. The slide glass was put into the beaker with pure ethanol and moved it lightly for about 15 to 60 seconds to decolorize.
9. The slide glass was washed.
10. The safranine solution was put on the slide glass and dyed it for 1 minute.
11. It was washed and dried as well.
12. A head microscope was used to observe bacteria. It was observed at 1000 to 1500 times.

Methodology in Thailand

First, the pH of pineapple, lime and starfruit was measured. After that, the fruit juice was made into powder with a spray drying method. To test their antibacterial properties, each fruit powder was dissolved in 10 mL of distilled water at the concentration of 1, 0.5, 0.25, 0.125 and 0.0625 g. The antibacterial activity against oral bacteria was evaluated by measuring the inhibition zone, and the minimum inhibitory concentration (MIC) was determined. The titration method was used to measure the amount of citric acid in pineapple juice, lime juice and starfruit juice.

Table 1. pH of pineapple juice, lime juice and star fruit juice from fruit powder 1 g, 0.5 g, 0.25 g, 0.125 g and 0.0625 g

Types of fruit	pH of 1 gram fruit powder	pH of 0.5 gram fruit powder	pH of 0.25 gram fruit powder	pH of 0.125 gram fruit powder	pH of 0.0625 gram fruit powder
Pineapple	3.73	3.80	3.93	4.22	4.43
Lime	1.23	1.62	2.12	2.49	2.68
Starfruit	1.42	1.73	2.29	2.56	3.48

4. Results

Results in Japan

Table 2. Measurement of fruit juice and mouthwash pH

Apple juice		Orange juice		Pineapple juice
3.96		3.88		3.36
MONDAMIN	Clinica	Systema	Damon	Listerine
7.51	6.33	6.21	2.97	3.62

Table 3. Measurement of fruit juice sugar content

Apple juice	Orange juice	Pineapple juice
15.4	10.1	12.9

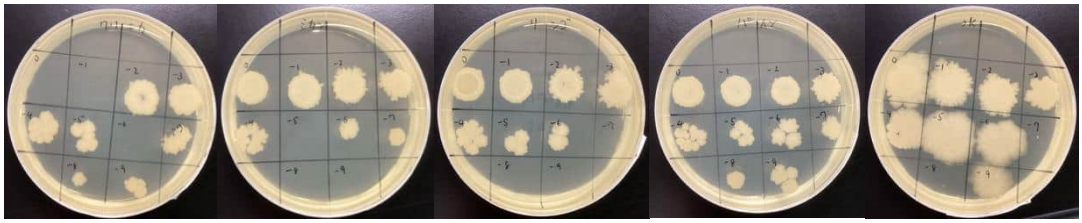

Clinica Orange Apple Pineapple water

Figure 1. State of plate (Trial 3)

Experiment 1, colony diameter
Table 4 shows the diameter of 1-5 independent colonies.

Table 4. Colony Diameter

Sample	Diameter(mm)												
	Trial 1				Trial 2					Trial 3			
Water	7.0	8.0	10.0		7.0	4.5	3.0	4.5	3.0	10.0	10.0	20.0	
Clinica	4.0	5.0	5.0		5.0	4.5	8.0			4.0	5.0	5.5	6.0
Orange	3.0	4.0	5.0		4.0	5.5	8.0			5.0	5.5	7.0	8.0
Apple	5.0	5.0	6.0	6.0	4.5					5.0	5.0	6.5	7.0
Pineapple	4.5	5.0	5.0	7.0	3.0	4.0	4.0	4.0		4.0	7.0	7.0	8.0

1. Standardized data

The data were standardized by dividing each colony diameter by the mean value of the control group (water) for that specific trial.
Figure 2 shows the distribution of the data.

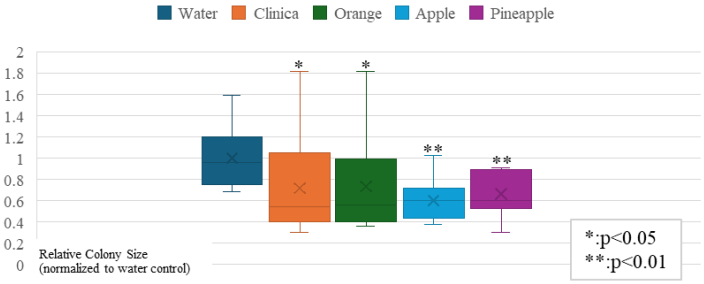

Figure 2. Box plot of Standardized Colony Diameter

2. Kruskal-Wallis Test

The Kruskal-Wallis Test was performed on the standardized data to compare the five groups. Significant difference was observed ($H=10.6705$, $p=0.0305$, $p>0.05$).

3. Mann-Whitney U test

The Mann-Whitney U test was performed on the standardized data to compare water and sample.
Clinica vs water: A significant difference was observed ($U=26.00$, $p=0.0406$, $p<0.05$).
Orange vs water: A significant difference was observed ($U=25.00$, $p=0.0344$, $p<0.05$).
Apple vs water: A highly significant difference was observed ($U=11.00$, $p=0.00333$, $p<0.01$).
Pineapple vs water: A highly significant difference was observed ($U=20.50$, $p=0.00493$, $p<0.01$).

Experiment 1, Colony count

Table 5. Colony Count

Sample	0	-1	-2	-3	-4	-5	-6	-7	-8	-9
Water	3	3	3	3	3	1	1	1	1	2
Clinica	0	0	3	3	3	3	3	3	1	1
Orange	3	3	3	3	3	3	3	1	1	2
Apple	3	3	3	3	3	3	3	2	2	3
Pineapple	3	3	3	3	3	3	3	2	2	2

Sample	0	-1	-2	-3	-4	-5	-6	-7	-8	-9
Water	3	3	3	3	3	3	3	1	1	1
Clinica	0	0	3	3	2	1	0	1	1	1
Orange	3	3	3	3	2	0	1	1	0	0
Apple	3	3	3	3	2	1	1	0	0	0
Pineapple	3	3	3	3	2	2	1	1	1	1

Sample	0	-1	-2	-3	-4	-5	-6	-7	-8	-9
Water	3	3	3	3	3	1	1	0	1	1
Clinica	0	0	3	3	2	1	1	2	2	2
Orange	3	3	3	3	2	1	0	0	0	0
Apple	3	3	3	3	2	1	1	0	0	0
Pineapple	3	3	3	3	3	1	1	2	1	1

Table 5 shows levels of colony count at each dilution stage. The numbers above the chart (0 to -9) represent dilution factors from 5^0 to 5^{-9}.
The occurrence was categorized into four levels: 3 (TNTC, indicated in red), 2 (dense colonies, 6-16 count, orange), 1 (independent colonies, 1-5 count, yellow), and 0 (no colonies, white).
A Kruskal-Wallis Test was performed using these level scores, and no significant difference was observed among the samples.

Results in Thailand

Clear Zone Assay of Lime, Starfruit, and Pineapple Powders Dissolved in 10 mL of Water

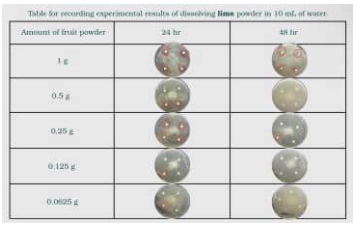

Figure 3. Experimental results of dissolving lime powder in 10 mL

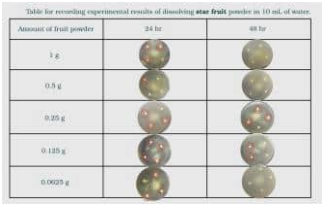

Figure 4. Experimental results of dissolving starfruit powder in 10 mL

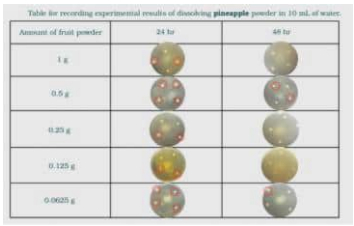

Figure 5. Experimental results of dissolving pineapple powder in 10 mL

Determination of the Minimum Inhibitory Concentration (MIC) of Lime Juice, Starfruit Juice, and Pineapple Juice.

Figure 6. The MIC values of lime juice, starfruit juice, and pineapple juice on the first day.

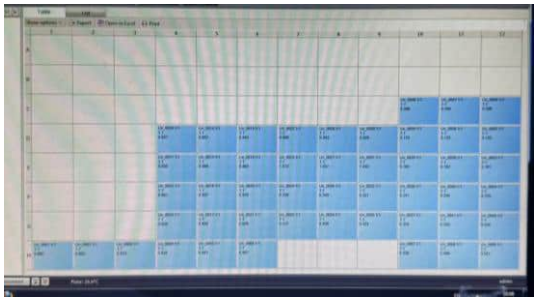

Figure 7. The MIC values of lime juice, starfruit juice, and pineapple juice after 19 hours of incubation.

Determination of Citric Acid Content by Titration

Table recording the experimental results of the citric acid values of lime juices, pineapple juices and star fruit juices by adding 0.1 mol/L NaOH. 32

Lime

	Volume of lime juice used (mL)	Volume of NaOH used at the endpoint (mL)
average	10	49.6 +- 0.153

Pineapple

	Volume of pineapple juice used (mL)	Volume of NaOH used at the endpoint (mL)
average	10	2.3 +- 0.0

Starfruit

	Volume of star fruit juice used (mL)	Volume of NaOH used at the endpoint (mL)
average	10	8.06 +- 0.06

Figure 8. Experimental results of the citric acid values of lime juice, pineapple juice and starfruit juice by adding 0.1 mol/L NaOH

4. Discussion

Discussion in Japan

1. Identification of oral bacteria

The bacteria used in this experiment were presumed to be Neisseria (non-pathogenic, oral resident flora). This is because the cells exhibited a coccus shape and were identified as Gram-negative via Gram staining.

2. Bactericidal effect and Bacteriostatic effect

As shown by the experimental results, fruit juices did not reduce the number of colonies. Instead, they inhibited the growth of colony size. These findings suggest that these samples did not have a bactericidal effect (action to kill bacteria) but exhibited a bacteriostatic effect (action to inhibit bacteria growth).

3. Contribution of pH, Sugar Content, and Specific Components

Pineapple: Among the three samples, pineapple showed the strongest inhibitory effect. This is likely

due to its lowest pH (3.36) and the presence of Bromelain (protein-digesting enzyme), which synergistically inhibited bacterial growth.
Apple: Among the three samples, apple showed the second strongest inhibitory effect. Although its pH was the highest (least acidic), it had a high sugar content. This suggests that osmotic pressure contributed significantly to its bacteriostatic effect.
Orange: Orange had moderate sugar content and pH levels compared to the other two samples. Consequently, its bacteriostatic effect was not as strong as that of pineapple or apple.

4. Antibacterial Effect of Clinica
In the experiments using Clinica, no colonies were observed at low dilution levels (5^0 and 5^{-1}). Similar results were obtained in a preliminary experiment using a higher bacterial concentration (OD_{600} 0.1). These findings suggest that the antibacterial effect of Clinica did not depend on the ratio of the agent to the number of bacteria. Instead, it reflects the inherent concentration-dependent potency of clinica.
Specifically, when the final concentration of clinica was 6.67%, it exceeded the Minimum Inhibitory Concentration (MIC), completely inhibiting initial adhesion to the agar medium and growth. On the other hand, when the final concentration fell below the MIC due to further dilution, the effect of Clinica shifted from "complete inhibition" to a "bacteriostatic effect," similar to the fruit juices.

Discussion in Thailand
Experimental results showed that lime had the highest antibacterial activity, followed by starfruit and pineapple, based on the inhibition zone. This correlates with the titration results, where lime required the highest volume to reach the endpoint. This suggests that the higher concentration of citric acid in lime plays a key role in inhibiting oral bacteria more effectively than the other fruits. From microplate reader analysis, bacterial growth in lime juice was 1% at a concentration of 0.75, In starfruit juice, it increased to 39.5% at the same concentration. In pineapple juice after 19 hours, bacteria growth was still present.

This project aimed to compare the antibacterial inhibitory effects against oral bacteria of key lime (Citrus hystrix) powder, Thai starfruit (Averrhoa carambola) powder, and Pattavia pineapple (Ananas comosus) powder.

Based on the experimental results, fruit juice powders at the concentration of 1, 0.5, 0.25, 0.125, and 0.0625 g dissolved in 10 mL of distilled water were tested using the agar diffusion method. The results showed that the key lime powder produced the largest clear zone, indicating the strongest antibacterial activity. Starfruit powder and pineapple powder showed similar clear zone sizes at the same concentrations.

Quantitative analysis of citric acid content revealed that key lime juice contained the highest average percentage of citric acid (31.5%), followed by starfruit juice (5.1%) and pineapple juice (1.4%). These findings suggest that the antibacterial activity observed may be related to the citric acid content present in each fruit.

The spray drying technique to converse fruit juice into powder enabled the longer storage of fruit juice, making it more convenient to evaluate antibacterial effectiveness. Therefore, this approach provided a practical method to dissolve fruit powder in water at the minimum inhibitory concentration (MIC) to inhibit oral bacteria. MIC refers to the lowest concentration that can stop the growth of bacteria. In this study, lime powder at 0.75 g dissolved in 10 mL of distilled water was the minimum concentration that could inhibit oral bacteria.

5. Conclusion

In conclusion, this project, which was a collaboration between Thailand and Japan, showed that fruit can help reduce the growth of oral bacteria. The fruit used in this study was able to inhibit bacteria that are related to tooth decay and gum disease. This suggests that fruit may be a natural way to help improve

oral health. Using natural products like fruit could be safer and more environmentally friendly than using chemical substances. However, more research is still needed to find the active compounds in the fruit and to see how it can be used effectively in oral care products in the future.

6. Acknowledgements

Sincere thanks should be delivered to Assistant Professor Dr. Piyangkul Lueangcharoenkit from the Department of Microbiology, Faculty of Science, Kasetsart University, for the provision of laboratory and equipment.

7. References

DeJesus, N. (2012). High acid levels in your mouth lead to cavities. *Air Force Medicine*. https://www.airforcemedicine.af.mil/News/Article/426104/high-acid-levels-in-your-mouth-lead-to-cavities/

Kato, Y. (2018). Bacteriostatic effect of lemon fruit juice: *Its potential as an oral rinsing agent. OMICS International*. https://www.omicsonline.org/open-access/bacteriostatic-effect-of-lemon-fruit-juice-it8217s-potential-as-an-oral-rinsing-agent-2332-0702-1000243-103051.html

Moahsomm, T. (2020). Project report on applying the Sufficiency Economy Philosophy and plant genetic conservation awareness for sustainable community development. *Google Drive*. https://drive.google.com/file/d/1P_ApfwLFMpEfXAIuV-EKIv0dAtPw-TtI/view?usp=drivesdk

Yapong, B. (2015). Efficiency of Mitis Salivarius Bacitracin agar stored for four weeks in isolating mutans streptococci from human saliva. *Chulalongkorn University Digital Journal*. http://161.200.36.106/cudj/upload/article//file_full_2848.pdf

Pangsomboon, K. (2001). Comparison of the effectiveness of 0.12% chlorhexidine mouthwash and special mouthwash (0.005% chloroxylenol) in reducing oral bacteria. *Prince of Songkla University Knowledge Bank*. https://kb.psu.ac.th/psukb/bitstream/2553/4008/14/217210.pdf

Chandel, S. (2017). The effect of sodium bicarbonate oral rinse on salivary pH and oral microflora: A prospective cohort study. *Journal of Clinical and Diagnostic Research*.

Meyer-Lippert, J. (2017). How pH affects oral health. *Side Effect Support*. https://sideeffectsupport.com/blogs/professionals/how-ph-affects-oral-health

Pattem, J. (2022). The dynamic interplay of dietary acid pH and concentration during early-stage human enamel and dentine erosion. *Frontiers in Dental Medicine*. https://www.frontiersin.org/journals/dental-medicine/articles/10.3389/fdmed.2022.1040565/full

Meurman, J. H., et al. (1996). Pathogenesis and modifying factors of dental erosion. *European Journal of Oral Sciences*. https://pubmed.ncbi.nlm.nih.gov/8804887/

Techasaengmanee, P. (2024). Antimicrobial effects against oral pathogens using 0.12% chlorhexidine combined with herbal extracts (Andrographis paniculata, fingerroot, Indian gooseberry, and eucalyptus). *Srinakharinwirot University Dental Journal.* https://ejournals.swu.ac.th/index.php/swudentj/article/download/15989/12774/57019

Darunarut, S. (2020). Antibacterial, anti-biofilm formation, and antioxidant activities of Chinese herbal extracts against oral bacteria. *Journal of Phetchaburi Rajabhat University Science,* 17(1), 33-44. https://has.hcu.ac.th/xmlui/bitstream/handle/123456789/1671/Antibacterial.pdf?sequence=1&isAllowed=y

Hiroyuki, T. (2006). Antibacterial Activity of Citrus Fruit Juices Against Vibrio Species. *Journal of Nutritional Science and Vitaminology*, 52(2), 157-160. https://doi.org/10.3177/jnsv.52.157

N C, P. (2014). In vitro Evaluation of Antibacterial Efficacy of Pineapple Extract (Bromelain) on Periodontal Pathogens. *Journal of International Oral Health, 6(5), 96-98.* https://pmc.ncbi.nlm.nih.gov/articles/PMC4229839/

Minasari, N. (2020). Effectiveness of Star Fruit Leaf Extract on the Growth of Streptococcus Sanguinis: An In Vitro Study. *World Journal of Dentistry*, 11(3), 196-200. https://doi.org/10.5005/jp-journals-10015-1731

Guy, W. (2003). Fatal Large-Volume Mouthwash Ingestion in an Adult: A Review and the Possible Role of Phenolic Compound Toxicity. *Journal of Intensive Care Medicine*, 18(3), 150-155. https://doi.org/10.1177/0885066602250783

Robert, M. (2009). Intoxication With Mouthwash Presenting as Psychosis and Delirium in a Combat Theater. *International Journal of AMSUS*, 174(8), 828-831. https://doi.org/10.7205/MILMED-D-03-5208

Shulman, J. (1997, September 1). Acute ethanol toxicity from ingesting mouthwash in children younger than 6-years of age. *Europe PMC*. https://academic.oup.com/milmed/article-abstract/174/8/828/4335695

John, L. (2023). *Bacteriostatic Antibiotics*. *StatPearls*

Supoltep, T. (2020). Chlorhexidine in Dentistry Part I: Functional Mechanism and Adverse Effects. *Journal of Khon Kaen Dent*, 23(3), 99-107. https://www.researchgate.net/profile/Suponteр-Teerakanok/publication/353794921_Chlorhexidine_in_Dentistry_Part_I_Functional_Mechanism_and_Adverse_Effects/links/611247ce1ca20f6f860f7d7d/Chlorhexidine-in-Dentistry-Part-I-Functional-Mechanism-and-Adverse-Effects.pdf

Meenakshisundaram, S. (2012). Optimization of spray drying process for developing seabuckthorn fruit juice powder using response surface methodology. *Journal of Food Science and Technology*, 51(12), 3731-3739. https://doi.org/10.1007/s13197-012-0901-y

京都大学資源生物学科教員（農学研究科）. (2012). 第 3 節　細菌の観察. *OpenCourseWare Kyoto University.* https://ocw.kyoto-u.ac.jp/wp-content/uploads/2012/04/2012_shigenseibutsukagakujikkenn_jikkenhou1-2_01-04-3.pdf

Efficacy of Extracts from Thai and Japanese *Piper nigrum* L. to Inhibit *Stachybotrys chartarum* and *Cladosporium* sp.

Supparada Kiatchalermporn[1], Khemmarat Wongvigran[1], Ayana Sasaki[2], Yuka Shibasaki[2], and Ayano Yoshida[2],

[1]*Chitralada School (Thailand)*

[2]*Ritsumeikan Moriyama High school (Japan)*

Abstract*:*

Poor indoor air quality is a major public health concern and is often associated with moisture-related fungal contamination, particularly *Stachybotrys chartarum* and *Cladosporium* sp. The demand for safe and environmentally friendly antifungal agents has increased interest in plant-derived compounds such as *Piper nigrum* L., whose primary bioactive alkaloid, piperine, exhibits broad-spectrum antifungal activity through disruption of fungal cell walls or membranes, interference with metabolic processes, and inhibition of biofilm formation. This study aims to evaluate the antifungal potential of *Piper nigrum* L. extracts from Thai and Japanese sources against indoor fungi, with a focus on *Stachybotrys chartarum* and *Cladosporium* sp.

Piper nigrum L. samples were obtained from commercial markets in Thailand and Japan, and then were dried, and extracted with ethanol. The crude extracts were concentrated by rotary evaporation, and piperine was identified by UV–Vis spectrophotometry, showing an absorption peak at 345 nm. In the Thai study, Stachybotrys chartarum was cultured for 14 days and evaluated for antifungal activity using the toxic plate method. The minimum inhibitory concentration (MIC) was determined to be 25 mg/mL, and the minimum fungicidal concentration (MFC) was established at 50 mg/mL, indicating clear inhibitory and fungicidal effects. In contrast, the Japanese study involved environmental fungal sampling and microscopic identification due to laboratory constraints. The predominant isolate was identified as *Cladosporium* sp., and no significant growth inhibition was observed under the applied conditions. The observed differences between the two studies are likely attributable to variation in fungal species, sampling methods, and the inability to apply precise MIC and MFC values. Overall, the findings suggest that *Piper nigrum* L. extract exhibits species-dependent antifungal activity and demonstrates strong potential against *Stachybotrys chartarum* under controlled experimental conditions.

Keywords*:* *Piper nigrum L.*; Piperine; *Stachybotrys chartarum, Cladosporium* spp.

---

1. Introduction

Poor indoor air quality, especially in damp or poorly maintained buildings, can increase the risk of respiratory diseases by allowing harmful molds such as *Stachybotrys chartarum* to grow. This mold is one of the most important species in its genus. Since 1993, exposure to *Stachybotrys chartarum* has been linked to serious lung problems in infants because it produces toxic substances that can damage tissues in the respiratory tract and may cause severe bleeding (Dylag et al., 2022). Similarly, *Cladosporium* sp. are among the most common indoor airborne molds, frequently found on damp building materials and household surfaces, and exposure to *Cladosporium* spores has been associated with allergic reactions, asthma exacerbation, and other respiratory symptoms in humans (Bensch et al., 2012; WHO, 2009). In Thailand and Japan, indoor mold contamination is a significant issue because of the hot and humid climate, the rainy season, and the widespread use of highly airtight buildings, which promote mold growth in indoor environments such as bathrooms, closets, and air-conditioning systems. Due to these health risks, there is growing interest in using natural

antifungal substances. Specifically, *Piper nigrum* L. (black pepper) is considered a possible option because it contains piperine as the main active compound (Hikul et al., 2018). Piperine has been shown to inhibit many types of fungi by disrupting cell walls or membranes, interfering with normal cell activity, and reducing biofilm formation. However, its effect on Stachybotrys chartarum has not been clearly studied. Therefore, it is interesting to study the potential of piperine to inhibit *Stachybotrys chartarum* and *Cladosporium* sp..

2. Methodology

Thailand

Step 1: Piperine Extraction
1.1 Wash *Piper nigrum L*. thoroughly.
1.2 Dry *Piper nigrum L*. at 60°C for 24 hours.
1.3 Grind the dried *Piper nigrum L.* by using a blender.
1.4 Store it in an opaque, airtight container.
1.5 Add 3 L of 95% ethanol until it covers the dried *Piper nigrum* L., then close the jar tightly, and leave at 25°C for 24 hours.
1.6 Filter by using a filter cloth and filter glass vacuum to collect the liquid extract.
1.7 Evaporate with a rotary evaporator.

Step 2: Identification of piperine in *Piper nigrum* L. extracts using UV-Vis spectrophotometer by running at wavelengths ranging from 200-500 nm

Step 3: Isolation of *Stachybotrys chatarum and* Identifying Fungal Species
3.1 Transfer a hyphal tip or single spore onto three fresh PDA plates. Open the plate at a 45° angle away from the operator.
3.2 Incubate the plates at room temperature in dark or dim light and monitor daily for 14 days and then examine the morphology of the plates on day 14 under a microscope.
3.3 Place a drop of Lactophenol Cotton Blue on a clean slide.
3.4 Cut a small piece of clear tape and gently touch the sticky side to the surface of the fungal colony to lift the hyphae and spores.
3.5 Carefully place the tape onto the stain.
3.6 Examine the prepared slide under the microscope.

- Microscopic morphology of Stachybotrys chatarum: hyphae are septate and grow both on and within the culture medium, sometimes forming rope-like structures. Conidiophores are simple or branched, bear clusters of monophialidic phialides at the apex, and change from hyaline to dark with age. Conidia form dark, slimy masses and are oval in Stachybotrys chartarum, averaging 4.5 × 9 µm, becoming dark and verrucose at maturity. (Marie-Alix d'Halewyn et al., n.d.)

Step 4: Minimum Inhibitory Concentration (MIC)
4.1 Prepare extract at the concentrations of 100, 50, 25, 12.5, 6.25, 3.12, 5.157 and 0.78 mg/mL
4.2 The toxic plate method is employed using the extract at different concentrations, with three replicates per concentration. Sterile distilled water, 33.33% DMSO and 16% DMSO, is used as controls. All plates are incubated at room temperature for 3 days. Toxicity testing is performed by

mixing *Stachybotrys chartarum* spores (10^5 spores /mL), PDA medium and the prepared *Piper nigrum* L. solution, divided equally among three wells, at a 50:50:50 μL ratio in each well.

Step 5: Minimum Fungicidal Concentration (MFC)
5.1 Based on the MIC results (25 mg/mL), concentrations of 25, 50, and 100 are selected where no visible fungal growth is observed. A control plate without the test substance is also included.
5.2 Fresh agar plates without the test substance are prepared, and fungal samples from the MIC plates at 25, 50, and 100 are transferred onto these plates to assess fungal regrowth.
5.3 Plates are observed for the presence or absence of fungal growth.

- Approximately 333 colonies are present in the initial inoculum, and a 10% survival threshold (33 colonies) is used to define fungicidal activity.

Japan

Step 1: Preparation of *Piper nigrum* L. Extract
1.1 Grind dried fruits of Malaysian *Piper nigrum* L. into a fine powder and weigh 500 g.
1.2 Transfer the powder into a volumetric flask and add 1.5 L of 95% ethanol until the sample is slightly covered.
1.3 Seal the flask tightly with aluminum foil and parafilm to prevent evaporation and then leave at room temperature for 24 hours.
1.4 Filter the mixture using filter paper to separate the solid residue and collect the liquid extract.
1.5 Use a rotary evaporator to remove the ethanol solvent until a paste-like crude extract is obtained.

Step 2: Environmental Fungal Sampling and Isolation
2.1 Prepare sterile PDA (Potato Dextrose Agar) plates.
2.2 Place the open PDA plates in a restroom environment for 24 hours to collect airborne fungal spores.
2.3 After exposure, seal the plates with parafilm and monitor daily for fungal colony development.

Step 3: Identifying Fungal Species
3.1 Collect a small sample of the fungal colony from the PDA plate using an experimental spatula.
3.2 Place the sample on a clean glass slide and add a drop of Acetic Dahlia for staining.
3.3 Examine the prepared slide under a light microscope to analyze hyphae and spore morphology.
3.4 Microscopic morphology of *Cladosporium* sp.: Conidiophores are dark, branched or unbranched and produce chains of pigmented, lemon-shaped conidia. Distinct dark scars (disjunctive scars) are visible where conidia are attached. Hyphae are septate and olive-to-brown in color.

Step 4: Antifungal Activity Assay
4.1 Disinfect the Biological Safety Cabinet (BSC) work surface with 70% ethanol and place all sterilized instruments inside.
4.2 Place a sterilized filter paper disk 1.0–1.5 cm from the edge of the PDA plate using sterile forceps.
4.3 Apply 10–20 μL of the *Piper nigrum* L. extract onto the center of the paper disk using a micropipette.
4.4 Seal the plates with parafilm and incubate in an incubator at 25–30°C for 6 days.
4.5 Measure the radial growth of fungal colonies daily and document morphological changes with photographs.

3. Results and discussion

Thailand

Step 2: Identification of piperine in *Piper nigrum L.* extracts using UV-vis spectrophotometer

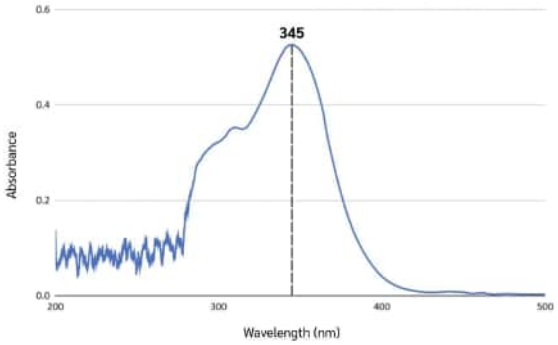

Figure 1. UV-Vis spectrum of Piperine in *Piper nigrum* L. extracts

The UV-Vis spectrophotometric analysis confirms the presence of Piperine in the *Piper nigrum L.* extracts. The spectrum shows a clear maximum absorption peak at 345 nm, which falls within the characteristic range for piperine (300–400 nm).

Step 3: Identifying Fungal Species

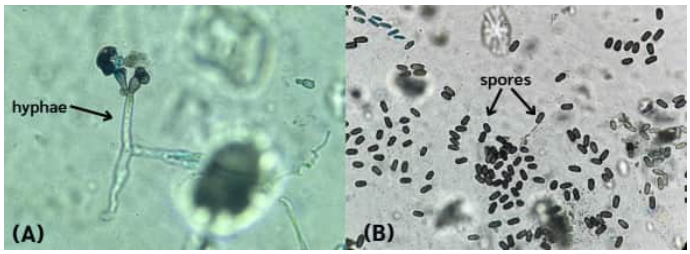

Figure 2. A,B: *Stachybotrys chatarum* under the light microscope at 40x magnification.

Step 4 :Minimum Inhibitory Concentration (MIC)

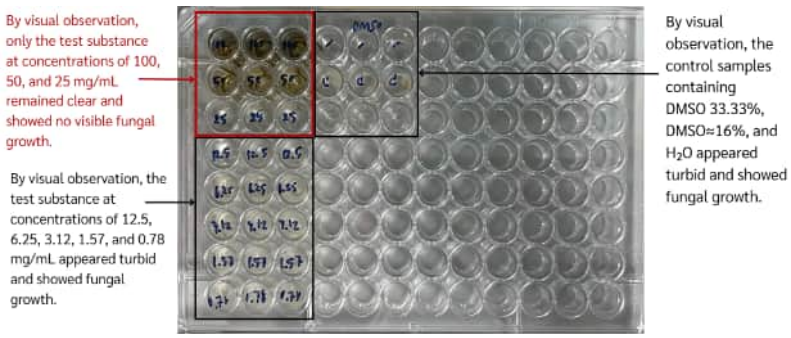

Figure 3. Toxicity (MIC) assay of *Piper nigrum* L. against *Stachybotrys chartarum* using the toxic plate method for 3 days

By visual observation, only the test substance at concentrations of 100, 50, and 25 mg/mL remained clear and showed no visible fungal growth. Therefore, the minimum inhibitory concentration (MIC) was determined to be 25 mg/mL

Step 5: Minimum Fungicidal Concentration (MFC)

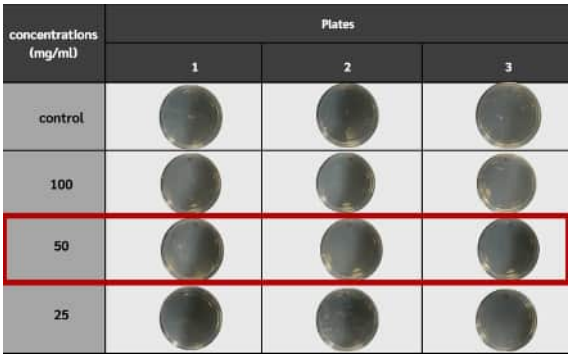

Figure 4. MFC results of *Piper nigrum* L. extracts against *Stachybotrys chartarum* on PDA plates

At the concentration of 50 mg/mL, approximately 26 fungal colonies were observed, which below the threshold. Therefore, the MFC was determined to be 50 mg/mL

Japan

Step 2: Environmental Fungal Sampling and Isolation

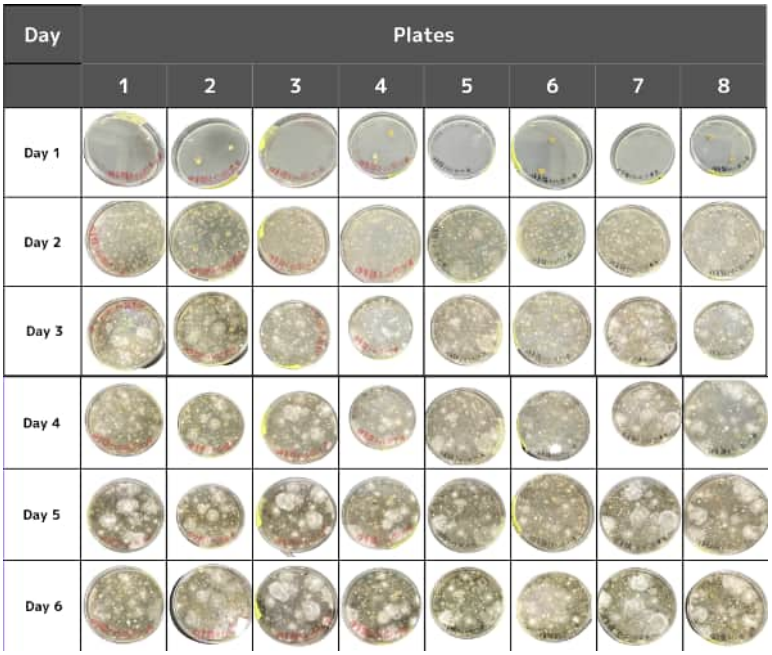

Figure 5. Mold cultivation (Cladosporium sp.)

Step 3: Identifying Fungal Species

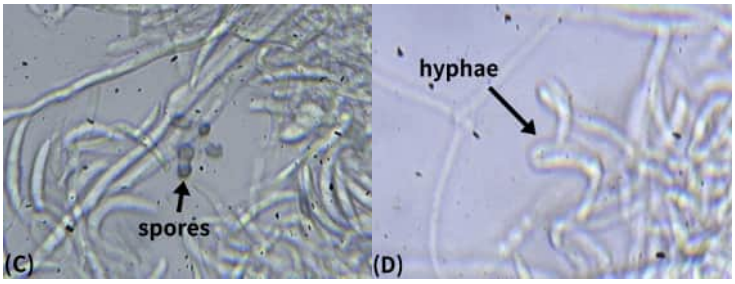

Figure 6. C,D: Cladosporium sp. under the light microscope at 40× magnification.

4.Conclusion

Thailand

The results showed that Piper nigrum L. extract from Thailand could inhibit the growth of Stachybotrys chartarum. The presence of piperine was supported by UV–Vis spectrophotometric analysis, which showed a clear maximum absorption peak at 345 nm. Piperine had a characteristic UV absorption range of 300–400 nm, and the observed peak fell within this range. The antifungal test showed a minimum inhibitory concentration (MIC) of 25 mg/mL and a minimum fungicidal concentration (MFC) of 50 mg/mL. Therefore, the results suggest that *Piper nigrum* L. extract is effective in inhibiting and killing *Stachybotrys chartarum*.

Japan

In this study, the antifungal activity of *Piper nigrum* L. extracts against environmental fungal samples was evaluated. Due to limitations in laboratory facilities, the experimental scope was focused on the extraction process and the microscopic identification of the collected fungi. The experimental results showed no significant difference in fungal growth between the treated group and the control group, indicating that the extract did not exhibit a prominent inhibitory effect under our specific testing conditions. Through microscopic observation, the target fungus was identified as *Cladosporium* sp. These findings suggest that the *Piper nigrum* L. extract may not possess sufficient antifungal activity against this particular species. The lack of observed inhibitory effect may be attributed to several factors, including the high environmental resistance of *Cladosporium* sp., the specific concentration of the extract applied, and the variations inherent in the environmental spore collection method used.

Comparison

The results indicate that *Piper nigrum* L. extract effectively inhibited the growth of *Stachybotrys chartarum* in the Thai study, as confirmed by MIC and MFC values, whereas no significant inhibitory effect was observed against *Cladosporium* sp. in the Japanese study. This suggests that the antifungal activity of the extract may depend on the fungal species and experimental conditions. To improve and adapt this approach, future studies should standardize the target fungi and experimental methods, apply optimized extract concentrations based on MIC and MFC values, and refine extraction procedures or evaluate purified piperine. Expanding tests to multiple indoor fungal species under controlled conditions would also help clarify the broader potential of *Piper nigrum* L. extract as a natural antifungal agent.

5. Acknowledgements

Thailand

Sincere thanks would be delivered to the Department of Microbiology, Faculty of Science, Kasetsart University, for providing the materials and the facilities in laboratories and the Department of Foreign Languages, Chitralada School, for giving valuable advice on the English language usage.

Japan

The authors would like to thank Professor Hanasaki of the Department of Applied Science, College of Life Sciences, Ritsumeikan University, and members of the Organic Materials Science Laboratory for their valuable cooperation.

6. References

Mariusz Dyląg. (2022, February 23). Update on Stachybotrys chartarum—Black Mold Perceived as Toxigenic andPotentially Pathogenic to Human. *National Library of Medicine*. https://pmc.ncbi.nlm.nih.gov/articles/PMC8945704/

Dalia Hikal. (2018, December). Antibacterial Activity of Piperine and Black Pepper Oil. *ResearchGate.* https://www.researchgate.net/publication/330471029_Antibacterial_Activity_of_Piperine_and_Black_Pepper_Oil

Piyapong Choochana. (2013). Development of piperic acid from piperine (*Piper nigrum Linn.*) for UVA protection. *Adobe Acrobat.* chrome-extension://efaidnbmnnnibpcajpcglclefindmkaj/https://rsuir-library.rsu.ac.th/bitstream/123456789/1715/1/PIYAPONG%20CHOOCHANA.pdf

Phitchapha Homa. (2019). Development of sunscreen containing from *Piper nigrum* L. (black pepper) extract in microemulsion form. *Adobe Acrobat.* https://rsuir-library.rsu.ac.th/bitstream/123456789/426/1/Phitchapha%20Homa.pdf

Marie-Alix d'Halewyn, M. Sc. microbiology - immunology and Pierre Chevalier, Ph. D., microbiology. (n.d.). *Stachybotrys chartarum. Institut national de santé publique du Québec.* https://www.inspq.qc.ca/en/moulds/fact-sheets/stachybotrys-chartarum

Bensch, K.(2012, July). The genus *Cladosporium*. *Studies in Mycology*.https://www.sciencedirect.com/science/article/pii/S0166061612000158

World Health Organization (WHO). (2009). WHO guidelines for indoor air quality: Dampness and mold. *World Health Organization*,https://www.who.int/publications/i/item/9789289041683

Make a disinfectant from the different bactericidal effects of medicinal herbs

Alissa Dubas[1], Kulsinee Potisen[1], Sopicha Ngamsuay[1],
Shiori Iwamoto[2], Rin Wada[2], Ami Miyahara[2], Yuna Makieda[2]
[1]Chulalongkorn University Demonstration Secondary School (Thailand)
[2]Kagoshima Chuo High School (Japan)

Abstract:
We conducted this study to develop a natural disinfectant suitable for people who are sensitive to chemical substances. As research materials, we selected four types of herbs—mugwort (Artemisia princeps), dokudami, lemongrass, and tea tree—which have long been traditionally used in Japan and Thailand. These herbs are known for their therapeutic properties, and we considered them promising candidates for safe alternatives to conventional disinfectants.
In this study, the active components of the herbs were extracted using purified water. Filter paper discs soaked in the extracts were placed on agar plates, and antibacterial activity was evaluated by measuring the diameters of the inhibition zones after several weeks using the disk diffusion method. For each herb, three extraction conditions were tested: frozen herbs, partially thawed herbs, and fresh herbs. A commercially available 75% alcohol-based disinfectant was used as a control. In addition, the pH of each extract was measured, based on the assumption that solutions with pH values closer to neutral are gentler on the skin.

Keywords：Medicinal herbs, disinfectant, plants, bacteria

Introduction:

Since the outbreak of COVID-19, hand sanitization has become a routine practice in public facilities and schools. Most commonly used disinfectants contain chemical substances such as alcohol and chlorine. Although these substances are highly effective in killing bacteria, they are also known to cause strong irritation. Against this background, there is a growing need to explore safer and more user-friendly disinfection methods that do not rely on chemical substances. Therefore, this study focuses on components derived from medicinal herbs and aims to investigate their bactericidal effects in order to reduce the use of chemical disinfectants.

In previous studies, among the six herbal extracts tested, extracts from perilla and rosemary were found to reduce bacterial colony counts, with rosemary showing particularly strong antibacterial activity. In addition, the combination of perilla and rosemary suppressed colony formation more effectively than either extract alone, suggesting a synergistic effect.

However, these previous studies mainly focused on whether antibacterial effects were present and did not sufficiently compare the strength of bactericidal activity as a disinfectant. Moreover, based on photographs of the Petri dishes used in earlier experiments, different types of bacteria appeared to have grown on each dish, which may have made it difficult to accurately compare antibacterial effects.

Therefore, in this study, we employed a variety of extraction methods and compared the effects obtained under different conditions. Furthermore, by measuring the sizes of inhibition zones, we quantitatively evaluated antibacterial activity and compared it with that of commercial disinfectants. In this way, our study aims to build on previous research by providing a clearer and more quantitative comparison of the antibacterial potency of herbal extracts.

Methodology1:

In this study, which focuses on the development of a herbal disinfectant, the initial objective was to determine whether herbal extracts exhibit antibacterial effects. To evaluate antibacterial activity, two preparatory steps were required. The first was the preparation of herbal extracts, and the second was the cultivation of bacteria necessary for testing. Following these preparations, the antibacterial activity of the extracts was evaluated in the main experiment.

Preliminary Experiment 1: Preparation of Herbal Extracts
In order to compare the antibacterial effects of herbs commonly used in two countries, four types of herbs were selected: yomogi (Artemisia princeps) and dokudami (Houttuynia cordata), which are widely used in Japan, and tea tree and lemongrass, which are commonly used in Thailand.

1. Each herb was collected and prepared under three conditions: dried, frozen, and fresh.
2. The herbs were mixed with water at a ratio of 1:6 to extract their active components.
3. The mixture was left to stand overnight.
4. The solution was filtered to remove solid residues.
5. The resulting liquid was used as the herbal extract.
6. In the final stage of developing the herbal disinfectant, the pH of each extract was measured. Extracts with pH values closer to those of commercially available disinfectants were considered to be safer for the human body.

Preliminary Experiment 2: Cultivation of Bacteria
To minimize variation in the experimental results, a single type of resident bacterium was used in this experiment.

1. Six agar plates were prepared, and a hand was lightly placed on each plate to allow resident bacteria to adhere.
2. As multiple types of resident bacteria grew on each plate, 14 bacterial colonies were selected, excluding fungi.
3. Using an inoculating loop, the selected colonies were subcultured three times to isolate a single bacterial strain.
4. As a result, a pure culture of a single bacterium was obtained.

Experiment 1: Antibacterial Effects of Herbal Extracts

The purpose of this experiment was to determine whether differences in herb type and extraction method affect antibacterial activity. A commercially available disinfectant was used as a control for comparison.

Method1:
A bacterial suspension (2 mL) prepared with purified water was dropped onto an agar medium and evenly spread over the entire surface using a glass spreader. Filter paper discs soaked in each herbal extract, as well as discs soaked in a commercial disinfectant, were then placed on the agar medium. The filter paper discs were prepared using a hole punch and had a radius of approximately 5 mm. After incubation, antibacterial activity was evaluated by observing the presence or absence of inhibition zones formed around the discs.
Inhibition zone: An inhibition zone is a circular area surrounding a disc impregnated with an antibacterial substance in which bacterial growth is suppressed, resulting in a visible region with no bacterial colonies.

Results1:
In Experiment I, no inhibition zones were observed in any of the 19 Petri dishes. This result was the same for both the paper discs soaked in the herbal extracts and those soaked in the commercial disinfectant. Therefore, no clear antibacterial effect was confirmed under the conditions used in this experiment.

Fig.1 Absence of Inhibition Zones

Discussion1:
There are two possible reasons why the expected results were not obtained. First, the single bacterial strain used in this experiment may have been too strong to be affected by the herbal extracts or the commercial disinfectant. Second, the amount or concentration of the extract absorbed into the paper discs may have been insufficient. As a result, the antibacterial components may not have diffused adequately into the agar medium, making it difficult to observe inhibition zones.

Conclusion1:
In Experiment I, the antibacterial effects of the herbal extracts could not be clearly confirmed. However, this experiment showed that the choice of bacterial strains and experimental conditions plays an important role in evaluating antibacterial activity. Based on these findings, the experimental conditions were revised and the methods improved for the next experiment.

Experiment2: Identification of Bacteria Suitable for Antibacterial Testing
Based on the results of Experiment 1, it was considered possible that the bacteria used were more resistant than the antibacterial effects of the disinfectant. Therefore, in Experiment 2, four types of bacteria were prepared, and their concentrations were varied. The objective was to identify bacterial strains that formed inhibition zones when treated with a commercially available disinfectant.

Method2:
Resident bacteria that had been previously collected were added to heat-sterilized purified water, and the suspension was mixed thoroughly. The bacterial suspension was then diluted to 10-fold and 100-fold concentrations.

Next, 2 mL of each diluted bacterial suspension was dropped onto agar media and evenly spread over the surface using a glass spreader. Filter paper discs soaked in a commercial disinfectant were then placed on the agar media in the same manner as in Experiment I. After incubation for one week, the presence or absence of inhibition zones was observed.

Results2:
Bacteria were successfully cultured in all Petri dishes. However, differences in growth patterns were observed depending on the type and concentration of bacteria. Some bacteria spread evenly over the agar surface, while others showed uneven or patchy growth. Regarding the bactericidal effect, no inhibition zones were observed in any of the Petri dishes, regardless of whether filter paper soaked in disinfectant or disinfectant solution directly dropped onto the agar was used.

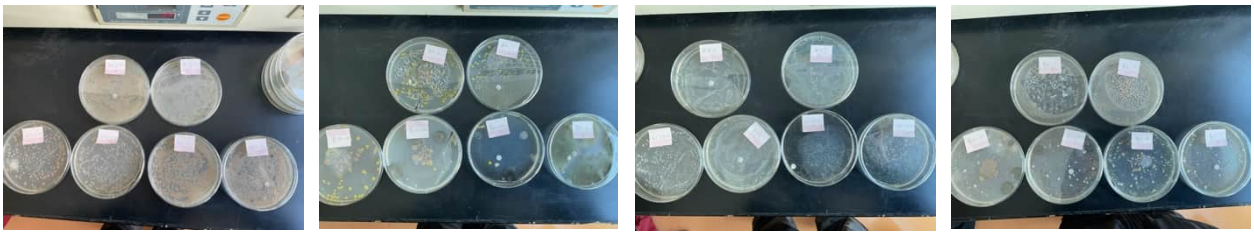

Fig.2. Bacteria 1 Bacteria 2 Bacteria 3 Bacteria 4

	vacteria1	vacteria2	vacteria3	vacteria4
1×(undiluted)	uniformly spread	patchy	uniformly spread	uniformly spread
10×dilution	patchy	no growth	uniformly spread	patchy
100×dilution	patchy	no growth	uniformly spread	patchy

Fig.3 Pattern of Bacterial Spread

Discussion2:
All bacteria used in this experiment were single strains derived from resident flora. Therefore, it is unlikely that the disinfectant had no bactericidal effect on all bacteria. One possible reason for the absence of inhibition zones is that the filter paper prepared using a hole punch was too small. Because of its small size, the disinfectant components may not have diffused sufficiently into the agar, making it difficult to evaluate the bactericidal effect accurately. In addition, differences in bacterial growth patterns suggested that bacteria spreading uniformly are more suitable for clearly identifying inhibition zones.

Conclusion2:
In Experiment II, bacteria suitable for evaluating bactericidal effects were tested using a commercial disinfectant. Although no inhibition zones were observed, differences in bacterial growth patterns were confirmed. These results indicate that improvements in experimental conditions, such as using bacteria that spread uniformly and larger filter paper, are necessary for accurate evaluation in future experiments.

Experiment3: Antibacterial Activity of Kaffir Lime and Lemongrass Extracts Against Mixed Skin Microbiota

Methodology3：
The experiment was divided into herb extraction and bacterial cultivation phases.

3.1 Preparation of Herbal Extracts
1. **Selection**: Kaffir lime leaves and Lemongrass stalks were selected due to their traditional medicinal use in Southeast Asia.
2. **Extraction**: The herbs were mixed with purified water at a ratio of 1:6
3. **Duration**: The mixture was left to stand overnight to allow active components to diffuse into the water.
4. **Filtration**: The solution was filtered to remove solid residues, obtaining a clear herbal extract.

3.2 Bacterial Cultivation and Testing
Instead of isolating single colonies, this study focused on the "natural mix" of bacteria found on the skin.
1. **Inoculation**: An agar medium was prepared, and a hand was placed lightly on the surface after a normal day of activity to transfer resident bacteria14.
2. **Application**: Filter paper discs (5 mm radius) were soaked in:
    - ○ Kaffir Lime extract.
    - ○ Lemongrass extract.
    - ○ 75% Alcohol (Control).

    +1
3. **Placement**: The discs were placed onto the agar medium immediately after the hand touch.
4. **Incubation**: The Petri dishes were sealed and left to sit for 48 hours.

3. Prediction of the Results
After 48 hours, the Petri dishes were examined for the formation of inhibition zones—areas where bacterial growth is visibly suppressed.

Fig.4 prediction of Result

Substance	Observation (48 Hours)
Kaffir Lime Extract	Clear circular area around disc
Lemongrass Extract	Moderate suppression observed
75% Alcohol (Control)	Strong suppression of growth
Water (Negative Control)	No inhibition; bacteria grew up to the disc

In contrast to the previous study where no inhibition zones appeared, the use of a general bacterial population and a shorter incubation time allowed for the observation of initial antibacterial activity before the most resistant strains could dominate the plate.

4. Result and Discussion

Because of the unsuccessful attempt in the cultivation of bacteria in the past months, we could not perform any experiment in 2.2 to demonstrate the antimicrobial activity of the extract to prove our hypothesis in time.

Overall conclusion:

In Experiment I, the antibacterial effects of herbal extracts were examined; however, no conclusive results were obtained because the bacterial strain used was too resistant to be affected by the extracts.

Based on the outcome of Experiment I, Experiment II was conducted to identify bacterial strains suitable for evaluating the antibacterial effects of herbal disinfectants. In this experiment, only a commercial disinfectant was used, and the type and concentration of bacteria were varied. Nevertheless, no inhibition zones were observed under any of the tested conditions.

These results indicated that there were further issues in the experimental procedure. As a result, this experiment did not reach the stage of testing the antibacterial effects of the herbal disinfectant. However, the findings clarified the limitations of the experimental design and provided important insights for improving future experiments.

References:

https://www.mcs-information.online/entry/MCS-petition-meeting
Chemical Sensitivity Information and Support Center
https://school.gifu-net.ed.jp/ena-hs/ssh/R02ssh/sc2/22046.pdf
https://school.gifu-net.ed.jp/ena-hs/ssh/R03ssh/sc3/32121.pdf
Oguri, Mahowa. “Producing a Disinfectant from Medicinal Herbs.”
https://www.eisai.co.jp/museum/herb/familiar/insecticide.html
Eisai Museum of Medicine. “Familiar Medicinal Herbs: Dokudami (Houttuynia cordata).”
https://www.chinoshioya.com/fs/chino2019ec/c/feature_wormouse?sort=04
Chinoshioya Co., Ltd. “Medicinal Herb Feature: Yomogi (Japanese Mugwort).”

Making more bio-nano fiber from fruits unique to each other's countries

Chanin Charoenrungsiri[1], Krit Kiattisirirote[1] Tamaki Nakajima[2], Ayano Okumachi[2], Hazuki Terada[2]
[1] *Kamnoetvidya Science Academy (Thailand)*
[2]*Kobe high school (Japan)*

Abstract:
Bio-nano fiber is fibrous materials made by refining polymer compounds derived from living organisms such as wood and some plants down to the nanometer （nm）scale. Taking advantage of enabling collaborative research with different countries, we considered to produce cellulose nano fibers from fruits unique to each other's country and compare their yields. In this study, although, wood is typically used for industrial cellulose nano fiber production aims to reduce environmental damage, such as deforestation, by utilizing fruit peels as an alternative raw material. First, impurities were removed, and the sample was bleached using NaClO adjusted its concentration to 22%(w/w). The bleached sample was subsequently filtered and dried to obtain cellulose nano fibers. In addition, we attached importance to be able to obtain cellulose nano fibers by using some chemicals to break hydrogen bonds without using advanced machines and chemicals like use in universities.

Keywords: Cellulose nano fiber（CNF）; fruit; NaClO

1. Introduction

To make human life better, researchers have long been studying and developing materials with useful properties. Cellulose nano fiber (CNF) is a material made by breaking down plant fibers, which mainly consist of cellulose, into extremely small fibers at the nanometer scale (1 nanometer is one billionth of a meter). CNF is very light—about one-fifth the weight of steel—but it is also very strong, with about five times the strength of steel. In addition, CNF has many excellent properties, such as high elasticity, high water absorption, and high transparency.

Because of these properties, CNF is expected to be used in many areas, including car parts, building materials, electronic devices such as displays, and even food products as a thickening agent. Since CNF is made from plants, it can be obtained from familiar natural resources. It is also an environmentally friendly material because it stores CO_2 and has a low environmental impact. For these reasons, CNF has attracted attention as a plant-based material that does not rely on petroleum and can help achieve a low-carbon society.

CNF is also expected to be used as a high-performance reinforcing material for plastics, possibly replacing carbon fiber. However, producing CNF requires large amounts of water and repeated mechanical processing, which makes it expensive to manufacture. As a result, CNF has not yet been widely used. In addition, materials such as carbon fiber and glass fiber are already commonly used, so reducing the production cost is the biggest challenge for CNF.

The purpose of this study is to reduce the production cost of CNF by using fruit peels instead of wood, which is usually used as the main raw material. Large amounts of fruit peels are thrown away during food processing, even though they contain a lot of cellulose. Using fruit peels effectively is important for recycling resources.

In this study, we attempt to produce CNF from fruit peels of fruits unique to different countries. By comparing the amount of CNF produced with the amount of cellulose in the fruit peels, we examine whether fruit peels are suitable as raw materials for CNF. We also aim to reduce raw material costs and environmental impact, and to find fruits that are especially suitable for CNF production.

Through recycling waste materials, this research aims to reduce deforestation and to propose a new way to use sustainable biomass resources. Ultimately, this study hopes to contribute to the practical use of CNF in society and to the realization of a low-carbon society.

2. Methodology

We wanted to find usefulness by producing results in an appropriate way depending on the location and an environment. Therefore, we conducted experiments in different ways. Show how we did it at a Japanese school in 1） and how we did it at a Thai school in 2）. In addition, it is determined that CNF have been produced if a translucent sheet could be made.

[1] Material

1） Three kind of peels, pineapple, persimmon, mandarin orange cut to a size of 5mm wide [5g]. NaClO adjusted its concentration to 22%（w/w）. HCl adjusted the pH to 2. NaOH adjusted its concentration to 50%(w/v)

2） Pineapple peels [5g]. $NaClO_2$ adjusted the concentration to 7.5% (w/w) and adjusted the pH to 3.8-4.0 by adding HCl. NaOH adjusted the concentration to 10% (w/w). NaBr and $NaClO_2$ adjusted the pH to be basic.

[2] Methods

1） Firstly, prepared peels were stirred in the HCl for 2 hours to remove impurities such as minerals. After that, it was filtered and washed. The remaining solids were added to NaClO solution and stirred at 30℃ for 2hours while maintaining its basic by adding NaOH. After the reaction, it was filtered and washed. The remaining solids put in the mixer with distilled water 50ml. Lastly, we put the obtained liquid in a dry oven at 50℃ all day night.

2） Heat the peels at 50℃ to dehydrate them. They were put in the water and heat it for 2hours to remove water-soluble compounds. Bleach with $NaClO_2$ adjust the pH to be acidic. Treat with NaOH at room temperature and filter to obtain cellulose. Mix cellulose with cellulase. The reference use TEMPO, however, we don't have it. Therefore, we used NaBr and $NaClO_2$ for instead.

3. Results

Here is a table of our results. We assume that ratio of cellulose contained in the peels as shown in the Table 1. The yield（%）was found by the formula shown in ①.

Table 1. The ratio of cellulose nano fiber yield to the amount of cellulose contained in the peel

Kind of fruit peels	Original cellulose content (%)	Yield (%)
Pineapples	-	- (*)
Persimmon	40	11
Mandarin Oranges	40	18

(*) …It couldn't make translucent sheet.

$$Yield(\%) = \frac{Yield(g)}{5 \times original\ cellulose\ content\ (\%)} \quad \cdots ①$$

4. Discussion

It is thought that the reason why the CNF derived from pineapple could not be produced was due to the use of cellulase. Cellulase is an enzyme that breaks down cellulose into glucose. Therefore, we couldn't obtain CNF from pineapples. Moreover, there is a difference in the yield of persimmons and mandarin oranges. We believe the reason lies in the strength of the peels' bond. At the stage of removing impurities, the binding of the mandarin orange was looser than persimmon.

5. Conclusion

[1] Conclusions
CNF can be made from fruit peels with school facilities. Furthermore, the one with soft peels have a higher yield.

[2] Prospects
We have possibilities that the yield of CNF can increases exponentially as the weight of the peels used increases. We want to conduct comparative experiment on the weight of the peels. What's more, we would like to examine the strength of CNF. By examining this, CNF derived from persimmon, which had a low yield, may also be useful because of the pectin.

6. References

Shiroshi Matsuki, Hidenori Kayano, Jun Takada, Hiroyuki Kono, Shuji Fujisawa, Tsuguyuki Saito, and Akira Isogai (2020). Nanocellulose Production via One-Pot Formation of C2 and C3] Carboxylate Groups Using Highly Concentrated NaClO Aqueous solution, https://pubs.acs.org/doi/pdf/10.1021/acssuschemeng.0c06515?ref=article_openPDF

Ayako Fujita (2019). Production of cellulose nano fibers derived from fruits and vegetables, Chemistry and education, 67(1), 26- 27, https://www.jstage.jst.go.jp/article/kakyoshi/67/1/67_26/_pdf

Yongqi Tian, Ruyang Huang, Yuanyuan Chen, Tao Wang, Jiulin Wu, Shaoyun Wang, (2025), The preparation and characterization of pineapple peel cellulose nanofibers and its application in oil-water emulsions, Carbohydrate Polymers, 353(1), 1-14, https://www.sciencedirect.com/science/article/abs/pii/S0144861725000268?via%3Dihub

National Institute of Advanced Industrial Science and Technology. (2022/07/06). AIST Magazine. What is cellulose nanofiber (CNF)? https://www.aist.go.jp/aist_j/magazine/20220706.html

Innovative bioplastic materials from food industries' wastes

Budrassakorn PRONRATTANARAKSA[1] Chomchan SUPBORNSUG[1]
Natnicha MONGKONSAWAT[1] Hana UEDA[2] Shiina AOYAGI[2] Harua WAKI[2]
[1]*Patumwan Demonstration School（Thailand）*
[2]*Risho Gakuen Osaka Ritsumeikan Junior & Senior High School（Japan）*

Abstract: This study developed bioplastic materials by combining chitosan with nutrients naturally contained in food waste, including mangosteens, apples, and lemon peels. Glycerol was used as a plasticizer, and its effects on the physical properties of the bioplastics were investigated. The results revealed that the glycerol content had a significant influence on flexibility and texture, demonstrating that food waste–derived components combined with chitosan have strong potential as sustainable and environmentally friendly materials, especially when glycerol is used as a plasticizer.

Keywords: food waste; SDGs-12; biodegradable plastic; Chitosan

1. Introduction

The amount of plastic waste is increasing every year, and a large amount of it is thrown away carelessly. This causes serious damage to the ocean and natural environments, and it has become a global problem. We wanted to find a way to reduce plastic waste and protect the environment. At the same time, many fruit peels are discarded as food waste every day. We thought that if fruit peels could be reused as biodegradable plastic, both waste problems could be solved at once. Therefore, we decided to research the production of biodegradable plastic from fruit peels.

2. Methodology

Chemicals and Experimental
1.Mangosteen peels / lemon peels / apple peels
2.Chitosan
3.Sodium hydroxide
4.Hydrochloric acid
5.Hydrogen peroxide
6.Acetic acid
7.Analytical balance
8.Magnetic stirrer
9.Temperature-controlled water bath
10.Hot air oven
11.Hydrophobic plate

Experiment

1Sample Preparation

1.1 Dry the mangosteen peels, grind them into powder, and sieve through a mesh.
1.2 Weigh 5 g of mangosteen peel powder using a 4-decimal-place analytical balance.
1.3 Weigh 5 g of chitosan.
2. Add 5 g of mangosteen peel powder into 100 mL of 10% (w/v) sodium hydroxide solution and boil at 100 °C for 2 hours while stirring continuously with a magnetic stirrer.
3. Centrifuge to separate the sodium hydroxide solution from the mangosteen peels at
4 °C for 15 minutes. 4. Decant and discard the sodium hydroxide solution.
5. Wash the mangosteen peels with distilled water and centrifuge to separate the liquid. Repeat until the wash water reaches pH 7.
6. Add 100 mL of 2 M hydrochloric acid (HCl) to the mangosteen peels and stir with a magnetic stirrer at 70 °C for 1 hour.
7. Centrifuge to separate hydrochloric acid from the mangosteen peels at 4 °C for 15 minutes.
8. Remove the hydrochloric acid by decanting the supernatant.
9. Wash the mangosteen peels with distilled water and centrifuge. Repeat until the wash water reaches pH 7.
10 Add concentrated hydrogen peroxide to bleach the mangosteen peels.
11. Prepare a 2% (w/v) chitosan solution by dissolving 5 g of chitosan in 250 mL of solution using 2% (v/v) acetic acid (prepared by mixing 20 mL acetic acid with 980 mL distilled water).
12. Mix the chitosan solution with mangosteen peel powder at a ratio of 50 mL of solution per 0.1 g of mangosteen peel powder.
13. Heat the mixture in a water bath at 40 °C to ensure good dispersion of the mangosteen peel powder.
14. Add glycerol at 20% (w/w) of chitosan (0.16 mL) and mix thoroughly using a magnetic stirrer.
15. Pour the mixture onto a hydrophobic plate.

16. Dry in a hot air oven at 50 °C for 1–2 days.
17. Repeat the experiment by adjusting the proportions of mangosteen peel powder and glycerol as follows:

Mangosteen Peel Powder (g)	Glycerol (mL)
5.0g	0.16
5.0g	0.0
lemon peel powder /apple peel Powder (g)	Glycerol (mL)
2.5g	0.16
3.0g	0.16

(1)

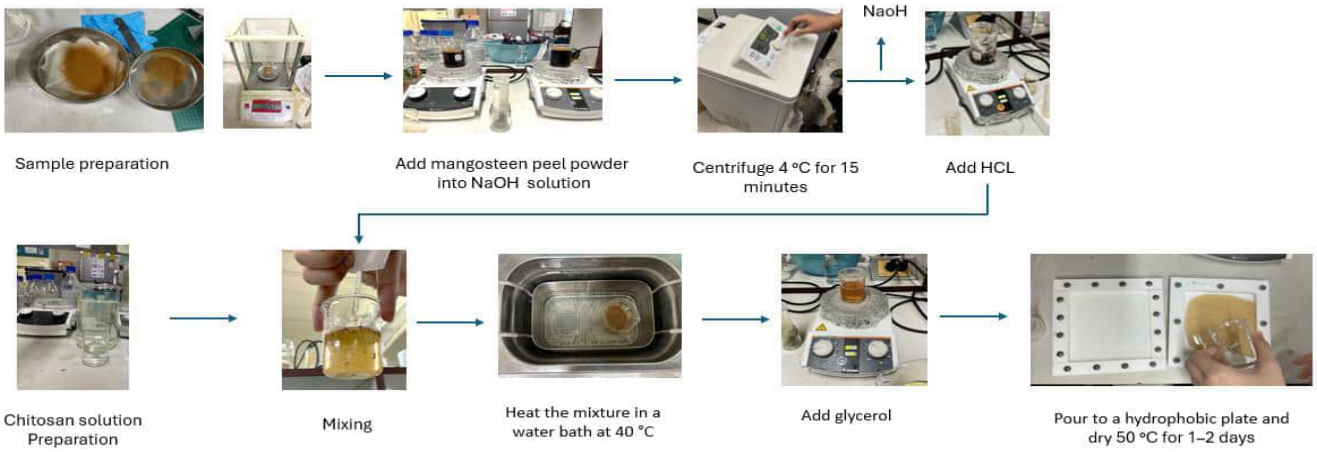

3. Results

Properties	Bioplastic with Glycerol	Bioplastic without Glycerol
		
External appearance	Translucent with scattered brown spots.wrinkles	Slightly less translucent than the glycerol sample, yellow to brown with small, dense brown specks
Texture	slightly crispy sheet with one side smooth but another side rough	Softer, jelly-like sheet with one side smooth but another side slightly rough
Texture	thin	thin
Tear resistance	low tear resistance	Very low tear resistance

Properties	Bioplastic with Glycerol	Bioplastic without Glycerol
		
External appearance	Slightly yellowish, translucent,	Slightly less translucent than the glycerol sample, yellow to brown with small, dense brown specks
Texture	mildly crisp sheet with similar smoothness on both sides.	mildly crisp sheet with similar smoothness on both sides.
Texture	thin	thin
Tear resistance	low tear resistance	Very low tear resistance

4. Discussion

The experiment showed that increasing the amount of glycerol made the bioplastics softer and more flexible. However, bioplastics with reduced or no glycerol were rigid and inflexible. We also conducted experiments using apple peels and lemon peels. Based on their different cellulose contents, 2.5 g of apple peel and 3.0 g of lemon peel were used, and glycerol was added to both samples. As a result, these bioplastics exhibited flexible properties similar to those of the mangosteen-based bioplastic. These bioplastics have potential for skin-related applications. They could be further developed by adding serum or active ingredients, with the aim of producing facial masks, acne patches, and scar treatment patches. One issue encountered during the preparation stage was that chitin was mistakenly used instead of chitosan. To resolve this problem, the experiment was repeated using highly concentrated acetic acid to dissolve the chitosan.

5. Conclusion

This project aimed to study the development of bioplastic materials from food industry waste, specifically mangosteen peels, apple peels, and lemon peels, using chitosan as the main polymer and glycerol as a flexible enhancer. This provides a way to reduce the environmental impact of using synthetic plastics.

The experimental results showed that the amount of glycerol significantly affected the properties of the bioplastic. Bioplastics with glycerol were softer, more flexible, and had better film-like properties, while bioplastics without glycerol were hard, brittle, and easily torn.

The developed bioplastic is thin, translucent, and can be molded into sheets, demonstrating its potential for application in skin-related products such as face masks, acne patches, and scar care patches. Further development is possible by adding active ingredients or skin-nourishing substances in the future.

In summary, this project demonstrates that food industry waste can be efficiently developed into environmentally friendly bioplastic materials, providing one approach to supporting the efficient and sustainable use of resources.

6. Acknowledgements

This research would not have been successfully completed without the guidance, knowledge, and support of our lecturers. The project team would like to express our sincere gratitude to Professor Ratana Rujiravanit, PhD, from the College of Petroleum and Petrochemical Engineering, Chulalongkorn University, and Surang Weraprasertsu from Patumwan Demonstration School, Srinakarinwirot University, for their valuable advice and continuous support throughout the

research process.
We also sincerely thank Krittanan Chansuk from the College of Petroleum and Petrochemical Engineering, Chulalongkorn University, for his guidance on operational procedures and the use of scientific equipment. We gratefully acknowledge all individuals and staff who provided samples, laboratory facilities, and assistance in experimental planning, data collection, and analysis.
We gratefully acknowledge all individuals and groups who contributed to this study, including the staff who provided samples and laboratory facilities, as well as those involved in experimental planning, execution, and data collection.
We also thank the teachers who assisted with sample collection, chemical handling, equipment operation, and data interpretation. This study was made possible by the support in supplying raw materials, and represents a step toward the beneficial use of waste materials and the reduction of environmental impact.
We are grateful to everyone who helped supply the raw materials; this study could not have been done without their support. Finally, we give our warm thanks to all who supported this research. This work is a step toward using waste in a useful way and lowering environmental harm, with the help of everyone involved.

7. References

(1)Food Composition Database Accessed December 3, 2025
https://fooddb.mext.go.jp/details/details.pl?ITEM_NO=7_07176_7

Exploring the allelopathic effects of radish and rosemary

Karin Kiyasu, Kogiku Shunsuke, Daichi Wakata
Ehime Prefectural Matsuyama Minami High School (Japan)

Abstract:

The effects on growth were investigated using rosemary, which is expected to have allelopathic effects, and daikon radish, which is said to have almost no effect. After growing them under five conditions, including indoors and outdoors, the rosemary did not wither, while the daikon radish tended to wither, especially under indoor conditions. Furthermore, transplanting rosemary, which has allelopathic effects, onto grown daikon radish was found to have an inhibiting effect on growth, but it was found that planting daikon radish from seed in an environment where rosemary already grows did not have any inhibiting effect on growth.

Keywords: allelopathic effects; rosemary; radish

1. Introduction

A high school in Japan proposed conducting an experiment on the allelopathy effect.
The allelopathy effect is a phenomenon in which plants release chemical substances produced within their bodies into their surroundings, which inhibit or promote the germination and growth of other plants. Rosemary is known as a plant that has an allelopathy effect, inhibiting the growth of other plants. On the other hand, radish is thought to have almost no allelopathy effect. Therefore, the purpose of this study was to investigate what differences in growth would occur if these plants were grown together.

2. Research method

The following five conditions were set for the experiment.
1. Radish seeds were planted, and once they grew, rosemary seedlings were planted in the same pot.
2. Radish seeds were planted and grown as is.
3. Radish seeds and rosemary seedlings were grown simultaneously in the same pot.
4. The same procedure as in 1, but grown indoors.
5. Radish seeds alone were planted and grown in nutrient-rich soil.

These five pots were grown for about a month and a half. They were also judged to have withered or not every week or so. However, all pots grown outdoors except for 4 were grown under a roof.

3. Results

Among the seedlings grown outdoors, the rosemary did not wither, but some of the radishes were seen to wither.
Among the seedlings grown indoors, the rosemary did not wither, but the radishes did. Furthermore, when rosemary, which has allelopathic effects, was transplanted onto mature radishes, it was found to have an inhibiting effect on their growth, but planting radishes from seed in an environment where rosemary already grows did not have any inhibitory effect on their growth.

Table 1: A table showing whether the plants in each pot died or not.

	1	2	3	4	5
11/10	—	—	—	—	—
11/18	N	N	N	N	—
11/25	N	N	N	N	—
12/8	N	N	N	w	N
12/16	N	N	N	w	N
12/26	w	w	w	w	N

1. Radish seeds were planted, and once they had grown, rosemary seedlings were planted in the same pot.
2. Radish seeds were planted and grown as is.
3. Radish seeds and rosemary seedlings were grown in the same pot at the same time.
4. The same procedure as 1, but grown indoors.
5. Radish seeds were grown in nutrient-rich soil.

注： N ・・ Not withered
w ・・ withered
— ・・Not germinated

Figures 1 and 2: Radish seeds grown indoors were planted, and once they had matured, rosemary seedlings were planted in the same pot.

Figures 3 and 4: At the start of the outdoor experiment and after the experiment.

4. Consideration

The following factors may have influenced the results of this experiment.
There may have been differences in the number of days and amount of water given indoors and outdoors.

The experiment was conducted in winter, which may not have been the optimum temperature conditions for basil germination.
The pots grown indoors were lined with water buckets, which may have caused the soil to become overly moist, leading to root rot of the radishes.
The pots used to plant the additional radishes in Experiment 4 were reused pots in which basil did not germinate, which may have affected the condition of the soil.
A roof was installed over the outdoor seedlings midway through the experiment, which changed the sunlight conditions and may have also affected their growth.
These factors combined may have affected the plant growth results.

5. Conclusion

In this study, the growth of radish plants was found to be particularly poor when grown indoors. However, it is highly likely that multiple factors, such as moisture content, temperature, sunlight, and soil condition, were influencing this, and it cannot be concluded that the allelopathic effect of rosemary was the sole cause.
In the future, it will be necessary to more accurately investigate the allelopathic effect by conducting experiments with more standardized cultivation conditions and clearly defined control areas.

6. Acknowledgements

We would like to express our deepest gratitude to the people who watered the plants while the Japanese high school students were away on a school trip.

7. References

Kyoko Takasuka, Misa Isshiki, Ayaka Ayashi.(2009). Research on the antibacterial and allelopathic properties of rosemary. FY2005 Designated Super Science High School Research and Development Implementation Report - Year 5, , 33.

Fujii, Yoshiharu. (2002). Plant allelopathy and its applications. BRAIN Techno News, (92), 13-18.

Japanese Society of Crop Science (ed.). (2010). Allelopathy. Glossary of Crop Science Terms. Association for Rural and Fishing Culture.

A Study on the Degradation of PLA Using Tomato-Derived Fungi

Mina Iwata[1], Hinako Iijima[1], Nanaka Igarashi[1], Aoi Tomatsuri[1], Monrada Thothong[2], Wadee Le[2], Natnicha Sripraman[2]

[1]*Ryugasakidaiichi senior high school (Japan)*

[2]*Princess Chulabhorn Science High School Mukdahan (Thailand)*

Abstract:

We have confirmed that PLA(biodegradable plastics) can be hydrolyzed by fungi that attach to rotting tomatoes. Therefore, it may be possible to use tomatoes and the mold that attaches to them as they rot to treat biodegradable plastic waste and reduce plastic use.

Keywords: biodegradable plastics; fungi

1. Introduction

Plastic waste currently has a negative impact on the environment. Biodegradable plastics can be degraded mainly through two stages—hydrolysis and microbial degradation—and therefore require a long time to decompose under natural conditions. We thought that hydrolysis limits the degradation of biodegradable plastics in natural environments and conducted this study to establish conditions and methods to accelerate the hydrolysis process. Tomatoes were used in this study because they are relatively inexpensive and because some fungi that attach to decaying tomatoes contain esterase, a degradation enzyme.

2. Methodology

Experiment 1

First, in order to culture molds adhering to tomatoes, mass measurements were conducted using an agar medium.

[Methods]

(1)A commercially available tomato (cultivar: *Furutica*) was left to decay at room temperature for 3 days to 1 week. The fungi that adhered to the tomato were isolated and cultured on potato dextrose agar prepared with 39 g of Potato Dextrose Agar.

(2)The grown fungi were cultured separately on new agar media according to their color (white, yellow, black, and no mold) and isolated. Hereafter, they are referred to as white mold, yellow mold, and black mold.

(3)A 5.0 mm piece of a biodegradable straw (hereafter referred to as “the straw”), whose mass had been measured in advance, was placed on each isolated fungus. The samples were incubated at 35 °C in an incubator under static conditions. After several days, the mass of the straw was measured again.

Experiment 2

To increase the contact area between the fungi and the material, the experiment was conducted using a liquid medium instead of a solid medium.

[Methods]

(1)Potato dextrose broth was placed in test tubes, and each of the three isolated fungi was added. Seven test tubes were prepared and cultured for each type of fungus.

(2)A 5.0 mm piece of a biodegradable straw, whose mass had been measured in advance, was placed into each test tube from (1). The samples were incubated at 35 °C in an incubator under static conditions, and the mass of the straw was measured periodically.

In this experiment, seven samples were prepared for each mold color.

Experiment 3

Based on the results of Experiment 2, it was considered that the straw itself absorbed water; therefore, a water absorption experiment was conducted.

[Methods]

(1)Distilled water was placed in four test tubes, and a 5.0 mm piece of a biodegradable straw, whose mass had been measured in advance, was added to each tube.

(2)The test tubes were incubated at 35 °C under static conditions in an incubator, and the mass of the straw was measured periodically.

Experiment 4

Assuming that differences in mold concentration affect the decomposition ability of biodegradable plastics, mass measurement version 2 (white mold only) was conducted in liquid culture medium.

[Methods]

(1) The white mold isolated in Experiment 1:(2) was cultured in a liquid culture medium in a test tube. Measurement experiments were conducted by varying the mold concentration and amount of white mold. Regarding concentration, the operation of transferring the fungus to the liquid culture medium once with a platinum loop was designated as concentration relative value 1, and the three samples were designated as concentration relative values 1, 2, and 3, respectively.

(2) A 5.0 mm biodegradable straw whose mass had been measured in advance was placed in (1) and placed in an incubator set to 35°C. The straw's mass was periodically measured.

3. Results

Experiment 1

Table 1(left): Change in the mass of the straw on agar medium inoculated with yellow mold(Unit: mg)

Table 2(right): Change in the mass of the straw on agar medium inoculated with white mold(Unit: mg)

	Yellow A	Yellow B	Yellow C	Yellow D
0 day	36	36	40	36
16 days	43	44	43	39
difference	7.0	8.0	3.0	3.0

	White A	White B	White C	White D
0 day	43	32	40	35
16 days	43	39	41	39
difference	0	7.0	1.0	4.0

Table 3(left): Change in the mass of the straw on agar medium inoculated with black mold(Unit: mg)

Table 4(right): Change in the mass of the straw on agar medium without mold(Unit: mg)

	Black A	Black B	Black C	Black D
0 day	38	35	43	48
16 days	39	41	44	45
difference	1.0	6.0	1.0	-3,0

	Nothing A	Nothing B	Nothing C	Nothing D
0 day	37	36	45	39
16 days	40	39	44	39
difference	3.0	3.0	-1.0	0

Experiment 2

Here we show the average mass of each mold color.

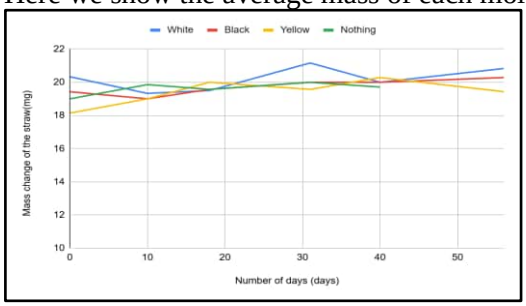

Fig. 1: Average mass change for each mold color

Experiment 3

Table 5: Mass Changes of Straws(Unit[mg])

	A	B	C	D
Day 0	20	17	18	19
Day 13	20	18	20	20
Day 21	24	20	20	22
Difference	4.0	3.0	2.0	3.0
Water Absorption Rate(%)	20.0	17.6	11.1	15.8

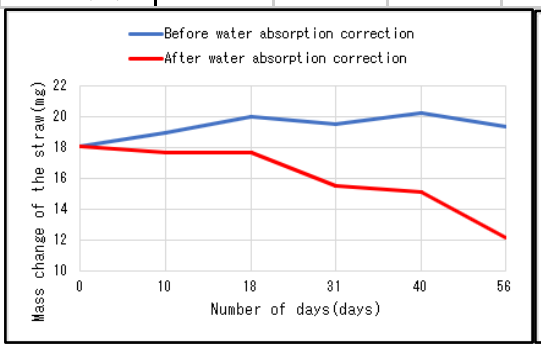

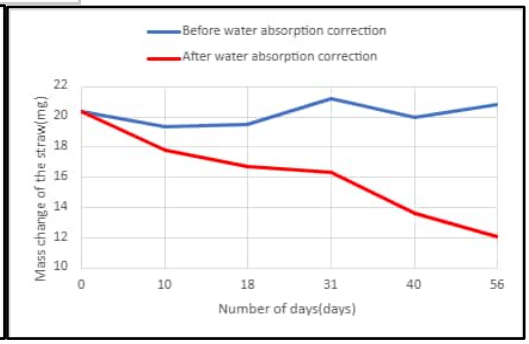

Fig. 2(left): Changes in mass of straws in yellow mold liquid culture

Fig. 3(right): Changes in mass of straws in white mold liquid culture

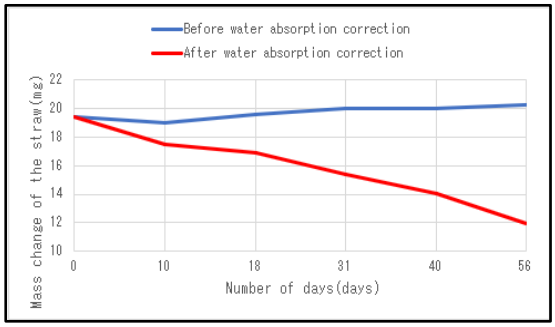

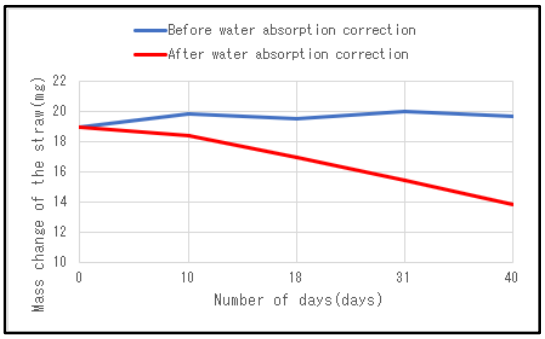

Fig. 4(left): Changes in mass of straws in black mold liquid culture

Fig. 5(right): Changes in mass of straws in liquid culture without mold

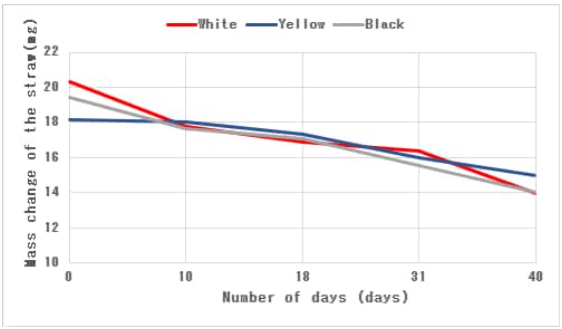

Fig. 6: Average Mass Changes for Each Mold Color

Experiment 4

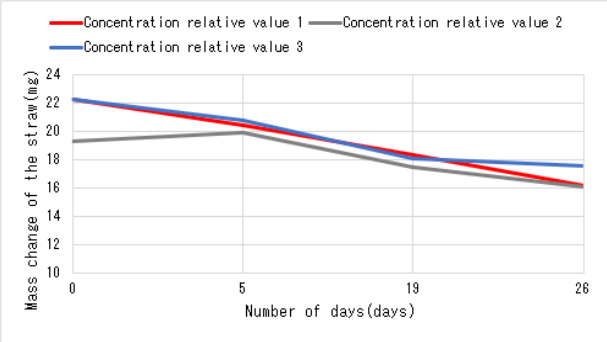

Fig. 7: Changes in mass of straws at different concentrations of white mold

4. Discussion

Experiment 1

In most cases, an increase in the mass of the straws was observed. It was inferred that the straws absorbed moisture from the agar, and the fungal effect did not manifest due to the small contact area with the fungi, likely caused by the shape of the straws.

Experiment 2

The mass of the straw did not decrease.

I assumed that the reason for this was that the straw had absorbed the culture medium, so I decided to carry out Experiment 3.

Experiment 3

From Table 5, we can see that the mass of straws A, B, C, and D increased after the water absorption experiment compared to before the experiment, which shows that the straws absorb water and increase in mass.

The water absorption rate was calculated as follows:

$$\text{The water absorption rate} = \frac{|Mass\ after\ water\ absorption - Mass\ before\ water\ absorption|}{Mass\ before\ absorbing\ water} \times 100$$

Therefore, the average water absorption rate is 16.1%. Fig. 2 to 5 show that many of the straws lost mass. Of these, white mold had the greatest average loss in straw mass, at 40%. During the measurement, the culture medium absorbed water into the straws and the culture medium entered the straw tube, so it is unlikely that it was completely removed and the mass of the straw alone measured. Measuring the dry mass is important.

Fig.5 shows that even after subtracting the mass loss of the straws in liquid culture without mold, there was still a decrease in the mass of the straws, indicating that the mass of the straws themselves had decreased. The mass loss was 6.4 mg (31%) for white mold, 3.2 mg (18%) for yellow mold, and 5.4 mg (28%) for black mold.

This shows that the mold that attaches to tomatoes as they rot has the ability to reduce the mass of biodegradable straws and hydrolyze biodegradable plastic.

Experiment 4

Even at a relative concentration of 1, the mass of the straw decreased sufficiently. No significant difference was observed in the results when the relative concentration was increased beyond this point.

5. Conclusion

We have confirmed that biodegradable plastics can be hydrolyzed by fungi that attach to rotting tomatoes. Therefore, it may be possible to use tomatoes and the mold that attaches to them as they rot to treat biodegradable plastic waste and reduce plastic use.

6. References

Kitamoto, H. (2021). *Biodegradation of polyesters by enzymes from epiphytic fungi*. Institute for Agro-Environmental Sciences, NARO. https://share.google/ZwjiswA45QbgGmjmg

Sasutomo. (2021, January 14). *"Marine plastic waste problem": Why now? What is the problem?*. Yahoo! JAPAN SDGs. https://sdgs.yahoo.co.jp/featured/21.html

Nature3D. (2019, December 2). *Biodegradation mechanism of PLA*. Nature3D. https://nature3d.net/explanation/pla_biodegrade_mechan

Ubon Ratchathani University. (n.d.). Preparation of Potato Dextrose Agar (PDA). Ubon Ratchathani: Ubon Ratchathani University.

Rungsaranon, C. (2021). Problems of promotion measures in biodegradable plastic products [Master's independent study, Chulalongkorn University]. Chulalongkorn University Intellectual Repository (CUIR). https://digital.car.chula.ac.th/cgi/viewcontent.cgi?article=8774&context=chulaetd

Soontornchai, S., Lertwisuttipaiboon, S., & Tosing, P. (2016). Bioplastics from agricultural crops to health and environment. Journal of Health and Health Management, 3(1), 24-37. https://he01.tci-thaijo.org/index.php/slc/article/download/221634/152796/719537

Suwan, K. (2016). Isolation and screening of actinomycetes capable of degrading bioplastics [Master's thesis, Chiang Mai University]. CMU Intellectual Repository. https://archive.lib.cmu.ac.th/full/T/2559/amicro80559kmsw_ch2.pdf

A Comparative Study of Bioplastic Production from Orange Peels in Thailand and Japan

Phakhwan Maneekan[1], Rinkarn Phangkeaw[1], Naraphat Wattanakul[1], Miyuka Kawai[2], Momoka Nagahata[2], Mei Nakagawa[2], Sumika Yamada[2]

[1]*Princess Chulabhorn Science High Schools (Thailand)*

[2]*Ikueinishi High School (Japan)*

Abstract:

Bioplastics are materials produced from natural and renewable resources and are considered environmentally friendly alternatives to conventional petroleum-based plastics. Orange peels were selected due to their high cellulose content and wide availability. The bioplastic was prepared using simple laboratory techniques with cornstarch as the main polymer and glycerol as a plasticizer to improve flexibility. This project aims to produce bioplastics from food waste, specifically orange peels, and to evaluate its basic properties. The properties of the produced bioplastic were evaluated through biodegradation and physical characteristic. Physically, the Japanese samples exhibited significant surface cracking compared to the smoother Thai samples, which likely facilitated faster decomposition. The comparative results show that bioplastics produced from orange peels in Japan exhibited a higher average weight loss after 10 days of soil burial than those produced in Thailand. The results of this study demonstrate that orange peel waste can be effectively used as a raw material for bioplastic production. The bioplastic produced shows potential as an environmentally friendly material and supports the use of food waste to reduce plastic pollution and promote sustainability.

Keywords: Bioplastics; Orange peels; Food waste; Biodegradation; Sustainable materials

1. Introduction

Plastics have become an essential part of daily life due to their convenience, durability, and wide range of applications. They are commonly used in packaging, household products, medical equipment, and industrial materials. However, most conventional plastics are produced from fossil fuels and are non-biodegradable, leading to a critical environmental crisis. Conventional petroleum-based plastics are resilient and non-biodegradable, leading to long-term accumulation in ecosystems and posing severe threats to marine life and human health. As fossil fuel reserves deplete, the transition toward sustainable alternatives has intensified. Bioplastics—polymers derived from renewable biomass—offer a promising solution due to their lower carbon footprint and inherent biodegradability.

Among various organic sources, orange peels present a highly viable raw material for bioplastic synthesis. Often discarded as agricultural waste, orange peels are rich in cellulose, starch, and pectin, which provide the necessary structural matrix for bioplastic formation. In this project, bioplastic materials were produced from Thai and Japanese orange peels using simple laboratory techniques and readily available materials. Glycerol was incorporated as a plasticizer to improve the cohesion of the mixture. This study aims to convert this specific food waste into a value-added bioplastic using glycerol as a plasticizer to overcome the common challenge of brittleness and enhance mechanical flexibility, assess and compare the suitability of bioplastics derived from both Thai and Japanese orange peels as eco-friendly alternatives to conventional plastic materials and specifically focuses on evaluating the environmental performance of the produced bioplastics through a biodegradation test.

2. Methodology

2.1 Materials

Table 1. Composition of Bioplastic Material

Materials	Quantity	Unit
Thai Sai Nam Pheng orange peels	25	g
Japanese Mikan orange peels	25	g
Cornstarch	25	g
Distill Water	15	ml
Glycerol	2.5	ml
Coconut Oil	2.5	ml
Lemon Juice	10	ml
Sodium Bicarbonate	2	g

Figure 1. Materials

2.2 Preparation of Bioplastic

2.3.1 The orange peels were boiled in water until they became soft and tender.

2.2.2 The boiled peels were transferred to a blender and processed until a fine, smooth puree was achieved

2.3.3 The orange peel puree was mixed with cornstarch, glycerol, coconut oil, sodium bicarbonate, and lemon juice in a container.

2.3.4 The mixture was allowed to rest until the effervescence caused by the chemical reaction between sodium bicarbonate and lemon juice ceased completely, ensuring all gas bubbles were dissipated before heating.

2.2.5 The mixture was transferred to a non-stick pan and heated over the lowest possible heat. Constant and vigorous stirring was applied to prevent the starch from scorching or overcooking. Heating continued until the mixture thickened into a clay-like, moldable consistency.

2.3.6 Upon thickening, the pan was removed from the heat. The stirring motion was switched to a pressing or kneading motion, using a spatula to press the material flat against the warm pan surface to force out any trapped air pockets.

2.2.7 The mixture was immediately transferred into molds while hot to ensure proper shaping before the material began to set.

2.2.8 The molded samples were dried in an oven for 2–4 hours. During this process, a thin layer of coconut oil was applied to the surface to retain moisture and prevent cracking

2.3 Biodegradation Test

The biodegradability was assessed by burying the samples in compost soil. To evaluate environmental degradability, small pieces of the produced bioplastic were dried in an oven at 50°C for 24 hours or until constant weight to establish an initial mass (W_0) and then buried in compost soil. After a period of 10 days, the samples were carefully removed, cleaned of soil debris, and weighed again (W_1). The degree of biodegradation was determined by calculating the weight loss percentage.

$$Biodegradability = \frac{W_0 - W_1}{W_0} \times 100$$

W_0 = Initial mass of the bioplastic sample (g) W_1= Final mass of the bioplastic sample after burial (g)

Figure 2. Biodegradation Test (Thailand)

Figure 3. Biodegradation Test (Japan)

3. Results

3.1 Physical Characteristics of Bioplastics

The Thai Sai Nam Pheng bioplastic samples appeared light yellow with a smooth, uniform surface and maintained their structural integrity well without cracking shown in Figure 3a. In contrast, the Japanese Mikan bioplastic samples were dark orange to reddish-brown and exhibited significant surface cracking and a rougher texture, indicating higher brittleness and uneven shrinkage during drying shown in Figure 3b.

Figure 3a. Thai Sai Nam Pheng bioplastic

Figure 3b. Japanese Mikan bioplastic

3.2 Biodegradation Test

The biodegradation test revealed a significant decrease in the weight of the bioplastic samples after 10 days of burial in compost soil. Specifically, the samples produced from Sai Nam Phueng orange peels tested in Thailand showed an average weight loss of 9.1%. This quantitative reduction in mass confirms that the material is susceptible to microbial decomposition, indicating that orange peel-based bioplastics can effectively break down under natural environmental conditions. The individual weight loss for each sample in Thailand and Japan are presented in Figure 4 and Figure 5, respectively.

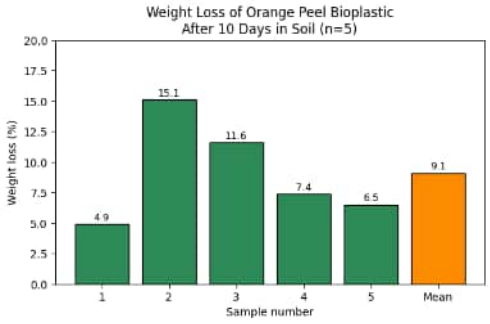

Figure 4. Weight loss of orange peel bioplastic (Thailand)

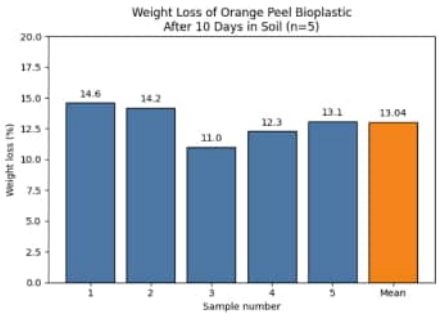

Figure 5. Weight loss of orange peel bioplastic (Japan)

Based on the comparative results shown in Figure 4 and Figure 5, the Mikan orange peel-based samples exhibited a higher average weight loss of 13.04%, compared to the 9.1% observed in the Thai samples. Although the degradation rate varies depending on environmental factors, the results demonstrate that orange peel bioplstics are capable of biodegradation in both countries.

4. Discussion

Physically, the Japanese samples appeared darker and exhibited significant surface cracking compared to the smoother Thai samples. The darker coloration is attributed to a combination of the high natural carotenoid content in Mikan peels and thermal browning reactions induced during the drying process, while the cracking likely resulted from rapid moisture loss during this process. Crucially, these structural features accelerated biodegradation by increasing the surface area accessible to soil microorganisms. Consequently, the comparative results show that bioplastics produced in Japan

exhibited a higher average weight loss after 10 days of soil burial than those produced in Thailand, indicating a faster biodegradation process. Despite the lower average weight loss observed in the Thai samples, a clear reduction in mass was still evident, confirming the potential of both as biodegradable alternatives.

5. Conclusion

The present study conclusively demonstrates the viability of utilizing orange peel waste from both Thailand and Japan as a sustainable raw material for bioplastic production. Soil burial tests verified that bioplastics from both sources degraded effectively, with Japanese samples exhibiting a faster degradation rate than Thai samples due to compositional differences. Physically, the material demonstrated adequate flexibility, but lower strength compared to conventional plastics. Overall, these findings validate the potential of converting orange peel waste into sustainable bioplastics. Further optimization of material formulation and extended biodegradation studies are recommended to enhance mechanical properties and broaden practical applications.

6. References

Mekonnen, T., Mussone, P., Khalil, H., & Bressler, D. (2013). Progress in bio-based plastics and plasticizing modifications. Journal of Materials Chemistry A, 1(43), 13379–13398. https://doi.org/10.1039/C3TA12555F

Chungsiriporn, J., Pongyeela, P., & Chairerk, N. (2023). Study on the preparation of biodegradable plastic from rice straw and chitosan. KKU Science Journal, 51(1), 69–77. https://doi.org/10.14456/kkuscij.2023.7

Marsi, N., Huzaisham, N. A., Hamzah, A. A., Zainudin, A. Z., Mohd Rus, A. Z., Leman, A. M., Rahmad, R., Mahmood, S., Abdul Rashid, A. H., Mohd Harun, D., & Darlis, N. I. (2020). Biodegradable plastic based on orange peel for packaging application. IOP Conference Series: Materials Science and Engineering, 864(1), 012184. https://doi.org/10.1088/1757-899X/864/1/012184

Sanyang, M. L., Sapuan, S. M., Jawaid, M., Ishak, M. R., & Sahari, J. (2015). Effect of plasticizer type and concentration on dynamic mechanical properties of sugar palm starch-based films. International Journal of Polymer Analysis and Characterization, 20(6), 627–636. https://doi.org/10.1080/1023666X.2015.1054107

Xie, F., Pollet, E., Halley, P. J., & Avérous, L. (2013). Starch-based nano-biocomposites. Progress in Polymer Science, 38(10-11), 1590-1628. https://doi.org/10.1016/j.progpolymsci.2013.05.002

Kato, M., Ikoma, Y., Matsumoto, H., Sugiura, M., Hyodo, H., & Yano, M. (2004). Accumulation of carotenoids and expression of carotenoid biosynthetic genes during maturation in citrus fruit. Plant Physiology, 134(2), 824–837. https://doi.org/10.1104/pp.103.031104

Study of Soil Quality and Carbon Sequestration under Sakura (Cherry Blossom) in Japan and Sri Trang (Blue Jacaranda) in Thailand

Natthawanee Chuhoithong[1], Tekawat Deepachoo[1], Waratchaya Kwannimit[1],Hamaya Moka[2], Shikata Wakana[2],Yamamota Chinatsu[2]

[1]*Princess Chulabhorn Science High School Trang (Thailand)*

[2]*Hyogo Perfectural Nagata High School (Japan)*

Abstract:

Global warming is a major environmental issue caused by the increasing concentration of carbon dioxide (CO_2) in the atmosphere. One effective natural approach to reduce atmospheric CO_2 is carbon sequestration by trees, which store carbon in their biomass and surrounding soil. However, the capacity of trees to grow and sequester carbon is strongly influenced by environmental factors, particularly soil quality, which varies across geographic regions.

This study investigates soil quality and carbon sequestration under Sri Trang trees *(Jacaranda mimosifolia)* in Thailand and Sakura trees *(Prunus serrulata)* in Japan. These two tree species were selected because they are endemic to their respective countries and share similar external characteristics, such as tree form and growth patterns, making them suitable for comparative analysis under different environmental conditions. Soil quality parameters, including soil texture, color, moisture content, pH, and temperature, were analyzed following the GLOBE protocol. Tree growth was evaluated using measurements of height and trunk circumference, while carbon sequestration potential was estimated using allometric equations.

This study shows that soil quality is closely related to tree growth and carbon sequestration. More suitable soil conditions are associated with higher tree growth and greater carbon storage, while less favorable soil conditions correspond to reduced performance. Overall, the findings confirm that soil quality plays an important role in determining the effectiveness of trees as a natural strategy for mitigating climate change.

Keywords: Global warming; Carbon sequestration; Soil quality; Tree growth; Endemic species

1. Introduction

The rapid increase in atmospheric carbon dioxide (CO_2) has intensified global warming and raised concerns about environmental stability. One natural approach to reduce excess atmospheric carbon is the use of vegetation, as trees absorb CO_2 through photosynthesis and store carbon in their biomass and surrounding soil.

Soil quality strongly influences tree growth and carbon sequestration. Properties such as soil texture, moisture, pH, and temperature affect root development and nutrient availability, leading to differences in tree growth and carbon storage across regions, even among species with similar external characteristics.

Sri Trang trees *(Jacaranda mimosifolia)* in Thailand and Sakura trees *(Prunus serrulata)* in Japan were selected because they are endemic species that represent their local ecosystems and share comparable external characteristics. This study aims to examine the relationship between soil quality, tree growth, and carbon sequestration under contrasting environmental conditions to better understand the role of soil in climate change mitigation.

2. Methodology

2.1 Site Selection and Tree Monitoring

Three study sites were chosen in both Trang (Thailand) and Nagata (Japan). At each site, three trees were selected for long-term monitoring and similar age. We measured

2.1.1 Tree Growth Defined by total height (m) and circumference at breast height (cm).

2.1.2 Soil Quality Following GLOBE protocols, we analyzed soil pH, moisture, color, and texture.

2.2 Carbon Sequestration Calculation

To estimate the carbon stored, we first calculated the total biomass using the allometric equation by Ogawa et al. (1965):

$$W_S = 0.0396\ (D^2H)^{0.933}$$

$$W_B = 0.00349\ (D^2H)^{1.030}$$

$$W_L = \left(\frac{28}{W_S + W_B} + 0.025\right)^{-1}$$

$$W_T = W_S + W_B + W_L$$

The carbon content was then estimated as 47% of the total dry biomass.

3. Results

3.1 Thailand

Table 1. Soil Quality at Study Sites in Thailand

Site	Color	Texture	Moisture (%)	pH
A	Red Brown	Loamy Sand	21.37	7
B	Yellow Brown	Sandy Loam	15.36	7
C	Dark Red	Loam	15.19	7

Graph 1. Height Growth Pattern of Sri Trang Trees.

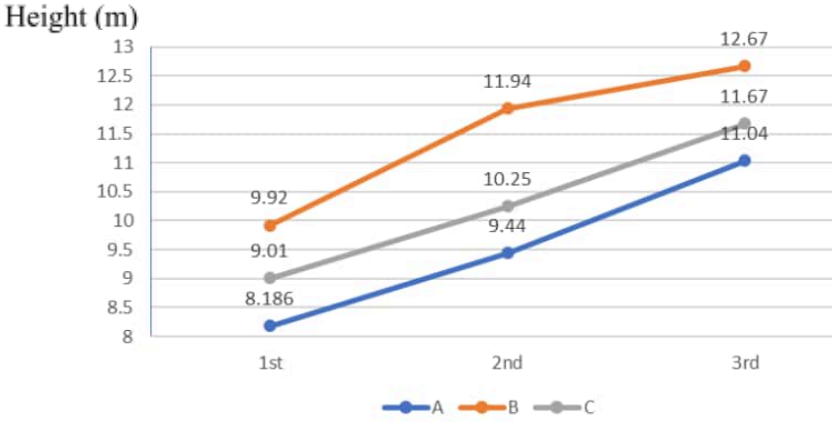

Graph 2. Circumference Growth Pattern of Sri Trang Trees.

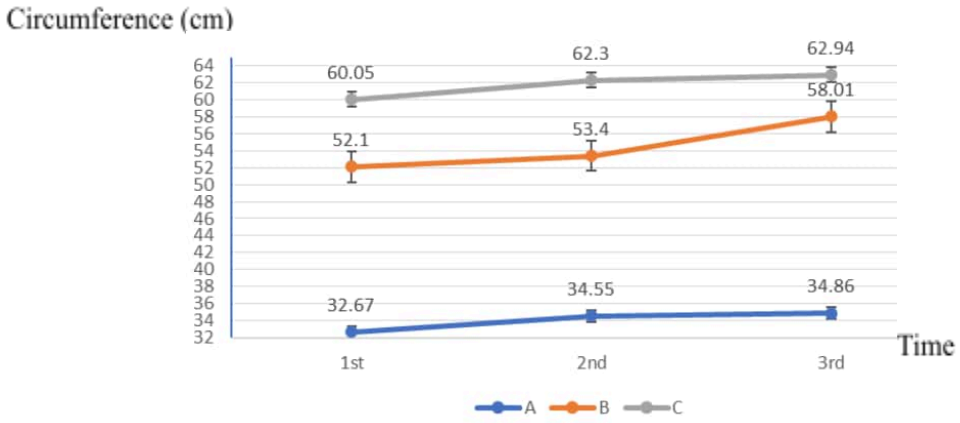

Graph 3. Carbon sequestration (kg C) of Sri Trang Trees

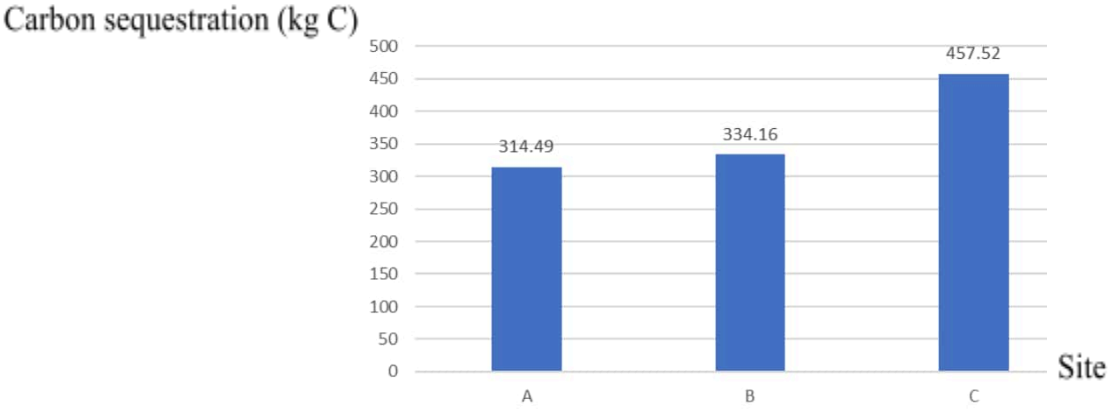

3.2 Japan

Table 2. Soil Quality at Study Sites in Japan

Site	Color	Texture	Moisture (%)	pH
A	Bistre	Soft	8.89	8
B	Coffee	Sarasara	6.98	6
C	Chamoisee	Pasapasa	2.93	7

Graph 4. Height Growth Pattern of Sakura Trees.

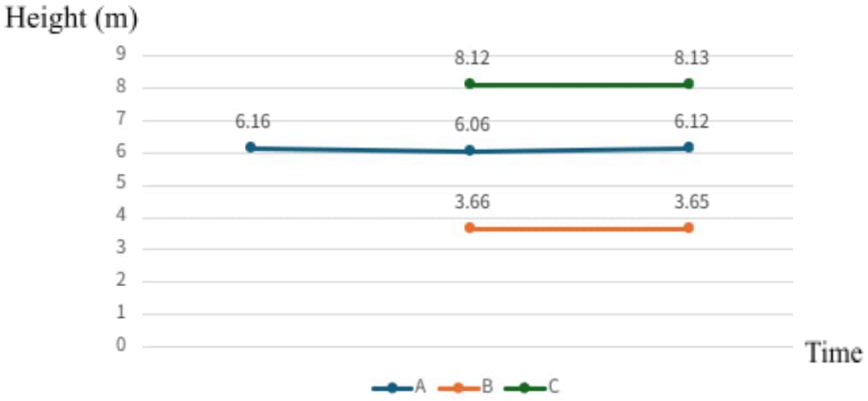

Graph 5. Circumference Growth Pattern of Sakura Trees.

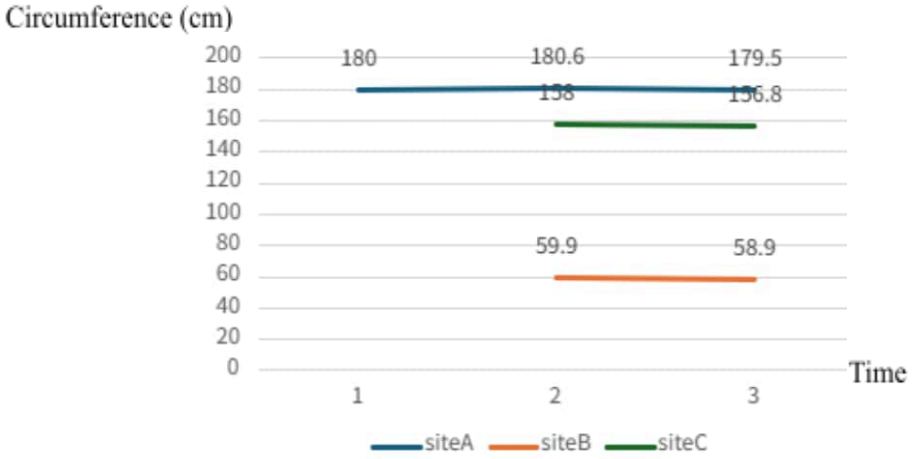

Graph 6. Carbon sequestration (kg C) of Sakura Trees

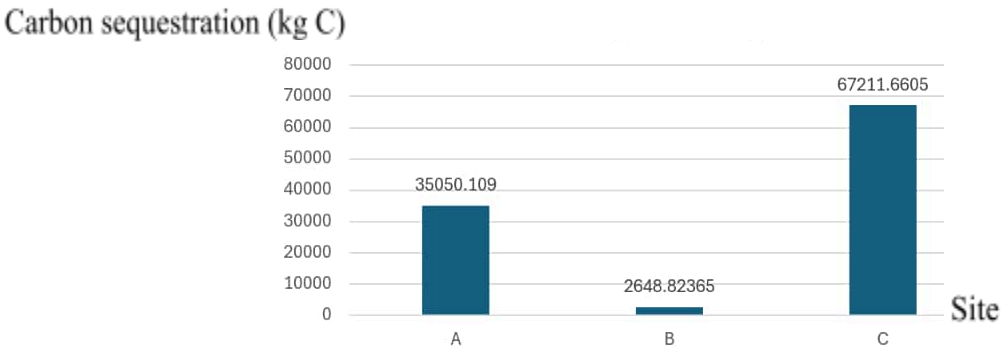

4. Discussion

In Thailand, Sri Trang trees showed higher growth and carbon storage, likely due to more suitable soil properties such as moisture, texture, and pH. Sri Trang trees are well adapted to red-brown soils with a loamy sand texture.
In Japan, Sakura trees showed growth and carbon storage patterns associated with soil properties such as moisture, texture, and pH. Sakura trees are well adapted to chamoisee soils with a pasapasa texture and tend to grow well under lower soil moisture conditions.

5. Conclusion

Ecological Comparative Analysis: Carbon Sequestration Potential and Growth of Sri Trang and Sakura Trees

A comparative study of growth dynamics and biomass accumulation between Sri Trang trees *(Jacaranda mimosifolia)* in Thailand and Sakura trees *(Prunus serrulata)* in Japan reveals key insights into the influence of edaphic factors on carbon sequestration potential. Although the two species share similar external morphological characteristics, their ecological performance differs markedly depending on environmental context.

Influence of Soil Physical and Chemical Properties on Carbon Sequestration

The results indicate that Sri Trang trees in Thailand exhibit higher growth rates and greater carbon sequestration capacity. This finding is consistent with plant physiological principles emphasizing soil specificity as a determinant of photosynthetic efficiency and energy accumulation. Sri Trang trees are

well adapted to red-brown soils with a loamy sand texture, which promotes effective drainage and aeration within the root zone. These soil conditions directly support enhanced biomass accumulation.

In contrast, Sakura trees in Japan display growth patterns associated with chamoisee soils and a pasapasa (loose and dry) soil texture. An important observation from the study is that Sakura trees are able to maintain stable physiological processes under lower soil moisture conditions. This reflects an adaptive strategy that supports survival and growth in temperate climates characterized by variability in soil water availability.

Research Implications

From a deeper analytical perspective, these findings support the academic principle that physical similarity does not imply functional equivalence. Factors that warrant further consideration in future research include:

Carbon Sequestration Efficiency:

The higher carbon sequestration capacity observed in Sri Trang trees within tropical environments may result from longer growing seasons combined with soil pH conditions that enhance nutrient availability.

Adaptability to Climate Change:

The ability of Sakura trees to grow effectively under low soil moisture conditions suggests potential drought tolerance, an important trait for green space planning under future climate change scenarios.

Conclusion

In conclusion, successful tree-based carbon sequestration strategies depend not solely on species selection based on external characteristics, but on ecological matching between soil properties and plant physiological requirements. This study provides a valuable foundation for informed decision-making in the selection of tree species for regional green space restoration aimed at both economic and environmental sustainability.

6. Acknowledgements

We would like to thank the ICRP program for facilitating this international collaboration. Special thanks to the GLOBE program for the scientific protocols and our teachers for their guidance.

7. References

Ogawa, H., Yoda, K., Ogino, K., & Kira, T. (1965). Comparative ecological studies on three main types of forest vegetation in Thailand. II. Plant biomass. *Nature and Life in Southeast Asia*, 4, 49-80.

The GLOBE Program. (2025). *Soil and Tree Protocols for Environmental Monitoring*.

The difference of microorganisms and water quality of water sources between Japan and Thailand.

Kiguchi Momoka[1], Osawa Kokoro[1], Kimura Koharu[1], Woramet Prayunhong[2], Natthakulwadee Tehair[2], Phanatchakorn Nuannim[2]
[1]Matsusho Gakuen High School (Japan)
[2]Princess Chulabhorn Science High School Trang (Thailand)

Abstract:

This research aimed to investigate and compare the water quality of aquatic resources in Thailand and Japan. The study areas included water sources around [2] Princess Chulabhorn Science High School, Trang Province, Thailand, and water sources around [1] Matsusho Gakuen High School in Japan. In addition, small aquatic organisms were surveyed to compare the biodiversity of living organisms in these water bodies. The results showed that the water temperature of the study sites in Thailand was significantly higher than that of Japan at the 0.05 level of statistical significance. However, there was no statistically significant difference in pH values between the water sources in Thailand and Japan. Furthermore, a greater diversity of small aquatic organisms was found in Thailand, including both zooplankton and phytoplankton, whereas the water sources in Japan were dominated mainly by algae.

Keywords: Water quality, Microorganisms

1. Introduction

Thailand and Japan differ significantly in terms of geography, climate, and environmental conditions, which lead to distinct patterns of biodiversity, particularly in aquatic ecosystems. Thailand is located in a tropical climate zone and is characterized by three seasons—summer, rainy season, and winter. As a result, water bodies in Thailand often contain relatively high levels of sediment due to heavy rainfall and surface runoff. In contrast, Japan is situated in a temperate climate zone with four distinct seasons, and its water bodies generally exhibit lower sediment levels and more stable environmental conditions.

These differences in climate and environmental characteristics play a crucial role in influencing water quality and the composition of aquatic ecosystems. Factors such as water temperature, pH, and sediment levels directly affect the survival and diversity of aquatic organisms, especially small organisms such as plankton and algae, which are sensitive to environmental changes. Consequently, variations in these factors may lead to differences in aquatic biodiversity between the two countries.

Therefore, this study focuses on examining water quality and small aquatic organisms in selected water sources in Thailand and Japan in order to compare the characteristics of aquatic biodiversity between the two regions. By analyzing environmental parameters and the diversity of small aquatic organisms, this research aims to provide a better understanding of how geographic and climatic differences influence aquatic ecosystems in both countries.

2. Methodology

2.1 Water Sample Collection

Water samples were collected from selected water sources in Japan and Thailand using sterile containers. All samples were labeled and transported for analysis.

2.2 Water Quality Measurement

Water quality parameters, including pH, temperature, and turbidity, were measured using standard instruments. The results were recorded for comparison.

2.3 Microscopic Observation

Microorganisms in the water samples were observed using a stereo microscope for larger organisms and a light microscope for microscopic organisms.

3. Results

Water quality parameters, including temperature, pH, and turbidity, were investigated in water sources located around [2] Princess Chulabhorn Science High School, Trang, Thailand and [1] Matsusho Gakuen High School, Japan. Three water sources were studied in each country. The results indicated that the average water temperature in Thailand was 29 °C, which was significantly higher than the average water temperature in Japan (25.33 °C) at the 0.05 level of statistical significance, as shown in Figure 1. However, there was no statistically significant difference in pH values between the water sources in Thailand and Japan at the 0.05 significance level, as shown in Figure 2.

Figure 1. Experimental results: Water temperature of water source

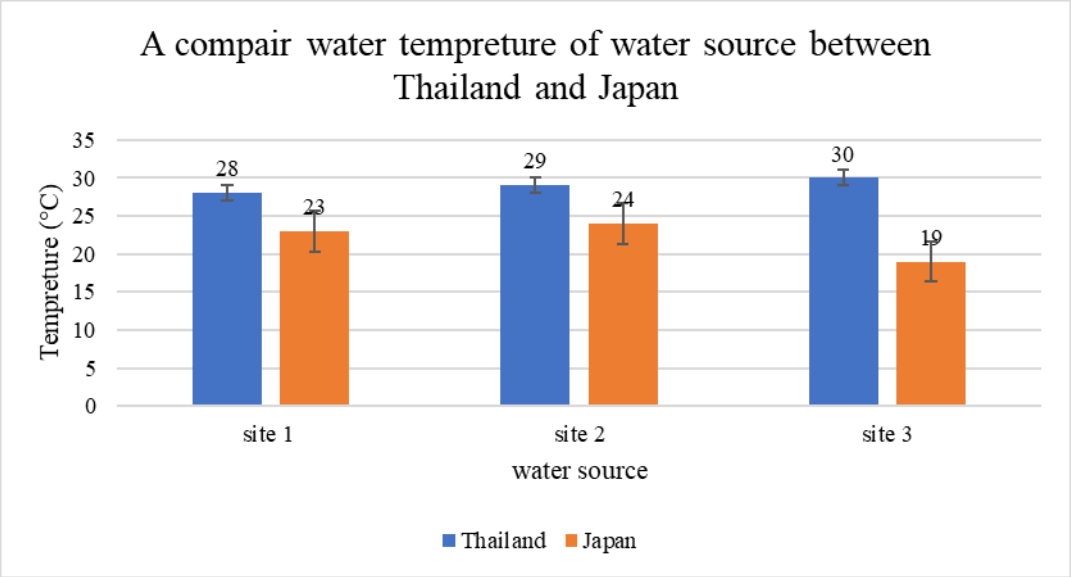

Figure 2. Experimental results: Water pH of water source

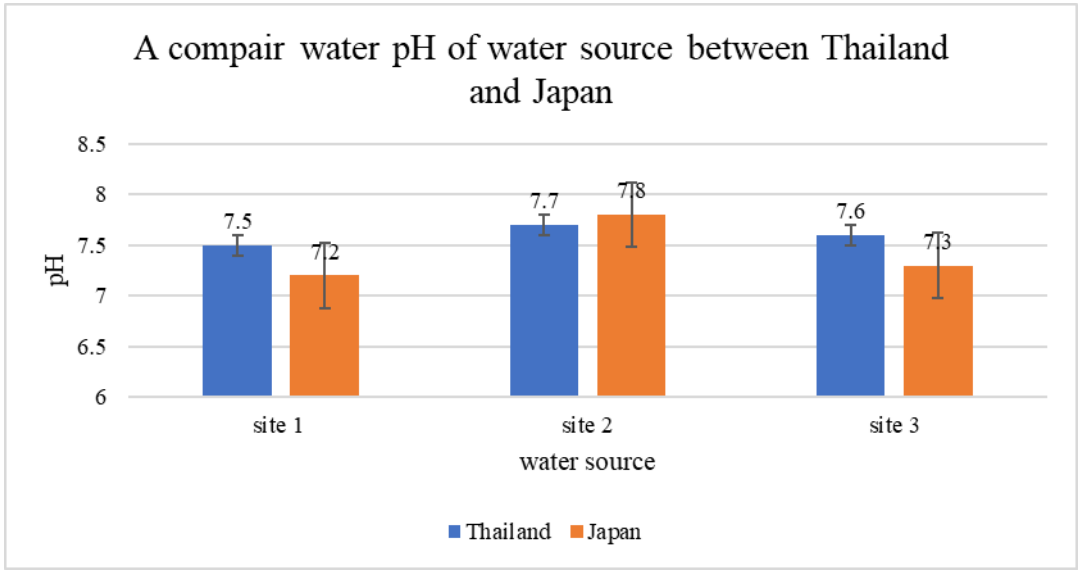

From the survey of microorganisms in the studied water sources, it was found that the diversity of microorganisms in Thailand was higher than that in Japan, whereas the water sources in Japan were dominated mainly by algae, as shown in Table 1.

Table 1. Experimental results: microorganisms in water sources

Thai microorganisms	Japanese microorganisms
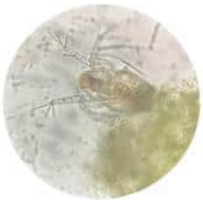 ***Daphnia sp.***	 ***Batrachospermum sp.***
 ***Acanthocystis* sp**	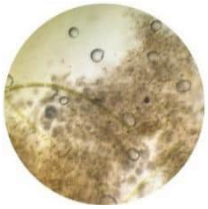 ***Spirogyra sp.***
 ***Stentor sp.***	 ***Green Algee***
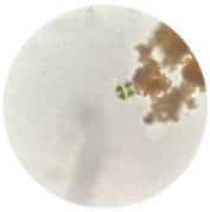 ***Cosmarium sp.***	
 ***Diatom & Cyanobacteria sp.***	

Chlamydomona sp.

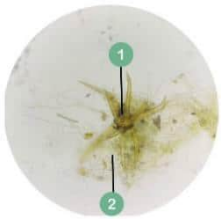

1. Asterionella sp.
2. Cladophora sp.

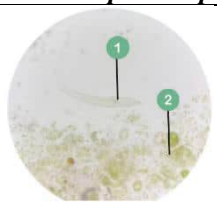

1. Rotifera sp.
2. Chlorella sp.

Trachelomona sp.

4. Discussion

Water temperature in Thailand was significantly higher at a 0.05 level of significance, supporting greater aquatic organism diversity, while clearer water in Japan with visibility exceeding 1 meter favored freshwater algae. Similar pH values ranging from 7.2 to 7.8 indicate minimal influence of pH.

5. Conclusion

Higher water temperatures in Thailand support greater aquatic organism diversity, including phytoplankton and zooplanktonsuch as Daphnia and Rotifera. Whereas cooler waters in Japan mainly favor freshwater algae. Lower turbidity in Japan (visibility > 1 m) promotes filamentous algae, while higher turbidity in Thailand suggests elevated nutrient availability and increased abundance of aquatic organisms. As pH values in both countries remain near neutral (about7.2-7.8), temperature and turbidity are the primary factors influencing organism community composition.

6. References

Bilotta, G. S., & Brazier, R. E. (2008). **Turbidity and aquatic ecosystems. Marine and Freshwater** Research. https://www.publish.csiro.au/mf/fulltext/mf20353 ITPO Tokyo. (n.d.). Rice Resin. *UNIDO*. https://itpo-tokyo.unido.org

Rabalais, N. N. (2019). **Turbidity and biodiversity in estuaries. ICES Journal of Marine Science.** https://academic.oup.com/icesjms/article/77/1/379/5620392

Microbial decontamination and structural integrity of recycled polycaprolactone (PCL) masks for sterile medical casts

Amane Fujioka[1], Chiari Kitada[1], Pitchayut Khampunnip[2], Natthaporn Wonglertsuwan[2]
[1]*Risho Gakuen Osaka Ritsumeikan Junior & Senior High School (Japan)*
[2]*Srinakharinwirot University Prasarnmit Demonstration School (Secondary) (Thailand)*

Abstract

Background: Radiotherapy for head and neck cancer relies on thermoplastic polycaprolactone (PCL) masks to ensure accurate patient positioning. Although these masks are physically reusable, they are rarely reused due to limited data regarding radiobiological effects after repeated exposure. Repurposing used PCL masks for medical applications that do not require radiobiological consideration- such as orthopedic casts- may significantly reduce medical waste.

Objective: To evaluate whether used thermoplastic PCL radiotherapy masks can be sterilized and recycled into medical casts without microbial contamination or loss of structural integrity.

Methods: This prospective jointed study was conducted between Srinakharinwirot university Prasarnmit demonstration school (Thailand) and Ritsumeikan Junior and Senior high school (Japan). In Thailand, microbial contamination was assessed using swab cultures from used PCL masks, with and without alcohol disinfection, cultured on agar plates from common nosocomial bacteria. In Japan, PCL masked were reheated, remolded, and subjected to repeated stretching and reshaping cycles to simulate reuse as orthopedic casts, assessing macroscopic deformation and structural stability.

Results: No bacterial growth was detected in either disinfected or non-disinfected masks throughout a one-month observation period. While the extensibility of the recycled PCL material tended to decrease after multiple reheating and remolding cycles, the application of manual pressure during the molding process ensured that the average conformability for each thickness remained above 70%.

Conclusion: This study demonstrates that discarded PCL thermoplastic radiation therapy masks can be safety disinfected and repurposed as medical casts without the risk of detectable microbial contamination. Furthermore, it was verified that even as the material undergoes physical hardening due to reuse,high molding precision can be maintained by incorporating manual pressure techniques. This approach presents a viable and environmentally sustainable alternative to conventional casting materials.

Keywords: Thermoplastic masks; PCL mask; Medical cast; recycled masks

---

1. Introduction

Radiotherapy is an essential treatment modality for head and neck cancer and requires thermoplastic polycaprolactone (PCL) immobilization masks to ensure precise patient positioning.[1] Although these masks are physically durable and theoretically reusable, they are typically discarded after treatment due to uncertainty regarding radiobiological safety following repeated radiation exposure.

Meanwhile, fracture management commonly employs cement casts due to their low cost, despite disadvantages such as weight, poor ventilation, and patient discomfort. Fiber casts offer improved performance but are substantially more expensive. The structural characteristics of thermoplastic PCL masks resemble those of modern casting materials, suggesting potential interchangeability. However, concerns remain regarding microbial contamination and material degradation after reuse. This study aimed to evaluate the feasibility of recycling used PCL radiotherapy masks into medical casts.

2. Methodology

This prospective joint study was conducted between Srinakharinwirot University Prasarnmit Demonstration School (SPSM), Thailand, and Risho Gakuen Osaka Ritsumeikan Junior & Senior High School, Japan. Sterilization experiments were conducted in Thailand, while material modeling and structural testing were conducted in Japan.

2.1 Microbial Contamination Study (Thailand)

Used PCL masks were divided into two groups: disinfected and non-disinfected. Three masks were used, with two swab samples collected per mask (nasal and oral regions). In the disinfected group, 70% alcohol was applied using sterile cotton balls prior to sampling. Samples were cultured on agar plates (picture 1) and incubated for Pseudomonas aeruginosa, Staphylococcus aureus, Staphylococcus epidermidis, and Bacillus cereus. Plates were observed weekly for one month.

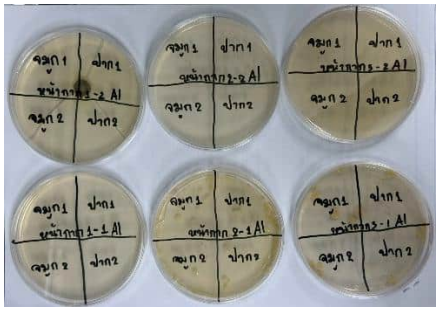

Picture 1. Culture plates

2.2 Structural Integrity and Reusability Testing (Japan)

In Japan, used PCL masks were reheated in warm water (60–65 °C) and subjected to a maximum of five cycles of reheating,stretching, and remolding to simulate reuse. Structural integrity was quantitatively evaluated by measuring the incremental stretch in each cycle while pulling the material with a constant force. To verify clinical molding precision, the material was molded onto the subject's knuckle (dorsum of the hand),and the fit was quantified by caculating the skin contact area ratio using the 100-square grid method with skin pigmentation. This approach present a feasible, environmentally sustainable alternative to conventional casting materials.

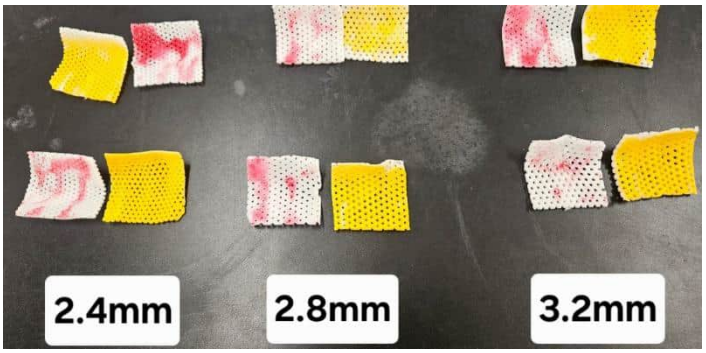

3. Results

3.1 Microbial Contamination

No bacterial growth was observed in any samples from either disinfected or non-disinfected groups throughout the observation period (Table 1).

Table 1. Bacterial culture

Bacteria	S. epidermidis		S. aureus		B. cereus		P. aeruginosa	
sample	Site 1 (nose)	Site 2 (mouth)	Site 1 (nose)	Site 2 (mouth)	Site 1 (nose)	Site 2 (mouth)	Site 1(nose)	Site 2(mouth)
Mask no.1	No growth	No growth	No growth	No growth	No growth	No growth	No growth	No growth
Mask no.2	No growth	No growth	No growth	No growth	No growth	No growth	No growth	No growth
Mask no.3	No growth	No growth	No growth	No growth	No growth	No growth	No growth	No growth

3.2 Structural Integrity

Following repeated remolding,the accumulation of thermal history led to a gradual decrease in material extensibility, however, by employing a manual pressure molding technique, it was possible to maintain a high contact area ratio, with the average of two trials for each thickness exceeding 70%,regardless of material degradation. This suggests that with the application of appropriate molding techniques, PCL with altered physical properties can still be precisely fitted to anatomical shapes, making its reuse as a cast highly realistic.

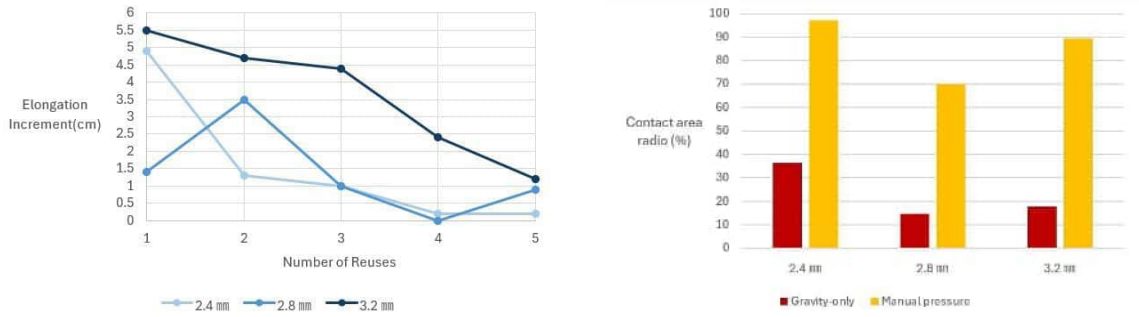

4. Discussion

This study demonstrates the feasibility of recycling used thermoplastic polycaprolactone (PCL) radiotherapy masks into medical casts by evaluating both microbial safety and structural integrity. The absence of detectable bacterial growth in both disinfected and non-disinfected samples suggests that used PCL masks, when properly handled and stored, may present a low risk of nosocomial contamination. These findings are consistent with the inherent properties of PCL, which is a hydrophobic thermoplastic polymer that does not readily support bacterial adhesion or biofilm formation[2].

Interestingly, no bacterial contamination was observed even in masks that did not undergo alcohol disinfection prior to culturing. This may be explained by several factors, including prior cleaning during clinical use, limited nutrient availability on the polymer surface, and the thermal exposure experienced by masks during the radiotherapy molding process. Nevertheless, alcohol disinfection remains recommended in clinical practice to minimize infection risk, especially when masks are repurposed for direct patient contact in orthopedic applications.

The structural integrity experiments conducted in Japan further support the suitability of recycled PCL masks as casting materials. The experimental results from Japan indicated a gradual decrease in material extensibility following repeated reheating cycles, suggesting subtle structural changes due to thermal history. However, no critical fractures or significant deformations were observed at the macro level. Most importantly, the results demonstrated that any loss in physical properties could be technically compensated for by employing a “manual pressure “molding technique. This confirms that recycled PCL remains highly capable of achieving the precise anatomical fit required for medical casts through appropriate handling.

Compared with traditional cement casts, recycled PCL casts may offer several advantages, including reduced weight, improved ventilation, and water resistance. While fiber casts share similar benefits, their higher cost can limit accessibility, especially in resource-constrained settings. Recycling radiotherapy PCL masks could therefore provide a cost-effective and environmentally sustainable alternative, contributing to the reduction of medical plastic waste.

Despite these promising findings, this study has several limitations. First, microbial testing focused on a limited number of common nosocomial bacteria and did not include fungal or viral pathogens. Second, structural integrity was assessed qualitatively rather than through quantitative mechanical testing such as tensile strength or load-bearing capacity. Third, the number of reuse cycles tested was limited, and long-term material fatigue was not evaluated. Finally, ethical constraints prevented in vivo testing on

patients, which would be necessary to fully assess clinical performance.

Future research should include standardized mechanical testing, expanded microbiological analysis, and evaluation of repeated sterilization methods such as autoclaving or ultraviolet irradiation. Clinical trials comparing recycled PCL casts with conventional casting materials in fracture management would further clarify their safety, effectiveness, and patient satisfaction.

5. Conclusion

This study demonstrates that discarded PCL thermoplastic radiotherapy masks can be safely sterilized and recycled into medical casts without detectable nosocomial contamination or significant loss of physical properties. The findings support reuse for at least three reshaping cycles, suggesting a viable strategy to reduce medical waste while providing an alternative casting material. Further studies are recommended to quantify mechanical strength and establish maximum reuse limits.

6. Acknowledgements

The authors gratefully acknowledge the Radiotherapy Department of Phramongkutklao Hospital for providing PCL masks used in this research.

7. References

1) Nagesh, M., Vadgaonkar, R., Sreelakshmi, K. K., Hajare, R., Parab, P., Dash, S., Reddy, R., Shende, V., Nawar, A., Biswas, R., Bula, S. R., Gagare, S., Belekar, D., Miriyala, R., & Mahantshetty, U. (2024). Assessment of usage, reuse and disposal of thermoplastic masks among radiotherapy technologists in India: A nationwide perspective. Technical Innovations & Patient Support in Radiation Oncology, 32, 100278. https://doi.org/10.1016/j.tipsro.2024.100278

2) Dash, T. K., & Konkimalla, V. B. (2012). Poly-ε-caprolactone based formulations for drug delivery and tissue engineering: A review. Journal of Controlled Release, 158(1), 15–33. https://doi.org/10.1016/j.jconrel.2011.09.064

2025-2026 International Collaborative Research Project Report

Issued April 2026

Issued by Ritsumeikan High School

1-1-1 Choshi Nagaokakyo City, Kyoto, JAPAN

TEL：+81-75-323-7111 FAX：+81-75-323-7123